Catching Collagen

A comparative test of destructive ZooMS sampling protocols against the non-destructive electrostatic membrane box sampling protocol using Châtelperronian and Mesolithic bone tools

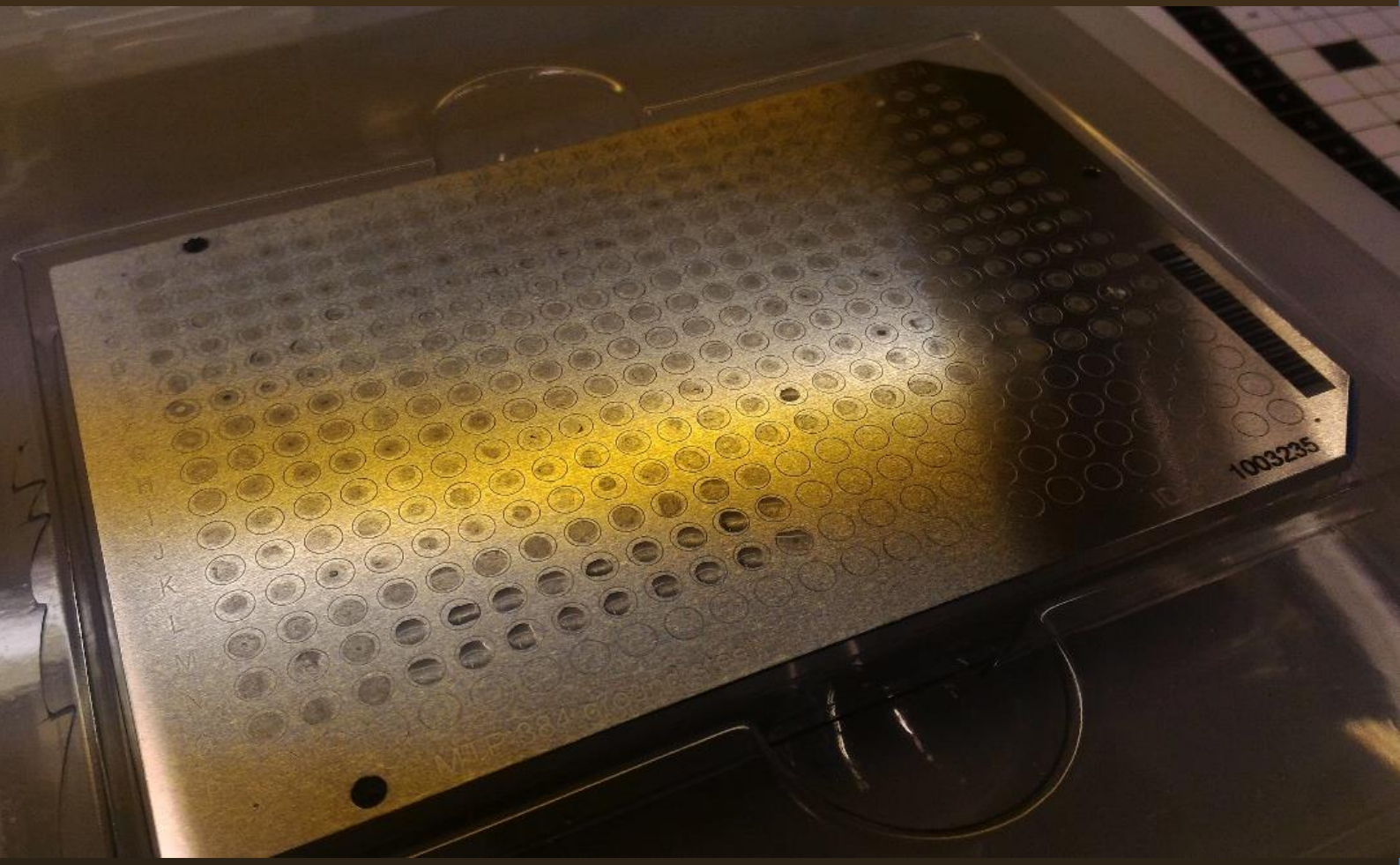

Joannes A. A. Dekker

Image: The MALDI Bruker plate MTP384 used in this research (own work).

Catching Collagen

A comparative test of destructive ZooMS sampling protocols against the non-destructive electrostatic membrane box sampling protocol using Châtelperronian and Mesolithic bone tools

Joannes A. A. Dekker,
S1617664

Bachelor Thesis
1043SCR1Y-1819ARCH

Supervisors:
Prof. dr. M. Soressi,
V. Sinet-Mathiot, MSc

University of Leiden,
Faculty of Archaeology

Leiden,
14-06-2019,
Final version

Table of Contents

Acknowledgements

A Bachelor thesis is supposed to be a student's first substantial and independent research project, but a student quickly discovers that one never can do research in complete isolation. There is a number of people, whose help was indispensable and who rightly deserve gratitude for their efforts.

First of all, I wish to thank my supervisors, prof. dr. Marie Soressi from Leiden University and Virginie Sinet-Mathiot, PhD student, from the Department of Human Evolution at the Max Planck Institute in Leipzig. In the first place I want to thank them for allowing me to apply ZooMS and to travel to the Max Planck Institute in Leipzig to do so. I greatly appreciate the opportunity presented to me.

Secondly, I owe thanks to dr. Frido Welker from the Max Planck Institute and the Natural History Museum of Denmark and dr. Hadi Izadi from the Yale School of Engineering and Applied Science. Both researchers chose to help me in their free time and were willing to answer my questions about the methodological complexities of ZooMS and intricate workings of electrostatic adhesion, respectively.

Furthermore I would like to express my gratitude to dr. Jason Laffoon from Leiden University, who gave me access to the Chemical Laboratory for the destructive sampling of the artefacts and who supervised the sampling.

My thanks also go to prof. dr. Jean-Jaques Hublin, the director of the Department of Human Evolution of the Max Planck Institute, for allowing me the use of the Department's facilities.

The Mesolithic North Sea bone points used in this thesis belong to private collectors and I wish to thank them for allowing me to analyse their prized artefacts. Without the cooperation of Aad Berkhout, Rick van Bragt, Maarten Drummen, Gideon de Jong, Mirjam Kruizinga, Trudy Langeveld, Erwin van der Lee, Johan Passchier, Sibo van Maren, Maarten Schoemaker, Willy van Wingerden and several others this thesis would have been incomplete.

As I myself lack the expertise for morphologically identifying bone, I want to express my thanks to dr. Laura Llorente Rodriguez, Andre Ramcharan, Wouter Bonhof, MSc and dr. William Rendu for making the morphological identifications of the Quinçay controls.

Lastly, I wish to thank my friends and family for their support.

1 Introduction

Bone is one of the most commonly found materials in the archaeological record. Bone is found at sites in all regions and of all periods, from the earlier hominins to the Second World War. Analysis of the encountered bones provides insight in what species were present at the site. The presence or absence of certain species can in turn be used to provide information on a variety of topics, among others climatic reconstruction, diet or domestication.

The species identification of a bone is usually achieved on basis of morphological characteristics, but a morphological approach is not always possible. Taphonomic processes or anthropic activity may obscure characterising features or fragment the bone. Consequently, unidentified bone remains are most often simple and small fragments or, in a minority of cases, bone tools. Additionally, morphological differences are not always present on all skeletal elements of closely related species. In those cases identification can still be made on a broader taxonomic level.

The species of a bone can be determined by histology (Hillier and Bell 2007, 260), but this method is time consuming and destructive (Buckley *et al.* 2017, 402; Cuijpers and Lauwerier 2008, 167). Furthermore, fragmented bone is often found in large quantities and is regarded as having little explanatory value. In the end this results in boxes full of unidentified bone fragments.

ZooMS is a proteomic identification method, which allows the cheap and fast identification of many bone fragments. The acronym stands for *Zooarchaeology by Mass Spectrometry* (Buckley *et al*. 2010, 14). Shortly summarised ZooMS works by unfolding the collagen structure, solubilising it and cleaving the collagen molecule into peptide chains. Mass spectrometry analysis allows the detection of peptide markers, which are peptide chains specific to certain taxonomic groups. Its application facilitates the identification of these boxes full of fragments, but at the moment most sampling techniques are destructive. Destructive sampling prevents the application of ZooMS to rare organic finds, like bone tools. Yet at the same time the species identification of bone tools would add greatly to our knowledge of the role bone tools played for past hominins.

In order to enable the species identification of precious organic finds several non-destructive ZooMS sampling protocols have been proposed. The most promising of these is the electrostatic membrane box protocol (Martisius *et al.* submitted). However, it remains untested how the membrane box compares to the commonly used

destructive sampling methods. It is therefore difficult for researchers to weigh the advantages and disadvantages of each protocol. This thesis aims to provide an overview of the differences between the established destructive ZooMS sampling protocols and the non-destructive electrostatic membrane box protocol in order to allow researchers to assess what sampling protocol is most suited for their research questions and material. To create this overview Châtelperronian bone and ivory tools from Quinçay, France, and Mesolithic bone and antler points from the Dutch shores of the North Sea will be analysed.

1.1 Developmental history of ZooMS

The developmental history of ZooMS reveals what aspects of the method can and have been improved. The original purpose of ZooMS was to find a way to distinguish bone of sheep (*Ovis aries*) from goat (*Capra hircus*). These two species are abundant at sites with domesticated animals and the characteristic features distinguishing them are often lost (Buckley *et al.* 2010, 14-16).

The idea that proteins could aid in taxonomic identification was already present in 1991 (Lowenstein and Scheuenstuhl 1991, 375). Lowenstein and Scheuenstuhl only attempted to clarify evolutionary relationships between already identified species and not to identify new samples. In 2000 Ostrom *et al.* suggested that proteins could perhaps be used to quickly identify species (Ostrom *et al.* 2000, 1043). Instead of collagen Ostrom *et al.* used osteocalcin, because they thought osteocalcin might preserve best in the archaeological record (Ostrom *et al.* 2000, 1044). The development of proteomic identification continued in 2008 when Buckley *et al.* managed to differentiate between bone samples belonging to cattle, chicken, human, rabbit and dog using the mass spectra of a part of the collagen molecule (Buckley *et al.* 2008, 327). This method was the direct precursor of ZooMS (Buckley *et al.* 2009, 3843).

Building on their earlier work Michael Buckley, Matthew Collins and Jane Thomas Oates published a more precise identification technique called ZooMS (Buckley *et al.* 2010, 14). The main difference between the 2008 protein identification technique and later ZooMS is what part of the collagen molecule is used. In 2008 only the telopeptides were used for identification. A collagen telopeptide is a peptide located near the end of the collagen protein, outside the triple helix structure (Greenblatt *et al.* 2017, 465), Telopeptides, however, only constitute around 1% of the total collagen sequence.

ZooMS uses the entire collagen protein (Buckley *et al.* 2009, 3843; Buckley *et al.* 2010, 14).

Current research projects are focussed on developing non-destructive sampling protocols for ZooMS by employing static electricity.

1.2 ZooMS compared to other biomolecular identification methods

There are alternative methods to identify uncharacteristic bones, such as ancient DNA analysis, tooth wear analysis and stable carbon isotope signatures. However, all these methods have significant limitations. DNA and its abilities are far better known than those of proteins, especially regarding species identification, but DNA degrades faster than collagen, is easily contaminated and DNA analysis is also expensive and time-consuming (Buckley and Kansa 2011, 278; Buckley *et al.* 2014, 632-633).

The main disadvantage of tooth wear analysis is that it requires undamaged teeth, limiting its applicability. Stable carbon isotope signatures distinguish between different ecological niches rather than directly distinguishing species.

Advantages of ZooMS are that collagen is easier to extract than other bone proteins, like osteocalcin (Collins *et* al. 2010, 6). Collagen can also be sampled directly from the bone, instead of requiring more complex preparation like DNA (Buckley *et al.* 2014, 633). The low cost and short analysis time also make ZooMS much more widely applicable than DNA analysis (Buckley *et al.* 2010, 14).

1.3 Destructive ZooMS sampling protocols

This thesis compares the two established destructive ZooMS sampling protocols: the cold acid and ammonium bicarbonate protocol, and three electrostatic non-destructive sampling protocols: eraser, membrane box and plastic bag protocol.

The cold acid protocol is the original method of sample preparation (Buckley *et al*. 2010, 15). In this protocol bone is demineralised in a hydrochloric acid (HCl) solution (Buckley *et al.* 2010, 15), which causes it to lose the majority of its weight and size (Van Doorn *et al.* 2011, 286).

The ammonium bicarbonate buffer protocol is often referred to by its shorter name, AmBic (Welker *et al.* 2015a, 281), which will be used for the rest of this thesis. The AmBic protocol yields less protein than the cold acid protocol (Van Doorn *et al.* 2011, 286), but it is much less destructive. Macroscopically the AmBic protocol causes no

change in bone size or weight. As the buffer only partially leaches the sample rather than dissolving it, the same sample can be analysed repeatedly (Van Doorn *et al.* 2011, 288).

The cold acid and AmBic protocol have been selected, because they represent the most commonly used and standardised protocols. Therefore they are the best comparisons for non-destructive protocols.

1.4 Non-destructive ZooMS sampling protocols

The reviewed non-destructive sampling protocols all employ static electricity to extract collagen from organic tissue. Due to the recent introduction of electrostatic sampling methods there is little empirical evidence for the limitations and the influence of variables on sampling results. Therefore expectations concerning the applicability and an understanding of how the methods work must be based on knowledge about static electricity as a whole. Although static electricity has been known since Antiquity, unfortunately its precise workings are still not understood.

The way in which the membrane box, plastic bag and eraser protocol generate static electricity differs fundamentally. The eraser and plastic bag protocols create static electricity by friction. They are triboelectric methods, *tribo* meaning rubbing in Greek (Williams 2012, 316). However, the membrane box protocol does not entail friction. Rather the entire design of the membrane box is supposed to prevent friction. The static electricity in the membrane box protocol is generated by separating two bodies from each other. The static electric charge is generated due to adhesion.

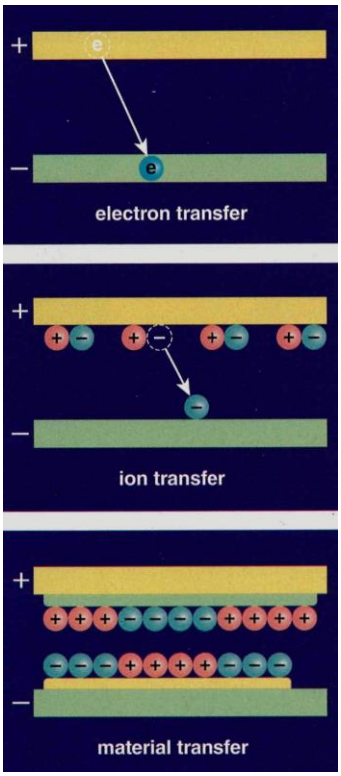

Figure 1 Three different ways to transfer charge, after Williams 2012, 320.

1.4.1 Triboelectric protocols: Eraser and plastic bag protocols

It is thought that triboelectric charges are in essence generated by mobile ions changing surface (fig. 1, middle image). Ions are mobile, if their counterion is either significantly larger or if the counterion is attached to a polymer (Williams 2012, 320). If two bodies are rubbed

against each other, mobile ions switch surface generating a force. The applied force is correlated with the strength of the charge, because it affects the depth from which ions can change surface (Williams 2012, 323).

In the eraser protocol rubbing the eraser against the target material creates an electrostatic charge (Fiddyment 2015, 15066). The generated charge causes collagen molecules to cling to the eraser waste. The eraser protocol is mostly applied to parchment (Fiddyment *et al.* 2015, 15066). One of the main advantages of the eraser protocol is that the actual sampling can be done by the people responsible for the preservation of the parchment. This minimises the risk that the target material is accidentally damaged during sampling (Fiddyment *et al.* 2015, 15067).
At the moment there is no published successful application of the eraser protocol on bone. The eraser's protocol success on parchment does not guarantee success on bone due to the significant difference in the organisation of collagen fibrils between parchment and bone. Besides the eraser protocol features heavy friction, which might damage microwear on worked bone. Therefore the eraser protocol will not be tested within this thesis.

The theory behind the plastic bag protocol is similar to the eraser protocol. Friction caused by movement inside the plastic bag, generates the triboelectric charge required for adhesion of bone particles. This protocol has been tested and the results showed that the principle works. However these results have not yet been published at time of writing.

1.4.2 Contact electrification protocol: Membrane box protocol

The first publication of the membrane box protocol is in press at the moment (Martisius *et al.* submitted). Membrane boxes consist of two halves, each of which is closed by a thin membrane. When an object is put in a membrane box, it is encapsulated by the two membranes (fig. 2). The intimate contact between the artefact and the two membranes generates static electricity. These electrostatic forces ensure that, when the object is removed again, bone micro-particles remain attached to the membranes.

The phenomenon of a charge arising due to two bodies touching and separating, is known as contact electrification and is the principle on which the membrane box

protocol is based (Baytekin *et al.* 2011, 308). It used to be thought that contact electrification arose due to a charge difference between the surfaces of two contacting bodies. However, contact electrification was also observed between two identical bodies. This presented a problem, because there should not be a charge difference between two bodies with equal charge and physical properties. Research revealed that instead of each surface having a general charge, it was comprised of a mosaic of negative and positive charges (Baytekin *et al.* 2011, 308) (fig. 3).

Figure 2 Mesolithic point P5 in its membrane box, own picture.

Thus, the general charge of a surface could be equal to or just slightly different from the other surface, whilst the generated electrical force would be much larger than expected (Baytekin *et al.* 2011, 309). What processes determine how many nanoscopic regions make up the mosaic and the magnitude of their charges remains largely unknown, although it is suspected that chemical and micromechanical properties of the material play a role (Baytekin *et al.* 2011, 308-311).

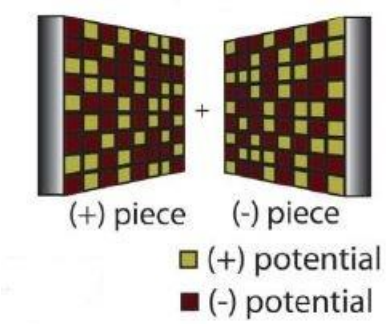

Figure 3 Schematic representation of the electrical charges on the surface of a positively charged object (left) and a negatively charged object (right) (Baytekin et al. *2011, 308).*

The nanoscopic mosaic of charges explains only part of the phenomenon of static electricity. Contact electrification occurs between any two materials and causes a charge transfer between them (Izadi *et al.* 2014, 1), which is carried by electrons (fig. 1, upper image) (Horn and Smith 1992, 363). Contrary to triboelectric forces, where the charge is carried by ions. However the strength of the adhesion induced by contact electrification differs immensely. It can be strong enough to deform materials and allows gecko's to cling to a surface, but it requires a sharp contact surface between the contacting bodies (Horn and Smith 1992, 363; Izadi *et al.* 2014, 1; Derjaguin and Smilga 1967, 4009). The strength of the electrostatic charge depends on myriad variables: the material of the contacting bodies, the electronic structure of the bodies, the surface roughness, the manner in

which contact between the bodies was established and what other physical processes were occurring during the establishment of contact (Horn and Smith 1992, 363; Derjaguin 1994, 223). Lastly there is also a positive correlation between the generated charge and the contact surface area (Persson *et al.* 2013, 1).

There is disagreement to what extent adhesive strength is determined by electrostatic forces or by other forces. Some claim that electrostatic attraction is the main force contributing to the adhesion between solid bodies (Derjaguin 1994, 223), whilst others claim that of the total amount of work performed by adhesion only a small part is contributed by contact electrification. Instead the majority of the work is performed by Van der Waals forces (Persson *et al.* 2013, 2-5). The disagreement on the mechanisms underlying adhesion might be obscured, however, by use of different variables: work versus force (Persson *et al.* 2013,1; Derjaguin 1994, 223).

In any case, contact electrification generates the adhesive forces necessary to catch the collagen on the membranes, enabling further analysis of the molecules.

1.5 Collagen

There are multiple types of collagen, each with its own chemical makeup (Shoulders and Raines 2009, 930). The ratios in which these types occur depends on the used tissue type. In bone, antler and dentine collagen type 1 is the dominant type (Welker 2018, 139). When referring to collagen in this thesis, collagen type 1 is meant.

The structure of collagen is one of the most important causes of its good preservation compared to other biomolecules. Collagen is formed by three strands. Two of these are α(1) strands and the third is a α(2) strand. The α(1) and α(2) strands are composed of different amino acid sequences. These three strands intertwine together to form a triple helix (fig. 4), which is called tropocollagen (Buckley 2016, 2). The strands are bound together by hydrogen bonds (Stryer 1981, 186). Considering that the function of collagen is to hold cells together, it is not surprising that it has such a robust structure (Stryer 1981, 185).

More than 30% of the amino acids in collagen is glycine. Around 20% is proline. Two other important amino acids are hydroxyproline and hydroxylysine (Kirby *et al.* 2013, 4852). It is the high content of proline and hydroxyproline, which gives collagen its stability (Stryer 1981, 191).

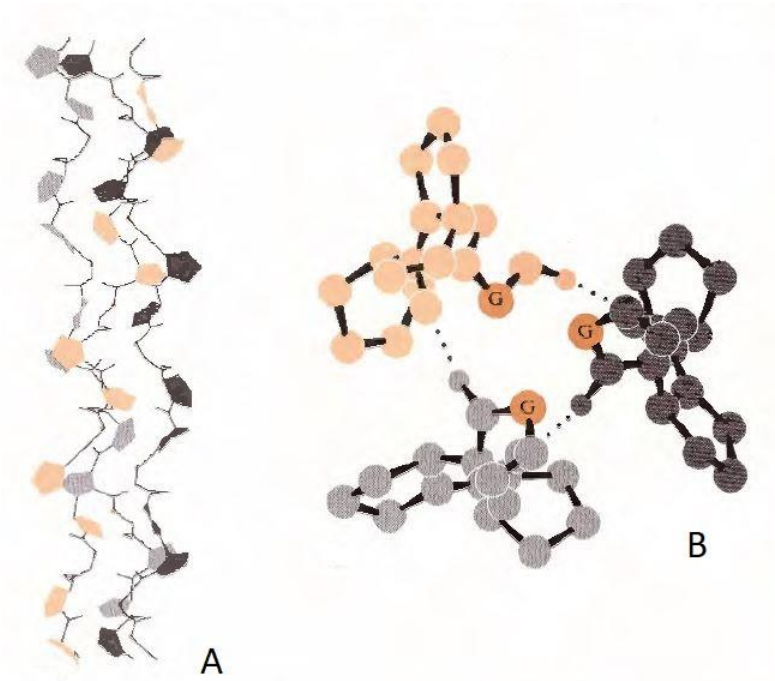

Figure 4 The triple helix structure of collagen, seen from side view A and end view B (Cantor and Schimmel 1980, 98).

Collagen can be found in high abundance in a variety of organic tissues (Kendall *et al.* 2018, 21). The most commonly encountered collagenous materials in archaeology are bone, dentine and antler. All three are also known to have been used for the production of formal tools during the Upper Palaeolithic (Langley 2016, 1). ZooMS was designed for bone, but is in theory also applicable to other collagenous materials. However, the differences in tissue structure might influence their suitability for electrostatic sampling. Bone consists of two tissue types: cortical and trabecular bone, but on a cellular scale bone consists of a single material. In contrast teeth are composed of two main materials: dentine and enamel. The difference in chemical composition between enamel and dentine is that enamel does not contain collagen, whilst dentine does (Lebon *et al.* 2014, 112).

Dentine can also be found in ivory. In fact, although ivory is commonly equated with tusks, ivory only refers to the dentine cores of tusks (Locke 2008, 423). Tusks are the incisors or canines of certain animal species. Instead of being covered with enamel like teeth, tusks have an outer layer of cementum (Locke 2008, 423), which also contains collagen (Kumar 2011, 152).

Dentine and bone contain similar amount of collagen (Heckel *et al.* 2016, 45), while antler has a higher collagen percentage (Jin and Shipman 2010, 92). In all three the collagen molecules are embedded in the crystal structure of hydroxyapatite, which serves as a protective layer for the collagen (Simpson *et al.* 2016, 29). Dentine, however,

has a larger mineral component than bone and antler, making it more resistant to diagenesis (Welker 2018, 141).

1.5.1 From Genome to Proteome

In order for a biomolecule to be usable for species identification it must vary between taxa. The degree of variation in the biomolecule determines the resolution of the identification method. Collagen, and other proteins, can be used for species identification, because proteins are reflections of specific parts of the DNA of a species. Certain parts of the DNA strand, called exons, code for proteins. When a protein is produced the relevant part of the DNA is first unfolded by an enzyme. An mRNA copy is then made of the DNA exon (Stryer 1981, 634). Every three nucleotides on the mRNA string code for one amino acid. The mRNA string leaves the cell nucleus and is transported to the ribosomes. In the ribosomes the mRNA is translated into amino acids, which in turn are assembled to form the protein (Stryer 1981, 642). The differences between taxa in the exon coding for collagen are linked to the separation time between the taxa (Stryer 1981, 635). In fact it is possible to study phylogeny using the amino acid composition of among other proteins collagen (Welker *et al.* 2015b, 81). If the split between two species was fairly recent, it is often not possible to distinguish the species with ZooMS analysis.

1.5.2 Collagen Preservation

For a protein to be usable in palaeoproteomics it is essential that it preserves well through time. The oldest bone used for ZooMS at time of writing is dated to 3.4 million years ago from a site called Beaver Pond in Canada (Rybczynski *et al.* 2013, 6). Apart from polar climates collagen also survives in other environments, albeit not as long. For example ivory tusks from the 17th century found at the bottom of the Indian Ocean could still be identified with ZooMS, although the outer layer of the tusks was collagen poor (Albéric *et al.* 2014, 126). Another example is a mammoth bone sample from the North dated to 60-20 ka, which contained half the collagen concentration of modern bone (Buckley *et al.* 2011, 2012).

These examples show that collagen can preserve in a variety of situations, but it is not unaffected by diagenesis. In order to assess if a sample is suitable for ZooMS or to explain why ZooMS might not provide expected results, it is necessary to understand the

mechanisms of collagen degradation. The main processes affecting collagen integrity are microbial attacks and hydrolysis. Any process that causes collagen demineralisation also leads to collagen loss (Tripp *et al.* 2018, 463). The reactions causing collagen loss are the same for bone, antler and dentine (Tütken and Vennemann 2011, 2; Kendall *et al.* 2018, 21). Of these processes it is thought that hydrolysis is the main mechanism of collagen degradation (Buckley and Collins 2011, 6). Hydrolysis is the process when an organic molecule reacts with water causing the original organic molecule to fragment (fig. 5) (britannica.com; Richards *et al.* 1967, 376). As a consequence heavier peptide markers are more vulnerable to diagenesis than smaller markers (Buckley and Collins 2011, 6). Hydrolysis is also responsible for degradation of DNA and it was thought that the place where the collagen was split by hydrolysis was randomly chosen, just like it is for DNA. However, it seems that collagen hydrolysis follows a pattern, albeit an ill-understood pattern (Dobberstein *et al.* 2009, 39).

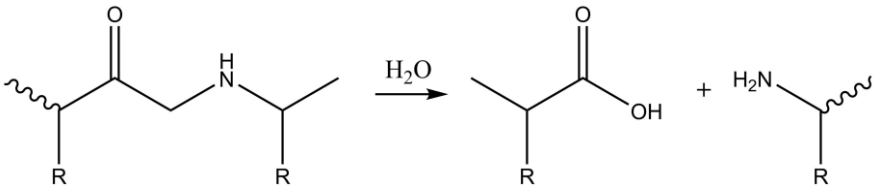

Figure 5 Reaction formula of hydrolysis, after Richards et al. 1967, 376.

Collagen degradation speed depends on the burial environment. Especially temperature seems to have large impact on collagen degradation. There is a clear correlation between thermal age of a sample and collagen loss, although the older the thermal age the less clear the pattern is (Dobberstein *et al.* 2009, 36).

Since successful application of molecular techniques depends on good preservation and analysis is often expensive and destructive, several techniques have been developed to test the preservation of organic tissues (Heckel *et al.* 2014, 134; Lebon *et al.* 2014, 115; Simpson *et al.* 2016, 32). The need for preservation tests became even more apparent, when it was discovered that macroscopically well preserved bone did not mean well preserved collagen (Simpson *et al.* 2016, 33; Tripp *et al.* 2018, 465). Of the various preservation tests deamidation tests collagen preservation directly (Li *et al.* 2010, 3607). Deamidation is a form of hydrolysis where an amide side group of the amino acids

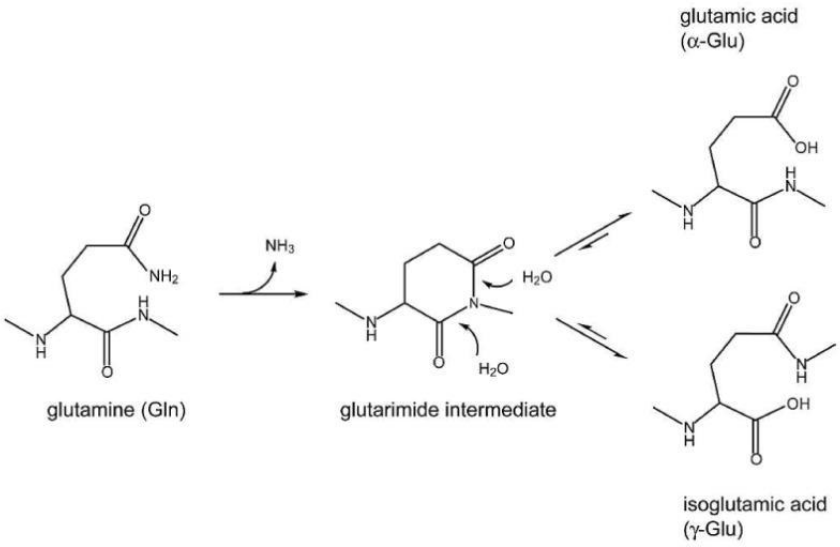

Figure 6 Schematic representation of glutamine deamidation (Li et al. 2010, scheme 1).

glutamine or asparagine is either separated or changed into another functional group (fig. 6) (Li *et al.* 2010, 3607). The lower the deamidation rate the more intact the collagen molecule. Artefacts with the same deamidation level likely share the same taphonomic history (Welker *et al.* 2017b, 25).

The established destructive ZooMS sampling protocols are able successfully identify artefacts from a wide range of preservation conditions. However, it remains to be established whether the non-destructive membrane box protocol shares the same robustness.

1.6 Research question and hypothesis

Therefore the main research question of this thesis is stated as following:

Is the electrostatic membrane box sampling protocol a suitable non-destructive alternative for current destructive ZooMS sampling protocols?

The sub-questions that will be addressed in order to determine if the membrane box is a suitable alternative are:

1) *What is the success rate of the membrane box protocol?*
2) *Are the identifications made with the membrane box protocol as precise as the identifications obtained from the destructive protocols?*
3) *Does the time the artefacts have been inside the membrane box affect the success rate of the membrane box identification?*

4) *Is the membrane box protocol applicable to artefacts with various taphonomic histories and chemical compositions?*
    a) *Is there a difference in success rate between the Quinçay and Mesolithic North Sea material?*
    b) *Is there a difference in success rate between dentine and bone samples?*

The success rate necessary for the membrane box protocol to be considered a suitable alternative depends on the research questions. A study using a large collection of fragmented bones in order to reconstruct a site's faunal spectrum will consider the success rate more important than the non-destructive nature of the sampling protocol, while for a research of precious organic artefacts non-destructive sampling is more important. When dealing with precious finds non-destructive sampling can balance out a lower success rate, due to enabling researchers to analyse a larger number of artefacts. For this study a success rate higher than 50% is considered sufficient, based on the reasoning that a sampling protocol should succeed more often than fail.

Based on an understanding of static electricity and empirical evidence from earlier attempts to apply electrostatic sampling strategies to archaeology it is hypothesised that the membrane box sampling protocol will:

- Provide identifiable spectra for the majority of the samples,

And

- That the spectra, obtained with the membrane box protocol, allow identification as precise as spectra, obtained according to the destructive sampling protocols and that thus the membrane box presents a suitable alternative for the established destructive ZooMS sampling protocols.

It is also expected that differences in burial conditions may influence the identification rate, but that in both datasets a majority of the samples can be identified. Since the Mesolithic North Sea material is more than 30 000 years younger than the Quinçay material, it is expected that the Mesolithic North Sea material will have a higher success rate. No significant difference between ivory and bone samples is expected.

1.7 Thesis outline

There is a clear demand for a reliable and well-tested non-destructive sampling strategy in archaeology and it is the aim of this thesis to provide empirical evidence for the

effectiveness of an electrostatic non-destructive sampling protocol for ZooMS, the membrane box protocol.

This thesis consists of six chapters. This first chapter serves to introduce the research and to provide the necessary background knowledge to understand the results and interpretation offered in this thesis.

In the second chapter, Materials, the used datasets are described. One dataset consists of possible bone or ivory tools from the Châtelperronian layers of Quinçay, France. The other dataset is comprised of Mesolithic bone points and one antler point from the North Sea. The archaeological context of the datasets will also be discussed.

The used methodology, from the sampling of the artefacts to the mass spectrometry analysis, will be extensively described in the chapter Methods.

In the fourth chapter, Results, the data obtained from the experiments is presented. The results will be grouped per dataset and used method.

In the fifth chapter, the Discussion, the results will be interpreted. The results from the different datasets and methods will be compared and the effectiveness of the membrane box method will be evaluated. Based on these comparisons an interpretation will be constructed and possible alternative interpretations will be briefly discussed as well. The limitations of the applied methods will also be addressed. Additionally improvements to the membrane box protocol will be suggested.

The thesis ends with an analysis of the general applicability of the membrane box protocol and the interpretation of the observed species distributions in the datasets.

2 Materials

Two datasets from different periods and localities are used for this research, because it allows a comparison of the results of the sampling protocols between different burial conditions. Different burial conditions may favour different sampling protocols. The first dataset consists of 22 possible bone tools, three morphologically identified bone fragments and three morphologically identified teeth from Quinçay, a Palaeolithic cave site in France. The other dataset consists of 10 osseous points found on the Dutch shores of the North Sea. These bone points are all attributed to the Mesolithic.
Three different sample preparation protocols will be applied to the 10 Mesolithic bone points as well as to the three morphologically identified bone fragments and teeth from Quinçay. The morphologically identified fragments serve as controls for the ZooMS analysis. It is suspected that out of the 22 possible bone tools from Quinçay, two may in fact be ivory. To control for the possibly different results of the preparation protocols for bone and ivory, three morphologically identified teeth were employed as a control group. Teeth can be used as a control group for ivory, because in both the collagen carrying component is dentine (section 1.5; Coutu *et al.* 2016, 419).

2.1 Quinçay

Most of the data used in this study comes from the French site Quinçay (fig. 7). The site is a limestone cave located near the city Poitiers. More detailed information regarding the stratigraphy of Quinçay can be found in appendix A.1 and more information on the Châtelperronian is in appendix A.2.

Figure 7 Location of Quinçay. The area in which Châtelperronian sites are found is shaded green (Roussel et al. 2016, 15).

The finds used in this study come from layers in the cave called Em, Ej, Sps, Sfj and Sfs, (tabs. 1 and 2). The layer of two of the 22 artefacts was not documented. These layers are associated with the Châtelperronian, a culture dated to 41-38 ka (Jöris and Street 2008, 782-789). The used Quinçay artefacts are bone tools and other remarkable osseous finds selected by M. Soressi.

Material from these layers at Quinçay has already been used for ZooMS analysis in earlier research. This research was able to identify 92.3% of its samples to family, genus or species level (Welker *et al.* 2017b, 19). This research does not employ the same dataset as Welker *et al.* 2017b, but because both datasets originate from the same layers at the same site, it can be assumed they underwent the same taphonomic processes. Therefore there is good reason to assume that the samples used for this research contain sufficient collagen as well.

Table 1: **The distribution of used artefacts and controls over the Châtelperronian layers at Quinçay**

Layer	Number of artefacts	Number of controls
Em	13	3
Ej	2	0
Sps	1	0
Sfj	1	1
Sfs	3	2
Undocumented	2	0

Table 2: Preliminary zooarchaeological and tool type interpretation of the Quincay artefacts (Soressi 2019, personal communication)

zooarchaeological determination prelim. / Tool type interpretation prelim.	Large mammal	Small mammal	Carnivore	Possibly antler	Possibly ivory	Indet.*	#
Possible awl/point						5	5
Possible point				1	1	1	3
Possible awl						1	1
Indet.*	3	2	1		1	7	13
#	3**	1***	1*	1	2	14	22

* Indet means undetermined.
** One of artefacts is thought to be either from a large mammal or a carnivore.
*** The artefact determined as small mammal is a rib fragment.

At the moment only preliminary determinations of the artefacts are available. A more detailed analysis of the artefacts is being done at the time of writing by Leiden Master-student Walter Mancini. For a detailed description of the artefacts, see appendix B. Photographs of the artefacts can be found in appendix C. The author labelled the Quinçay material with the letter Q and a sequential number. Numbers below 10 were used for the control specimens, above 10 for the possible bone tools.

2.2 Mesolithic bone points

The Mesolithic bone points used in this study were found on the shores of the Dutch province Zuid-Holland. The points were washed ashore and thus none of them were found in situ. It is thought that they were originally deposited in Doggerland, but the last parts of Doggerland became submerged around 8,0 ka (Leary 2009, 227). Now finds from Doggerland are washed up by the currents (Verhart 1988, 177). Additional information about the archaeological context of Doggerland can be found in appendix A.3.

There has been no in depth research on how being submerged in the North Sea for roughly 8000 years affects collagen preservation, but a research on 10th century bones from the Mediterranean showed no significant change in the organic matrix of collagen (Arnaud *et al.* 1978, 418).

ZooMS analysis has also been successfully applied on bone from the North Sea, dated to 60-20 ka (Buckley *et al.* 2011, 2012). Therefore there is no reason to assume a priori that North Sea artefacts will be unsuited for ZooMS.

The bone points used in this research were not found as part of any excavation or survey. They were found by private collectors, who often walk along the beaches in search of archaeological material and Pleistocene faunal remains. Some of these collectors graciously offered to loan their finds to the author as part of a larger research project investigating the selection of certain species as raw material for projectile point production.

The points analysed here were found on six beaches: the Zandmotor, Maasvlakte 1, Maasvlakte 2, ‘s Gravenzande, Hoek van Holland and Rockanje (fig. 8). The bone points are attributed to the Mesolitihic on the basis of the earlier C^{14} dating of three different points (Verhart 1986, 178). The morphological characteristics of other bone points found on the Dutch shores indicate that they are all part of the same homogenous group (Verhart 1988, 177). The points used in this research fall within that homogenous group and are therefore considered Mesolithic. Mesolithic bone points in general are divided into two main categories based on length: larger or smaller than 88.5 mm (Verhart 1986, 161; Spithoven 2015, 43). The points in this study range in length from 26 to 165 mm, where most are smaller than 88.5 mm. One of the bone points (P5) was previously identified as antler by Dick Mol.

Additional information on the Mesolithic North Sea points used in this research can be found in appendix B. Photographs of the artefacts are located in appendix C. The Mesolithic North Sea bone points were labelled by the author with the letter P followed by a sequential number.

Figure 8 Map of the beaches, where the points have been found, indicating the Zandmotor, Maasvlakte 1, Maasvlakte 2, 's Gravenzande, Hoek van Holland and Rockanje (after:

3 Methods

The various ZooMS protocols only differ in the way, in which they extract collagen from organic tissue. The methodology employed to select the samples and to analyse the collagen is the same for all protocols.

3.1 Sample Selection

All suspected Châtelperronian bone tools from Quinçay were used in this research, thus there was no further selection between the Quinçay artefacts. On the Quinçay bone tools only the membrane box protocol was used, except for Q31, which was in a plastic bag. Q31 is significantly smaller than all the other artefacts, which is probably why it was not put in a membrane box years ago. It was decided to use the plastic bag protocol for Q31, because no membrane box was available at the time.
Selection criteria had to be formulated for the Quinçay controls and the Mesolithic bone points, since the collectors had provided more points, than could be analysed.

3.1.1 Selecting the Quinçay controls

Control samples are necessary to screen for errors affecting the entire batch and also serve to expose systematically erroneous identifications, by for example human error in interpretation.
The Quinçay controls had to be similar to the possible tools for as many variables as possible. There were no Quinçay finds available with the exact same context as the possible tools, meaning same layer, same square and sub-square and same depth. Therefore we selected finds that shared the same layer, square and depth square as one of the possible tools. These are Q2, Q3 and Q4. Q6 is from the same square and layer as some possible tools, but was found 10 cm above the nearest tool. Q1 and Q7 are not from the same square or depth as some of the tools, but they were closest to a possible tool compared to the alternatives. Another criterion was that the controls had to be morphologically identifiable. Morphological identification was done by Dr. Laura Llorente Rodriguez, Andre Ramcharan and Wouter Bonhof RMSc, all affiliated to the Zooarchaeological Laboratory at Leiden University and by Dr. William Rendu (University of Bordeaux).
Due to the suspicion that the dataset contains both bone and ivory artefacts, controls for bone and for dentine were included. Unfortunately no ivory finds from Quinçay were available as control. However, Q1, a lamella of a mammoth molar, should function as a

control for mammoth dentine, because the dentine in tusk is identical to dentine in other teeth (Coutu *et al.* 2016, 419).
The Quinçay controls were analysed according to the cold acid, AmBic and membrane box protocol.

3.1.2 Selecting the Mesolithic Points

The primary reason for developing non-destructive sample preparation protocols is to prevent unnecessary damage to artefacts. Yet this research destructively samples 10 Mesolithic points twice, for the cold acid and the AmBic protocol. The reason the Mesolithic points are sampled destructively, instead of using unworked bone fragments, is twofold. First of all, in contrast with Quinçay, it is impossible to find controls from the same context. Even if a bone would be found next to a point, this does not mean that both were deposited at the same site. Due to the lack of context and presumed heterogeneity there are few variables that could be controlled for.
Secondly, the Mesolithic points used in this research were designated for ^{14}C dating at Groningen. The ^{14}C dating is part of another research project. The destructive sampling required for ZooMS is much smaller than the amount required for ^{14}C (10 mg average versus a minimum of 50 mg). By using artefacts already designated for destructive sampling, the damaging of any further artefacts is prevented.
All the Mesolithic points were analysed according to the cold acid, AmBic and membrane box protocol.

3.2 Sampling protocols

The term ZooMS does not denote a single protocol. Since its first publication in 2009-2010, various variants have been suggested. These variants differ from the original method in their sample preparation protocol. The five main variants are:

Destructive protocols:

- The cold acid protocol, the original ZooMS protocol, which uses HCl to denaturalise the collagen structure (Buckley *et al.* 2010, 15).
- The AmBic protocol, which dissolves the soluble collagen in a bone (Van Doorn *et al.* 2011, 283).

Non-destructive protocols:

- The eraser protocol, analyses eraser waste from rubbing the target material (Fiddyment *et al.* 2015, 15066).

- The membrane box protocol, analyses tiny amounts of collagen attached to the membrane, after a bone fragment is removed from the encapsulating membranes (Martisius *et al.* submitted).
- The plastic bag protocol samples residue collagen left behind in plastic bags by friction.

An overview of the differences between the reviewed ZooMS protocols is shown in Table 3. Although the eraser protocol is not tested in this thesis, it is added to table 3 for a complete overview of the characteristics of non-destructive ZooMS protocols.

The cold acid and AmBic protocol both require a destructive sample from the artefact. The sample size used in the available literature varies significantly. Most studies seem to use samples smaller than 20 mg (Van Doorn *et al.* 2011, 283; Welker *et al.* 2016, 11163). Another study states that samples should be smaller than 30 mg (Welker *et al.* 2017a, 4; Welker *et al.* 2017b, 17). In this study a sample size between 10 and 30 mg was adopted. A sample size of around 20 mg was aimed for. It was decided to adopt the 20 mg upper boundary, because there is much uncertainty regarding the preservation conditions of collagen in the North Sea. Since resampling would not be practically feasible and unnecessarily destructive the best course of action seemed to take larger initial samples. Samples were taken using either a scalpel, a set of pliers or a fretsaw (fig. 9). With the scalpel bone was scraped or sawed off from the point. The pliers were used to break off small protrusions of bone. The fretsaw was used, when the pliers could not be used. The fretsaw was considered more efficient than the scalpel in sawing through bone. All sampling was done wearing nitryl gloves.

Sampling was done in the Chemical Laboratory at the Faculty of Archaeology, Leiden University. The workspace was cleaned twice by spraying it with 95% ethanol and then wiping it with chem wipes. The equipment used to sample was cleaned once with ethanol. Sampling of material was done above a weighing paper. The sample was then transferred into an Eppendorf tube and weighed on a scale (accuracy ± 0.1 mg). Between different samples the workspace and tools were thoroughly cleaned with ethanol according to the aforementioned procedure.

Figure 9 Used pliers and fretsaw, own work.

Table 3: Overview of differences in ZooMS sampling protocols

*Fiddyment *et al.* state that they combined the solubilisation and digestion step into a single incubation in both AmBic and Trypsin at 37°C for 4 hours at a later stage in their research.

	Cold acid (van Doorn *et al*. 2011, 283)	AmBic (van Doorn *et al*. 2011, 283)	Eraser, according to Fiddyment *et al.* 2015, 15070	Membrane box (Martisius *et al*., submitted)	Plastic-bag
Destructive sampling	Yes	Yes	No	No	No
Electrostatic principle	n/a	n/a	Friction	Contact electrification (Baytekin *et al.* 2011, 308)	Friction
Demineralisation	0.5 M HCl, at 4°C, for 40 h	n/a	n/a	n/a	n/a
Solubilisation	AmBic, pH 8, 65°C for 1 h	AmBic, pH 8, 65°C for 1 h	*AmBic, pH 8, 65°C for 1 h	AmBic, pH 8, 65°C for 1 h	AmBic, pH 8, 65°C for 1 h
Digestion	1 µL trypsin at 37°C for 17:15 h	1 µL trypsin at 37°C for 17:15 h	*1 µL trypsin at 37°C for 18 h	1 µL trypsin at 37°C for 17:15 h	1 µL trypsin at 37°C for 17:15 h
Clean-up	0.1% TFA in 1:1 acetonitrile and distilled water	0.1% TFA in 1:1 acetonitrile and distilled water	0.1% TFA in 1:2 acetonitrile and distilled water	0.1% TFA in 1:1 acetonitrile and distilled water	0.1% TFA in 1:1 acetonitrile and distilled water
Peptide filtration	Thermo C18 ZipTips	Thermo C18 ZipTip	C18 Milipore	Thermo C18 ZipTip	Thermo C18 ZipTip
Protein sample re-usable?	No	Yes	No	No	No
Mass spectrometer	Bruker autoflex LRF MALDI-TOF	Bruker autoflex LRF MALDI-TOF	Bruker Ultraflex III MALDI-TOF	Bruker autoflex LRF MALDI-TOF	Bruker autoflex LRF MALDI-TOF

If pliers were used to sample, the sample was held within a beaker glass to prevent any bone from scattering and contaminating the rest of the laboratory. The beakers were used only for one sample and then cleaned with soap after which they were left to dry in air.

3.2.1 The Cold Acid Protocol

In this research 250 µL 0.5 M HCl was added to the Eppendorf tubes with the samples to free the collagen. The samples were centrifuged at 10000 RPM for 30 seconds in a Heraeus Megafuge 16 Centrifuge from the company Thermo Scientific, in order to homogenise the samples. After 40 hours of demineralisation the acid was removed from the tubes and the tubes were rinsed thrice with ammonium bicarbonate buffer (NH_4HCO_3, Sigma-Aldrich) to neutralize the pH. The rinsing procedure involved adding 200 µL ammonium bicarbonate buffer, vortexing and centrifuging the tube. The ammonium bicarbonate buffer was then pipetted out of the tube and discarded. After the third rinse the pH of the tubes was between 7 and 8. The pH was measured using Fisherbrand pH sticks. Once the final rinse had been discarded, 100 µL ammonium bicarbonate buffer was added. The buffered samples were then incubated in a heating block at 65 °C for one hour to gelatinize the soluble collagen fraction. The soluble collagen fraction was separated from the insoluble fraction by centrifugation at 10000 RPM for one minute. Subsequently 50 µL of the supernatant was transferred onto a closable plate in order to store the samples before filtering the peptides.

3.2.2 The AmBic Protocol

For the AmBic protocol collagen was extracted similarly to the cold acid protocol, only with omission of the acid demineralisation step. Samples were directly incubated in a heating block with 100 µL ammonium bicarbonate at 65 °C for one hour. After heating, the samples were centrifuged at 10000 RPM for one minute.

3.2.3 The Membrane Box Protocol

The membrane boxes used in this research were from Abemus (reference numbers 12, 13 and 115). These boxes consist of two equal halves (fig. 10). Each half is covered by a tight membrane of polyurethane. The boxes themselves are made of polystyrene. The

artefact was placed in the centre of the box. Upon closing the box, the membranes encapsulated the artefact.

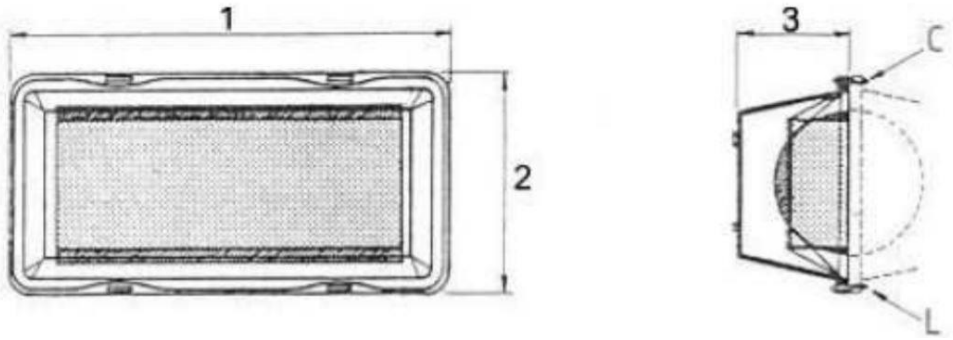

Figure 10 Schematic drawing of a membrane box, 1 is the length, 2 width and 3 depth, www.abemus.fr.

All membrane boxes except P5 were new. The membrane box of P5, however, had been used before to contain a lithic tool. The used membrane box was first cleaned by spraying the membranes with ethanol and subsequently with distilled water. The box was then left to dry for 4.5 hours before use.

Vinyl gloves were worn, when placing the artefacts into the membrane box. P5 is again an exception. It was handled with nitryl gloves. The different treatment of P5 was due to the availability of material and for no other reason.

The Mesolithic bone points and Quinçay control specimens, except P5, were in their membrane boxes for 12 days before sampling. P5 was in the membrane box for 10 days. The precise date on which the possible tools from Quinçay were placed in the membrane boxes is unknown, but it is known that this was more than 10 years ago.

In order to extract the bone from the collagen 200 µL of ammonium bicarbonate buffer was incubated at 65 °C for one hour. The heated buffer was pipetted into an Eppendorf tube. A drop of the heated buffer was placed on the surface of the membrane after the artefacts had been removed from the boxes (fig. 11). Using the pipet the drop was dragged systematically over the entire surface of the membrane box. The drop was then pipetted in the Eppendorf tube containing the heated buffer. This process was repeated for every membrane box. Afterwards the samples were incubated in a heating block again at 65 °C for one hour and centrifuged at 10000 RPM for one minute.

Figure 11 Membrane box sampling, picture from Virginie Sinet-Mathiot.

3.2.4 The Plastic Bag Protocol

The method to extract bone from a plastic bag is very similar to the membrane box protocol. 200 µL ammonium bicarbonate buffer was heated up to 65 °C for one hour and pipetted into an Eppendorf. First the ammonium bicarbonate buffer is pipetted in the plastic bag. The drops are steered over the bottom fold, because it is thought most of the residue is located there. The ammonium bicarbonate buffer is then collected from the bag using a pipet. Subsequently, the bag is cut open and the surface is sampled by moving a drop ammonium bicarbonate buffer across the surface.
Once the plastic bag sample was in an Eppendorf tube, it was incubated in a heating block at 65 °C for one hour and centrifuged at 10000 RPM for one minute. After centrifugation 50 µL of the supernatant was pipetted onto the closable storage plate.

3.3 Trypsin digestion

After all the samples had been placed on the closable plate 1 µL trypsin (produced by Promega, number #V5111) was added to the samples. Trypsin digestion was performed to cleave the collagen molecules, thereby creating the peptide fragments (Buckley and Kansa 2011, 273). The samples were left overnight at 37 °C to digest. After 17:15 hours trypsin digestion was terminated by adding 1 µL 20% TFA (trifluoroacetic acid, VWR).

3.4 Zip-tip Filtration

To remove any particulate sample impurities the peptide fragments must be filtered from the samples, before they can be analysed with mass spectrometry. Filtering is done using ZipTips (Thermo C18 Tips, #87784) (Welker *et al.* 2017b, 17). ZipTips are a form of reversed phase chromatography. Hydrophobic molecules, like proteins, bind to the ZipTips. The impurities do not bind to the ZipTip and wash away (Molnár and Horváth 1976, 1498). The attraction of the peptides to the eluent is larger than the peptides' attraction to the ZipTip, allowing their extraction (thermofisher.com).
Zip-tips were first conditioned with 0.1% TFA in 1:1 acetonitrile and distilled water and subsequently washed with 0.1% TFA in distilled water. Then the digested peptides were pipetted in the filters. They remaining sample buffer is discarded. In order to collect the peptides the 0.1% TFA in 1:1 acetonitrile is passed through the filters. This 0.1% TFA in 1:1 acetonitrile solution contained the peptide fragments and was spotted on a MALDI plate.

3.5 Spotting on the MALDI plate

Once the peptides have been extracted and isolated from the samples, they were spotted on a MALDI Bruker plate MTP384 target ground steel BC, which has a barcode and transponder (fig. 12).

One in every 9 spots on the MALDI plate was spotted with a calibrant. The used calibrant is the Bruker calibrant for 1000-3200Da #8206193 for the Leipzig laboratory. On the other spots 1 µL of the samples is spotted. Every sample is spotted three times on the MALDI plate. After spotting 1 µL of the sample on the plate, 1 µL of sample matrix was added to each spot. The sample matrix consists of α-cyano-4-hydroxycinnamic acid (CHCA; Sigma, #C2020-10G).

The plate number was 20, run number 20190201_VSM12.

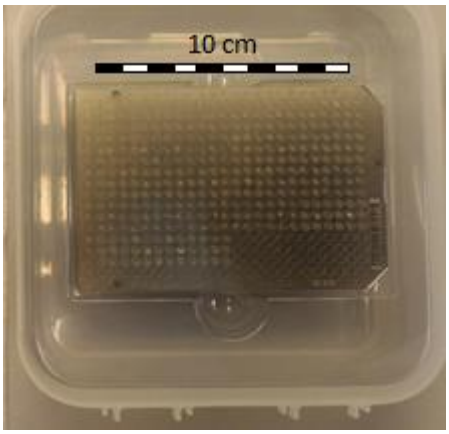

Figure 12 The MALDI plate, picture from Virginie Sinet-Mathiot.

3.6 The Mass Spectrometer

The different protocols described above only affect the preparation of the sample before it enters the mass spectrometer. The type of mass spectrometer used for ZooMS analysis is the same for all sampling protocols: the MALDI-TOF MS. The MALDI-TOF MS along with the LC-MS/MS is the most commonly used mass spectrometer for ancient proteomic research. MALDI-TOF MS stands for Matrix-Assisted Laser Desorption/Ionisation Time-Of-Flight Mass-Spectrometry (Welker 2018, 139). The MALDI-TOF MS works in the following way: at an ion source a pulsed laser heats the spots on the MALDI plate. Due to this energy influx the sample matrix evaporates. As the sample matrix molecules ablate from the MALDI plate they desorb the peptides. Without a sample matrix, the peptides would not leave the plate. The laser has also caused the peptides to become ionised (Guerrera and Kleiner 2005, 72). These peptide ions are subjected to an electric field, which causes the ions to accelerate. The velocity an ion reaches is a product of its mass. As an ion leaves the electric field it speeds through an uncharged (drift) region, before hitting a detector. The detector measures

the time of impact (Chapman 2000, 462). The mass spectrometer used in this research also contains a reflector. The ions first hit the reflector and are bounced back through the drift region to the detector (fig. 13) (Boesl 2017, 92). Time of impact allows the calculation of velocity, which enables the calculation of the ion's mass. This type of mass spectrometer is able to detect ions of all sizes (Chapman 2000, 463). In the case of ZooMS the ions are ionised collagen peptides.

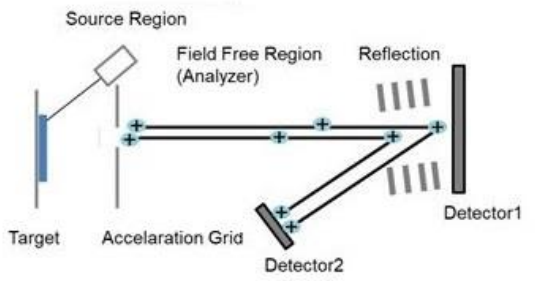

Figure 13 Schematic drawing of a reflector mass spectrometer, creative-proteomics.com.

The mass spectrometer used for this thesis was an autoflex LRF MALDI-TOF from the company Bruker (fig. 14). It was set in reflector mode. The method used is RP_700-3500_Da. The Flex control program was used and the raw data were converted into .txt files by Flex Analyses (Bruker). The mass spectrometer itself is located at Fraunhofer 121, Leipzig. The triplicate spectra are merged through a custom script in R and the combined spectrum is identified in mMass (Strohalm *et al.* 2010, 4648).

3.7 Spectrum Identification

The spectra were analysed with the aid of the open source program Mmass (Strohalm *et al.* 2010, 4648). Identification was done on basis of the biomarkers P1, A, B, C, P2, D, E, F and G. The criterion for the original markers A to G was that the markers should have at least three variants among the 14 species (Buckley *et al.* 2009, 3845). The biomarkers P1 and P2 were postulated by Kirby *et al.* using MALDI-TOF analysis (Kirby *et al.* 2013, 4852). The database used in this research defined its biomarkers on basis of the amino acid sequences derived from either genetic research or LC-MS/MS observation (Welker *et al.* 2016, appendix 5). The sample spectra were compared against a database containing Holocene and Pleistocene fauna (Welker *et al.* 2016, 11163) by the author and verified by Virginie Sinet-Mathiot, PhD-student. The identifications of P3 and P29 were verified by Dr. Frido Welker as well.

Figure 14 The autoflex LRF MALDI-TOF mass spectrometer used in this research, picture from Virginie Sinet-Mathiot.

3.7.1 Interpreting a mass spectrum

To demonstrate the process of identifying a sample based on its mass spectrum an example is given on basis of figure 15. In figure 15 the mass spectra of Q2.1 and P29.1 (Quincay control sample and a Mesolithic bone point) are displayed. Q2.1 and P29.1 were chosen, because both samples contain all the diagnostic biomarkers and because the mass spectra of Q2.1 and P29.1 differed the most from each other. On the vertical axis the intensity of the peak is noted. The higher the peak the more present the peptide is. The horizontal axis displays the m/z (mass /charge ratio). The m/z is what characterises a certain peptide fragment and determines its speed in the mass spectrometer. The biomarker peaks have been marked and labelled in the picture. It becomes immediately clear that, although all the labels are associated with a peak, this is not necessarily the highest peak in its immediate surroundings. It is common to see a series of peaks at an interval of 1 m/z. If such a series of peaks represents a biomarker, then one of the first peaks should match the m/z value of the biomarker. The series of peaks is caused by the presence of H, C, N, O and P isotopes. There are isotopes that are 1 u, or several u, heavier than the dominant isotope. These isotopes form a small portion of all the atoms of the element. Peptide fragments are large enough to contain significant amounts of heavier isotopes.

One also notices that in the above list of biomarkers only A, F and G and not A1, A2, F1, F2, G1 and G2 are mentioned, yet they are labelled as peaks in the example below. That is because A1, F1 and G1 are a hydroxylated versions of the same biomarker. The difference between the 1 and 2 biomarker is always 16 m/z, equal to an oxygen atom. The 1 and 2 are two versions of the same biomarker and if one is found, the other is expected as well (Sinet-Mathiot 2019, personal communication). P1 and P2 are an exception to this rule, because P1 is not a hydroxylated version of P2.

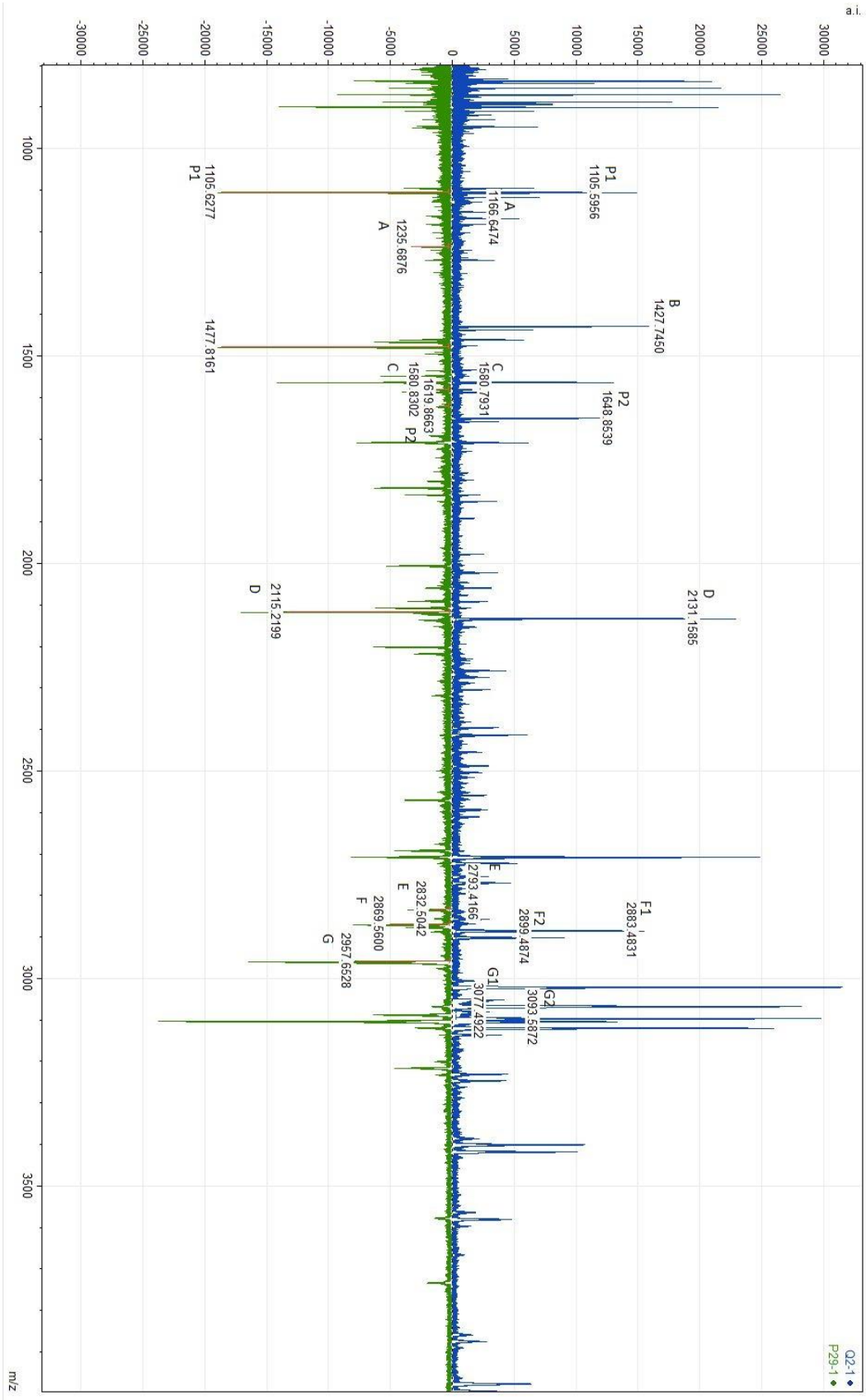

Figure 15 Labelled spectra of Q2.1 and P29.1.

4 Results

Tables 4 and 5 give an overview of the peptide markers present in the processed samples and the identification of each sample made on basis of the combinations of the values for the peptide markers. Table 4 shows the results from the Quinçay artefacts, while table 5 displays the results from the Mesolithic bone points. If a sample could not be identified, its identification is listed as ‘empty’. Empty refers to the fact that the mass spectrum of the sample is empty of any collagen peptide marker peaks, meaning no collagen has preserved.

Table 4 Quinçay Biomarkers, .1 suffix indicates cold acid protocol, .2 suffix indicates buffer protocol, .3 or no suffix means membrane box protocol. Q31 is plastic bag protocol.

ZooMS number	Layer	Square	Depth	P1	A	B	C	P2	D	E	F	G	Identification
Q1.1	Sfs	7M(4-7)	16	1105	x	1453	1579	x	2115	2808	2853+2869	3015	Elephantidae
Q1.2	Sfs	7M(4-7)	16	1105	x	1453	1579	x	2115	2808	2853	x	Elephantidae
Q1.3	Sfs	7M(4-7)	16	x	x	x	x	x	x	x	x	x	Empty
Q2.1	Em	3K(4)	19	1105	1150+1166	1427	1580	1648	2131	2792	2883+2899	3077+3093	Rangifer tarandus
Q2.2	Em	3K(4)	19	1105	1150+1166	1427	1580	1648	2131	2792	2883+2899	3093	Rangifer tarandus
Q2.3	Em	3K(4)	19	x	x	x	x	x	x	x	x	x	Empty
Q3.1	Em	(5L(8))	19	1105	1182+1198	1427	1550	x	2145	x	2883+2899	2999	Equus sp
Q3.2	Em	(5L(8))	19	1105	x	1427	1550	x	2145	x	2883+2899	x	Equus sp
Q3.3	Em	(5L(8))	19	x	x	x	x	x	x	x	x	x	Empty
Q4.1	Em	3L(7)	19	1105	1150+1166	1427	x	1648	2131	x	2883+2899	3093	Rangifer tarandus
Q4.2	Em	3L(7)	19	1105	1150+1166	1427	1580	1648	2131	2792	2883+2899	3093	Rangifer tarandus
Q4.3	Em	3L(7)	19	x	x	x	x	x	x	x	x	x	Empty
Q6.1	Sfj	8M(2)	18	1105	1150+1166	1427	1580	1648	2131	2792	2883+2899	3093	Rangifer tarandus
Q6.2	Sfj	8M(2)	18	1105	1166	1427	1580	1648	x	x	x	x	Rangifer tarandus
Q6.3	Sfj	8M(2)	18	x	x	x	x	x	x	x	x	x	Empty
Q7.1	Sf	7M(1)	12	1105	1150+1166	1427	1580	1648	2131	2792	2883+2899	3093	Rangifer tarandus
Q7.2	Sf	7M(1)	12	1105	1166	1427	x	1648	x	x	2883	x	Rangifer tarandus
Q7.3	Sf	7M(1)	12	x	x	x	x	x	x	x	x	x	Empty
Q10	Em (f)	4k (3)	18	x	x	x	x	x	x	x	x	x	Empty
Q11	Sfs	8m (9)	>20	x	x	x	x	x	x	x	x	x	Empty

ZooMS number	Layer	Square	Depth	P1	A	B	C	P2	D	E	F	G	Identification
Q12	Em sfs DIII	4L		x	x	x	x	x	x	x	x	x	Empty
Q13	Em eff. DIII	4L		x	x	x	x	x	x	x	x	x	Empty
Q14	Sfj	8N (7+4+8)	21	x	x	x	x	x	x	x	x	x	Empty
Q15	Sfs	9N	<>21	1105	x	1453	x	x	x	x	2853	x	Elephantidae + Carnivora
Q16	Ej-m (165-32-51)	3K (4)	17	x	x	x	x	x	x	x	x	x	Empty
Q17	Ej ou Em			x	x	x	x	x	x	x	x	x	Empty
Q18	Sfs	8M (5)		x	x	x	x	x	x	x	x	x	Empty
Q19		10K (1-2)	<>15	x	x	x	x	x	x	x	x	x	Empty
Q20	S DIII <S	4M		x	x	x	x	x	x	x	x	x	Empty
Q21	Em 3 (182-95-46)	3k (6)	>19	x	x	x	x	x	x	x	x	x	Empty
Q22	Em	1K(8)	>21	x	x	x	x	x	x	x	x	x	Empty
Q23	Em	5K (5)	16	x	x	x	x	x	x	x	x	x	Empty
Q24	Em	3K (6)	<19	x	x	x	x	x	x	x	x	x	Empty
Q25	Em	5K (3)	<17	x	x	x	x	x	x	x	x	x	Empty
Q26	Sfs	8M (9)	>20	x	x	x	x	x	x	x	x	x	Empty
Q27	Em	3K (6)	>19	x	x	x	x	x	x	x	x	x	Empty
Q28	Em 4	5L (5-6) (190-56-55)	>19	x	x	x	x	x	x	x	x	x	Empty
Q29	Em 8	3L (4) (186-0-33)	>19	x	x	x	x	x	x	x	x	x	Empty
Q30	Em	3J (3)	>19	x	x	x	x	x	x	x	x	x	Empty
Q31	Em	3K (6)	>20	x	x	x	x	x	x	x	x	x	Empty

Table 5 Mesolithic Biomarkers, .1 suffix indicates cold acid protocol, .2 suffix indicates buffer protocol, .3 or no suffix means membrane box protocol.											
ZooMS number	Site	P1	A	B	C	P2	D	E	F	G	Identification
P1.1	ZM	1105	1180+1196	1427	1550	1648	2131	2792	2883+2899	3017+3033	Cervid + saiga
P1.2	ZM	1105	1196	1427	1550	1648	2131	2792	2883+2899	3017	Cervid + saiga
P1.3	ZM	x	x	x	x	x	x	x	x	x	Empty
P3.1	ZM	1105	1235	1477	1580	1619	2115	2832	2869	2957	Human
P3.2	ZM	1105	1235	1477	x	1619	2115	2832	2869	2957	Human
P3.3	ZM	x	x	x	x	x	x	x	x	x	Empty
P5.1	MV2	1105	1180+1196	1427	1550	1648	2131	2792	2883+2899	3017+3033	Cervid + saiga
P5.2	MV2	1105	1180+1196	1427	1550	1648	2131	2792	2883	3017+3033	Cervid + saiga
P5.3	MV2	x	x	x	x	x	x	x	x	x	Empty
P6.1	MV2	1105	1180+1196	1427	1550	1648	2131	2792	2883+2899	3017+3033	Cervid + saiga
P6.2	MV2	1105	1180+1196	1427	1550	1648	2131	2792	2883+2899	3017+3033	Cervid + saiga
P6.3	MV2	1105	1180+1196	1427	1550	1648	2131	2792	2883+2899	3017+3033	Cervid + saiga
P7.1	ZM	1105	1180+1196	1427	1550	1648	2131	x	2883+2899	3017+3033	Cervid + saiga
P7.2	ZM	1105	1180+1196	1427	1550	1648	2131	2792	2883+2899	3017+3033	Cervid + saiga
P7.3	ZM	1105	x	1427	x	x	x	x	2883+2899	x	Castor + Equus + Cervid + Caprinae
P28.1	HvH	1105	1180+1196	1427	1550	1648	2131	2792	2883+2899	3017+3033	Cervid + saiga
P28.2	HvH	1105	1180+1196	1427	1550	1648	2131	2792	2883+2899	3017+3033	Cervid + saiga
P28.3	HvH	x	x	x	x	x	x	x	x	x	Empty
P29.1	MV1	1105	1235	1477	1580	1619	2115	2832	2869	2957	Human
P29.2	MV1	1105	1235	1477	1580	1619	2115	2832	2869	2957	Human
P29.3	MV1	x	x	x	x	x	x	x	x	x	Empty
P30.1	Ro	1105	x	x	x	x	x	x	x	x	Empty

ZooMS number	Site	P1	A	B	C	P2	D	E	F	G	Identification
P30.2	Ro	x	x	x	x	x	x	x	x	x	Empty
P30.3	Ro	x	x	x	x	x	x	x	x	x	Empty
P31.1	MV2	1105	1180+1196	1427	1550	1648	2131	2792	2883+2899	3017+3033	Cervid + saiga
P31.2	MV2	1105	1180+1196	1427	1550	1648	2131	2792	2883+2899	3017+3033	Cervid + saiga
P31.3	MV2	x	x	x	x	x	x	x	x	x	Empty
P41.1	MV2	1105	1180+1196	1427	1550	1648	2131	2792	2883+2899	3017+3033	Cervid + saiga
P41.2	MV2	1105	1180+1196	1427	1550	1648	2131	2792	2883	3017+3033	Cervid + saiga
P41.3	MV2	x	x	x	x	x	x	x	x	x	Empty

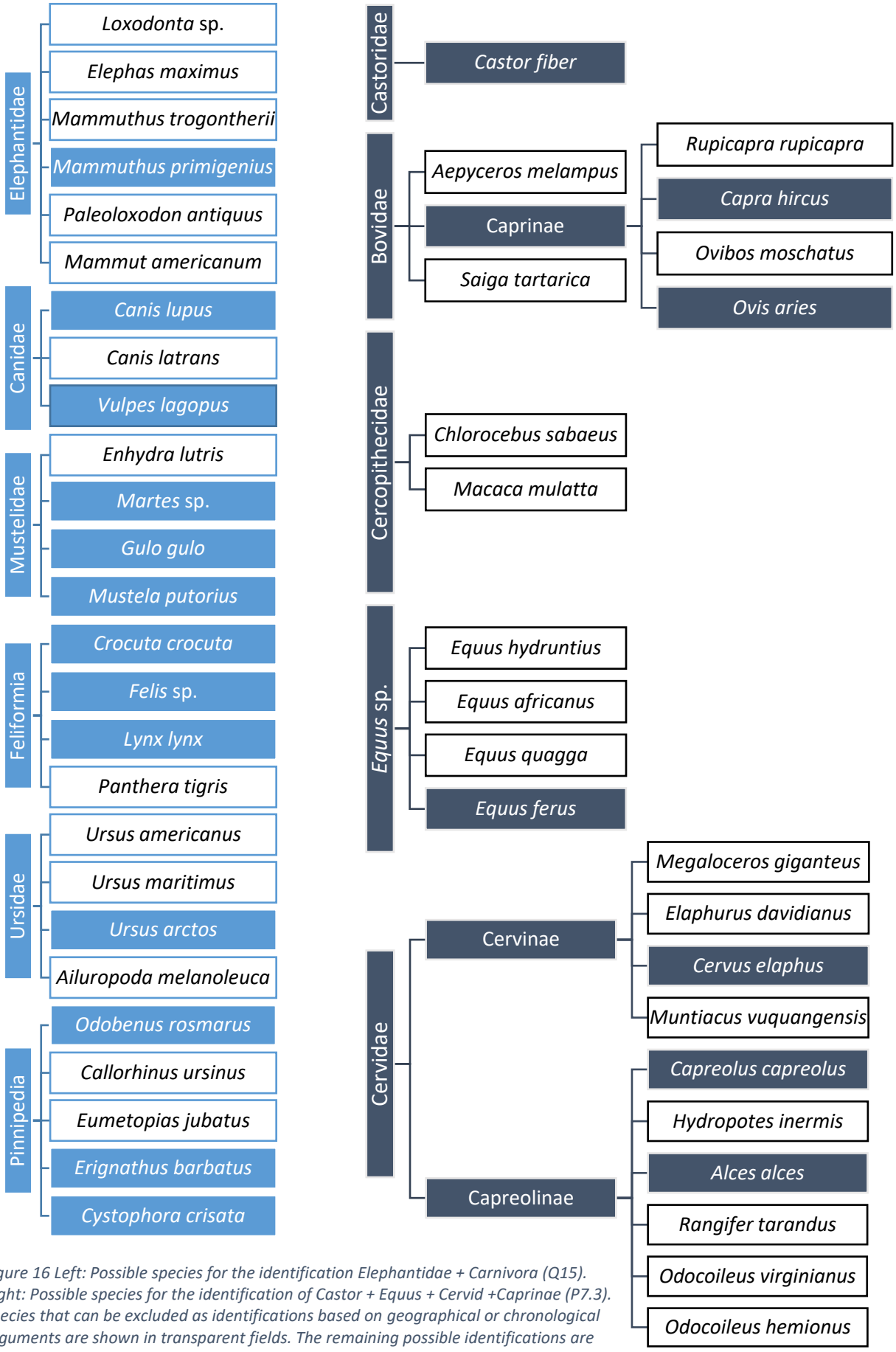

Figure 16 Left: Possible species for the identification Elephantidae + Carnivora (Q15). Right: Possible species for the identification of Castor + Equus + Cervid +Caprinae (P7.3). Species that can be excluded as identifications based on geographical or chronological arguments are shown in transparent fields. The remaining possible identifications are presented in opaque fields.

4.1 Taxonomic Identifications by ZooMS

The identifications of Q7.2, Q15 and P7.3 are based on respectively four, three and three peptide markers. Identifications based on fewer peptide markers are as accurate as identifications based on all nine peptide markers. Depending on the circumstances they can be as precise or less precise in their identification.

Q15 is an example of the reduced precision, due to fewer present peptide markers, as can be seen in table 4. Q15 was the one Quinçay artefact, for which the membrane box provided collagen for an identification. The specific species matching with the Elephantidae + Carnivora identification are listed in figure 16.

For Q15 the ZooMS identification cannot be more specific than the clade Pinnipedia and the families Felidae, Elephantidae, Mustelidae and Ursidae. However the morphological analysis and archaeological context of the artefacts might be able to narrow down the possibilities. The two main reasons to exclude a species as a possible identification is that its geographical range does not encompass the find location or that the species is not contemporaneous with the dating of the site. The species that can be excluded based on their geographical range are listed in table 6. Species that were not locally present at the time of deposition are listed in table 7.

Table 6: Species excluded as possible Elephantidae + Carnivora identifications based on geographical range

Elephantidae	Canidae	Mustelidae	Feliformia	Ursidae	Pinnipedia
Loxodonta sp. (Blanc 2008, 4)	*Canis latrans* (Kays 2018, 1)	*Enhydra lutris* (Doroff and Burdin 2015, 2)	*Panthera tigris* (Goodrich *et al.* 2015, 3)	*Ursus maritimus* (Wiig *et al.* 2015, 2)	*Callorhinus ursinus* (Gelatt *et al.* 2015, 2)
Elephas maximus (Choudhury *et al.* 2008, 2)				*Ursus americanus* (Garshelis *et al.* 2016, 2)	*Eumetopia jubatus* (Gelatt and Sweeney 2016, 2)
Mammut americanum (britannica.com)				*Ailuropoda melanoleuca* (Swaisgood *et al.* 2017, 1)	

Table 7: Possible Elephantidae + Carnivora identifications that were not present during the Châtelperronian					
Elephantidae	Canidae	Mustelidae	Feliformia	Ursidae	Pinnipeida
Mamuthus trogontherii (Wei *et al.* 2010, 961)					
Paleoloxodon antiquus (Stuart 2005, 173)					

The remaining possible identification are listed in table 8.

Table 8: Remaining possible identifications of Elephantidae + Carnivora *Both of the Pinnipedia have been sighted as far south as Spain in modern times. Although there are no known occurrences of the two species at Châtelperronian sites, this may be due to lack of exploitation by Neanderthals. Therefore they cannot be excluded as possibility. **There is one documented find of *Odobenus rosmarus* in Rozel, France, dated to 115-113 ka (Van Vliet-Lanoë *et al.* 2006, 256). ***Although the spectrum of *Ursus spelaeus* is unknown, it is included in the identification of Ursidae.					
Elephantidae	Canidae	Mustelidae	Feliformia	Ursidae	Pinnipedia
Mammuthus primigenius (Villaluenga *et al.* 2012, 506)	*Canis lupus* (Villaluenga *et al.* 2012, 506)	*Martes* sp. (Villaluenga *et al.* 2012, 512)	*Crocuta crocuta* (Villaluenga *et al.* 2012, 506)	*Ursus arctos* (Villaluenga *et al.* 2012, 512)	*Erignathus barbatus** (Kovacs 2016, 3)
	Vulpes lagopus (Welker *et al.* 2015a, 282)	*Gulo gulo* (Stewart *et al.* 2003, 225)	*Felis* sp. (Stewart *et al.* 2003, 225)	*Ursus spelaeus**** (Villaluenga *et al.* 2012, 506)	*Cystophora crisata** (Bellido *et al.* 2007, 1)*
		Mustela putorius (Stewart *et al.* 2003, 225)	*Lynx Lynx* (Stewart *et al.* 2003, 225)		*Odobenus** *rosmarus*

Out of the 10 tested Mesolithic bone points 7 were identified as Cervid + saiga. Is identification is comprised of the species:

Alces alces	*Megaloceros giganteus*	*Aepyceros melampus*
Elaphurus davidianus	*Cervus elaphus*	*Saiga tatarica*

For European Pleistocene samples this is commonly noted as Cervid + saiga, since the impala (*Aepyceros melampus*) does not occur in Europe (Lorenzen *et al.* 2006, 128). Pere Davids deer (*Elaphurus* davidianus) likewise does not live in Europe (Meijaard and Groves 2004, 187). *Saiga*

tartarica was extinct in Europe in the Mesolithic and can thus be excluded (Nadachowski *et al.* 2016, 360). The date of the extinction of *Megaloceros giganteus* is controversial. A recent comprehensive study of ^{14}C dates of *Megaloceros giganteus* specimens suggests that by the Holocene *Megaloceros giganteus* had gone extinct in Europe (Lister and Stuart 2019, 3).
Therefore in this case the Cervid + saiga identification denotes *Alces alces* and *Cervus elaphus*.
The Castor + Equus + Cervid + Caprinae identification of P7.3 is again very broad and refers to the species listed in figure 16.

The possible identifications as presented in figure 16 can be further specified as well. Table 9 shows what species are excluded due to geographical reasons. Table 10 contains the species not present in Doggerland in the Mesolithic and Table 11 reveals the possible identifications.

Table 9: Species excluded as possible Castor + Equus + Cervid + Caprinae identifications based on geographical range

Castoridae	Bovidae	Cercopithecidae	*Equus* sp.	Cervidae
	Aepyceros melampus (Lorenzen *et al.* 2006, 128)	*Chlorocebus sabaeus* (Dolotovskaya *et al.* 2017, 472)	*Equus africanus* (Schulz and Kaiser 2013, 115)	*Elaphurus davidianus* (Meijaard and Groves 2004, 187)
	Rupicapra rupicapra (Masini and Lovari 1988, 346)		*Equus quagga* (Schulz and Kaiser 2013, 115)	*Muntiacus vuquangensis* (Turvey *et al.* 2016, 2252)
				Hydropotes inermis (Lister 1984, 211)
				Odocoileus virginianus (Gilbert *et al.* 2006, 114)
				Odocoileus hemionus (Gilbert *et al.* 2006, 114)

Table 10: Possible Castor + Equus + Cervid + Caprinae identifications not present during the Mesolithic in Doggerland				
Castoridae	Bovidae	Cercopithecidae	*Equus* sp.	Cervidae
	Saiga tartarica (Nadachowski *et al.* 2016, 360)	*Macaca mulatta* (Elton and O'Regan 2014, 125-126)	*Equus hydruntinus* (Crees and Turvey 2014, 24)	*Megaloceros giganteus* (Lister and Stuart 2019, 3)
				Rangifer tarandus (Sommer *et al.* 2014, 300)

Table 11: Remaining possible identifications of *Castor* + *Equus* + Cervid + Caprinae				
Castoridae	Bovidae	Cercopithecidae	*Equus* sp.	Cervidae
Castor fiber (Vervoort-Kerkhoff and van Kolfschoten 1988, 96)	*Capra hircus* (Vervoort-Kerkhoff and van Kolfschoten 1988, 96)		*Equus ferus* (Vervoort-Kerkhoff and van Kolfschoten 1988, 96)	*Cervus elaphus* (Vervoort-Kerkhoff and van Kolfschoten 1988, 96)
	Ovis aries (Vervoort-Kerkhoff and van Kolfschoten 1988, 96)			*Capreolus capreolus* (Vervoort-Kerkhoff and van Kolfschoten 1988, 96)
				Alces alces (Vervoort-Kerkhoff and van Kolfschoten 1988, 96)

The cold acid and AmBic protocol gave two kinds of identification for the Mesolithic North Sea bone points: Cervid + saiga or human (fig. 17; tab. 5). The presence of human was very much unexpected. Human bone artefacts are rare and the two human points (P3 and P29, fig. 18 and appendix C) are not dissimilar from the other bone points in morphology and typology.

The identifications made with the membrane box method did not show any humans. The spectra obtained for P7 with the cold acid and AmBic protocol indicated a Cervid + saiga identification, while the spectrum obtained with the membrane box protocol identified P7 as Castor + Equus + Cervid + Caprinae (tab. 5). Based on the identification made with the cold acid (P7.1) and the AmBic (P7.2) protocols (tab. 5) it seems clear that P7 was either from a *Alces alces* or *Cervus elaphus*. One of the three times the membrane box protocol yielded sufficient collagen, the identification could be made to genus/species level.

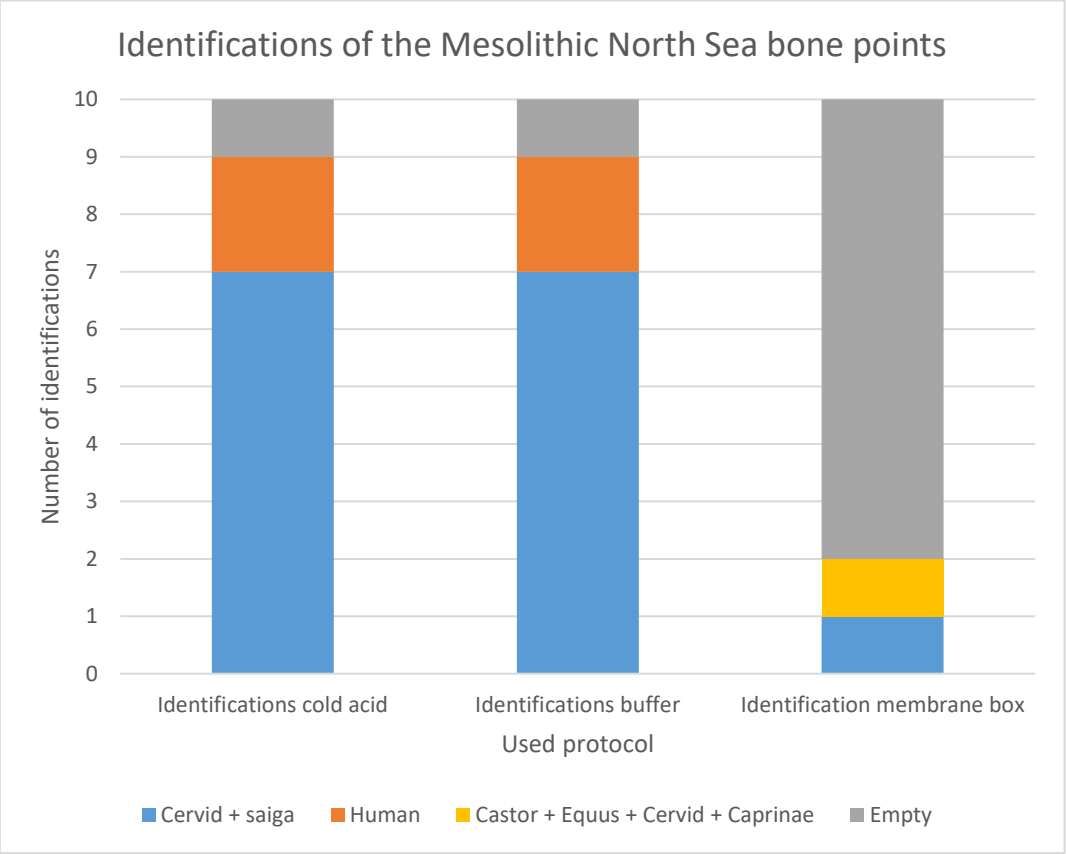

Figure 17 ZooMS identifications of the Mesolithic North Sea bone points, sorted by used protocol.

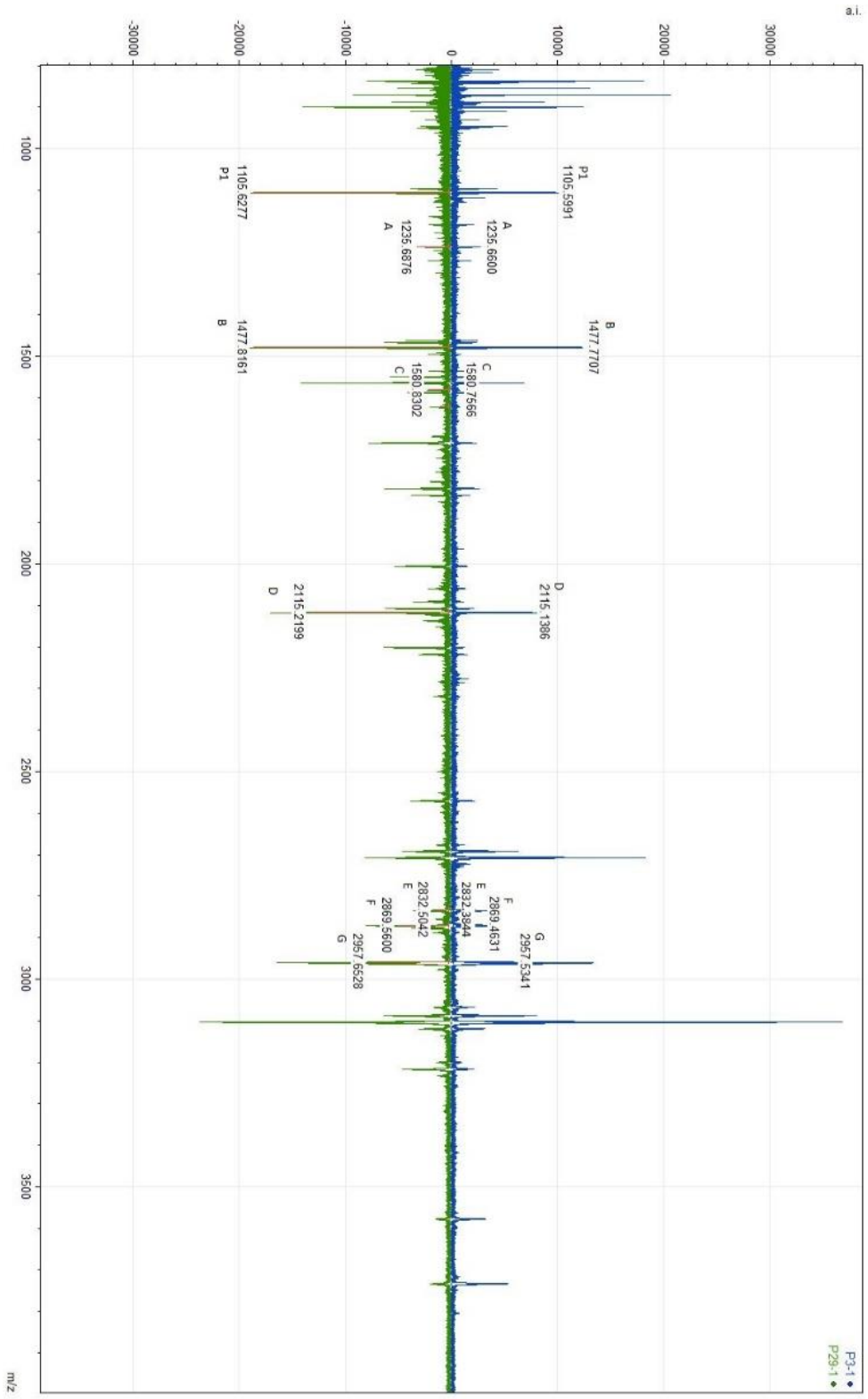

Figure 18 Mass spectra of P3 and P29, the human bone points.

4.2 Success rates of the ZooMS sampling protocols

The identification rate of the cold acid protocol has been displayed in table 12. Table 13 shows the success rate of the AmBic protocol and table 14 contains the success rate of the membrane box protocol.

Table 12: Cold acid identification success rate	**Identified**	**Empty**	**Total**	**Success rate**
Quinçay cold acid	6	0	6	100%
North Sea bone point cold acid	9	1	10	90%
Total	15	1	16	93.8%

Table 13: AmBic *identification success rate*	**Identified**	**Empty**	**Total**	**Success rate**
Quinçay buffer	6	0	6	100%
North Sea bone point buffer	9	1	10	90%
Total	15	1	16	93.8%

Table 14: *Membrane box identification success rate*	**Identified**	**Empty**	**Total**	**Success rate**
Quinçay membrane boxes	1	26	27	3.8%
North Sea bone point membrane boxes	2	8	10	20%
Total	3	17	41	7.3%

Tables 12 and 13 show that there is a difference in the success rate of both the cold acid and AmBic protocol between the Quinçay material and the North Sea bone points. However, applying Fisher's test (Fisher 1922, 93) to the success rate of the cold acid protocol shows that there is no significant difference (p=1.00) between the success rate of the Quinçay and North Sea material. Since the success rates for the cold acid and AmBic protocol are the same, there is also no statistical difference between the Quinçay and material for the AmBic protocol.

The difference between the success rate of the Quinçay membrane boxes and the North Sea bone point membrane boxes seems substantial (20% vs 3.8%). Executing Fisher's statistical test (Fisher 1922, 93) on this 2x2 contingency table gives a p value of 0.17, indicating that there is no statistical difference between the success rate of the membrane box protocol for the Quinçay and North Sea material.

The plastic bag protocol is not included in the table, because it was applied to only one artefact Q31. In the one case that the plastic bag protocol was applied, it did not yield an identification.

North Sea bone point P30 could not be identified with any of the three protocols. Most likely P30 does not contain sufficient collagen for ZooMS analysis.

The identifications made by both the cold acid protocol and AmBic protocol for the Quinçay control match completely. Differences between the morphological analyses and the ZooMS identifications were observed, but the results of the different morphological analyses vary significantly (tab. 15). At first sight only two of the seven controls have a matching morphological and ZooMS identification. All mismatches between the first morphological analysis and the ZooMS analysis were identified as *Rangifer tarandus* by ZooMS.

The second morphological analysis was done with the knowledge of what the ZooMS identification was, but in the case of Q2 and Q6 it was deemed very unlikely that the fragments were *Rangifer tarandus* (Llorente Rodriguez and Ramcharan 2019, personal communication).

The reason the third morphological analysis did match with the ZooMS identification, is that there is quite large temporal variation in the morphology of *Rangifer tarandus*. *Rangifer tarandus* found at Châtelperronian sites are larger and differ in some morphological traits compared to modern specimens (Rendu 2019, personal communication). This temporal variation explains, why morphological analysis based on a Holocene reference collection differs from a morphological analysis performed by a zooarchaeologist, who has worked extensively on Châtelperronian material.

Table 15: Morphological analyses of the Quinçay control samples.

The 1st and 2nd morphological identifications were performed at Leiden University, while the 3rd identification was provide by Dr. William Rendu.

ZooMS number	1st morphological identification	2nd morphological identification	3rd morphological identification	ZooMS identification
Q1	*Mammuthus primigenius*	N/A	N/A	Elephantidae
Q2	*Cervus* sp.	*Cervus* sp.	*Rangifer tarandus*	*Rangifer tarandus*
Q3	*Equus caballus*	N/A	N/A	*Equus* sp.
Q4	*Sus* sp.	*Rangifer tarandus*	*Rangifer tarandus*	*Rangifer tarandus*
Q6	*Bos* sp.	*Bos* sp.	*Rangifer tarandus*	*Rangifer tarandus*
Q7	*Bos taurus*	*Rangifer tarandus*	*Rangifer tarandus*	*Rangifer tarandus*

5 Discussion

The results of this research shed new light onto electrostatic sampling, but before the results can be discussed in detail the limitations of ZooMS as an identification tool must be considered. These considerations help to put the identifications provided by this research into the right perspective. After reviewing the identifications, the Quinçay and North Sea datasets will be compared in order to determine any biases that may have influenced the success rates of the different methods. In turn, the success rates of the four applied protocols will be discussed and the various factors influencing the success rates of the electrostatic sampling protocols will be addressed. Based on these considerations a revised membrane box protocol is proposed.

5.1 Limitations of ZooMS

The choice of mass spectrometer determines the way in which the mass of a molecule is measured, which influences the possibilities for analysis later on. When selecting a type of mass spectrometer for research the advantages and disadvantages of the type of mass spectrometer must be taken into account. All ZooMS research uses the MALDI-TOF MS to analyse the composition of the collagen molecule. However, the MALDI-TOF MS is not the only type of mass spectrometer that can be used for proteomic analysis. The other commonly used category of mass spectrometers is the LC-MS/MS (Liquid Chromatography-tandem – Mass Spectrometry).

5.1.1 Advantages and disadvantages of LC-MS/MS relative to MALDI-TOF MS analysis

Although the use of a LC-MS/MS is more expensive and time consuming than MALDI-TOF MS (Buckley *et al.* 2008, 325), the LC-MS/MS has the advantage that it shows the amino acid sequence of the detected peptides (Welker 2018, 138). Hence the LC-MS/MS has been used to search for new peptide markers to improve the resolution of species identification (Buckley *et al.* 2011, 2007; Welker *et al.* 2017a, 11).

It has also been observed, that some of the peptide markers are not always detected by the MALDI-TOF MS, because the peptide markers are present in a too low intensity. The low intensity results in a low peak indiscernible from the noise. The LC-MS/MS shows the amino acid sequence of the peptide fragment and thus peptide markers can be correctly identified even if they are only present in low intensity. The amino acid identifications made during LC-MS/MS analysis are probability based. Using the mass of a peptide fragment an algorithm reports the chance that the peptide fragment has the identified amino acid sequence. However, especially in the case where there are multiple peptide markers with the same mass, there is a risk of false positives. In those cases, a peptide fragment is identified as a peptide marker for one species, while for example it is in fact a deamidated peptide

marker of another species (Buckley 2016, 11). The fact that the LC-MS/MS does detect all peptide markers does provide LC-MS/MS analysis with more precision compared to MALDI-TOF analysis. For example the LC-MS/MS is able to distinguish between the members of the family Rhinocerotidae (rhinoceroses), while the MALDI-TOF MS is unable to do so (Welker *et al.* 2017a, 11).

The lack of the preciseness of the ZooMS identifications is a serious drawback. For example, the Cervid + saiga identification covers the subfamily Cervini, two bovids and another cervid and that is the most specific identification ZooMS is able to give. Although it is often possible to reduce the list of possible species based on the archaeological context (tabs. 6, 7, 8, 9, 10 and 11), it is not uncommon to end with several species as possible identification.

5.1.2 Selecting sample size

In section 3.2 it was already mentioned that there are large differences in the reported sample sizes for the destructive ZooMS protocols. Studies were found reporting 1 mg (Charlton *et al.* 2016, 56), 5 mg (Van Doorn *et al.* 2011, 283), 10 mg (Bradfield *et al.* 2018, 7) and 10-30 mg (Welker *et al.* 2017a, 4; Welker *et al.* 2017b, 14). When destructively sampling artefacts for ZooMS this large variation in reported sample size presents a conundrum for a researcher. If the sample is too small, the analysis will fail and an artefact will have been needlessly damaged. A too large sample is also unnecessarily damaging.

The large variation in sample size can be explained due to differences in collagen preservation. If collagen is well preserved as little as 2 mg is needed, where badly preserved collagen requires larger samples. Sample size is therefore decided on case-by-case basis (Welker and Sinet-Mathiot 2019, personal communication). If there is no data available about the collagen preservation prior to the ZooMS analysis 10 mg should be maintained as an average sample size. In this research 10 mg had been maintained as the lower boundary of the sample size, due to uncertainty regarding the collagen preservation of the Mesolithic North Sea points. The good quality of collagen extracted from the Mesolithic North Sea points in this research indicates that smaller samples will most likely also provide sufficient collagen for ZooMS analysis.

5.2 Quinçay possible bone tool identifications

Unfortunately, only one of the possible bone tools from Quinçay could be identified on basis of its mass spectrum (table 4). This bone specimen (Q15) (fig. 19) was one of the two artefacts that was suspected to be ivory (Appendix B). Although ZooMS cannot exclude that Q15 is from certain carnivores (tab. 8), morphological examination can help to narrow down the possible identifications. The morphology of Q15 was examined by André Ramcharan from the Zooarchaeology Laboratory at Leiden University and he identified the artefact as ivory. However, the texture of the artefact is dissimilar to *Mammuthus primigenius* ivory (Soressi 2019, personal communication). The alternative would be *Odobenus rosmarus.* There are few examples of *Odobenus rosmarus* at Neanderthal sites (Van Vliet-Lanoë *et al.* 2006, 256), but their geographic distribution during the Pleistocene is not well known. The large increase in sea level during the Holocene and drowning of Pleistocene coastal sites is likely one of the causes of the lack of knowledge on *Odobenus rosmarus* distribution.

Figure 19 Q15, photo by Walter Mancini.

5.3 North Sea bone point identifications

All the North Sea bone points, except one, could be identified using ZooMS (tab. 5). The quality of the collagen allowed an identification to the most specific level possible with ZooMS. Based on the archaeological context this was specified even further. In the end, only two or three species were used to create the bone points analysed in this research: *Alces alces* or *Cervus elaphus* and *Homo sapiens* (fig. 17).

From the start *Cervus elaphus* and *Alces alces* were considered as possible species of which the points could have been made, along with *Bos primigenius*, *Equus caballus* and *Capreolus capreolus* (Verhart 1988, 171). It was thought that the bones of these animals would be most suited for point production, as long and straight bones were required (Verhart 1988, 171). The majority of morphologically identified North Sea bone points from Europe are also made of *Cervus elaphus* bone (Dickson 2001, 436). Important to note is that ZooMS cannot differentiate between collagen

containing materials. Of the seven *Cervus elaphus* or *Alces alces* identifications one (P5) was identified as antler by Dick Mol. The ZooMS analysis neither confirms nor rejects this.

Two similar studies using ZooMS on bone points from Taforalt, Morocco, dated to 15077-13892 cal. BP (Desmond *et al.* 2018, 151) and from 9 South African sites dated to 300-1700 AD were published recently (Bradfield *et al.* 2018, 11). They show a selection for the use of *Gazella* sp. and bovids respectively (Desmond *et al.* 2018, 154; Bradfield *et al.* 2018, 11). Both studies admit that they are not able to fully explain the rational behind a selection for *Gazella* sp. and bovids. In the case of Taforalt, Desmond *et al.* suggest that there is a connection between the shape of the tool and the used species (Desmond *et al.* 2018, 154-155). In South Africa the selection of species for point production can be partially explained by selection on functionality (Bradfield *et al.* 2019, 2430). Bradfield *et al.* and Desmond *et al.* do both suggest that there might be a symbolic component to the observed species selection (Bradfield *et al.* 2019, 2430; Desmond *et al.* 155).

In contrast to the use of cervid bone, the use of human bone was not expected. Since modern contamination by the analysts is a known risk for proteomic and DNA analyses it must be made certain that the identification is of actual ancient human. In this case it seems extremely unlikely that the two points identified as human are contamination. First of all, the spectra were unambiguous (fig. 18, appendix D). If a sample had been contaminated by modern human collagen one would expect to see both the human biomarkers as well as the biomarkers of another species. Secondly, both the cold acid and ammonium bicarbonate protocol samples indicated a human identification. The samples taken from the bone points for these protocols were small pieces that were removed from the butt of the point and thus contain both the inner and outer layers of the point. Because collagen from the inside of the point was analysed contamination of the outer surface of the point can be excluded as cause of the human identification. Possible contamination would also have had to occur before spotting on the MALDI plate, because all samples were spotted in triplicate on the MALDI plate. The only other option to explain the spectra of these two points, apart from a human origin, is if insufficient collagen was preserved in the points themselves and if these four samples had been contaminated in the laboratory. This scenario is more unlikely than a human identification of the points, because it is less parsimonious and because the order of magnitude of the intensity, in which the peptide markers are present, is similar for all identified Mesolithic North Sea points. If modern contamination had been present, it would have had a higher intensity than the archaeological samples.

The working of human bone is not unknown in prehistory, although it is rare. The oldest example of hominin worked as a tool is a Neanderthal skull fragment from La Quina dated to MIS 4 (Verna and d'Errico 2001, 147-154). Other examples are skull-cups from Gough's Cave in England dated to 14700 cal. BP (Bello *et al.* 2011, 2), a burin probably used to work hide from Perdigões, Portugal, dated around 4500-4200 cal. BP (Cunha *et al.* 2016, 1107-1110) and a chisel made from a human femur dated to 3500-3700 BP found at Gohar Tepe, Iran (Soltysiak and Gręzak 2015, 362-363). At Gough's Cave the skull-cups were accompanied by indicators that cannibalism was practiced at the site (Bello *et al.* 2011, 10) and at Perdigões there are instances in which human and animal bone seem to be treated the same (Cunha *et al.* 2016, 1110). At Gohar Tepe and La Quina there are no clear indicators of systematic extraordinary treatment of hominin remains (Soltysiak and Gręzak 2015, 364; Verna and d'Errico 2001, 155). In both articles the authors admit that it is not possible to determine, if the selection of hominin bone for tool production carried any intentional meaning, or whether the producer might not have been aware of the hominin origin of the bone.
At the moment there are no published examples of projectile points made from human bone. Due to the lack of information on the archaeological context of the North Sea points little can be said at the moment. It is very interesting that apart from *Cervus elaphus* or *Alces alces* the only species identified by this research is *Homo sapiens*, but caution must be exercised in constructing an interpretation based on two datapoints.

5.3.1 Selection on availability?

A possible explanation for a selection for *Cervus elaphus* or *Alces alces* for the production of bone points is that these species were the most available. In that case a selection for *Cervus elaphus* and *Alces alces* combined would be expected at Mesolithic sites. Since none of the points was found in the context of a site, sites from Britain and the Netherlands are used to test this hypothesis (fig. 20). The most commonly found species at Mesolithic sites in North-western Europe are *Bos primigenius, Cervus elaphus, Capreolus capreolus* and *Sus* scrofa (Overton and Elliot 2018, 336). At three out of seven English sites the majority of the number of identified specimens (NISP) was *Cervus elaphus*. At two others the dominant species was *Bos primigenius* and another two sites the majority of the NISP was *Sus scrofa* (Overton and Elliot 2018, 336). At Zutphen-Ooijerhoek, the Netherlands, no single species forms a majority of the NISP. *Sus scrofa* is the largest minority with 40%, while *Cervus elaphus* and *capreolus capreolus* follow at 35% and 25% respectively (Overton and Elliott 2018, 336).
The percentage of *Sus scrofa* versus *Cervus elaphus* and *Bos primigenius* seems to be larger in South English sites compared to North England (Overton and Elliot 2018, 341). Interestingly bone and antler points have been found in North England, but not South England (Overton and Elliot 2018, 341-342).

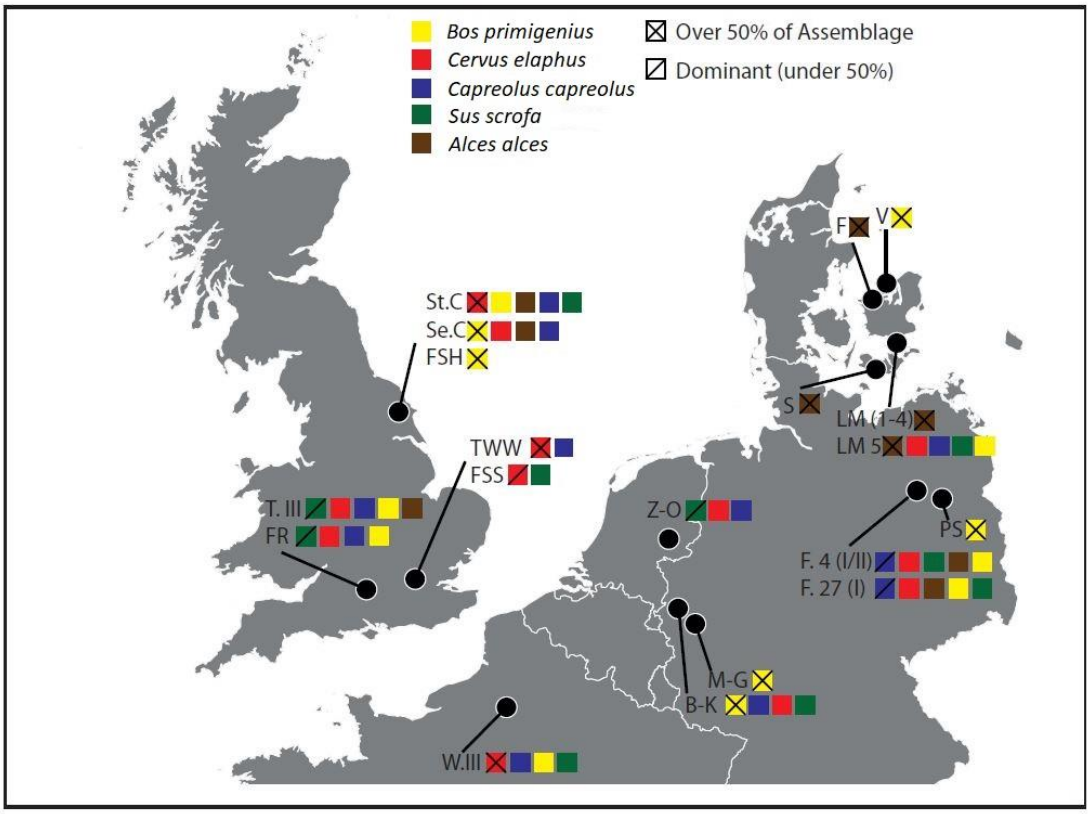

Figure 20 Overview of the dominant species at Mesolithic sites, after Overton and Elliot 2018, 339. Acronyms of the sites: St.C: Star Carr, Se.C: Seamer Carr, FSH: Flixton School House Farm, TWW: Three Ways Wharf, FSS: Former Sanderson Site, T.III: Thatcham III, FR: Faraday Road, W.III: Warluis IIIb, Z-O: Zutphen-Ooijerhoek site M, B-K: Bedburg-Königshoven, M-G: Mönchengladback-Geneicken, F.4 (I/II): Friesack 4 (complex I and II), F.27 (I): Friesack 27, PS: Postdam Schlaatzm, LM1-5: Lundby Mose 1-5, S: Skottemarke, F: Favrbo, V: Vig.

Although at none of the reviewed sites fish remains formed a significant component of the NISP, stable isotope studies on Mesolithic North Sea human remains indicate that a significant portion of their diet consisted of freshwater animals (Van der Plicht *et al.* 2016, 115). It must therefore be taken into consideration that the terrestrial fauna found, represent only a portion of the Mesolithic diet. The overview of faunal remains at Mesolithic sites shows that *Cervus elaphus* was exploited in large numbers. There does not seem to be a general dominance of *Cervus elaphus* in Mesolithic North-western European sites, but most of the *Cervus elaphus* dominant sites are close to former Doggerland. Combined with the fact that sites from Doggerland itself are lacking, the identification of a majority of the bone points as *Cervus elaphus* should not be surprising. What is surprising is the complete absence of *Bos primigenius, Capreolus capreolus* and *Sus scrofa* among the bone points. Should the raw material of bone points have been selected purely on availability, then bone points of *Bos primigenius, Capreolus capreolus* and *Sus scrofa* are expected as well.

The use of human bone for projectile points cannot be explained from an availability point of view. For human bone to be the most available bone either the diet of the Mesolithic people of Doggerland would have to consist for a large portion of human or the degree of interpersonal violence should

have been extremely high. Both the faunal assemblages as the stable isotope data do not support extensive cannibalism and the latter scenario is extremely unlikely.

5.3.2 Selection on durability?

Rather than just using the most available bones, it could be that the apparent selection for *Cervus elaphus* or *Alces alces* bone is, because their bone is biomechanically more suited for a projectile point than other available material. It has been argued that there is a trade-off between the stiffness and toughness of bone (Currey 2004, 576). Stiff bones are suited for enduring longer periods of relatively lower stress, while tough bones are able to resist short periods of high stress (e.g. high velocity impacts) (Currey 2004, 578). The place of a skeletal element on the stiff-tough spectrum is adapted to the needs of the species (Currey 2004, 570). When skeletal elements are used as projectile points the stiff-tough spectrum is linked to a penetration power-durability trade-off (Margaris 2006, 193).

Of the materials used for the North Sea points, antler is expected to have the least penetration power, because it is the toughest and least stiff. Experimental research shows that Mesolithic type *Cervus elaphus* bone (Spithoven 2018, 65) , Gravettian bone (Knecht 1993, 41) and Nenana (An Upper Palaeolithic Alaskan technocomplex) *Bos taurus* bone (Wood and Fitzhugh 2018, 10) and Aurignacian, Gravettian (Knecht 1993, 43) and Magdalenian antler points all have sufficient penetration depth for hunting (Pokines 1998, 878). The fact that the penetration power of both bone and antler points of various typologies is adequate to kill large mammals indicates that selection on functionality would prioritise the most durable materials.

The shock absorbent abilities of projectile points are most important for their durability (Margaris 2006, 193). Shock absorption is measured by the required work to fracture. Research on the biomechanics of bone has focused on the elasticity and does not report the work to fracture. Due to an inverse relation between the elastic modulus and the work to fracture, the relative shock resistance of bone can be inferred.

Table 16 gives an overview of elastic moduli reported in literature based on three criteria:

EITHER

1. The species is phylogenetically close to a species identified as raw material of a bone point.

OR

2. The species was present in Mesolithic Doggerland and could have served as an alternative raw material for bone point production.

   AND

3. The elastic modulus of the species was reported in at least two studies.

For many species relevant to this research the elastic moduli are unavailable. As it is suspected that most bone points were produced from metapodia (Verhart 1988, 171), lack of elaborate data on metapodial elastic moduli hampers direct assessment of the biomechanical suitability of a species for projectile point production. Besides, most of the elastic moduli were measured on hydrated samples. Dry bone and antler has a higher elastic modulus (tab. 16; Currey 2006, 127). It must be taken into account that the projectile points were likely dry when used and thus would have a higher elastic modulus than listed in table 16. Nevertheless table 16 might be helpful indirectly.

Table 16: Reported Young's elastic modulus of bone for relevant species according to 15 studies:
Blob and Snelgrove 2006, Chen *et al.* 2008, Chen *et al.* 2009, Currey 1988a, Currey 1988b, Currey 1990, Currey 2006, Currey *et al.* 2009, Keller *et al.* 1990, Kieser *et al.* 2014, Landete-Castillejos *et al.* 2007, MacGregor and Currey 1983, Margaris 2006, Reilly and Burstein 1975 and Shah *et al.* 2008.
*The study by Kieser *et al.* 2014 uses the elastic modulus of Keller *et al.* 1990 for the *Homo sapiens* femur.

Species	Blob and Snelgrove 2006 (GPa)	Chen *et al.* 2008	Chen *et al.* 2009 (GPa)	Currey 1988a (GPa)	Currey 1988b (GPa)	Currey 1990 (GPa)	Currey 2006 (GPa)	Currey *et al.* 2009 (GPa)	Keller *et al.* 1990 (GPa)	Kieser *et al.* 2014 (GPa)	Landete-Castillejos *et al.* 2007 (GPa)	MacGregor and Currey 1983 (GPa)	Margaris 2006 (GPa)	Reilly and Burstein 1975 (GPa)	Shah *et al.* 2008 (GPa)
Alces alces antler (hydrated)	11.6	-	-	-	-	-	-	-	-	-	-	-	-	-	-
Rangifer tarandus antler (hydrated)	-	-	-	6.41	-	8.1	8.1	-	-	-	-	-	5.68	-	5.8
Cervus elaphus antler (hydrated)	-	-	-	6.71	-	7.2	7.2	7.30	-	-	5.27	-	-	-	-
Cervus elaphus antler (dry)	-	-	-	-	-	-	-	17.50	-	-	-	13.55	-	-	-
Cervus elaphus femur (hydrated)	-	-	-	-	-	-	-	22.39	-	3.8	-	-	-	-	-
Cervus canadensis antler (dry)	-	7.5	7.6	-	-	-	-	-	-	-	-	-	-	-	-
Cervus canadensis antler (hydrated)	-	-	6.98	-	-	-	-	-	-	-	-	-	-	-	-
Cervus canadensis limb bone (hydrated)	-	-	-	-	-	-	-	-	-	-	-	-	16.14	-	-

Odocoileus virginianus radius (hydrated)	-	-	-	-	-	-	-	-	-	-	-	-	9.75	-	-
Dama dama radius (hydrated)	-	-	-	-	-	25.5	-	-	-	-	-	-	-	-	-
Dama dama tibia (hydrated)	-	-	-	26.84	-	26.8	26.8	-	-	-	-	-	-	-	-
Capreolus capreolus femur (hydrated)	-	-	-	-	-	18.4	-	-	-	-	-	-	-	-	-
Equus caballus femur (hydrated)	-	-	-	21.22	-	24.5	24.5	-	-	-	-	-	-	-	-
Ovis aries metacarpus (hydrated)	-	-	-	18.95	-	-	-	-	-	-	-	-	-	-	-
Ovis aries femur (hydrated)	-	-	-	-	-	-	-	-	-	3.8	-	-	-	-	-
Homo sapiens femur (hydrated)	-	-	-	-	-	-	16.7	-	12.1	12.1*	-	-	-	17.4	-
Bovine femur (hydrated)	-	-	-	18.49	19.58	26.1	26.1	-	-	-	-	-	-	22.7	-
Bos taurus tibia (hydrated)	-	-	-	-	-	-	-	-	-	-	-	17.24	-	-	-

As table 16 shows, there is considerable variation in the reported elastic moduli of the same skeletal element from the same species (e.g. *Cervus canadensis* antler (dry) 7.5 ↔ 7.6 GPa and *Cervus elaphus* femur 3.8 ↔ 22.39 GPa). There is also an unexpectedly large intraspecies differences between different skeletal elements. The difference between the elastic moduli of *Ovis aries* femur and metacarpus is similar to the maximum observed interspecies variation in elastic modulus. However, the large differences between the elastic moduli reported in Kieser *et al.* 2014 and the other studies in table 16 raise doubts on the extent to which the values reported in different studies can be compared. Moreover, Kieser *et al.* 2014 report an elastic modulus for *Cervus elaphus* and *Ovis aries* femur much lower than that of *Rangifer tarandus* and *Cervus elaphus* antler. Bone elastic moduli lower than antler elastic moduli are suspect, because of the functional difference between bone and antler. Antler needs to be able to withstand huge impacts experienced during fighting between deer (Currey 2006, 124-125).
Due to these issues, the shock absorption of a skeletal element of a species will only be ranked relative to other skeletal elements reported within the same study.

Due to lack of available data on elastic moduli of *Cervus elaphus* or *Alces alces* bone, it is not possible to conclude that deer bone would have provided more durable or less durable projectile points than bones of other species. Although Currey *et al.* 2009 provides an elastic modulus for a *Cervus elaphus* femur, no bones of other animals are reported in the same study. The *Cervus elaphus* antler however is considerably more shock resistant than bone and an antler point would likely be more durable (Currey 2006, 130).
Interestingly enough antler points have been found as well on the Dutch shores of the North Sea. Two earlier studies report that based on morphology 13.8% (N=389) (Spithoven 2015, 48) and 25% (N=165) (Verhart 1988, 161) of the found North Sea points are made of antler (Spithoven 2015, 48; Verhart 1988, 161). The rest is made of bone. As mentioned in section 2.4 one of the specimens was identified as antler (P5) by Dick Mol on basis of its morphology. ZooMS analysis identified P5 as *Cervus elaphus* or *Alces alces* (tab. 5). Since only one out of the seven *Cervus elaphus* or *Alces alces* identifications is made of antler it seems that there was no selection for antler.

The elastic modulus of the *Homo sapiens* femur is reported in the same study (Currey 2006, 130) alongside the elastic moduli of antler, *Dama dama* tibia, *Equus caballus* and bovine femora. Since the points P3 and P29 (Appendix B) are too large to be made from human metapodia there is a chance that they were made of a long bone. Table 16 shows that the human femur is actually more shock absorbent than either *Equus caballus, Dama dama* and bovine femora.

5.4 Influence of external factors on membrane box collagen extraction

Although tables 12, 13 and 14 revealed no significant difference in success rates of the sampling protocols between the Châtelperronian dataset from Quinçay and the Mesolithic dataset from the North Sea, this is no proof that both datasets have the same quality of collagen preserved. There are several reasons why possible differences between the two datasets have to be taken into account. First of all, the burial conditions of both datasets are widely different. The Quinçay dataset was found in a cave, whereas the North Sea points were recently washed ashore. Secondly, there is a significant age difference between the two datasets. The Quinçay material dates to the Châtelperronian, while the North Sea points are Mesolithic. Thirdly, the Quinçay and North Sea material have not been in membrane boxes for the same amount of time.

5.4.1 Influence of burial conditions

The burial conditions of the material from Quinçay and the North Sea are very different, which could have caused a difference in results. Salt in the seawater may have reduced the charging capacity of the North Sea bone points (Welker 2019, personal communication). In solution salt splits in its two ions: Na^+ and Cl^-. These ions bind to polarised sites on the collagen molecule, reducing its overall charge. However, usually the salt ions recrystallize again when the solution evaporates. Since the bone points had been dry for at least months it is possible that the salt ions have recrystallized instead of remaining attached to the collagen molecule. Besides, the collectors reported to have desalinated their artefacts, possibly removing the influence of salt. There was one destructively sampled North Sea point (P30), which could not be identified. It seems likely that this is due to lack of collagen.

Although all destructively sampled Quinçay samples could be identified, this difference between the Quinçay and North Sea dataset cannot be interpreted as a result of better burial conditions at Quinçay. The sample size is too small. Previous ZooMS analysis performed on bones from the Châtelperronian layers at Quinçay reported that 92.3% of the samples could be identified to family, genus or species level using destructive sampling protocols (Welker *et al.* 2017b, 19). If the 92.3% success rate is used to predict the success rate of all destructively sampled artefacts in this thesis, then one would expect to obtain 6 (5.54) identifiable spectra from the Quinçay material and 9 (9.23) identifiable spectra from the North Sea dataset.

These predictions seem to match with the observed success rates. If a binomial distribution for the success of the identification is assumed, where the chance to successfully identify an artefact is 92,3%, then 6 successful identifications out of 6 artefacts, yield an exceedance probability of p=0.618. 9 successful identifications out of 10 gives an exceedance probability of p=0.551. In both

cases it cannot be proven that there is a significant difference between the observed and assumed success rate, but one should be careful concluding that the burial conditions for Quinçay and the North Sea are equivalent. Such a claim requires a larger sample size.

5.4.2 Influence of the age of artefacts on collagen quality

The difference in age between the datasets could also have had impact on the success rates. The North Sea bone points are over 30 000 years younger than the Quinçay material. Therefore it is expected that the North Sea bone points would have less degraded collagen. However, it may be that the difference in collagen preservation is not large enough to affect the ZooMS analysis. There are many instances, in which ZooMS has been successfully applied to samples much older than the artefacts used in this research (Welker *et al.* 2017a, 4). In fact there have been cases in which collagen from the Late Pleistocene was not significantly different from modern collagen (Buckley and Collins 2011, 3).

As the destructive methods yielded good quality collagen for both the Quinçay as the North Sea artefacts, it seems that the issue lies with the quantity rather than quality of collagen extracted by the membrane box protocol.

5.4.3 Influence of membrane box storage time on collagen extraction

The Quinçay material had been in the membrane boxes since 2007, while the North Sea material only spent 12 days inside membrane boxes. Yet the results in table 12 provide no indication that the time the artefacts spent inside the membrane box influences the extraction of collagen. If the time in the membrane box mattered, the Quinçay dataset should have shown a larger identification rate for the membrane boxes than the North Sea points. There are experiments that show that time required for maximal charge generation by contact electrification varies from 2 seconds to 15 min (Baytekin *et al.* 2011, 310, Lowell and Rose-Innes 1980, 962). Other scholars argue that time of contact is much less important (Horn and Smith 1992, 363). In any case the time the artefacts spent in the membrane boxes should have been enough to generate the maximum charge of contact electrification (Lowell and Rose-Innes 1980, 962).

Although it is not possible to discount storage time and environmental conditions as factors influencing the success rate, the data show that it is unlikely that environmental conditions are the dominant factor determining the identification rate.

5.5 Protocol success rates

The results show a clear difference in success rates of the collagen sampling protocols (Tables 12, 13 and 14). The cold acid and AmBic protocol performed well for both datasets, with success rates 100% for Quinçay and and 90% for the North Sea points, respectively. There was only one instance, in which both destructive protocols failed, P30. In all other cases the mass spectra contained distinct peaks for all biomarkers (Appendix D).

In contrast to the destructive sampling protocols the identification rate of the non-destructive membrane box protocol is very low (table 12). For Quinçay the success rate was 3.8%, while for the North Sea bone points it was 20%. Because the protocols are identical once the samples are transferred onto the storage plate, the explanation for the low success rate of the membrane box protocol must be sought before that moment in the protocol (Methods 3.6).
There are two possible explanations:

1. either the contact adhesive forces between bone and membrane were too weak to trap bone particles on the membrane,
   or
2. the adhesive forces were stronger than the desorption of bone from the membrane by heated ammonium bicarbonate buffer.

The same reasoning applies to the plastic bag protocol, which did not yield enough collagen for an identification. A value judgement on the plastic bag protocol cannot be given on basis of a single experiment.
The results of the membrane box protocol indicate that the protocol is sound in principle, but lacking in application. One possibility to improve the success rate of the membrane box protocol is to increase the adhesion of the collagen onto the membrane. As the main force contributing to the adhesion between solid bodies is electrostatic attraction induced by contact electrification (Derjaguin 1994, 223), ways to increase the electrostatic forces must be considered.
Although it is possible that the adhesive forces were too strong, rather than too weak, this is extremely unlikely. Static electricity is practically nullified by moisture (Visser 1995, 182). Since a drop of ammonium bicarbonate buffer has been dragged over the surface of the membrane, electrostatic adhesion should have been eliminated or severely reduced (Izadi and Zandieh 2017, 28).

5.6 Toward improving electrostatic sampling by contact electrification

The recommendations to improve the non-destructive collagen sampling protocol in this thesis will focus on the membrane box protocol instead of the plastic bag protocol. There are three main reasons for this.

1. The static electric charge that must be enhanced, can be generated by contact electrification or by friction (section 1.2). Friction is considered the main mechanism for creating a electrostatic charge in the plastic bag protocol, but contact electrification contributes to the charge as well. Contact electrification is also responsible for generating the electrostatic charge in the membrane box protocol. Thus by enhancing the charge generated by contact electrification both the membrane box and plastic bag protocol will improve.
2. Friction increase is not without risk. In the current protocol it is assumed that the friction an artefact endures over time, whilst gently being move around in a plastic bag, is sufficient to extract collagen. This level of friction is harmless to the microwear and general structure of the artefact. Applying increased friction risks to damage the artefact or obscure any microwear and should therefore be avoided.
3. One of the main strengths of the plastic bag protocol was its accessibility. It can be done using common plastic bags, in which artefacts are often already stored. Suggestions to change the material or the form of the plastic bag would eliminate the protocol's accessibility. The recommendations made in this thesis do involve the contact material and its form.

The magnitude of contact electrification is dependent on the charged area, surface charge density, separation distance, charge penetration depth, the atmospheric conditions, material properties (Izadi and Zandieh 2017, 7) and repeated contact (Lowell and Rose-Innes 1980, 965).

5.6.1 Charged area

Since all surfaces have a certain degree of roughness, the area of intimate contact is not equal to the area of contact visible with the naked eye. It can be assumed that the charged area is of the same order of magnitude as the apparent area of contact (Lowell and Rose-Innes 1980, 953). The intimate contact area can be increased by either exerting pressure on the materials (Lowell and Rose-Innes 1980, 954) or by increasing the roughness of the surface (Chen *et al.* 2018, 4). A surface with features on both the nano and micro scaled was observed to provide the largest electrostatic charge (Chen *et al.* 2018, 6).

5.6.2 Separation distance

As not the entire area of visible contact is actually in intimate contact, the rest of the artefact's surface is separated from the membrane by a certain distance. The influence of the separation distance on the electrostatic charge is complex. The two main forces involved in contact electrification, the electrostatic adhesion force and the intermolecular Van der Waals forces, both vary non-linearly with separation distance.

The electrostatic adhesion force increases when the distance between the artefact and the membrane decreases (Izadi and Zandieh 2017, 7). However, increased separation distance can also lead to increased electrostatic adhesion when the dielectric constant of the medium that separates the objects decreases; for instance when the gap between the artefact and the membrane is filled by air molecules (Izadi and Zandieh 2017, 27).

The Van der Waals force component of adhesion decreases rapidly as the separation distance increases. However, at extremely short distances, the Van der Waals attractive force actually becomes repulsive.

Due to this trade-off between the electrostatic and the Van der Waals forces component of adhesion, it seems that a separation distance between 5 and 20 nm provides the largest electrostatic charge (Izadi and Zandieh 2017, 22-27).

5.6.3 Surface charge density

The charge density is dependent on material properties and thickness of the membrane (Zhou *et al.* 2014, 1571). Charge density can be manipulated under the influence of an electric field. Electrical fields are commonly employed in toner printers in order to cause particles to adhere to a surface (Hays and Sheflin 2005, 688). A negative electric field enhances the charge density of a negatively charged material and vice versa (Zhou *et al.* 2014, 1570) by polarising the material if it is an insulator, such as bone (Ruffato *et al.* 2014, 2). Experiments show that collagen is charged slightly more positive than glass (Mesquida *et al.* 2018, 2). A negatively charged field would therefore increase the charge difference between the artefact and the membrane, increasing the electrostatic forces.

5.6.4 Charge penetration depth

The deeper the charge penetrates a material, the more the charge is spread over a larger volume. A smaller charge penetration depth means a larger portion of the charge is conserved at the surface. Therefore the smaller the charge penetration depth, the larger the electrostatic forces (Izadi and Zandieh 2017, 7). Charges reach a higher penetration depth in conductive materials and friction also increases penetration depth (Izadi and Zandieh 2017, 23).

However experiments have measured that sometimes an enhancement of the electrostatic forces comes paired with an increased charge penetration depth. This can be explained by the fact that if a larger volume of an object is affected by the electric charge, more molecules will be able to participate in electron transfer (Izadi and Zandieh 2017, 23).

5.6.5 Atmospheric conditions

In humid conditions electrostatic forces are reduced or completely eliminated (Matsusaka *et al.* 2010, 5787; Visser 1995, 183). Under normal atmospheric pressure the air can become ionised by the contact electrification induced charge. The ionised air particles reduce the charge of the dielectric. It must be stressed that the ionisation of air is a possibility and not a certainty (Lowell and Rose-Innes 1980, 955). Both the influence of humidity and the ionisation of air particles can be prevented by worked in a vacuum of a strength around 10^{-3} torr (Lowell and Rose-Innes 1980, 955).

5.6.6 Material properties

Lastly, the choice of material significantly influences the generated charge. The polymers able to generate the largest charge upon contact, are fluoropolymers (Izadi and Penlidis 2013, 590). The main reason these polymers are able to generate such a large charge is, because they contain a carbon atom with dangling bond (Matsusaka *et al.* 2010, 5785). There are rankings called triboelectric series[1], which show what materials are able to generate larger contact electrification charges. It is not the absolute position of a material on this series that matters, but its position relative to the material it contacts. A material is negatively charged, if it contacts a material placed higher on the triboelectric series (Galembeck *et al.* 2014, 64283) and the larger the difference between two materials on the triboelectric series, the greater the generated charge (tab. 17). As collagen is quite positively charged (section 5.6.3) (Mesquida *et al.* 2018, 2), the membrane needs to consist of a material at the bottom of a triboelectric series. The membranes in the membrane boxes were composed of polyurethane, which is already quite low on the triboelectric series (tab. 17) (Diaz and Felix-Navarro 2004, 282). Polymers that are ranked lower on the triboelectric series are polyethylene, polypropylene and polytetrafluoroethylene (Teflon) (Diaz and Felix-Navarro 2004, 282). Replacing the membrane with one of the aforementioned polymers would increase the electrostatic forces.

[1] Although in section 1.2 it is written that triboelectricity and contact electrification are fundamentally different, the concept of the triboelectric series was coined before the distinction between contact electrification and triboelectricity was made. Thus a triboelectric series can be applied both for triboelectrically induced and contact electrification induced charges.

Table 17: Shortened triboelectric series, after Diaz and Felix-Navarro 2004, 282.	
Charge	**Material**
Positively charged	Collagen
	Glass
	Nylon
	Cotton
	Polyester
	Polyurethane
	Polyethylene
	Polyvinyl chloride (PVC)
Negatively charged	Polytetrafluoroethylene (Teflon)

5.6.7 Repeated contact

Apart from the aforementioned characteristics there is another way to increase the generated charge and the amount of transferred material. Repeatedly contacting the membrane at the same place with an artefact will increase the generated charge (Lowell and Rose-Innes 1980, 965). The fact that an increase in charge penetration depth was recorded after repeated contact also suggests an increase in electrostatic forces (Izadi and Zandieh 2017, 23). Although it would be difficult to place the artefact back on the precise same spot on the membrane, this will likely not matter. Even if the artefact touches the membrane on different spots an electrostatic charge will still be generated and material transfer will still occur.

5.7 Suggestions for revising the membrane box protocol

In the previous sections several options to increase electrostatic adhesion are mentioned. Some of these are more easy to incorporate into the existing protocol than others. At the moment there is no way to predict and quantify to what extent the suggested changes will improve the existing membrane box protocol. The revised protocol below differs in multiple aspects from the original membrane box protocol, but it would be good practice to also test single aspects in order to determine what factors are dominant in generating the electrostatic charge. Apart from advancing the understanding of static electricity in general, it might also allow 'streamlining' of the protocol. For example the introduction of an electric field might be practically difficult. Should experiments show that an electric field contributes less to the generated electrostatic forces than the use of

polyethylene as contact material, then a researcher could decide to not employ an electric field, but instead to analyse more samples.

5.7.1. Suggestion 1: Changing the material

The first suggestion is to exchange the polyurethane membranes for either Teflon or polyethylene. Teflon would be preferable, as it is ranked lowest on the triboelectric series (Diaz and Felix-Navarro 2004, 282). However polyethylene might be more accessible than Teflon, as its applications amongst others include common plastic food wrap (Albert Heijn cling foil). The latter would also be low-cost, and easily accessible.

5.7.2 Suggestion 2: Controlling laboratory conditions

Secondly, the experiment should take place in a humidity controlled environment. Although a vacuum is advised in section 5.6.5, this might not be feasible. It is advised to take precautions to ensure an environment as dry as possible. Before placing the artefact on the membrane the charge of the membrane can be enhanced by rubbing it with a negatively charged roller (Izadi 2019, personal communication).

5.7.3 Suggestion 3: Repeated contact

Lastly, membrane-bone contact should be broken and re-established multiple times by opening and closing the membrane box. The duration of contact and number of times establishing contact suggested here are mainly arbitrary. This suggestion should be experimentally calibrated, especially since the conflicting data on the time needed to establish maximum charge (section 5.4.3), (Baytekin *et al.* 2011, 310; Lowell and Rose-Innes 1980, 962).

5.7.4 Additional suggestions

The following two suggestions might not be feasible to implement on a large scale.

1. Surface features on both the micro and nano level would greatly increase electrostatic adhesion (Chen *et al.* 2018, 6). Ideally, a membrane with nano and micro level features should be used.
2. On each side of the membrane box a negatively charged electrode could be placed. The electrodes will bring the entire membrane box under the influence of a negative electric field, which will enhance the membranes' charge density. Since most scholars in the field of electrostatic adhesion do not work on the sampling of biomolecules the literature does not give clear recommendations regarding the characteristics of the electric field. One study,

which applied an electric field in order to increase electrostatic adhesion, used a voltage potential of 2-4 kV (Ruffato *et al.* 2014, 3). Another research found that 5 V was enough to enhance electrostatic adhesion (Zhou *et al.* 2014, 1570). The use of a high voltage electrical field requires safety measures. The field strength required to manipulate the electrostatic forces depends on the thickness of the material. The research applying a 5 V field used a film with a thickness of 2.4 µm (Zhou *et al.* 2014, 1570).

5.8 Alternative non-destructive sampling methods

Apart from the aforementioned electrostatic sampling protocols, a recent study showed that protein can also be sampled non-destructively using C_8 resins (Manfredi *et al.* 2017, 3311). The study used a film composed of 70% cation/anion exchange resins and C_8 resins and 30% ethyl-vinyl acetate. The principle of these resins is that proteins will bind to the resins (Manfredi *et al.* 2017, 3311). The method was tested on replica canvas, wood paintings and frescos and 16th century Italian frescos (Manfredi *et al.* 2017, 3313). A strip of the resin – ethyl-vinyl acetate film was moisturised with ultrapure water and placed on the target surface for 30 minutes. Ammonium acetate was used to elute the protein from the film strip. Afterwards the proteins were denatured using trifluoroethanol, alkylated with dithiothreitol and analysed with LC-MS (Manfredi *et al.* 2017, 3313). Using this method it was possible to extract the proteins beta-casein, alpha-S1-casein and kappa-casein from the 16th century frescos (Manfredi *et al.* 2017, 3315)., The resin – ethyl-vinyl film also succeeded in capturing collagen from the replica canvases, wood paintings and frescos (Manfredi *et al.* 2017, 3314). Additionally it was shown that the resin – ethyl-vinyl film did not leave any traces or residue on the target surface (Manfredi *et al.* 2017, 3316).

The fact that this method succeeded in sampling collagen non-destructively is worthy of interest. However, for archaeological applications it is worrisome that collagen was found in the replica frescos, but not in the 16th century frescos. It may be that this is because the 16th century frescos used a different binding agent than the replica frescos. Based on the presence of the casein protein it was suggested that a mixture of milk and albumin was used as binding agent for the 16th century frescos, while rabbit skin glue was used for the replicas (Manfredi *et al.* 2017, 3311-3315). In that case the 16th century frescos would not have contained any collagen, explaining the discrepancy between the results of the frescos and historical frescos.

6 Conclusion

The primary aim of this research was to test the applicability of the membrane box protocol as a non-destructive alternative for the current destructive collagen sampling ZooMS protocols. The sub-questions were meant to help defining the criteria for a suitable alternative.

1) *What is the success rate of the membrane box protocol?*
2) *Are the identifications made with the membrane box protocol as precise as the identifications obtained from the destructive protocols?*
3) *Does the time the artefacts have been inside the membrane box affect the success rate of the membrane box identification?*
4) *Is the membrane box protocol applicable to artefacts with various taphonomic histories and chemical compositions?*
    a) *Is there a difference in success rate between the Quinçay and Mesolithic North Sea material?*
    b) *Is there a difference in success rate between dentine and bone samples?*

As a secondary objective the ZooMs identification of the artefacts presented in this thesis enabled study of the species selection patterns of the tools from Quinçay and the Mesolithic North Sea bone points.

6.1 Membrane box protocol a suitable alternative?

With regards to the first sub-question, the success rate of the membrane box protocol was in 8.1% (3/37). For the Quinçay possible bone tools the success rate was 3.8% and for the North Sea bone points a success rate of 20% was achieved. Despite the seemingly large difference in success rate in the two datasets, the difference is not statistically significant (tab. 12) according to Fisher's test ($p=0.17$). A success rate of at least 50% is deemed necessary for a suitable sampling protocol, see section 1.6.

The second criterion for a suitable alternative is the precision of its identifications. In two out (Q15 and P7) of the three cases (Q15, P6 and P7) that the membrane box protocol did extract enough collagen for identification, the identification was less precise than the identification of the same artefact obtained with the cold acid and AmBic protocol (tabs. 4 and 5).

There are large differences in the age, burial conditions and the time the artefacts spent inside the membrane box between the Quinçay and North Sea artefacts. Of these the time spent inside the membrane box can be directly controlled and is thought to have the least impact on the amount of collagen extracted (section 5.4.3).

As no significant difference was observed between the Quinçay and North Sea dataset (tab. 12) it can be concluded that the membrane box protocol is applicable to artefacts with various taphomonic histories and that neither age, burial conditions nor time was the dominant factor determining the success rate of the membrane box protocol.

Some tools from Quinçay were suspected to be ivory. It was intended to test if the ivory artefacts provided similar success rates as the bone tools. The structural differences between the collagenous materials might influence the generated electrostatic charge and thus the membrane box protocol's success rate. However, because only one of the Quinçay possible tools was identified with the membrane box protocol there is not enough data to answer this question.

It seems that the membrane box protocol is not yet a suitable alternative to the current destructive ZooMS sampling protocols. The success rate of the membrane box protocol is much lower than that of the destructive cold acid and AmBic protocols (tabs. 12, 13 and 14). The cold acid and AmBic protocol are able to offer a certain level of assurance that, if collagen is preserved in the artefact, a ZooMS identification will be possible. The membrane box protocol is not able to offer such an assurance.
However, it must be stressed that the membrane box protocol does extract sufficient collagen for identification in some cases, indicating that it is possible to extract collagen using electrostatic adhesion. Although the non-destructive methods might not be able to reach the success rates of the destructive protocols, they can undoubtedly be significantly improved. Specific suggestions to improve electrostatic sampling of collagen are made.

6.2 Species selection patterns of the Mesolithic North Sea points

The identifications of the bone projectile points from Mesolithic Doggerland do indicate certain patterns of selection for the raw material. This thesis was not able to explain the selection for *Cervus elaphus* or *Alces alces* bone from either a functional or a availability point of view. At the moment a comparative overview of the work to fracture or elastic moduli of various skeletal elements (primarily metapodia) of the species present in Mesolithic Doggerland is required in order to test if the selected species were biomechanically most suited for projectile points.
Apart from a selection for *Cervus elaphus* or *Alces* alces this research has also revealed the use of human bone for projectile points by the Mesolithic people of Doggerland. Tools made of human bone are rare and often singular finds. Although the two finds are insufficient evidence to interpret

the human working of bone as a custom, they raise the possibility and warrant further research into the North Sea bone points.

6.3 Further research

The results of this research indicate several promising directions for further research. First of all, the revised protocol as written in section 5.7 might be a first step in improving the success rate of the membrane protocol. The Quinçay dataset used in this research would be ideal for testing future versions of the membrane box protocol. Since the protocol is non-destructive the artefacts are not damaged and the number of variables in future experiments would be minimalised.

Secondly, it must be stressed that electrostatic sampling is very much an interdisciplinary subject. Its advance could be accelerated by establishing cooperation with scholars from other fields, like physics. The scholarly debate in the field of electrostatics deals with the same topics as archaeological research like this thesis, namely: how to control contact electrification induced charges. Yet the intended applications and models designed in electrostatics do not match well with what is required for archaeological research. The same scenario applies to the study of the biomechanics of bone. Medical researchers have the tools and the knowledge to provide the answer to archaeological questions. However, because the clinical relevance of such research is often unclear, it is not done. The result is insufficient data to answer archaeological questions.

Apart from improving the membrane box protocol it would be useful to develop the application of a resin – ethyl-vinyl acetate film, following Manfredi *et al.* 2017, to archaeological bone.

Should the success rate of the membrane box protocol indeed be improved, then more North Sea bone points should be sampled in order to test if the pattern observed in this thesis holds true. If indeed 20% of the bone points is produced from human bone, this would be a most rare example of the systemic working of human bone for tool production.

In section 5.3 there was a discourse on the possibility that selection for availability or function might explain the pattern of species identifications observed in the bone points. As it was not the primary aim of this thesis the discussion focused only on some aspects of selection for availability or functionality. Experiments measuring the work to fracture of skeletal elements of animals present in Mesolithic Doggerland are also suggested as further research. Such experiments would allow testing of the hypothesis that raw material of the Mesolithic North Sea bone points was selected for its

durability. Other explanations of the observed selection should also be investigated. Do the used species reflect the most commonly hunted species or were they the most available in the landscape? Is there a difference in used species between different find locations? The availability of species was touched upon briefly, but only eight sites were discussed. A more extensive overview is required to truly test this hypothesis. Possible variation in the selection pattern through time must also be considered. In fact at the time of writing, a project by the RCE and the Centre for Isotope Research of Groningen University is working on a project to C^{14} date North Sea bone points from the Dutch shores, amongst which the ten points used in this research.

7 Abstract

In this thesis the membrane box protocol, a new non-destructive electrostatic collagen sampling protocol for ZooMS (Zooarchaeology by Mass Spectrometry), is compared for the first time to the destructive cold acid and ammonium bicarbonate buffer sampling protocols. The new sampling protocol employs electrostatic adhesive forces, generated by contact electrification between a polyurethane membrane and an osseous artefact, to extract miniscule amounts of collagen from the artefact onto the membrane.

The membrane box, cold acid and AmBic protocols were applied to 6 morphologically identified bone and dentine fragments from the Châtelperronian layers of Quinçay, France, and 10 Mesolithic bone and antler projectile points found on the Dutch shores of the North Sea. Moreover, the membrane box protocol was applied on 21 possible Châtelperronian bone and ivory tools from Quinçay.

The success rate of the membrane box protocol appeared to be low (Quinçay: 3.7%, North Sea: 20%) compared to the cold acid (Quinçay: 100%, North Sea: 90%) and the AmBic protocol (Quinçay: 100%, North Sea: 90%). These results show the possibility to non-destructively extract collagen using electrostatic adhesion, but also indicate the need for improvement of the membrane box protocol.

Literary analysis of electrostatic adhesion yielded several opportunities for improvement of the membrane box protocol. Of which the most easy implementable are: replacement of the polyurethane membrane by a polyethylene or polytetrafluoroethylene (Teflon) membrane, limitation of atmospheric humidity, enhancement of the membrane's electrostatic charge by applying friction and repeated contact between artefact and membrane.

Of the 10 Mesolithic North Sea bone points 7 were identified as *Cervus elaphus* or *Alces alces*. Two other bone points were identified as *Homo sapiens*. These two Mesolithic bone points form a rare example of the production of formal tools from human bone. The 7 *Cervus elaphus* or *Alces alces* bone points hint at selection for *Cervus elaphus* or *Alces alces* bone for projectile point production.

Further research is required to test the suggestions for improvement of the membrane box protocol and to test the pattern of selection for *Cervus elaphus/Alces alces* and *Homo sapiens* bone for projectile point production.

Bibliography

Albéric, M., A. Gourrier, K. Müller, I. Zizak, W. Wagemaier, P. Fratzl and I. Reiche, 2014. Early diagenesis of elephant tusk in marine environment. *Palaeogeography, Palaeoclimatology, Palaeoecology* 416, 120-132. **DOI:** 10.1016/j.palaeo.2014.09.006.

Arnaud, G., S. Arnaud, A. Ascenzi, E. Bonucci and G. Graziani, 1978. On the problem of the preservation of human bone in sea-water. *Journal of Human Evolution* 7, 409-420. **DOI:** 10.1016/S0047-2484(78)80091-8.

Baytekin, H., A. Patashinski, M. Branicki, B. Baytekin, S. Soh and B. Grzybowski, 2011. The Mosaic of Surface Charge in Contact Electrification. *Science* 333(6040), 308-312. **DOI**: 10.1126/science.1201512.

Bellido, J., J. Castillo, M. Farfán, J. Mons and R. Real, 2007. First records of hooded seals (*Cystophora crisata*) in the Mediterranean Sea. *Marine Biodiversity Records* 1(e74), 1-2. **DOI:** 10.1017/S1755267207007804.

Bello, S., S. Parfitt and C. Stringer, 2011. Earliest directly-dated human skull-cups. *PLoS ONE* 6(2), e17026, 1-12. **DOI:** 10.1371/journal.pone.0017026.

Blanc, J., 2008. *Loxodonta africana*. *The IUCN Red List of Threatened Species 2008*, e.T12392A3339343. **DOI:** 10.2305/IUCN.UK.2008.RLTS.T12392A3339343.en.

Blob, R. and J. Snelgrove, 2006. Antler stiffness in moose (*Alces alces*): correlated evolution of bone function and material properties? *Journal of Morphology* 267, 1075-1086. **DOI:** 10.1002/jmor.10461.

Bocherens, H., D. Drucker and S. Madelaine, 2014. Evidence for a ^{15}N positive excursion in terrestrial foodwebs at the Middle to Upper Palaeolithic transition in south-western France: Implications for early modern human palaeodiet and palaeoenvironment. *Journal of Human Evolution* 69, 31-43. **DOI:** 10.1016/j.jhevol.2013.12.015.

Boesl, U., 2017. Time-of-flight mass spectrometry: introduction to the basics. *Mass Spectrometry Reviews* 36, 86-109. **DOI:** 10.1002/mas.21520.

Bradfield, J., T. Forssman, L. Spindler and A. Antonites, 2018. Identifying the animal species used to manufacture bone arrowheads in South Africa. *Archaeological and Anthropological Sciences*, 1-16.

Brooks, A., S. Bradley, R. Edwards and N. Goodwyn, 2011. The palaeogeography of Northwest Europe during the last 20,000 years. *Journal of Maps* 7(1), 573-587. **DOI**: 10.4113/jom.2011.1160.

Buckley, M., M. Collins, J. Thomas-Oates, 2008. A method for isolating the collagen (I) α2 chain carboxytelopeptide for species identification in bone fragments. *Analytical Biochemistry* 374, 325-344. **DOI:** 10.1016/j.ab.2007.12.002.

Buckley, M., M. Collins, J. Thomas-Oates and J. Wilson, 2009. Species identification by analysis of bone collagen using matrix-assisted laster desorption/ionisation time-of-flight mass spectrometry. *Rapid communications in mass spectrometry* 23, 3843-3854. **DOI:** 10.1002/rcm.4745.

Buckley, M., S. Kansa, S. Howard, S. Campbell, J. Thomas-Oates and M. Collins, 2010. Distinguishing between archaeological sheep and goat bones using a single collagen pep.tide. *Journal of Archaeological Science* 37, 13-20. **DOI:** 10.1016/j.jas.2009.08.020.

Buckley, M. and M. Collins, 2011. Collagen survival and its use for species identification in Holocene – Lower Pleistocene bone fragments from British archaeological and paleontological sites. *Antiqua* 1(1), 1-7. **DOI:** 10.4081/antiqua.2011.e1.

Buckley, M. and S. Kansa, 2011. Collagen fingerprinting of archaeological bone and teeth remains from Domuztepe, South Eastern Turkey, 2011b. *Archaeological and Anthropological Sciences* 3: 271-280. **DOI:** 10.1007/s12520-011-0066-z.

Buckley, M., N. Larkin and M. Collins, 2011. Mammoth and Mastodon collagen sequences; survival and utility. *Geochimica et Cosmochimica Acta* 75, 2007-2016. **DOI:** 10.1016/j.gca.2011.01.022.

Buckley, M., S. Fraser, J. Herman, N. Melton, J. Mulville and A. Pálsdóttir, 2014. Species identification of archaeological marine mammals using collagen fingerprinting. *Journal of Archaeological Science* 41, 631-641. **DOI:** 10.1016/j.jas.2013.08.021.

Buckley, M. 2016. Species identification of bovine, ovine and porcine type 1 collagen; comparing peptide mass fingerprinting and LC-based proteomics methods. *International Journal of Molecular Sciences* 17(445), 1-17. **DOI:** 10.3390/ijms17040445.

Buckley, M., V. Harvey and A. Chamberlain, 2017. Species identification and decay assessment of Late Pleistocene fragmentary vertebrate remains from Pin Hole Cave (creswell Crags, UK) using collagen fingerprinting. *Boreas* 46, 402-411. **DOI:** 10.1111/bor.12225.

Cantor, C. and P. Schimmel, 1980. *The conformation of biological macromolecules.* San Francisco: W. H. Freeman and Company.

Chapman, J. (eds), 2000. *Mass Spectrometry of Proteins and Peptides*. Totowa: Humana Press.

Charlton, S., M. Alexander, M. Collins, N. Milner, P. Mellars, T. O'Connell, R. Stevens and O. Craig, 2016. Finding Britain's last hunter-gatherers: A new biomolecular approach to 'unidentifiable' bone fragments utilising bone collagen. *Journal of Archaeological Science* 73, 55-61. **DOI:** 10.1016/j.jas.2016.07.014.

Chen, P., A. Lin, Y. Seki, A. Stokes, J. Peyras, E. Olevsky, M. Meyers and J. McKittrick, 2008. Structure and mechanical properties of selected biological materials. *Journal of the Mechanical Behaviour of Biomedical Materials* 1, 208-226. **DOI:** 10.1016/j.jmbbm.2008.02.003.

Chen, P., A. Stokes, J. McKittrick, 2009. Comparison of the structure and mechanical properties of bovine femur bone and antler of the North American elk (*Cervus elaphus canadensis*). *Acta Biomaterialia* 5, 693-706. **DOI:** 10.1016/j.actbio.2008.09.011.

Chen, L., Q. Shi, Y. Sun, T. Nguyen, C. Lee and S. Soh, 2018. Controlling surface charge generated by contact electrification: strategies and applications. *Advanced Materials* 30(1802405), 1-15. **DOI:** 10.1002/adma.201802405.

Choudhury, A., D. Lahiri Choudhury, A. Desai, J. Duckworth, P. Easa, A. Johnsingh, P. Fernando, S. Hedges, M. Gunawardena, F. Kurt, U. Karanth, A. Lister, V. Menon, H. Riddle, A. Rübel and E. Wikramanayake, 2008. *Elephas maximus*. *The IUCN Red List of Threatened Species* 2008: e.T7140A12828813. **DOI:** 10.2305/IUCN.UK.2008.RLTS.T7140A12828813.en.

Coles, B., 2000. Doggerland: the cultural dynamics of a shifting coastline, in: Pye, K. and J. Allen (eds), *Coastal and Estuarine Environments: sedimentology, geomorphology and geoarchaeology*. London: The Geological Society of London, 393-401. **DOI:** 10.1144/GSL.SP.2000.175.01.27.

Collins, M., M. Buckley, H. Grundy, J. Thomas-Oates, J. Wilson and N. van Doorn, 2010. ZooMS: the collagen barcode and fingerprints. *Spectroscopy Europe* 22(2), 6-10.

Coutu, A., G. Whitelaw, P. le Roux and J. Sealy, 2016. Earliest Evidence for the Ivory Trade in Southern Africa: Isotopic and ZooMS Analysis on Seventh-tenth Century AD Ivory from KwaZulu-Natal. *African Archaeological Review* 33, 411-435. **DOI:** 10.1007/s10437-016-9232-0.

Crees, J. and S. Turvey, 2014. Holocene extinction dynamics of *Equus hydruntinus*, a late-surviving European megafaunal mammal. *Quaternary Science Reviews* 91, 16-29. **DOI:** 10.1016/j.quascirev.2014.03.003.

Cuijpers, S. and R. Lauwerier, 2008. Differentiating between bone fragments from horses and cattle: a histological identification method for archaeology. *Environmental Archaeology* 13(2), 165-179. **DOI:** 10.1179/174963108X343281.

Cunha, C., N. Almeida, B. Santander, T. Tomé, P. Saladié, A. Valera, N. Cabaço and A. Silva, 2016. A case of human bone chalcolithic technology from the Perdigões site (Alentejo, Portugal). *International Journal of Osteoarchaeology* 26, 1106-1112. **DOI:** 10.1002/oa.2518.

Currey, J., 1988a. The effect of porosity and mineral content on the Young's modulus of elasticity of compact bone. *Journal of Biomechanics* 21(2), 131-139. **DOI:** 10.1016/0021-9290(88)90006-1.

Currey, J., 1988b. The effects of drying and re-wetting on some mechanical properties of cortical bone. *Journal of Biomechanics* 21(5), 439-441. **DOI:** 10.1016/0021-9290(88)90150-9.

Currey, J., 1990. Physical characteristics affecting the tensile failure properties of compact bone. *Journal of Biomechanics* 23(8), 837-844. **DOI:** 10.1016/0021-9290(90)90030-7.

Currey, J., 2004. Incompatible mechanical properties in compact bone. *Journal of Theoretical Biology* 231, 569-580. **DOI:** 10.1016/j.jtbi.2004.07.013.

Currey, J., 2006. The adaptation of mechanical properties to different functions, in: Currey, J., *Bones: Structure and Mechanics*. Princeton: Princeton University Press, 124-145.

Currey, J., T. Landate-Castillejos, J. Estevez, F. Ceacero, A. Olguin, A. Garcia and L. Gallego, 2009. The mechanical properties of red deer antler bone when used in fighting. *The Journal of Experimental Biology* 212, 3985-3993. **DOI:** 10.1242/jeb.032292.

Derjaguin, B. and V. Smilga, 1967. Electronic theory of adhesion. *Journal of Applied Physics* 38(12), 4609-4616. **DOI:** 10.1016/0043-1648(68)90663-7.

Derjaguin, B., 1994. Problems of Adhesion. *Progress in Surface Science* 45(1-4), 233-231. **DOI:** 10.1016/0079-6816(94)90053-1.

Desmond, A., N. Barton, A. Bouzouggar, K. Douka, P. Fernandez, L. Humphrey, J. Morales, E. Turnern, M. Buckley, 2018. ZooMS identification of bone tools from the North African Later Stone Age. *Journal of Archaeological Science* 98, 149-157. **DOI:** 10.1016/j.jas.2018.08.012.

Diaz, A. and R. Felix-Navarro, 2004. A semi-quantitative tribo-electric series for polymeric materials: the influence of chemical structure and properties. *Journal of Electrostatics* 62, 277-290. **DOI:** 10.1016/j.elstat.2004.05.005.

Dickson, D.B., 2001. *Western European Mesolithic, in Peregrine, P.N. and M. Ember. Encyclopedia of prehistory. Vol. 4: Europe*. College Station, Texas: Texas A&M University, 436-444.

Dobberstein, R., M. Collins, O. Craig, G. Taylor, K. Penkman and S. Ritz-Timme, 2009. Archaeological collagen: Why worry about collagen diagenesis? *Archaeological and Anthropological Sciences* 1, 31-42. **DOI:** 10.1007/s12520-009-0002-7.

Dolotovskaya, S., J. Torroba Bordallo, T. Haus, A. Noll, M. Hofreiter, D. Zinner and C. Roos, 2017. Comparing mitogenomic timetress for two African savannah primate genera (*Chlorocebus* and *Papio*). *Zoological Journal of the Linnean Society* 181, 471-483. **DOI:** 10.1093/zoolinnean/zlx001.

Van Doorn, N., H. Holland and M. Collins, 2011. A novel and non-destructive approach for ZooMS analysis: ammonium bicarbonate buffer extraction. *Archaeological and Anthropological Sciences* 3, 281-289. **DOI:** 10.1007/s12520-011-0067-y.

Doroff, A. and A. Burdin, 2015. *Enhydra lutris*. *The IUCN Red List of Threatened Species* 2015: e.T7750A21939518. **DOI:** 10.2305/IUCN.UK.2015-2.RLTS.T7750A21939518.en.

Elton, S. and H. O'Regan, 2014. Macaques at the margins: the biogeography and extinction of *Macaca sylvanus* in Europe. *Quaternary Science Reviews* 96, 117-130. D**OI:** 10.1016/j.quascirev.2014.04.025.

D'Errico, F., J. Zilhão, M. Julien, D. Baffier and J. Pelegrin, 1998. Neanderthal acculturation in Western Europe. *Current Anthropology* 39, S1-S44. **DOI:** 10.1086/204689.

D'Errico, F., B. Borgia and A. Ronchitelli, 2012. Uluzzian bone technology and its implications for the origin of behavioural modernity. *Quaternary International* 259, 59-71. **DOI:** 10.1016/j.quaint.2011.03.039.

Fiddyment, S., B. Holsinger, C. Ruzzier, A. Devine, A. Binois, U. Albarella, R. Fischer, E. Nichols, A. Curtis, E. Cheese, M. Teasdale, C. Checkley-Scott, S. Milner, K. Rudy, E. Johnson, J. Vnouček, M. Garrison, S. McGrory, D. Bradley and M. Collins, 2015. Animal origin of 13th century uterine vellum revealed using noninvasive peptide fingerprinting. *PNAS* 112(49), 15066-15071. **DOI:** 10.1073/pnas.1512264112.

Fisher, R., 1922. On the interpretation of χ^2 from contingency tables, and the calculation of p. *Journal of the Royal Statistical Scoiety* 85(1), 87-94. **DOI:** 10.2307/2340521.

Galembeck, F., T. Burgo, L. Balestrin, R. Gouveia, C. Silva and A. Galembeck, 2014. Friction, tribochemistry and triboelectricity: recent progress and perspectives. *Royal Society of Chemistry Advances* 4, 64280-64298. **DOI:** 10.1039/c4ra09604e.

Garshelis, D., B. Scheick, D. Doan-Crider, J. Beecham and M. Obbard, 2016. *Ursus americanus*(errata version published in 2017). *The IUCN Red List of Threatened Species* 2016, e.T41687A114251609, accessed on 25-4-2019. **DOI:** 10.2305/IUCN.UK.2016-3.RLTS.T41687A45034604.en.

Gelatt, T., R. Ream and D. Johnson, 2015. *Callorhinus ursinus*. *The IUCN Red List of Threatened Species*2015, e.T3590A45224953, accessed on 25-4-2019. **DOI:** 10.2305/IUCN.UK.2015-4.RLTS.T3590A45224953.en.

Gelatt, T. and K. Sweeney, 2016. *Eumetopias jubatus*. *The IUCN Red List of Threatened Species* 2016, e.T8239A45225749. **DOI:** 10.2305/IUCN.UK.2016-1.RLTS.T8239A45225749.en, accessed on 25-4-2019.

Gilbert, C., A. Ropiquet and A. Hassanin, 2006. Mitochondrial and nuclear phylogenies of Cervidae (Mammalia, Ruminantia): Systematics, morphology, and biogeography. *Molecular Phylogenetics and Evolution* 40, 101-117. **DOI:** 10.1016/j.ympev.2006.02.017.

Goodrich, J., A. Lynam, D. Miquelle, H. Wibisono, K. Kawanishi, A. Pattanavibool, S. Htun, T. Tempa, J. Karki, Y. Jhala and U. Karanth, 2015. *Panthera tigris*. *The IUCN Red List of Threatened Species* 2015: e.T15955A50659951, accessed on 25 April 2019. **DOI:** 10.2305/IUCN.UK.2015-2.RLTS.T15955A50659951.en.

Greenblatt, MTsai and M. Wein, 2017. Bone turnover markers in the diagnosis and monitoring of metabolic bone disease. *Clinical Chemistry* 63(2), 464-474. **DOI:** 10.1373/clinchem.2016.259085.

Guerrera, I. and O. Kleiner, 2005. Application of mass spectrometry in proteomics. *Bioscience Reports* 25(1/2), 71-93. **DOI:** 10.1007/s10540-005-2849-x.

Hays, D. and J. Sheflin, 2005. Electrostatic adhesion of ion and triboelectric-charged particles. *Journal of Electrostatics* 63, 687-692. **DOI:** 10.1016/j.elstat.2005.03.031

Heckel, C., K. Müller, R. White, H. Floss, B. Conrad and I. Reiche, 2014. Micro-PIXE/PIGE analysis of Palaeolithic mammoth ivory: Potential chemical markers of provenance and relative dating. *Palaeogeography, Palaeoclimatology, Palaeoecology* 416, 133-141. **DOI:** 10.1016/j.palaeo.2014.09.010.

Heckel, C., K. Müller, R. White, S. Wolf, N. Conrad, C. Normand, H. Floss and I. Reiche, 2016. F-content variation in mammoth ivory from Aurignacian context: Preservation, alteration, and implications for ivory-procurement strategies. *Quaternary International* 403, 40-50. **DOI:** 10.1016/j.quaint.2015.11.105.

Higham, T., R. Jacobi, M. Julien, F. David, L. Basell, R. Wood, W. Davies and C. Ramsey, 2010. Chronology of the Grotte du Renne (France) and implications for the context of ornaments and human remains within the Châtelperronian. *PNAS* 107(47), 20234-20239. **DOI:** 10.1073/pnas.1007963107.

Hillier, M. and L. Bell, 2007. Differentiating human bone from animal bone: a review of histological methods. *Journal of Forensic Science* 52(2), 249-263. **DOI:** 10.1111/j.1556-4029.2006.00368.x.

Horn, R. and D. Smith, 1992. Contact electrification and adhesion between dissimilar materials. *Science* 256(5055), 362-364. **DOI:** 10.1126/science.256.5055.362.

Hublin, J., 2015. The modern human colonisation of western Eurasia: when and where? *Quaternary Science Reviews* 118, 194-210. **DOI:** 10.1016/j.quascirev.2014.08.011.

Izadi, H. and A. Penlidis, 2013. Polymeric bio-inspired dry adhesives: Van der Waals or electrostatic interactions? *Macromolecular Reaction Engineering* 7, 588-608. **DOI:** 10.1002/mren.201300146.

Izadi, H., K. Stewart and A. Penlidis, 2014. Role of contact electrification and electrostatic interactions in gecko adhesion. *Journal of the Royal Society Interface* 11, 1-4. **DOI:** 10.1098/rsif.2014.0371.

Izadi, H. and A. Zandieh, 2017. Bio-inspired dry adhesives: contact electrification and electrostatic interactions, in *Kirk-Othmer Encyclopedia of Chemical Technology*. John Wiley & Sons, 1-35. **DOI:** 10.1002/0471238961.koe00034.

Jin, J. and P. Shipman, 2010. Documenting natural wear on antlers: a first step in identifying use-wear on purported antler tools. *Quaternary International* 211, 91-102. **DOI:** 10.1016/j.quaint.2009.06.023.

Jöris, O. and M. Street, 2008. At the end of the ^{14}C time scale – the Middle to Upper Palaeolithic record of western Eurasia. *Journal of Human Evolution* 55, 782-802. **DOI:** 10.1016/j.jhevol.2008.04.002.

Kays, R. 2018. *Canis latrans*. *The IUCN Red List of Threatened Species* 2018, e.T3745A103893556. **DOI:** 10.2305/IUCN.UK.2018-2.RLTS.T3745A103893556.en.

Keller, T., Z. Mao and D. Spengler, 1990. Young's modulus, bending strength, and tissue physical properties of human compact bone. *Journal of Orthopaedic Research* 8, 592-603. **DOI:** 10.1002/jor.1100080416.

Kendall, C., A. Eriksen, I. Kontopoulos, M. Collins, and G. Turner-Walker, 2018. Diagenesis of archaeological bone and tooth, 2018. *Palaeogeography, Palaeoclimatology, Palaeoecology* 491, 21-37. **DOI:** 10.1016/j.palaeo.2017.11.041.

Kieser, D., S. Kanade, N. Waddell, J. Kieser, J. Theis and M. Swain, 2014. The deer femur – a morphological and biomechanical animal model of the human femur. *Bio-Medical Materials and Engineering* 24, 1693-1703. **DOI:** 10.3233/BME-140981.

Kirby, D., M. Buckley, E. Promise, S. Trauger and T. Holdcraft, 2013. Identification of collagen-based materials in cultural heritage. *Analyst* 138, 4849-4858. **DOI:** 10.1039/c3an00925d.

Knecht, H., 1993. Early Upper Palaeolithic approaches to bone and antler projectile technology. *Archaeological Papers of the American Anthropological Association* 4, 33-47. **DOI:** 10.1525/ap3a.1993.4.1.33.

Kovacs, K., 2006. *Erignathus barbatus. The IUCN Red List of Threatened Species 2016*, e.T8010A45225428. **DOI:** 10.2305/IUCN.UK.2016-1.RLTS.T8010A45225428.en.

Kumar, G, 2011. *Orban's Oral Histology & Embryology*. Elsevier India. **E-ISBN:** 9788131238011.

Lahr, M. and R. Foley, 1998. Towards a theory of modern human origins: geography, demography and diversity in recent human evolution. *Yearbook of physical anthropology* 41, 137-176. **DOI:** 10.1002/(SICI)1096-8644(1998)107:27+<137::AID-AJPA6>3.0.CO;2-Q.

Landete-Castillejos, T., J. Currey, J. Estevez, E. Gaspar-López, A. Garcia and L. Gallego, 2007. Influence of physiological effort of growth and chemical composition on antler bone mechanical properties. *Bone* 41, 794-803. **DOI:** 10.1016/j.bone.1007.07.013.

Langley, M., 2016. Late Pleistocene osseous projectile technology and cultural variability, in Langley, M. (ed), *Osseous Projectile Weaponry. Vertrebrate Paleobiology and Paleonanthropology.* Dordrecht: Springer. **DOI:** 10.1007/978-94-024-0899-7_1.

Leary, J., 2009. Perceptions of and responses to the Holocene flooding of the North Sea lowlands. *Oxford Journal of Archaeology* 28(3), 227-237. **DOI:** 10.1111/j.1468-0092.2009.00326.x.

Lebon M., A. Zazzo and I. Reiche, 2014. Screening in situ bone and teeth preservation by ATR-FTIR mapping. *Palaeogeography, Palaeoclimatoloy, Palaeoecology* 416, 110-119. **DOI:** 10.1016/j.palaeo.2014.08.001.

Lévêque, F., 1979. Note a propos de trois gisements Castelperroniens de Poitou-Charentes. *Dialektikê Cahiers de Typologie Analytique*, 25-40. **DOI**: 10.5281/zenodo.2584119.

Lévêque, F., G. Gouraud and F. Bouin, 1997. Contribution à l'étude des occupations préhistoriques de la grotte de la grande roche de la plématrie à Quinçay (Vienne). *Group vendéen d'études préhistoriques* 33, 5-8.

Li, X., C. Lin and P. O'Connor, 2010. Glutamine deamidation : differentiation of glutamic acid and y-glutamic acid in peptides by electron capture dissociation. *Analytical Chemistry* 82(9), 3606-3615. **DOI :** 10.1021/ac9028467.

Lister, A., 1984. Evolutionary and ecological origins of British deer. *Proceedings of the Royal Society of Edinburgh* 82B, 205-229. **DOI:** 10.1017/S0269727000003754.

Lister, A. and A. Stuart, 2019. The extinction of the giant deer *Megaloceros giganteus* (Blumenbach): New radiocarbon evidence. *Quaternary International*, 1-19. **DOI:** 10.1016/j.quaint.2019.03.025.

Locke, M., 2008. Structure of ivory. *Journal of Morphology* 269, 423-450. **DOI:** 10.1002/jmor.10585.

Lorenzen, E., P. Arctander and H. Siegismund, 2006. Regional genetic structuring and evolutionary history of the impala *Aepyceros melampus*. *Journal of Heredity* 97(2), 119-132. **DOI:** 10.1093/jhered/esj012.

Lowell, J. and A. Rose-Innes, 2012. Contact electrification. *Advances in Physics* 29(6), 947-1023. **DOI:** 10.1080/00018738000101466.

Lowenstein, J. and G. Scheuenstuhl, 2015. Immunological methods in molecular palaeontology. *Philosophical Transactions of the Royal Society B Biological Sciences* 333, 375-380. **DOI:** 10.1098/rstb.1991.0087.

MacGregor, A. and J. Currey, 1983. Mechanical properties as conditioning factors in the bone and antler industry of the 3rd to the 13th century AD. *Journal of Archaeological Science* 10, 71-77. **DOI:** 10.1016/0305-4403(83)90129-2.

Manfredi, M., E. Barberis, F. Gosetti, E. Conte, G. Gatti, C. Mattu, E. Robotti, G. Zilberstein, I. Koman, S. Zilberstein, E. Marengo and P. Righetti, 2017. Method for non-invasive analysis of proteins and small molecules from ancient objects. *Analytical Chemistry* 89, 3310-3317. **DOI:** 10.1021/acs.analchem.6b03722.

Margaris, A., 2006. *Alutiiq engineering: the mechanics and design of skeletal technologies in Alaska's Kodiak archipelago* (PhD thesis, University of Arizona).

Martisius, N., F. Welker, T. Dogandžic, M. Grote, W. Rendu, V. Sinet-Mathiot, A. Wilcke, S. McPherron, M. Soressi and T. Steele, under review. Non-destructive ZooMS identification reveals strategic bone tool raw material selection by Neanderthals. *Science Reports*.

Masini, F. and S. Lovari, 1988. Systematics, phylogenetic relationships and dispersal of the chamois (*Rupicapra* spp.) *Quaternary Research* 30, 339-349. **DOI:** 10.1016/0033-5894(88)90009-9.

Matsusaka, S., H. Maruyama, T. Matsuyama and M. Ghadiri, 2010. Triboelectric charging of powders: A review. *Chemical Engineering Science* 65, 5781-5807. **DOI:** 10.1016/j.ces.2010.07.005.

Meijaard, E. and C. Groves, 2004. Morphometrical relationships between South-east Asian deer (Cervidae, tribi Cervini): evolutionary and biogeographic implications. *Journal of Zoology, London* 263, 179-196. **DOI:** 10.1017/S0952836904005011.

Mesquida, P., D. Kohl, O. Andriotis, P. Thurner, M. Duer, S. Bansode and G. Schitter, 2018. Evaluation of surface charge shift of collagen fibrils exposed to glutaraldehyde. *Scientific Reports* 8(10126), 1-7. **DOI:** 10.1038/s41598-018-28293-1.

Molnár, I. and C. Horváth, 1976. Reverse-phase chromatography of polar biological substances: separation of catechol compounds by high-performance liquid chromatography. *Clinical Chemistry* 22(9), 1497-1502.

Moree, J. and M. Sier (eds), 2015. Twenty metres deep! The Mesolithic period at the Yangtze Harbour site – Rotterdam Maasvlakte, the Netherlands. Early Holocene landscape development and habitation. *BOORrapporten 566*. Bureau Oudheidkundig Onderzoek Rotterdam, Rotterdam.

Nadachowski, A., G. Lipecki, U. Ratajczak, K. Stefaniak and P. Wojtal, 2016. Dispersal events of the saiga antelope (*Saiga tartarica*) in Central Europe in response to the climatic fluctuations in MIS 2 and the early part of MIS 1. *Quaternary International* 420, 357-362.
DOI: 10.1016/j.quaint.2015.11.068.

Nocete, F., J. Vargas, T. Schuhmacher, A. Banerjee and W. Dindorf, 2013. The ivory workshop of Valencina de la Concepción (Seville, Span) and the identification of ivory from Asian elephant on the Iberian Peninsula in the first half of the 3rd millennium BC. *Journal of Archaeological Science* 40, 1579-1592. **DOI:** 10.1016/j.jas.2012.10.028.

Ostrom, P., M. Schall, H. Gandhi, T. Shen, P. Hauschka, J. Strahler and D. Gage, 2000. New strategies for characterising ancient proteins using matrix-assisted laser desorption ionisation mass spectrometry. *Geochimica et Cosmochimica Acta* 64(6), 1043-1050. **DOI:** 10.1016/S0016-7037(99)00381-6.

Overton, N. and B. Elliot, 2018. Animals in a wider context. In Milner, N., C. Conneller and B. Taylor (eds), *Star Carr Volume 2: Studies in Technology, Subsistence and Environment*. York: White Rose University Press, 334-343. **DOI:** 10.22599/book2.

Pasty, J., S. Costamagno, V. Mistrot, V. Laroulandie, P. Alix, C. Ballut, H. Pasty-Vande Walle and R. Murat, 2012. Biostratigraphic and palaeoenvironmental implications of the Middle Palaeolithic and

Châtelperronian occupations of La Tour Fondue site in Chauriat (Puy-de-Dôme, France). *Paleo, Revue d'archéologie préhistorique* 23, 1-38.

Peeters, J. and G. Momber, 2014. THe southern North Sea and the human occupation of northwest Europe after the Last Glacial Maximum. *Netherlands Journal of Geosciences* 93(1-2), 55-70. **DOI:** 10.1017/njg.2014.3.

Persson, B., M. Scaraggi, A. Volokitin and M. Chaudhury, 2013. Contact electrification and the work of adhesion. *EPL* 103(36003), 1-5. **DOI:** 10.1209/0295-5075/103/36003.

Pfeifer, S., W. Hartramph, R. Kahlke and F. Müller, 2019. Mammoth ivory was the most suitable osseous raw material for the production of the Late Pleistocene big game projectile points. *Scientific Reports* 9(2303), 1-10. **DOI:** 10.1038/s41598-019-38779-1.

Plicht, J. van der, L. Amkreutz, M. Niekus, J. Peeters and B. Smit, 2016. Surf'n turf in Doggerland, dating, stable isotopes and diet of Mesolithic human remains from the southern North Sea. *Journal of Archaeological Science: Reports* 10, 110-118. **DOI:** 10.1016/j.jasrep.2016.09.008.

Pokines, J., 1998. Experimental replication and use of cantabrian Lower Magdalenian antler projectile points. *Journal of Archaeological Science* 25, 875-886. **DOI:** 10.1006/jasc.1997.0269.

Richards, J., D. Cram and G. Hammond, 1967. *Elements of organic chemistry.* Kogakusha: McGraw-Hill.

Reilly, D. and A. Burstein, 1975. The elastic and ultimate properties of compact bone tissue. *Journal of Biomechanics* 8(6), 393-396. **DOI:** 10.1016/0021-9290(75)90075-5.

Roussel, M. and M. Soressi, 2010. La Gronde Roche de la Plématrie à Quinçay (Vienne). L'évolution du Châtelperronien revisitée, in Buisson-Catil, J. and J. Primault (eds), *Préhistoire entre Vienne et Charente – Hommes et sociétés du Paléolithique*. Chauvigny: Association des Publications Chauvinoises, 203-219.

Roussel, M., M. Soressi and J. Hublin, 2016. The Châtelperronian conundrum: Blade and bladelet lithic technologies from Quinçay, France. *Journal of Human Evolution* 95, 13-32. **DOI:** 10.1016/j.jhevol.2016.02.003.

Ruebens, K., S. McPherron and J. Hublin, 2015. On the local Mousterian origin of the Châtelperronian: Integrating typo-technological, chronostratigraphic and contextual data. *Journal of Human Evolution* 86, 55-91. **DOI:** 10.1016/j.jhevol.2015.06.011.

Ruffatto, D., A. Parness and M. Spenko, 2014. Improving controllable adhesion on both rough and smooth surfaces with a hybrid electrostatic/gecko-like adhesive. *Journal of the Royal Society* 11(20131089), 1-10. **DOI:** 10.1098/rsif.2013.1089.

Rybczynski, N., J. Gosse, C. Harington, R. Wogelius, A. Hidy and M. Buckley, 2013. Mid-Pliocene warm-period deposits in the High Arctic yield insight into camel evolution. *Nature Communications* www.nature.com/naturecommunications. **DOI:** http://dx.doi.org/10.1038/ncomms2516.

Schulz, E. and T. Kaiser, 2013. Historical distribution, habitat requirements and feeding ecology of the genus *Equus* (Perissodactyla). *Mammal Review* 43, 111-123. **DOI:** 10.1111/j.1365-2907.2012.00210.x.

Shah, S., J. DesJardins and R. Blob, 2008. Antler stiffness in caribou (*Rangifer tarandus*): Testing variation in bone material properties between males and females. *Zoology* 111, 476-482. **DOI:** 10.1016/j.zool.2007.12.001.

Shoulders, M. and R. Raines, 2009. Collagen structure and stability. *The Annual Review of Biochemistry* 78, 929-958. **DOI:** 10.1146/annurev.biochem.77.032207.120833.

Simpson, J., K. Penkman, B. Demarchi, H. Koon, M. Collins, J. Thomas-Oates, B. Shapiro, M. Stark and J. Wilson, 2016. The effects of demineralisation and sampling point variability on the measurement of glutamine deamidation in type I collagen extracted from bone. *Journal of Archaeological Science* 69, 29-38. **DOI:** 10.1016/j.jas.2016.02.002.

Soltysiak, A. and A. Gręzak, 2015. Worked human femur from Gohar Tepe, Iran. *International Journal of Osteoarchaeology* 25, 361-365. **DOI:** 10.1002/oa.2296.

Sommer, R., J. Kalbe, J. Ekström, N. Benecke and R. Liljegren, 2014. Range dynamics of the reindeer in Europe during the last 25,000 years. *Journal of Biogeography* 41, 298-306. **DOI:** 10.1111/jbi.12193.

Spithoven, M., 2015. *Spitsen van been en gewei uit Zuid-Holland, Nederland, een typologische intra-site vergelijking.* Leiden (unpublished Bachelor thesis Leiden University).

Spithoven, M., 2018. *Mesolithic Doggerland, where the points are small, a functional analysis of the small barbed bone points*. Leiden (unpublished Master thesis Leiden University).

Staubwasser, M., V. Drăguşin, B. Onac, S. Assonov, V. Ersek, D. Hoffmann and Daniel Veres, 2018. Impact of climate change on the transition of Neanderthals to modern humans in Europe. *PNAS* 115(37), 9116-9121. **DOI:** 10.1073/pnas.1808647115.

Stewart, J., T. van Kolfschoten, A. Markova and R. Musil, 2003. Neanderthals as part of the broader Late Pleistocene megafaunal extinctions? In Ander, T. van and W. Davies (eds), *Neanderthals and*

Modern Humans in the European Landscape during the Last Glaciation: Archaeological Results of the Stage 3 Project. Camebridge: McDonald Institute for Archaeological Research, 221-231.

Strohalm, M., D. Kavan, P. Novak, M. Volný and V. Havlíček, 2010. mMass 3: a cross-platform software environment for precise analysis of mass spectrometric data. *Analytical Chemistry* 82(11), 4648-4651. **DOI:** 10.1021/ac100818g.

Stryer, L., 1981. *Biochemistry*. New York: W. H. Freeman and Company.

Stuart, A., 2005. The extinction of woolly mammoth (*Mammuthus primigenius*) and straight-tusked elephant (*Palaeoloxodon antiquus*) in Europe. *Quaternary International* 126-128, 171-177. **DOI:** 10.1016/j.quaint.2004.04.021.

Swaisgood, R., D. Wang and F. Wie, 2017. *Ailuropoda melanoleuca*. *The IUCN Red List of Threatened Species* 2016, e.T712A121745669, accessed on 25-4-2019.

Tripp, J., M. Squire, R. Hedges and R. Stevens, 2018. Use of micro-computed tomography imaging and porosity measurements as indicators of collagen preservation in archaeological bone. *Palaeogeography, Palaeoclimatology, Palaeoecology* 511, 462-471.
DOI: 10.1016/j.palaeo.2018.09.012.

Turvey, S., J. Hansford, S. Brace, V. Mullin, S. Gu and G. Sun, 2016. Holocene range collapse of giant muntjacs and pseudo-endemism in the Annamite large mammal fauna. *Journal of Biogeography* 43, 2250-2260. **DOI:** 10.1111/jbi.12763.

Tütken, T. and T. Vennemann, 2011. Fossil bones and teeth: Preservation or alteration of biogenic compositions? *Palaeogeography, Palaeoclimatology, Palaeoecology* 310, 1-8.
DOI: 10.1016/j.palaeo.2011.06.020.

Verhart, L., 1988. Mesolithic barbed points and other implements from Europoort, the Netherlands. *Oudheidkundige Mededelingen uit het Rijksmuseum van Oudheden te Leiden* 68, 145-194.

Verna, C. and F. d'Errico, 2011. The earliest evidence for the use of human bone as a tool. *Journal of Human Evolution* 60, 145-157. **DOI:** 10.1016/j.jhevol.2010.07.027.

Vervoort-Kerkhoff, Y. and T. van Kolfschoten, 1988. Pleistocene and Holocene mammalian faunas from the Maasvlakte near Rotterdam (The Netherlands). *Mededelingen Werkgroep voor Tertiare en Kwartaire Geologie* 25(1), 87-98.

Villaluenga, A., A. Arrizabalaga and J. Rios-Garaizar, 2012. Multidisciplinary approach to two Chatelperronian series: lower IX layer of Labeko Koba and X level of Ekain (Basque Country, Spain). *Journal of Taphonomy* 10(3-4), 499-520.

Visser, J., 1995. Particle adhesion and removal: a review. *Particulate Science and Technology* 13(3-4), 169-196. **DOI:** 10.1080/02726359508906677.

Vliet-Lanoë, B. van, D. Cliquet, P. Auguste, E. Folz, D. Keen, J. Schwenninger, N. Mercierm P. Alix, Y. Roupin, M. Meurisse and H. Seignac, 2006. L'abri sous-roche du Rozel (France, Manche): un habitat de la phase récente du Paléolithique moyen dans son contexte géomorphologique. *Quaternaire* 17(3), 207-258. **DOI :** 10.4000/quaternaire.826.

Wei, G., S. Hu, K. Yu, Y. Hou, X. Li, C. Jin, Y. Wang, J. Zhao and W. Wang, 2010. New materials oft he steppe mammoth, *Mammuthus trogontherii*, with discussion on the origin and evolutionairy patterns of mammoths. *Science China Earth Sciences* 53(7), 956-963. **DOI:** 10.1007/s11430-010-4001-4.

Welker, F., M. Soressi, W. Rendu, J. Hublin and M. Collins, 2015a. Using ZooMS to identify fragmentary bone from the Late Middle/Early Upper Palaeolithic sequence of Les Cottés, France. *Journal of Archaeological Science* 54, 279-286. **DOI:** 10.1016/j.jas.2014.12.010.

Welker, F., M. Collins, J. Thomas, M. Wadsley, S. Brace, E. Cappellini, S. Turvey, M. Reguero, J. Gelfo, A. Kramarz, J. Burger, J. Thomas-Oates, D. Ashford, P. Ashton, K. Rowsell, D. Porter, B. Kessler, R. Fischer, C. Baessmann, S. Kaspar, J. Olsen, P. Kiley, J. Elliott, C. Kelstrup, V. Mullin, M. Hofreiter, E. Willerslev, J. Hublin, L. Orlando, I. Barnes and R. MacPhee, 2015b. Ancient proteins resolve the evolutionary history of Darwin's South American ungulates. *Nature* 522, 81-84. **DOI:** 10.1038/nature14249.

Welker, F., M. Hajdinjak, S. Talamo, K. Jaouen, M. Dannemann, F. David, M. Julien, M. Meyer, J. Kelso, I. Barnes, S. Brace, P. Kamminga, R. Fischer, B. Kessler, J. Stewart, S. Pääbo, M. Collins and J. Hublin, 2016. Palaeoproteomic evidence identifies archai hominins associated with the Châtelperronian at the Grotte du Renne. *PNAS* 113(40), 11162-11167. **DOI:** 10.1073/pnas.1605834113.

Welker, F., G. Smith, J. Hutson, L. Kindler, A. Garcia-Moreno, A. Villaluenga, E. Turner and S. Gaudzinski-Windheuser, 2017a. Middle Pleistocene protein sequences from the rhinoceros genus *Stephanorhinus* and the phylogeny of extant and extinct Middle/Late Pleistocene Rhinocerotidae. *PeerJ* 5, 3033. **DOI:** 10.7717/peerj.3033.

Welker, F., M. Soressi, M. Roussel, I. van Riemsdijk, J. Hublin and M. Collins, 2017b. Variations in glutamine deamidation for a Châtelperronian bone assemblage as measured by peptide mass fingerprinting of collagen. *Science & Technology of Archaeological Research* 3(1), 15-27. **DOI:** 10.1080/20548923.2016.1258825.

Welker, F., 2018. Palaeoproteomics for human evolution studies. *Quaternary Science Reviews* 190, 137-147. **DOI:** 10.1016/j.quascirev.2018.04.033.

Wiig, Ø., S. Amstrup, T. Atwood, K. Laidre, N. Lunn, M. Obbard, E. Regehr and G. Thiemann, 2015. *Ursus maritimus*. *The IUCN Red List of Threatened Species* 2015: e.T22823A14871490, accessed on 25-4-2019. **DOI:** 10.2305/IUCN.UK.2015-4.RLTS.T22823A14871490.en.

Williams, M., 2012. What creates static electricity? *American Scientist* 100, 316-323.

Wißing, C., H. Rougier, I. Crevecoeur, M. Germonpré, Y. Naito, P. Semal and H. Bocherens, 2016. Isotopic evidence for dietary ecology of late Neanderthals in North-Western Europe. *Quaternary International* 411, 327-345. **DOI:** 10.1016/j.quaint.2015.09.091.

Wood, J. and B. Fitzhugh, 2018. Wound ballistics: the prey specific implications of penetrating trauma injuries from osseous, flaked stone, and composite inset microblade projectiles during the Pleistocene/Holocene transition, Alaska U.S.A. *Journal of Archaeological Science* 91, 104-117. **DOI:** 10.1016/j.jas.2017.10.006.

Zhou, Y., S. Wang, Y. Yang, G. Zhu, S. Niu, Z. Lin, Y. Liu and Z. Wang, 2014. Manipulating nanoscale contact electrification by an applied electric field. *Nano Letters* 14, 1567-1572. **DOI:** 10.1021/nl404819w.

Zilhão, J., F. d'Errico, J. Bordes, A. Lenoble, J. Texier and J. Rigaud, 2006. Analysis of Aurignacian interstratification at the Châtelperronian-type site and implications for the behavioural modernity of Neanderthals. *PNAS* 103(33), 12643-12648. **DOI:** 10.1073/pnas.0605128103.

Websites:

https://www.britannica.com/science/hydrolysis, accessed on 27-4-2019.

https://www.britannica.com/animal/mastodon, accessed on 25-4-2019.

www.creative-proteomics.com/technology/maldi-tof-mass-spectrometry.htm, accessed on 27-4-2019.

https://www.thermofisher.com/nl/en/home/life-science/protein-biology/protein-mass-spectrometry-analysis/sample-prep-mass-spectrometry/c18-columns-peptide-clean-up-mass-spectrometry.html, accessed on 23-4-2019.

List of figures

Figures

Tables

Appendices

Appendix A: Archaeological context

A.1 Quinçay

Quinçay is a limestone cave near Poitiers, in western France. It was excavated by François Lévêque from 1968 to 1990. The cave can be divided into two parts, a front area with numerous limestone blocks, and the back, which lacks large limestone blocks (fig. 21) (Lévêque 1997, 5). In the front area the names of stratigraphical units start with E, while the stratigraphic units start with an S in the back area (Welker *et al.* 2017b, 16). The back area was the focus of the 1968-1990 excavation (Lévêque *et*

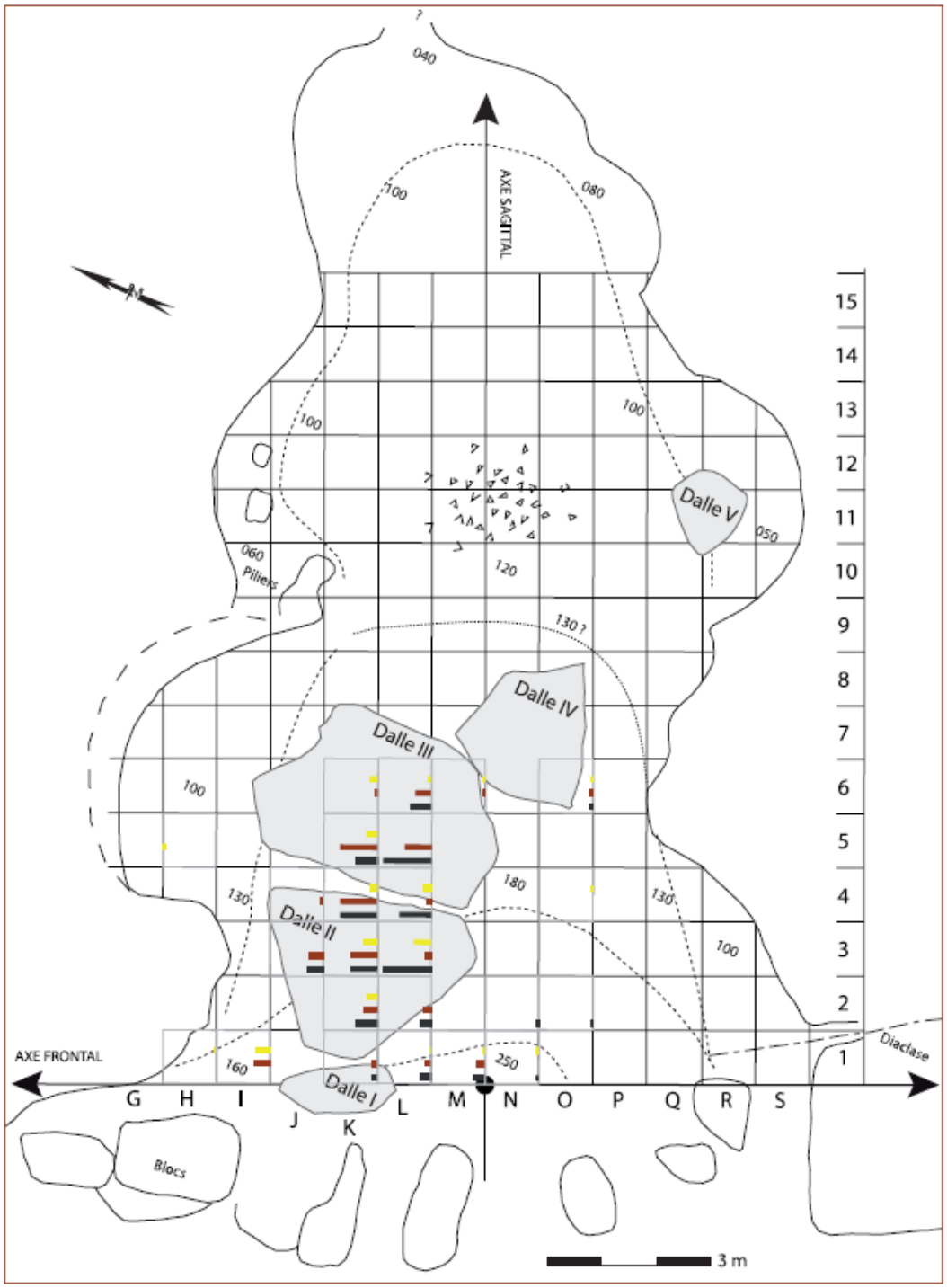

Figure 21 Excavation plan of Quinçay (Roussel and Soressi 2010, 205).

al. 1997, 5). Lévêque described four main archaeological layers in the front part of the site: Ej, Em, En and Eg (from top to bottom) (Lévêque 1979, 25-26). Each front layer is linked with a posterior layer: Ej is linked to Sj, Em to Sm, Sfs and Sj, En to Sfi and Eg to Sg. Layers Ej, Em and En are attributed to the Châtelperronian (Lévêque 1979, 25), while Eg has been attributed to the Mousterian of the Acheulean Tradition (Roussel and Soressi 2010, 217). Some Mesolithic and Neolithic artefacts were found on the surface of the cave as well, but these periods do not constitute a separate layer (Lévêque 1997, 5). The layers Em and En contain the most artefacts. Compared to each other, Em contains more retouched tools, while En contains more flakes (Lévêque 1979, 25). The fact that most retouched tools were found in Em most likely correlates with the fact that the possible bone tools predominantly originate from Em.

A.2 The Châtelperronian

To put the species interpretation of the Quinçay artefacts in perspective it is important to understand their context, including the associated culture. All the Quinçay artefacts come from the Châtelperronian, which is a culture from southwest France dated to 41-38 ka (Jöris and Street 2008, 782-789). The dating of the Châtelperronian is controversial because of unreliability in the ^{14}C dates (Ruebens *et al.* 2015, 77).

The Châtelperronian is considered to be one of the transitional industries. The transitional industries are thought to represent the technological transition from the Middle Palaeolithic to the Upper Palaeolithic. The Châtelperronian does not constitute a distinct time period on a continental scale. Both Middle Palaeolithic (Mousterian) and Upper Palaeolithic (Proto-Aurignacian) sites are contemporary to Châtelperronian sites. However, on a local scale the three are distinct (Ruebens *et al.* 2015, 79). The change from Middle to Upper Palaeolithic is often equated with a transition from Neanderthals to AMH (Anatomically Modern Humans) in Europe (Lahr and Foley 1998, 157). The Châtelperronian seems to dispute this association. The Châtelperronian features characteristics of Upper Palaeolithic industries (Hublin 2015, 200; Higham *et al.* 2010, 20234). Yet technological analysis (Ruebens *et al.* 2015, 76), stratigraphical analysis (Welker *et al.* 2016, 11166; Zilhão *et al.* 2006, 12648) and the hominin remains found in Châtelperronian layers (Hublin 2015, 201; Welker *et al.* 2017b, 25) all indicate an association between the Châtelperronian and Neanderthals.

The authorship of the Châtelperronian is relevant for the interpretation of the species identification by ZooMS for several reasons. First of all formal bone tools have often been referred to as a hallmark of modern behaviour (d'Errico *et al.* 2012, 59). If the ZooMS analysis shows that there was a clear selection for certain species in tool production, this would support the view that Neanderthals made formal bone tools and thus had modern behaviour. Secondly, in order to interpret whether the tools

were made of the most available species or whether there was selection on other criteria, the diet of the producers must be known. If it is known, which species produced the tools, then stable isotope analyses of relevant hominin remains combined with the remains of butchered fauna can be used to reconstruct their diet.

The Châtelperronian seems to be trapped between two cold phases (Staubwasser *et al.* 2018, 9116), which were characterised by lower temperature, increased aridity and a reduction of forests in favour of steppes (Staubwasser *et al.* 2018, 9118-9119). This last cold phase seems to have caused a reduction in hominin activity. At several sites a nearly artefact sterile layer is found above the Châtelperronian (Staubwasser *et al.* 2018, 9120).

The faunal remains at Châtelperronian sites provide a hypothesis for what the species distribution of the Châtelperronian bone tools should be, if there is no selection for particular animals. If the species distribution of the bone tools differs significantly from the common species distribution at Châtelperronian sites, it seems likely that there was a selection for certain specific animals. The macrofauna at many Châtelperronian sites is composed of mainly bovids, reindeer and horses (Welker *et al.* 2015a, 282), indicating a cold climate (Pasty *et al.* 2012, 34). The bovids are thought to be the most commonly hunted species at Châtelperronian sites (Bocherens *et al.* 2014, 35). However, there is large variation in Neanderthal diet. For example, late Neanderthals at Goyet, Belgium, seem to have predominantly eaten mammoths (Wißing *et al.* 2016, 342).

A.3 Mesolithic Doggerland

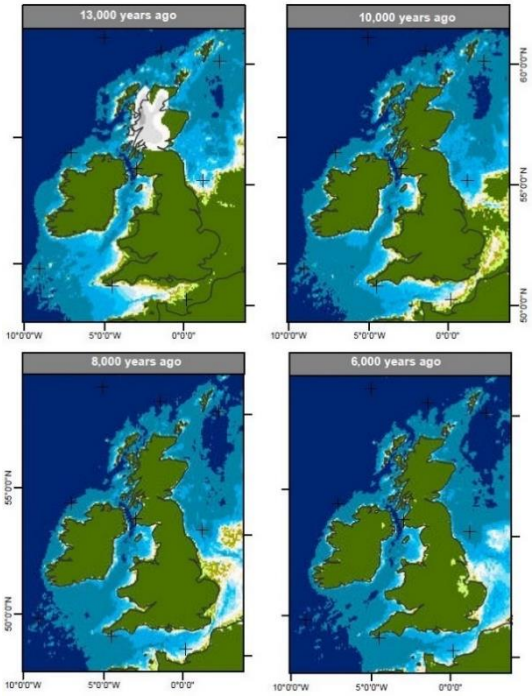

Figure 22 Changing size of Doggerland through time, (Brooks et al. 2011).

Figure 23 Extent of Doggerland around 10 ka. Red dot denotes Maasvlakte 2, Moree and Sier 2015, 313.

Doggerland is the name for the parts of the North Sea that were dry during much of the Pleistocene up to the Mesolithic (Coles 2000, 393). It is named after the Dogger Bank, fish rich shallows in the North Sea. At the end of the Palaeolithic, Doggerland connected the British Isles to the European mainland and the North Sea was dry up to the latitude of York, (fig. 22) (Brooks *et al.* 2011, appendix). At the beginning of the Holocene the sea level started to rise, steadily flooding Doggerland. During the Mesolithic Doggerland still covered a large part of the south of the North Sea and connected South England to the Netherlands and Germany (fig. 23) (Moree and Sier 2015, 313).

It is thought that throughout the flooding of Doggerland it was occupied by Anatomically Modern Humans (AMH) (Peeters and Momber 2014, 58-60). During the Mesolithic there were still only hunter-gatherers in Europe. The $\delta^{15}N$ of Mesolithic AMH found in the North Sea or on the coast of the Netherlands indicated that the protein in their diet originated from freshwater animals for the most part (Van der Plicht *et al.* 2016, 115).

Appendix B: Additional information on the analysed artefacts

Additional information on the Quinçay morphologically identified controls														
ZooMS Number	Box number	Unit	Square	Depth	TissueType	Morphological notes	Length before (mm)	Length after (mm)	Weight before (g)	Weight after (g)	Weight sample (mg)	Protocol	Sampling method	Sampling location comments
Q1.1		Sfs	7M(4-7)	16	Tooth	Lamella mammoth molar	42,9	41,6	8,86	8,80	30,4	CA	Pliers	Protrusion at the base
Q1.2		Sfs	7M(4-7)	16	Tooth	Lamella mammoth molar	42,9	41,6	8,86	8,80	22,6	B	Pliers	Protrusion at the base
Q1.3		Sfs	7M(4-7)	16	Tooth	Lamella mammoth molar	42,9		8,86			MB	MB	
Q2.1	2	Em	3K(4)	19	Tooth	Molar, *Cervus* sp.	23,6	23,3	4,85	4,79	19,3	CA	Pliers	Corner of the root
Q2.2	2	Em	3K(4)	19	Tooth	Molar, *Cervus* sp.	23,6	23,3	4,85	4,79	15,4	B	Pliers	Corner of the root
Q2.3	2	Em	3K(4)	19	Tooth	Molar, *Cervus* sp.	23,6		4,85			MB	MB	
Q3.1	4	Em	5L(8)	19	Tooth	Incisor, *Equus caballus* juvenile	37,6	37,4	10,24	10,02	14,4	CA	Pliers	Tip of the root
Q3.2	4	Em	5L(8)	19	Tooth	Incisor, *Equus caballus* juvenile	37,6	37,4	10,24	10,02	21,8	B	Pliers	Tip of the root
Q3.3	4	Em	5L(8)	19	Tooth	Incisor, *Equus caballus* juvenile	37,6		10,24			MB	MB	
Q4.1	3	Em	3L(7)	19	Bone	2nd phalange, *Sus* sp.	19,6	18,2	3,31	3,27	18,6	CA	Pliers	Edge at the base
Q4.2	3	Em	3L(7)	19	Bone	2nd phalange, *Sus* sp.	19,6	18,2	3,31	3,27	14,5	B	Pliers	Edge at the base
Q4.3	3	Em	3L(7)	19	Bone	2nd phalange, *Sus* sp.	19,6		3,31			MB	MB	
Q6.1	4	Sfj	8M(2)	18	Bone	Mandible, *Bos* sp., juvenile	64,2	64,2	10,45	10,36	23,5	CA	Pliers	Lower edge
Q6.2	4	Sfj	8M(2)	18	Bone	Mandible, *Bos* sp., juvenile	64,2	64,2	10,45	10,36	26,1	B	Pliers	Lower edge
Q6.3	4	Sfj	8M(2)	18	Bone	Mandible, *Bos* sp., juvenile	64,2	64,2	10,45	10,36		MB	MB	
Q7.1	3	Sf	7M(1)	12	Bone	Metacarpus, *Bos taurus* juvenile	30,1	28,4	7,84	7,78	25	CA	Pliers	Protrusion at the base
Q7.2	3	Sf	7M(1)	12	Bone	Metacarpus, *Bos taurus* juvenile	30,1	28,4	7,84	7,78	21,5	B	Pliers	Protrusion at the base
Q7.3	3	Sf	7M(1)	12	Bone	Metacarpus, *Bos taurus* juvenile	30,1		7,84			MB	MB	

Additional information on the Quinçay possible bone tools											
ZooMS number	Sample number	Unit	Square	Depth	TissueType	Morphological notes	Length (mm)	Width (mm)	Protocol	Sampling	Remarks
Q10	14	Em (f)	4k (3)	18	Bone	Most likely bone, either long bone of carnivore or small to medium size bone of big mammal (deer, horse). Pointy end on one side and fracture on other one (proximal?, distal?) heavy polishing on two surfaces. Long fracture on other (internal) side.	85	8	MB	MB	
Q11	10 (piece n1)	Sfs	8M (9)	20	Bone	Bone(?) fragment, (Awl ?, point ?) Distal end, Polished on three surfaces, Long fracture on one lateral surface, breaking fracture on marginal end.	43	7	MB	MB	
Q12	5	Em Sfs DIII	4L		Bone	Bone, distal end of a pointy object, squished on two sides, interesting aspects are the pointy end, and the fracture break at the marginal end. Also, presence of black points-striations.	50	12	MB	MB	
Q13	8	Em eff. DIII	4L		Bone	Bone, most certainly a rib, signs of polishing on the whole piece. Read note on actual piece for exact stratigraphic context (note in French)	115	8	MB	MB	
Q14	20	Sfj	8N (7+4+8)	21	Antler?	Antler (?) Distal End (Spear Point?). Fracture at both ends and lateral side toward the tip, heavy signs of dark areas (burning?), the internal side has a concave base, look for signs manufacture techniques (Splitting?)	80	15	MB	MB	
Q15	13	Sps	9N	21	Ivory?	Bone (?) could also be Ivory, Medial part, Fractures at both ends but different kinds of fractures: one end is more truncated while other one is more stepped. Light signs of parallel striations on longitudinal side, Signs of manufacture (Splitting)	70	13	MB	MB	
Q16	17	Ej-m (165-32-51)	3K (4)	17	Bone	Bone (?) Medial fragment of a Point or Awl, Fractured at both ends, Signs of polishing and parallel striations on the whole length, perpendicular cut marks at about half way.	48	5	MB	MB	
Q17	9	Ej or Em			Bone	Bone, distal end of a pointy object (Point?) Beautifully shaped, Signs of manufacture show no splitting but instead heavy grinding/polishing. Very interesting fracture on marginal end.	42	7	MB	MB	Def. tool
Q18	6	Sfs	8M (5)		Bone	Bone, Medial Fragment, Fractured on both ends, little black stains (Burning? Dirt?).	30	8	MB	MB	
Q19	2		10K (1)	15	Bone	Bone, (Point?, Awl?) distal end, Signs of polishing on the whole length, Small fracture break on the pointy tip and truncated fracture on other marginal end, light signs of black stains (burning? dirt?).	43	5	MB	MB	
Q20	15	DIII	4M		Bone	Bone (Looks like a flat bone) Medial Fragment, signs of polishing and cut marks on longer side, Fractures on concave side, Broke half way, Black and Brown stains, NOTE(Os Gravè).	75	11	MB	MB	Def. tool
Q21	3	Em (182-95-46)	3K (6)	19	Bone	Bone fragment, distal end, fairly thick so maybe large mammal (deer, horse), Very pointy and heavily polished End (Awl for hide working?), it seems no signs of manufacture (so perhaps was just a pointy Bone Fragment) but then heavily used on one side.	64	10	MB	MB	Def. tool

ZooMS number	Sample number	Unit	Square	Depth	TissueType	Morphological notes	Length (mm)	Width (mm)	Protocol	Sampling method	Remarks
Q22	16	Em	1K (8)	21	Bone	Bone Fragment, Medial part, fairly thick bone so maybe large mammal (deer, horse) long bone, No clear signs of manufacture and use (like splitting or polishing) but very interesting features. First, 8 parallel cut marks on long side unequally distributed (not regular) and also Brownish/Red stains (Ochre?)	63	14	MB	MB	Def. tool
Q23		Em	5K (5)	16	Ivory?	Bone(?) Ivory(?) Fragment, (Spear Point?) Distal End, looks like a flat long bone, presence of Black and Brown stains, Signs of Breaking on 4 parts (Post-depositional)	75	20	MB	MB	Def. tool
Q24	18	Em	3K (6)	19	Bone	Bone Fragment, Medial part, no signs of manufacture and light signs of use (polishing). Also, very interesting parallel striations (around 12) almost look red in colour	40	7	MB	MB	Def. tool
Q25		Em	5K (3)	17	Bone	Bone Fragment, Distal End, Breaking fractures on both Ends, Presence of dirt	34	13	MB	MB	
Q26	11 (piece n.8)	Sfs	8M (9)	20	Bone	Bone Fragment, Medial Part, Most likely a Rib judging from its shape, Brownish and Red stains present, light cut marks, light sign of use (polishing)	52	10	MB	MB	
Q27	4	Em	3K (6)	19	Bone	Bone Fragment, Medial Part of a relatively small bone, Possible signs of manufacture (Splitting) and polishing on one side, (inside small box)	30	10	MB	MB	
Q28	1	Em	5L (5-6) (190-56-55)	19	Bone	Bone Fragment, Distal pointy end, (Point? Awl?), light parallel to long axis, heavy signs of manufacture and use (shaping by grinding) and polishing, Look for breaking fracture on the tip, plus breaking fracture on other end.	30	4	MB	MB	Def. tool
Q29	19	Em	3L (4) (186-0-33)	19	Bone	Bone Fragment, Medial Part, Flat bone most likely Rib of a small mammal, Step fractures at both ends, little notch on one side near the End, Multiple Horizontal reddish striation marks, Breaking fracture perpendicular to long axis near the End	20	8	MB	MB	
Q30	12	Em	3J (3)	19	Bone	Bone Fragment, Rectangular shape, Could be splitted Rib of small mammal, Fractured at both ends and ventral side	15	8	MB	MB	
Q31		Em	3K (6)	20	Bone	Bone Fragment, Pointy shape, very small (Point? Awl?) Peculiar fracture on ventral side.	12	4	PB	PB	Def. tool

Reference table Quinçay dataset				
ZooMS number	**Q**(uinçay)X.Y, where the value of the suffix indicates the used protocol			
Box number	The number of the box from which the control samples were taken.			
Unit	Stratigraphical layer in which the bone fragment has been found.			
Cultural attribution	The cultural attribution of the bone fragment. All Quinçay samples are thought to be Châtelperronian.			
Square	The square according to the site grid, in which the fragment was found.			
Depth (arbitrary units)	The depth at which the fragment was found.			
Tissue Type	Antler	Bone	Ivory	Tooth
Length before (mm)	Length as measured before sampling.			
Length after (mm)	Length as measured after sampling.			
Weight before (g)	Weight as measured before sampling.			
Weight after (g)	Weight as measured after sampling.			
Weight sample (mg)	Weight of the sample as measured.			
Protocol	**CA** (Cold acid)	**B** (Ammonium bicarbonate buffer)	**MB** (Membrane box)	**PB** (Plastic bag)
Sampling method	Pliers		Membrane box	
Sampling location comments	Comments on where the sample was taken from the bone fragment.			
Remarks	Def. tool = definitely tool			

Additional information on the Mesolithic North Sea bone points													
ZooMS number	Collection number	Find number	Unit	TissueType	Morphological notes	Length before (mm)	Length after (mm)	Weight before (g)	Weight after (g)	Weight sample (mg)	Protocol	Sampling method	Sampling location comments
P1.1	28	1	ZM	bone		66,1	66,1	5,1	5,1	17,8	CA	Scalpel	Scalpel
P1.2	28	1	ZM	bone		66,1	66,1	5,1	5,0	10,8	B	Pliers	Base
P1.3	28	1	ZM	bone		66,1		5,1			MB	MB	
P3.1	28	3	ZM	bone		49,3	44,1	4,0	2,6	17,0	CA	Scalpel	Base, the non barb side
P3.2	28	3	ZM	bone		49,3	44,1	4,0	2,6	21,0	B	Fretsaw	Top of the base
P3.3	28	3	ZM	bone		49,3		4,0			MB	MB	
P5.1	86	1	MV2	antler	*Cervus elaphus*	165,0	163,0	16,4	16,2	12,0	CA	Scalpel	Residue
P5.2	86	1	MV2	antler	*Cervus elaphus*	165,0	163,0	16,4	16,2	17,7	B	Split, Pliers	Top
P5.3	86	1	MV2	antler	*Cervus elaphus*	165,0		16,4			MB	MB	Reused MB
P6.1	1000	1	MV2	bone		132,4	132,4	13,2	13,7	10,0	CA	Scalpel	Trabecular bone
P6.2	1000	1	MV2	bone		132,4	132,4	13,2	13,7	9,5	B	Scalpel, Split	Trabecular bone at the base
P6.3	1000	1	MV2	bone		132,4		13,2			MB	MB	
P7.1	27	1	ZM	bone		139,9	139,0	17,4	17,1	21,3	CA	Scalpel	Base
P7.2	27	1	ZM	bone		139,9	139,0	17,4	17,1	14,6	B	Split	-
P7.3	27	1	ZM	bone		139,9		17,4			MB	MB	
P28.1	37	4	HvH	bone		92,5	92,0	7,9	7,7	11,5	CA	Scalpel	Base
P28.2	37	4	HvH	bone		92,5	92,0	7,9	7,7	11,5	B	Split	-
P28.3	37	4	HvH	bone		92,5		7,9			MB	MB	
P29.1	34	1	MV1	bone		63,7	63,0	3,6	3,5	23,5	CA	Scalpel	Trabecular bone
P29.2	34	1	MV1	bone		63,7	63,0	3,6	3,5	27,5	B	Pliers	Base
P29.3	34	1	MV1	bone		63,7		3,6			MB	MB	
P30.1	14	121	Ro	bone		26,8	24,7	0,9	0,9	15,2	CA	Scalpel	C14, trabecular
P30.2	14	121	Ro	bone		26,8	24,7	0,9	0,9	16,3	B	Split	-
P30.3	14	121	Ro	bone		26,8		0,9			MB	MB	
P31.1	30	1	MV2	bone		79,0	75,4	5,1	4,9	44,5	CA	Scalpel	Trabecular bone
P31.2	30	1	MV2	bone		79,0	75,4	5,1	4,9	15,3	B	Split	-
P31.3	30	1	MV2	bone		79,0		5,1			MB	MB	
P41.1	41	3	MV2	bone		38,9	38,5	1,9	1,9	28,2	CA	Pliers	Base
P41.2	41	3	MV2	bone		38,9	38,5	1,9	1,9	27,6	B	Pliers	Base
P41.3	41	3	MV2	bone		38,9		1,9			MB	MB	

Reference table Mesolithic North Sea bone points					
ZooMS number	**P(**oint)X.Y, where the value of the suffix indicates the used protocol.				
Collection number	The number of the private collector, as listed in the database.				
Find number	The number of the points, as listed in the database.				
Unit	**ZM** (Zandmotor)	**MV2** (Maasvlakte 2)	**SGZ** (’s Gravenzande)	**HvH** (Hoek van Holland)	**Ro** (Rockanje)
Cultural attribution	All points are thought to be Mesolithic.				
Tissue Type	Bone	Ivory	Antler		
Length before (mm)	Length as measured or listed in database in mm.				
Length after (mm)	Length measured after sampling in mm.				
Weight before (g)	The weight of the point before sampling as measured or listed in database.				
Weight after (g)	The weight of the point after sampling as measured.				
Weight sample (mg)	The weight of the sample sampling as measured (mg).				
C14	All listed bone points are designated for C14 dating.				
Protocol	**CA** (Cold acid)	**B** (Ammonium bicarbonate buffer)	**MB** (Membrane box)	**PB** (Plastic bag)	
Sampling method	Pliers	Scalpel	Fretsaw	Split (Split means that the sample taken earlier was split into two samples)	Membrane box
Sampling location comments	Comments on where on the point the sample was taken.				

Appendix C: Artefact photographs

C.1 Quinçay morphologically identified controls, before sampling

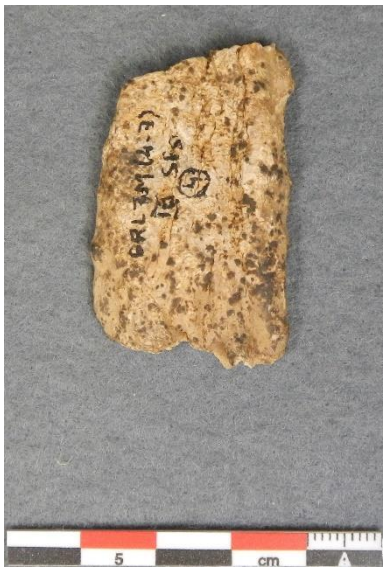

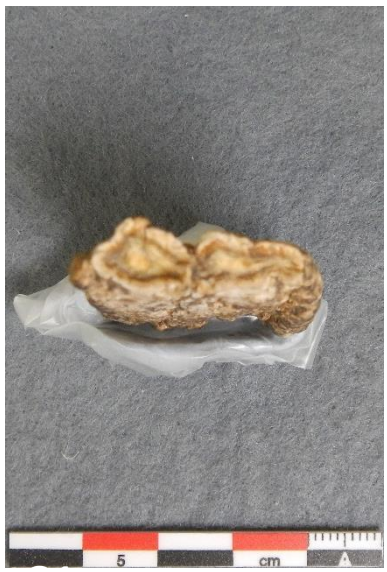


Q3


Q3

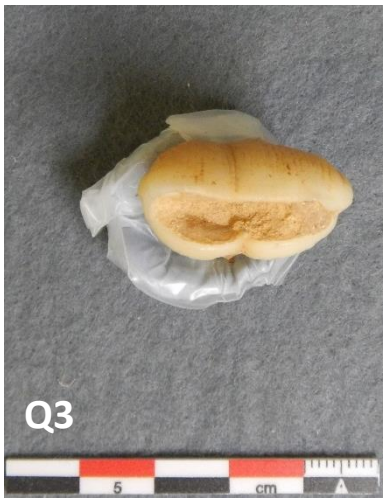
Q3


Q4


Q4


Q4


Q4


Q4


Q5
10 cm

Q5
10 cm
1:2


Q5
10 cm

Q5
10 cm

Q5
10 cm
1:2


Q6
5 cm

Q6
5 cm


Q6
5 cm
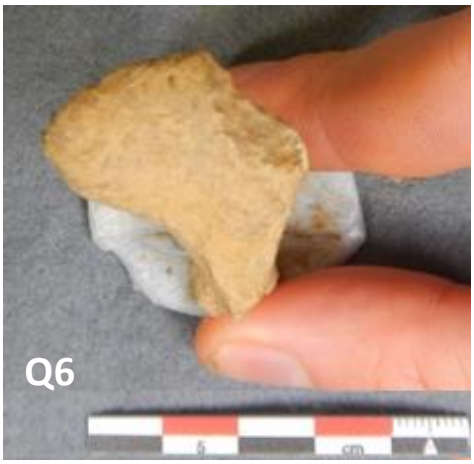
Q6
5 cm


Q7
Q7
Q7
Q7
Q7
Q7

C.2 Quinçay possible bone tools

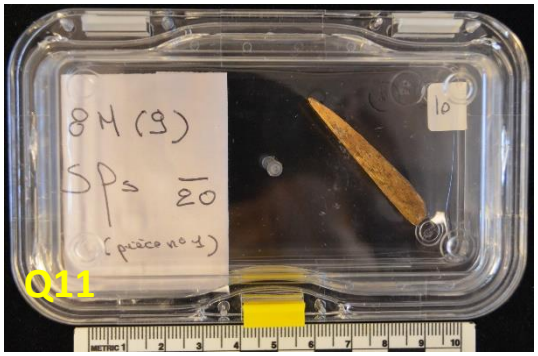

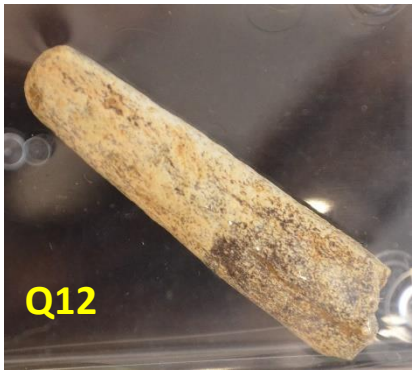


Q14

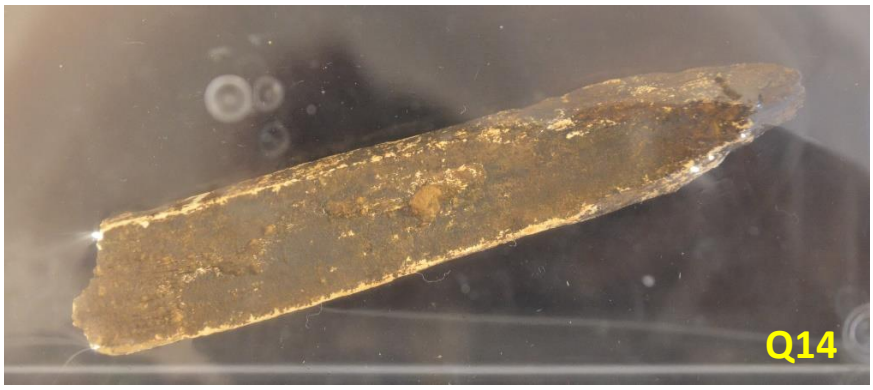
Q14


Q15


Q15

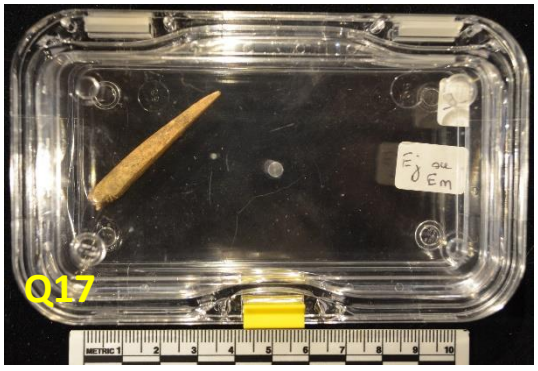
Q17


Q17

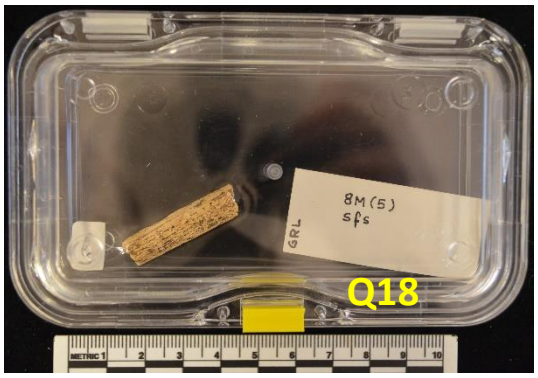
Q18


Q18

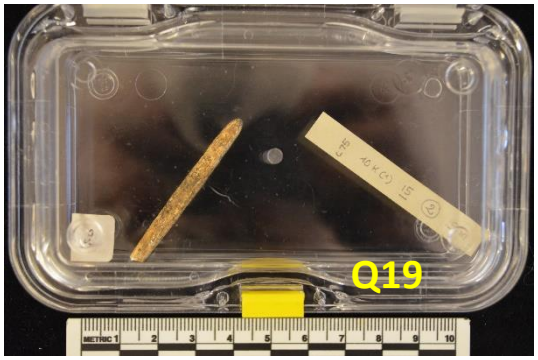
Q19


Q19


Os grave
Q20


Q20


Q21

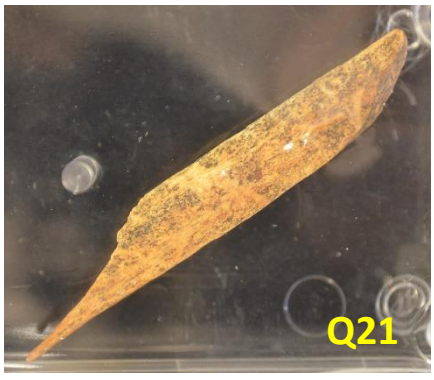
Q21


Q22


Q22


Q23


Q23

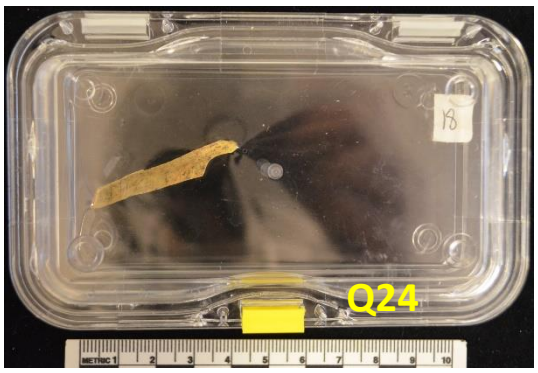
Q24

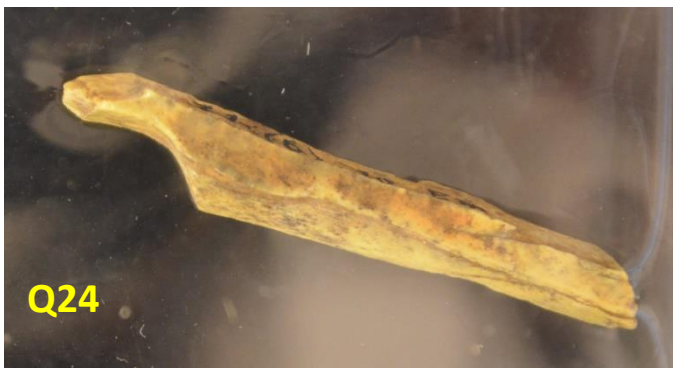
Q24


GRL
5K (3)
Em 17
Q25


Q25


Q26


Q26


Q27


Q27


Q28


Q28

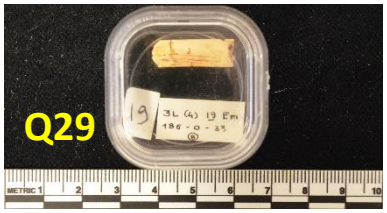
Q29

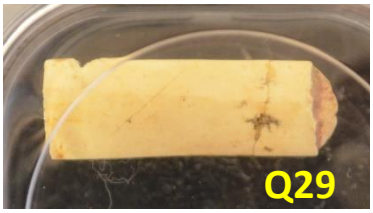
Q29

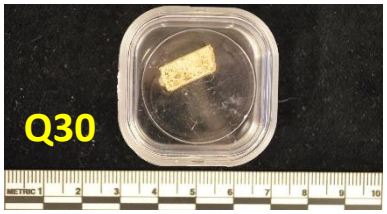
Q30


Q30


Q31

C.3 Mesolithic North Sea bone points, before sampling

1:2

1:2

1:2

1:2


P30


P30


P31


P31


P41


P41

C.4 Quinçay morphologically identified controls, after sampling

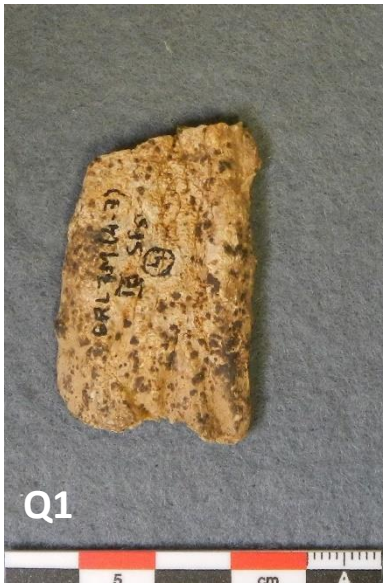


Q3
5
cm


Q3
5
cm


Q3
5
cm


Q3
5
cm


Q4
5
cm


Q4
5
cm


Q4
5
cm

1:2

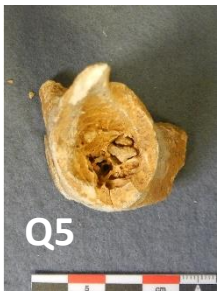

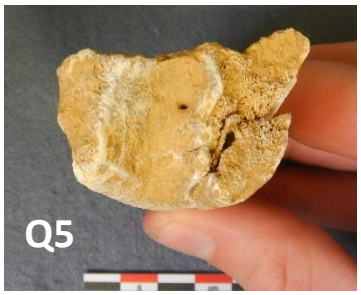

1:2


Q6
5
cm


Q6
5
cm


Q7
5
cm


Q7
5
cm


Q7
5
cm


Q7
5
cm

C.5 Mesolithic North Sea bone points, after sampling

1:2

1:2

1:2

1:2

1:2

1:2


P31
5
cm


P31
5
cm


P41
5
cm


P41
5
cm

Appendix D: Labelled mass spectra

D.1 Quinçay morphologically identified controls

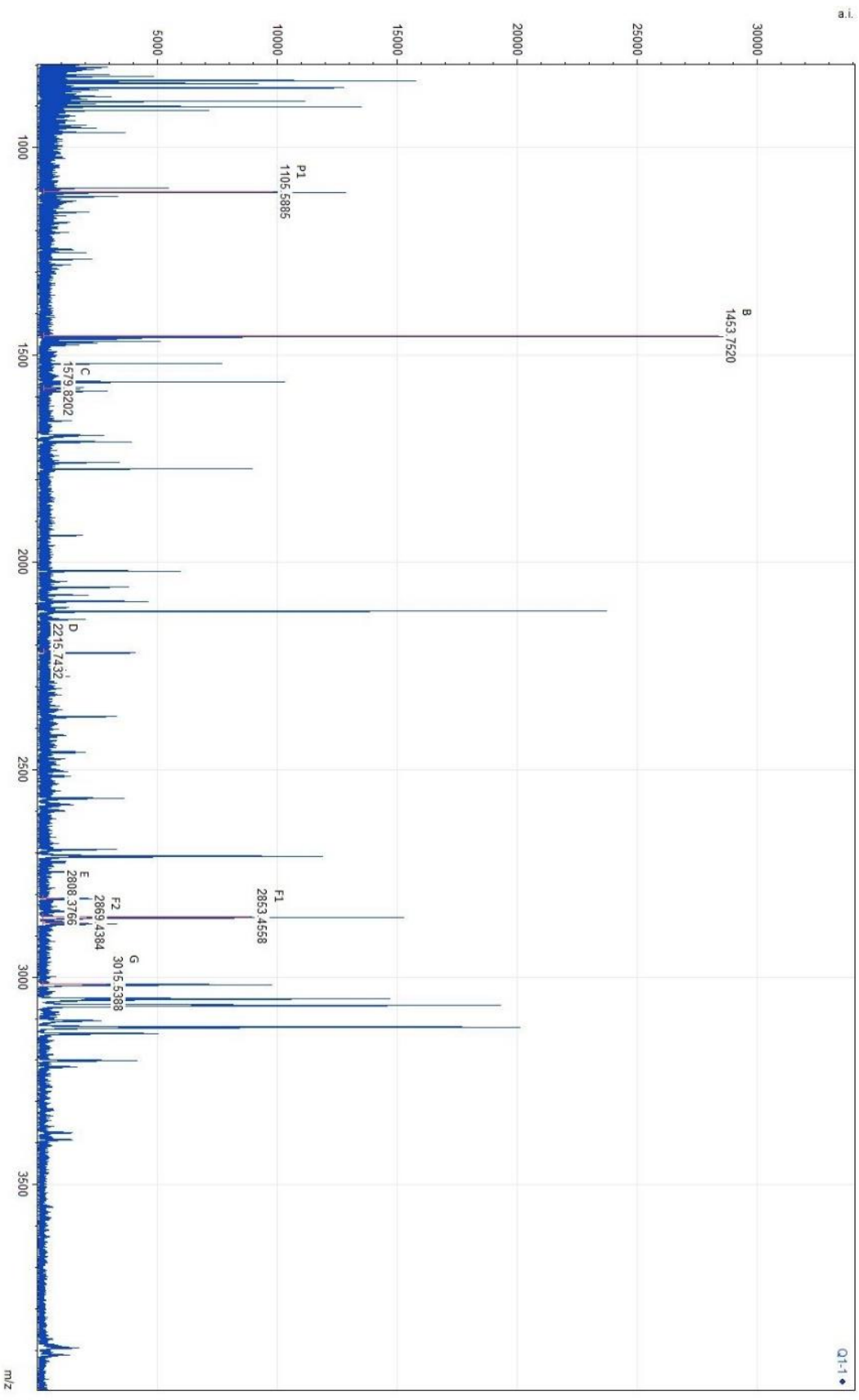

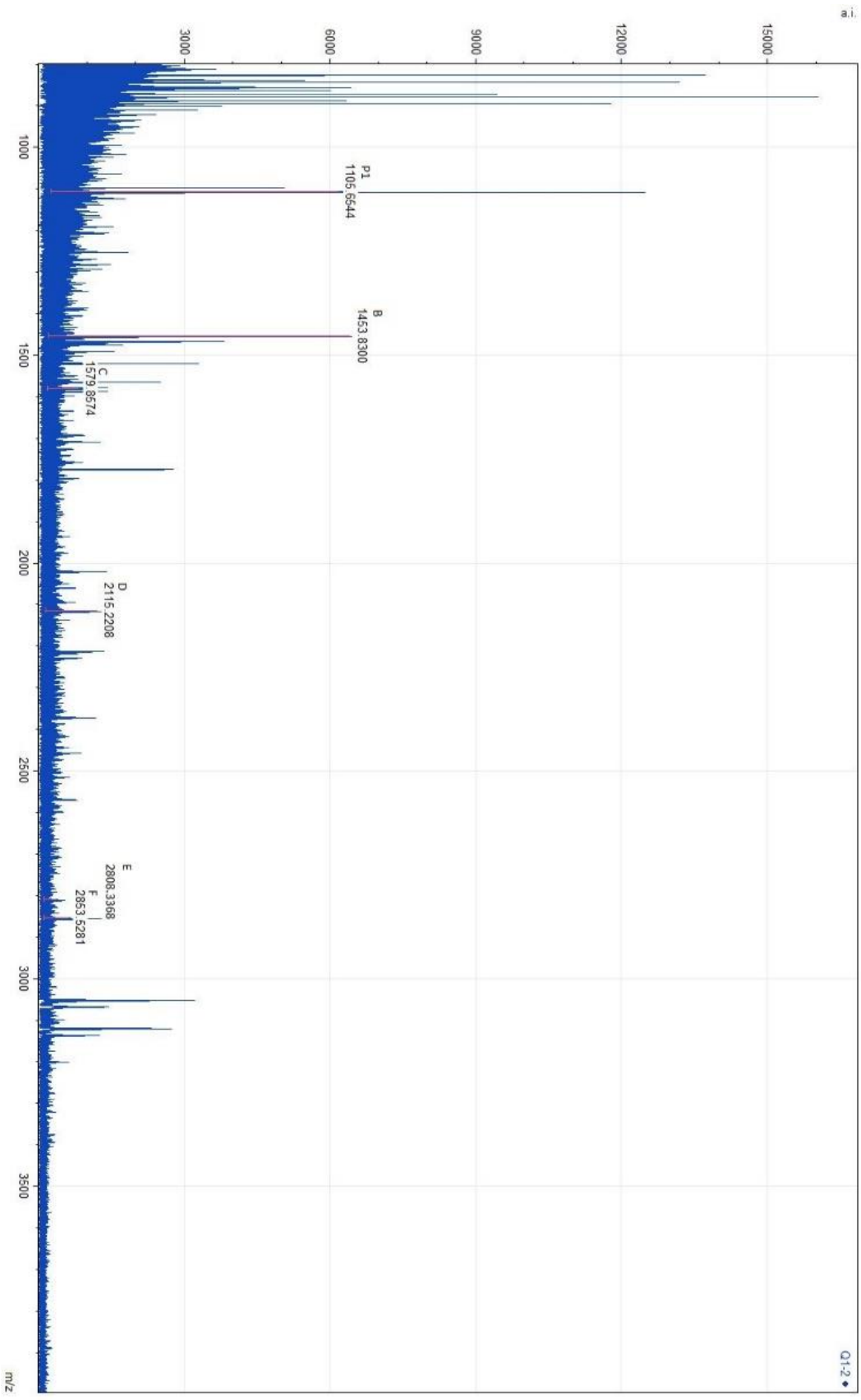
a.i.
3000
6000
9000
12000
15000
1000
1500
2000
2500
3000
3500
m/z
P1
1105.6544
B
1453.8300
C
1579.8574
D
2115.2208
E
2808.3368
F
2853.5281
Q1:2

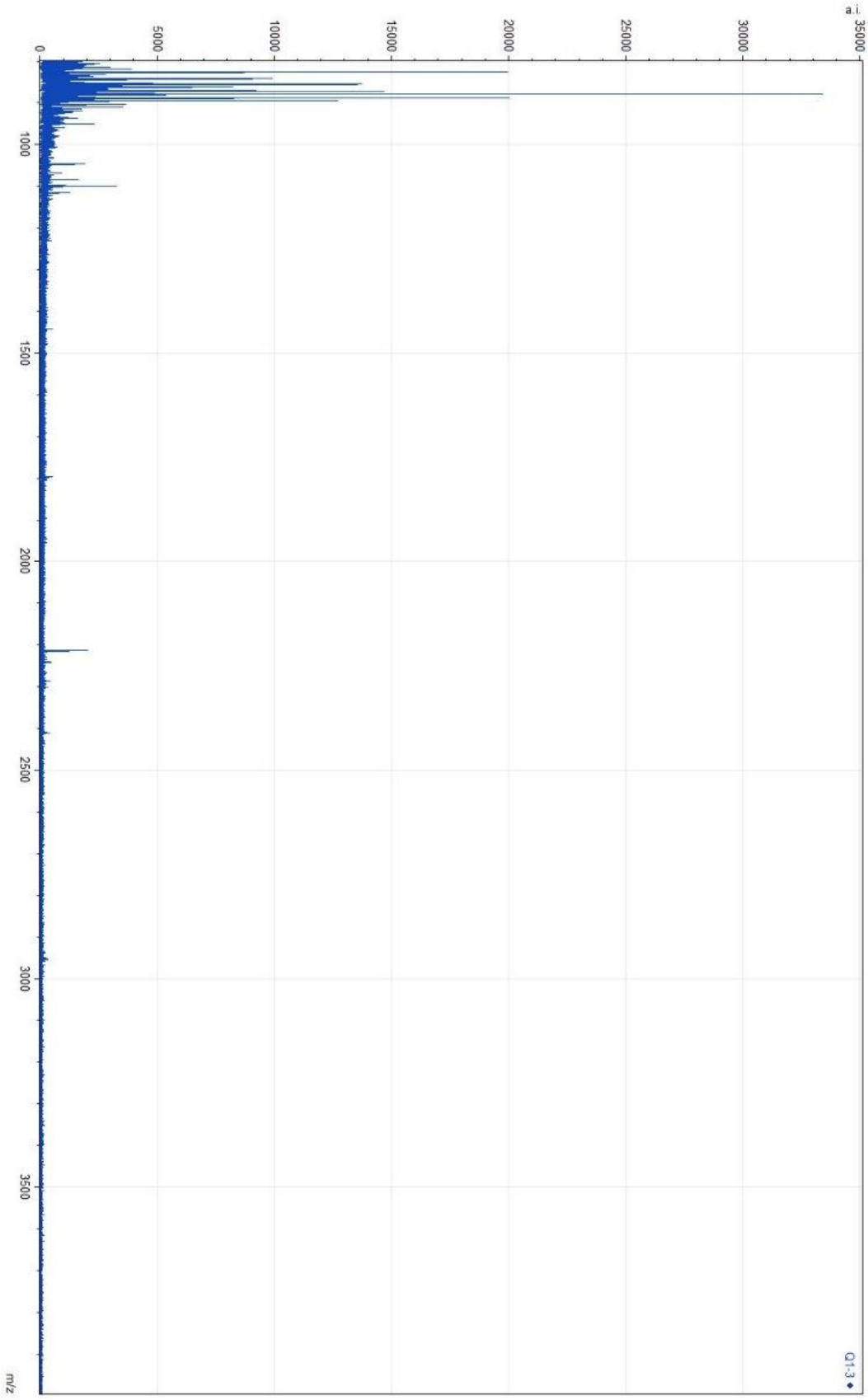
a.i.
0
5000
10000
15000
20000
25000
30000
35000
1000
1500
2000
2500
3000
3500
m/z
Q1:3

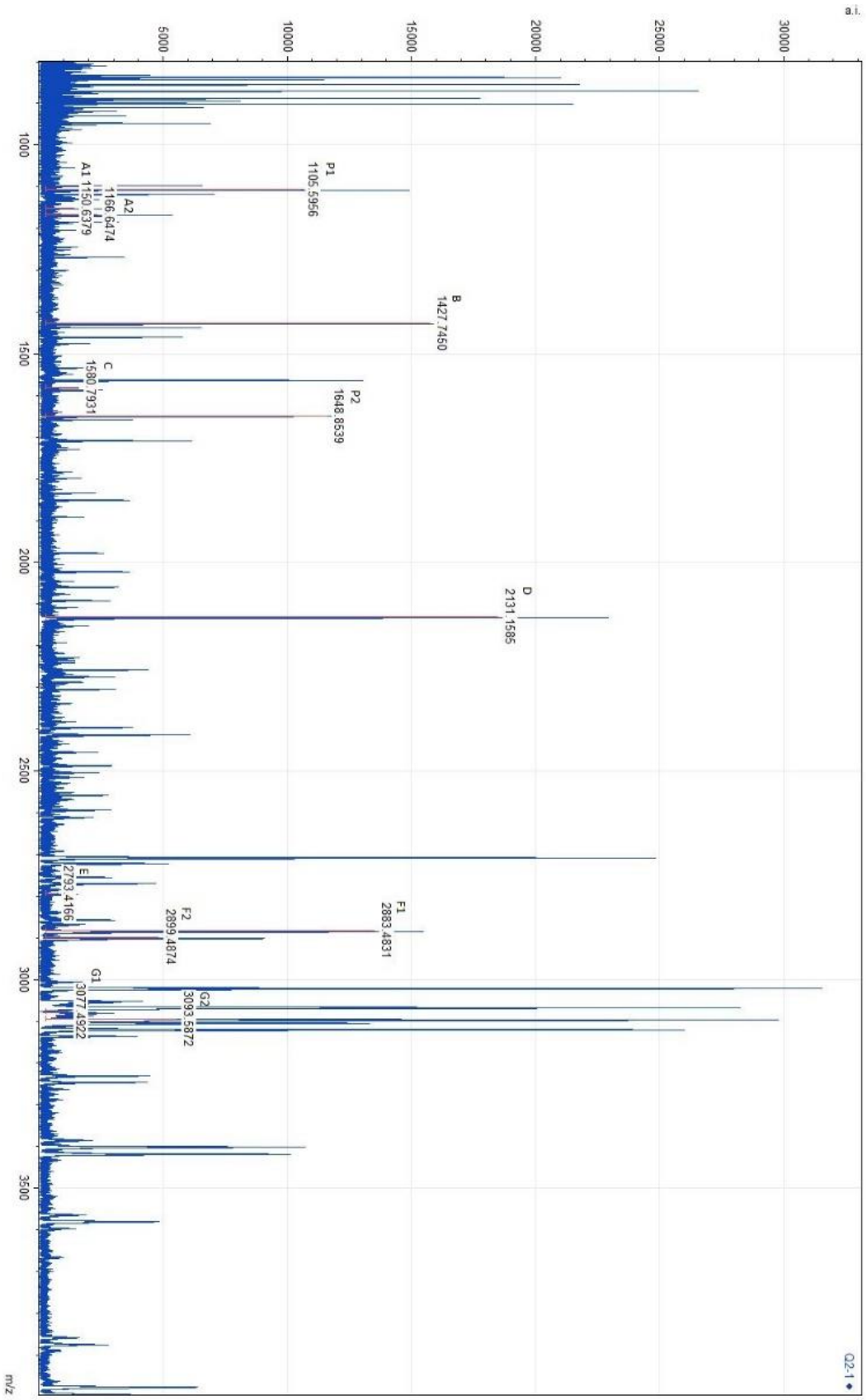
a.i.
5000
10000
15000
20000
25000
30000
1000
1500
2000
2500
3000
3500
m/z
P1
1105.5956
A2
1166.6474
A1
1150.6379
B
1427.7450
C
1580.7931
P2
1648.8539
D
2131.1585
E
2793.4166
F2
2899.4874
F1
2883.4831
G1
3077.4922
G2
3093.5872
Q2-1

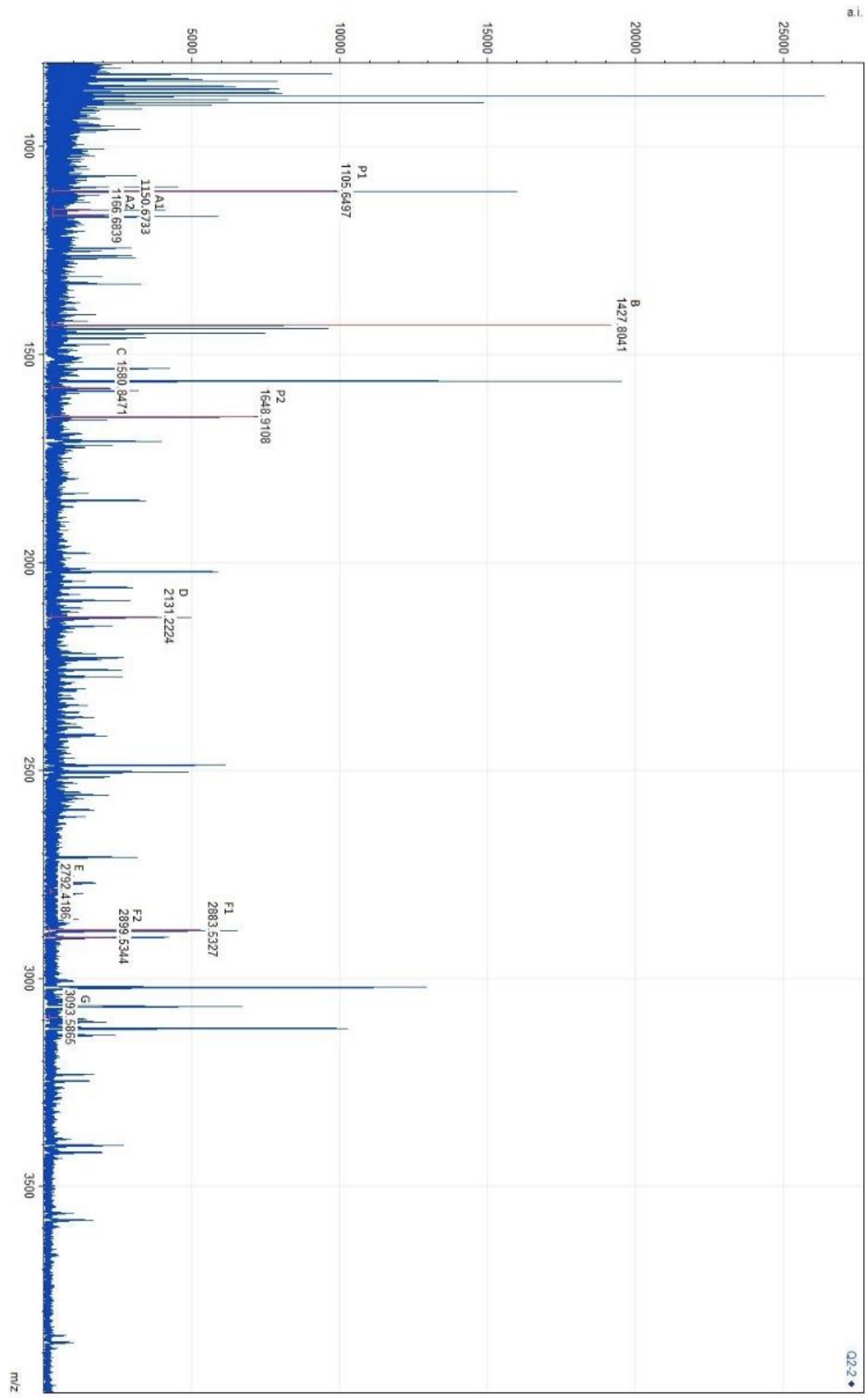
a.i.
5000
10000
15000
20000
25000
1000
1500
2000
2500
3000
3500
m/z
P1
1105.6497
A1
1150.6733
A2
1166.6839
B
1427.8041
C 1580.8471
P2
1648.9108
D
2131.2224
E
2792.4186
F1
2883.5327
F2
2899.5344
G
3093.5865
Q2-2

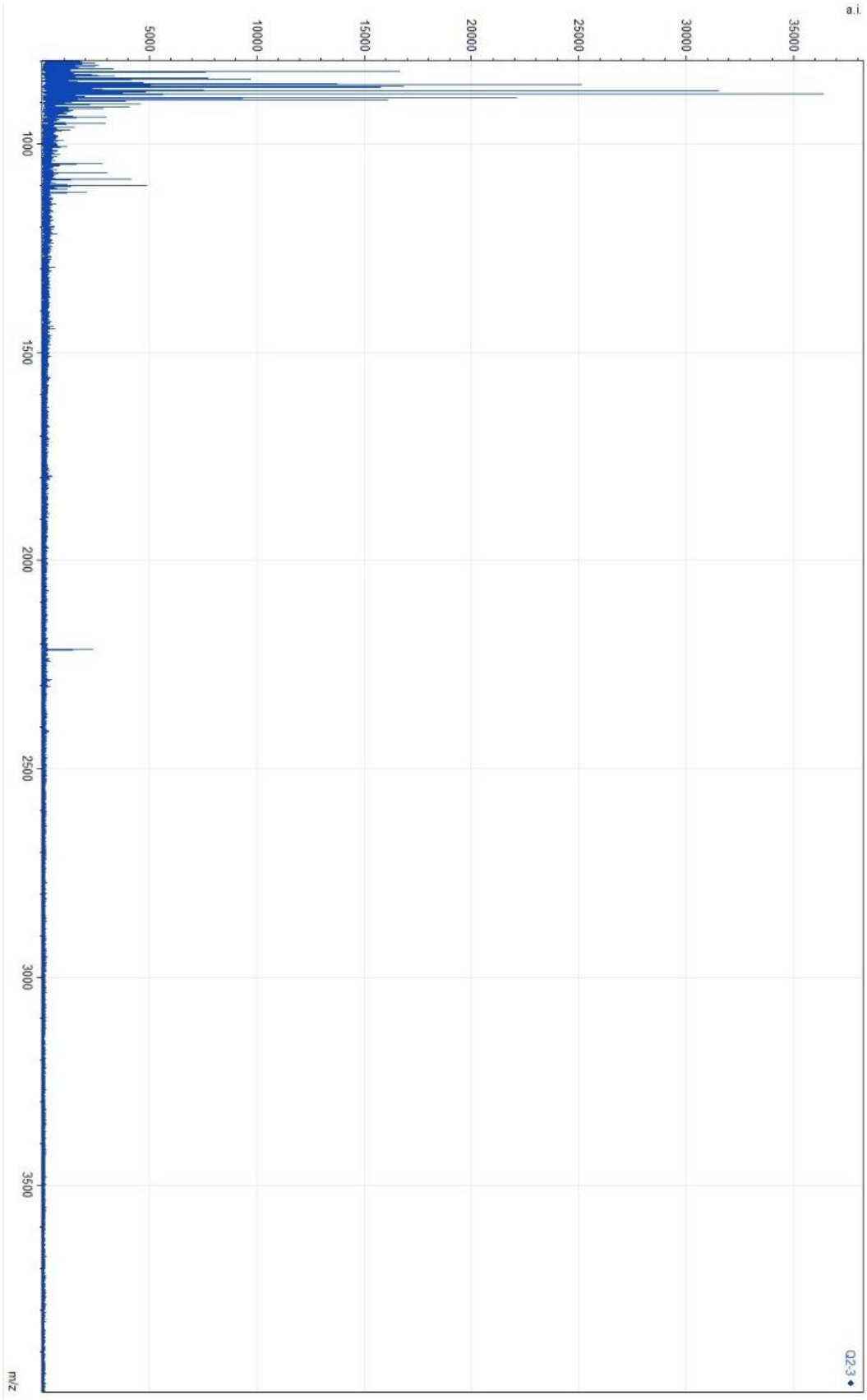
a.i.
5000
10000
15000
20000
25000
30000
35000
1000
1500
2000
2500
3000
3500
m/z
Q2-3

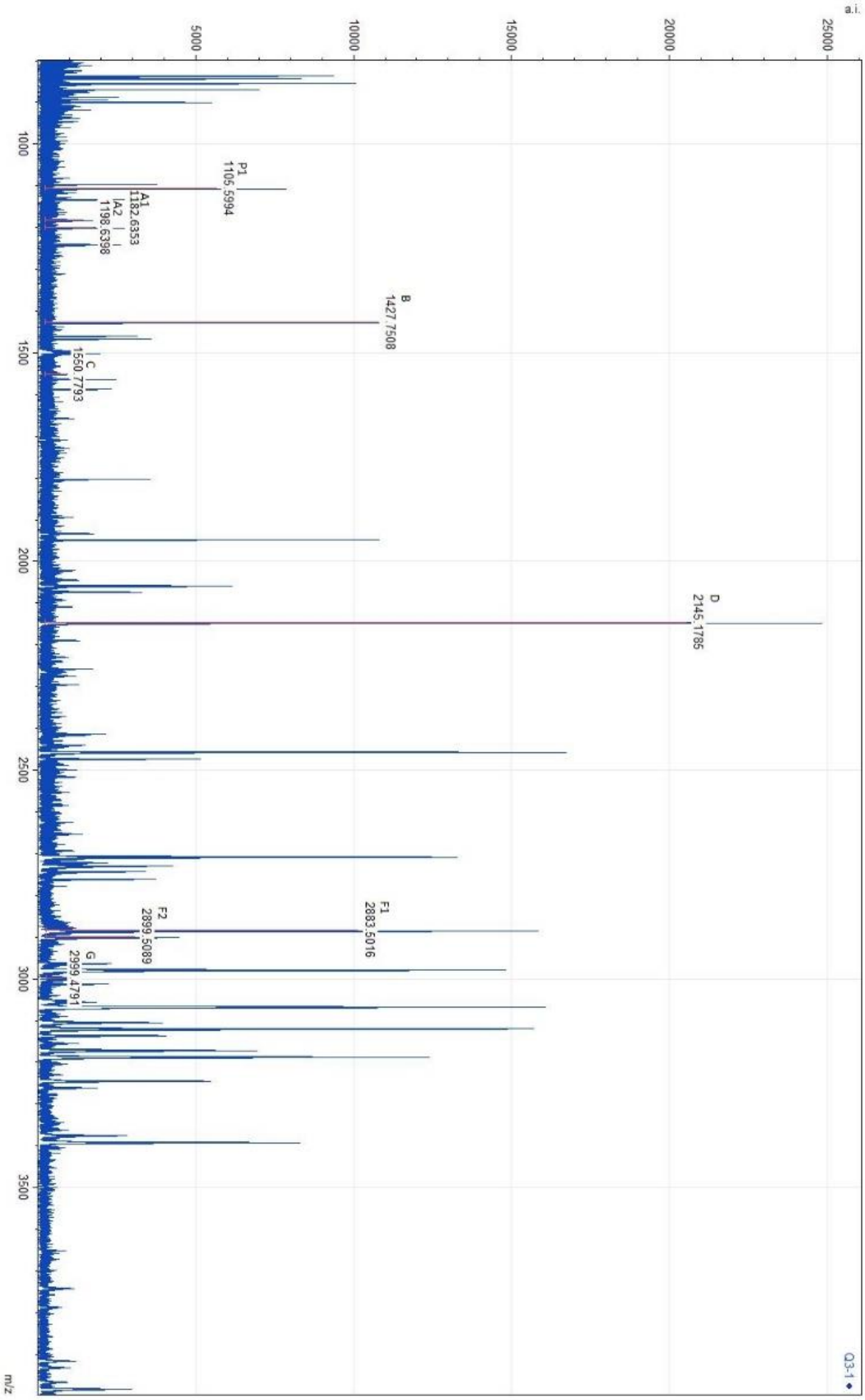
a.i.
25000
20000
15000
10000
5000
1000
1500
2000
2500
3000
3500
m/z
P1
1105.5994
A1
1182.6333
A2
1198.6398
B
1427.7508
C
1560.7793
D
2145.1785
F1
2883.5016
F2
2899.5089
G
2999.4791
Q3-1

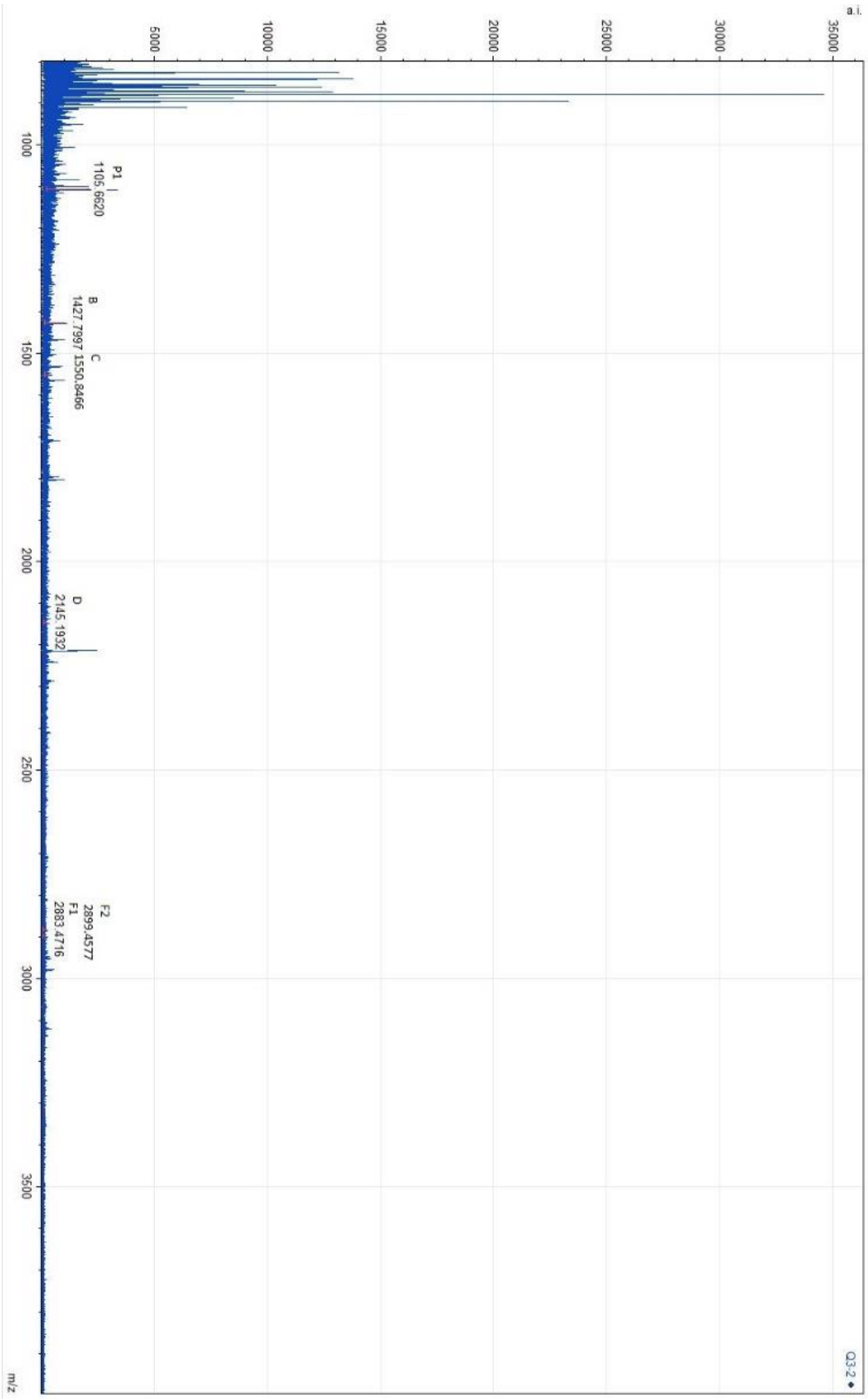
a.i.
5000
10000
15000
20000
25000
30000
35000
1000
1500
2000
2500
3000
3500
m/z
P1
1105.6620
B
1427.7997
C
1550.8466
D
2145.1932
F2
2899.4577
F1
2883.4716
Q3 2 ◆

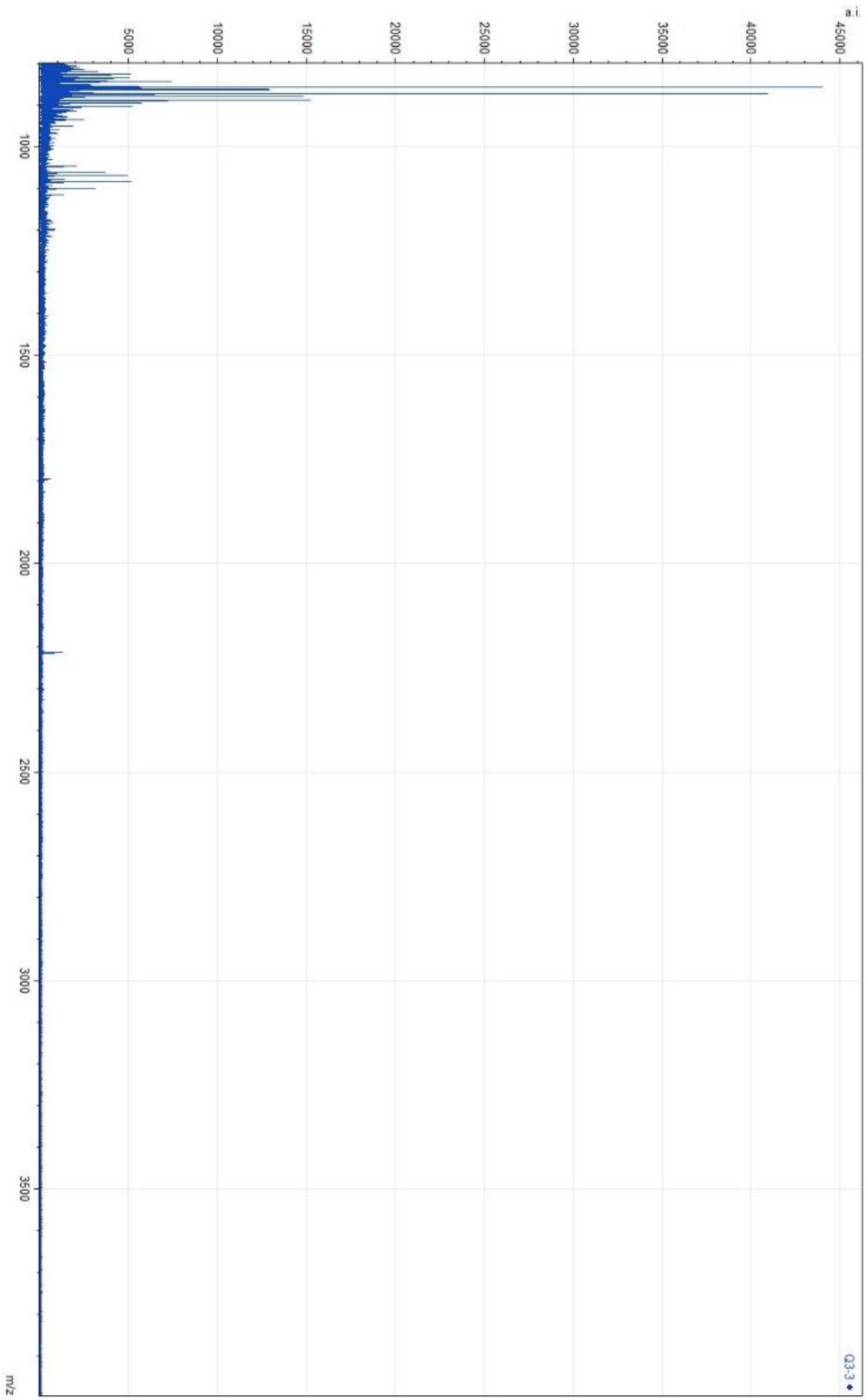
a.i.
5000
10000
15000
20000
25000
30000
35000
40000
45000
1000
1500
2000
2500
3000
3500
m/z
Q3-3

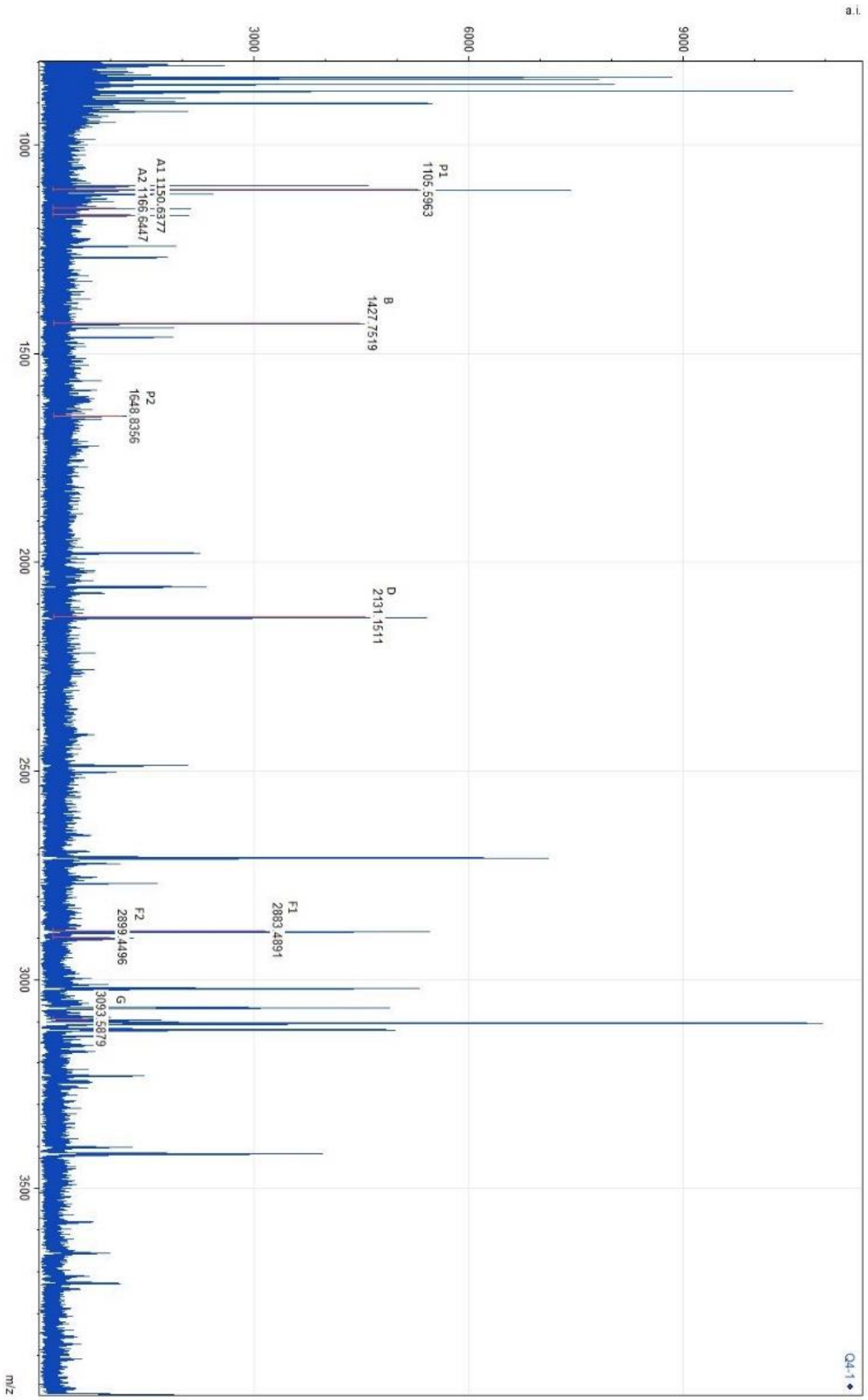
a.i.
3000
6000
9000
1000
1500
2000
2500
3000
3500
m/z
P1
1105.5963
A1 1150.6377
A2 1166.6447
B
1427.7519
P2
1648.8356
D
2131.1511
F1
2883.4891
F2
2899.4496
G
3093.5879
Q4-1

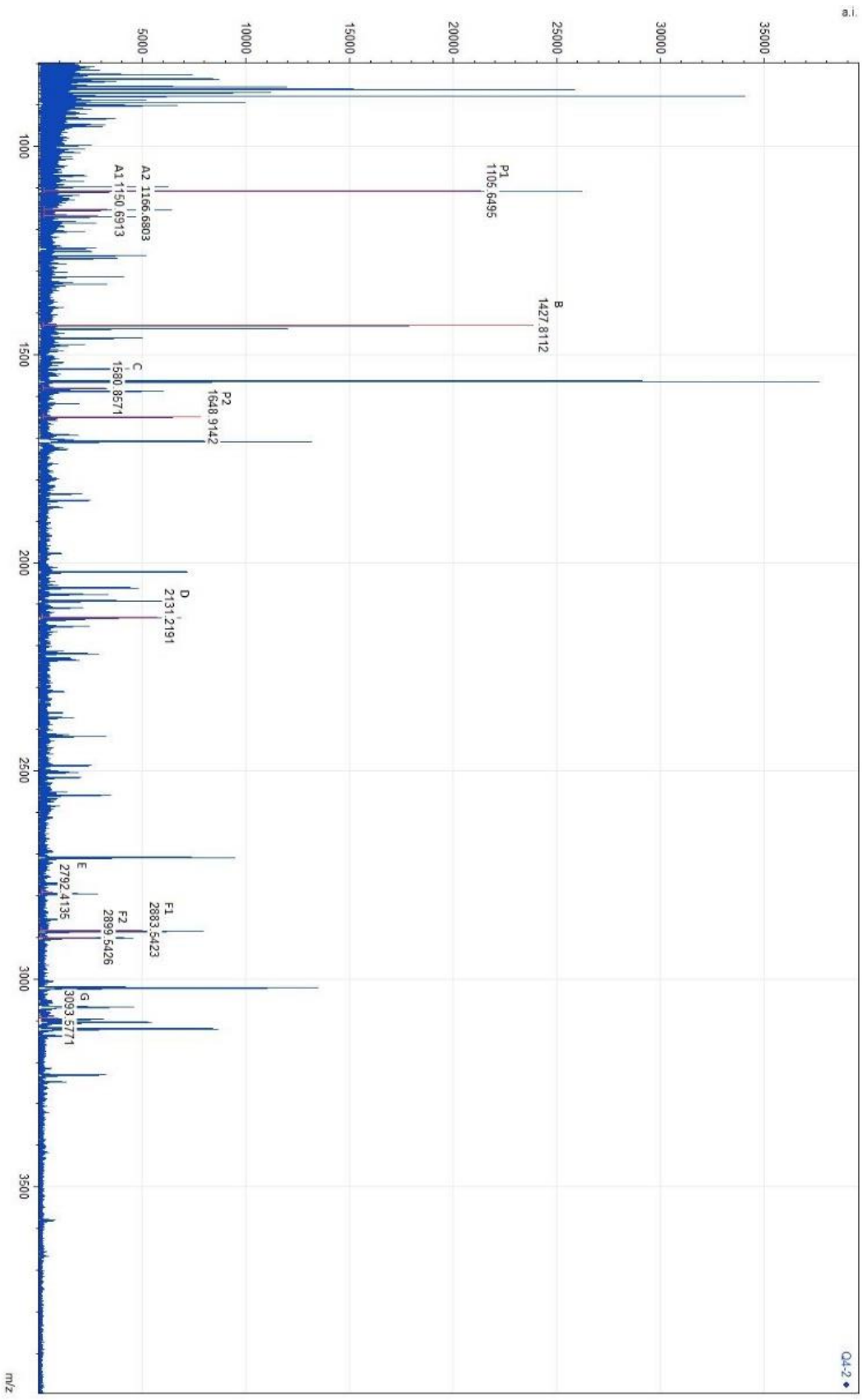
a.i.
5000
10000
15000
20000
25000
30000
35000
1000
1500
2000
2500
3000
3500
m/z
A1 1150.6913
A2 1166.6803
P1 1105.6495
B 1427.8112
C 1580.8571
P2 1648.9142
D 2131.2191
E 2792.4135
F2 2899.5426
F1 2883.5423
G 3093.5771
Q4-2

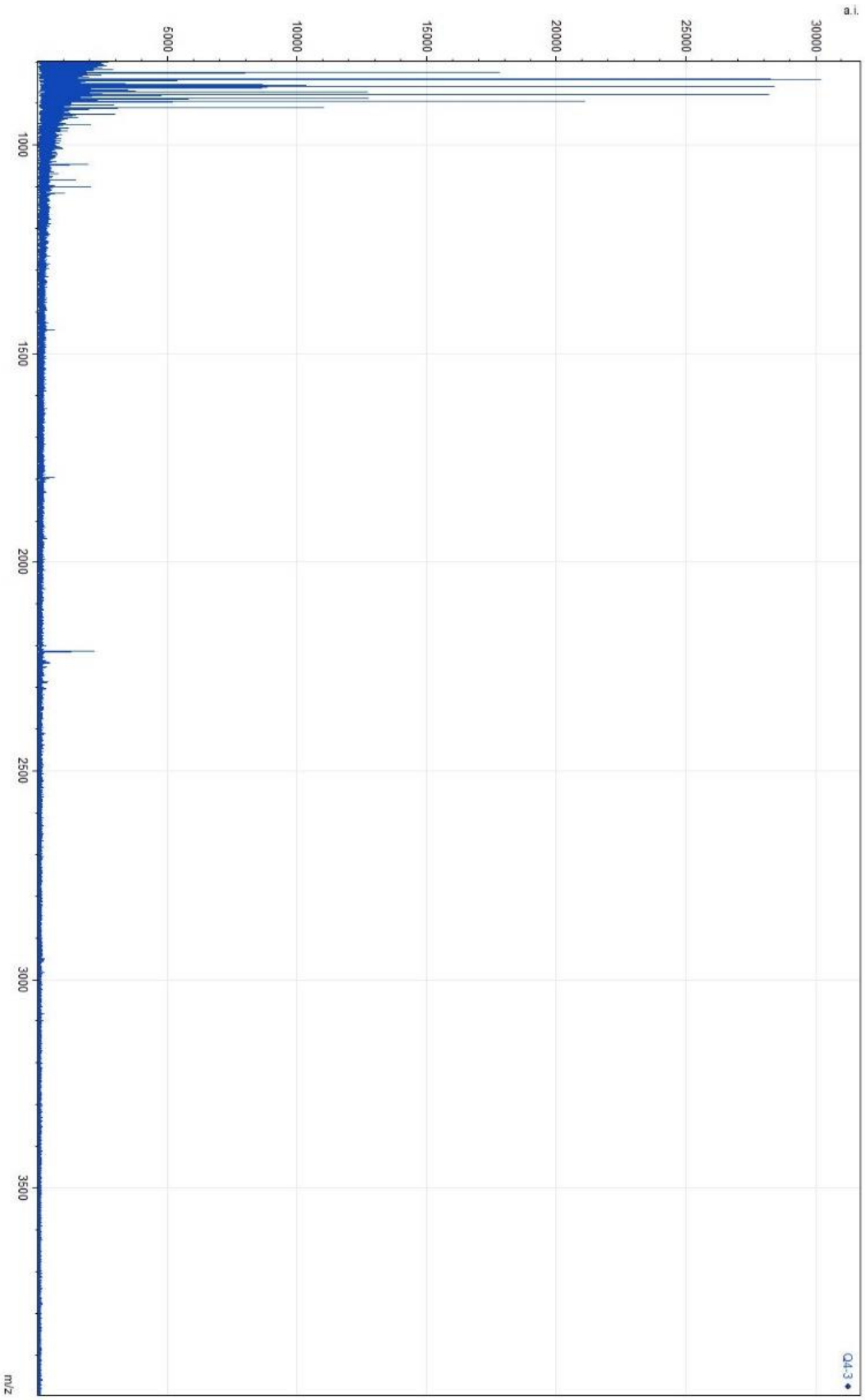
a.i.
5000
10000
15000
20000
25000
30000
1000
1500
2000
2500
3000
3500
m/z
Q4-3

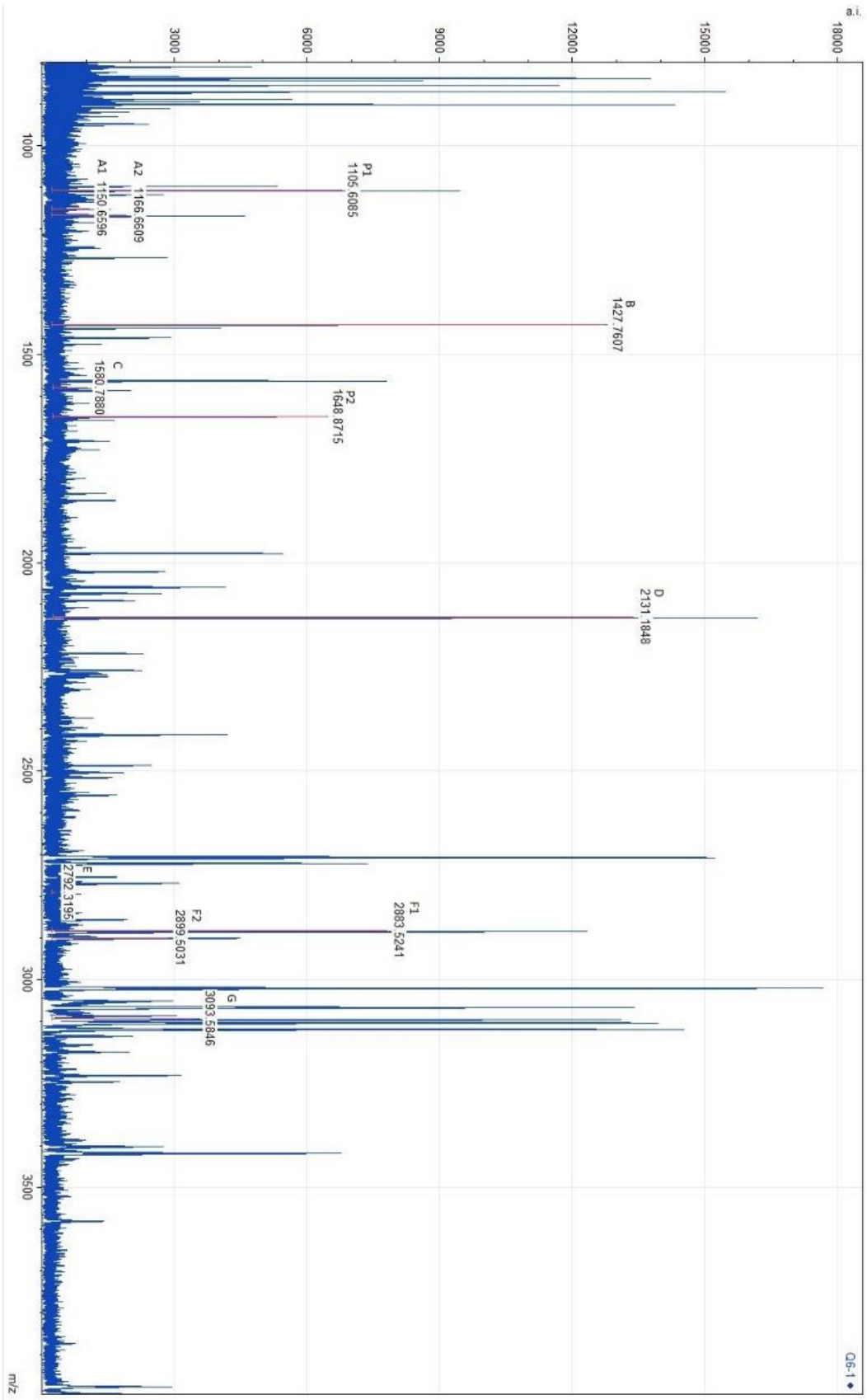
a.i.
18000
15000
12000
9000
6000
3000
1000
1500
2000
2500
3000
3500
m/z
A1
1150.6596
A2
1166.6609
P1
1105.6085
B
1427.7607
C
1580.7880
P2
1648.8715
D
2131.1848
E
2792.3195
F2
2899.5031
F1
2883.5241
G
3093.5846
Q6-1

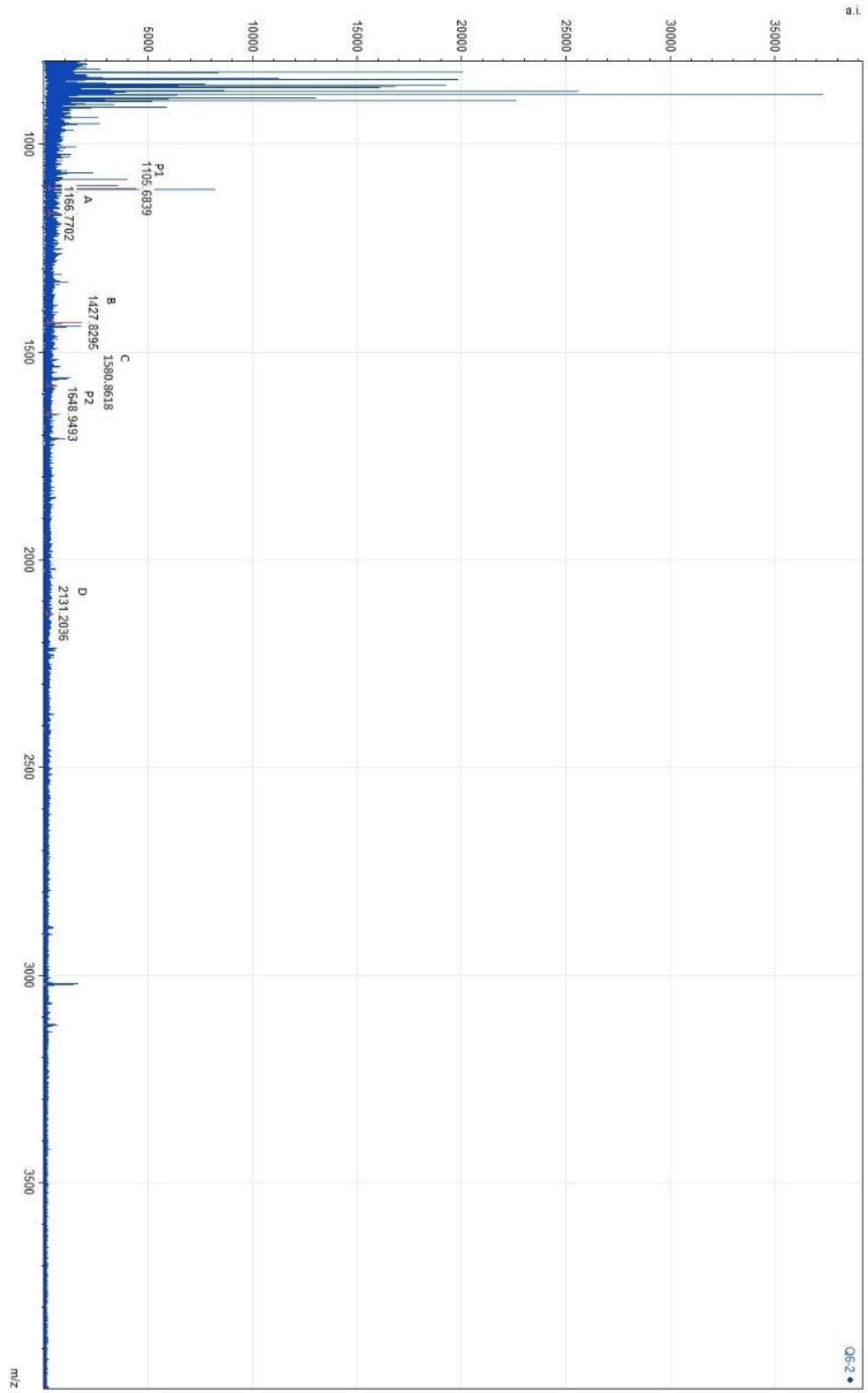
a.i.
5000
10000
15000
20000
25000
30000
35000
1000
1500
2000
2500
3000
3500
m/z
P1
1105.6839
A
1166.7702
B
1427.8295
C
1580.8618
P2
1648.9493
D
2131.2036
Q6-2

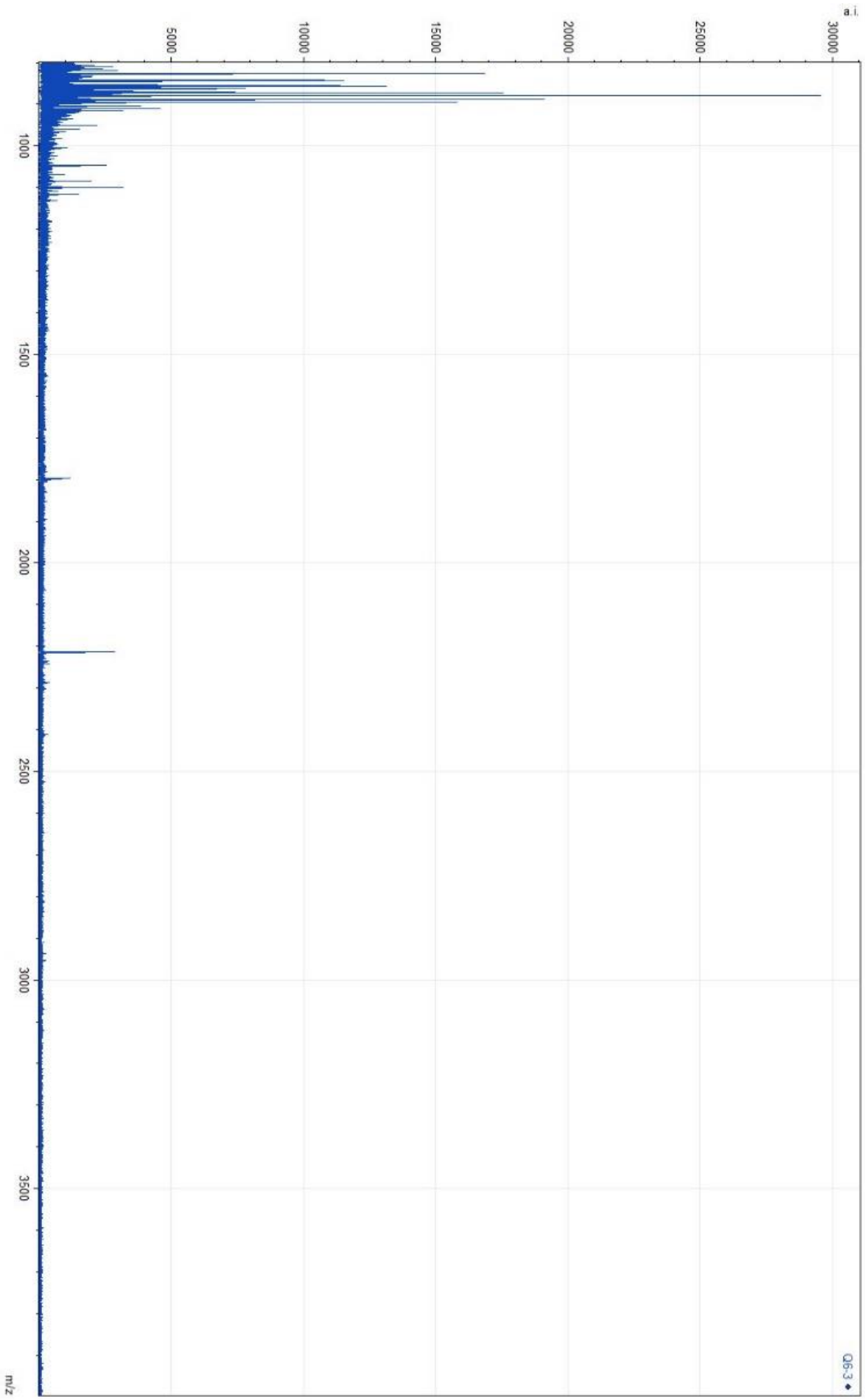
a.i.
5000
10000
15000
20000
25000
30000
1000
1500
2000
2500
3000
3500
m/z
Q6-3

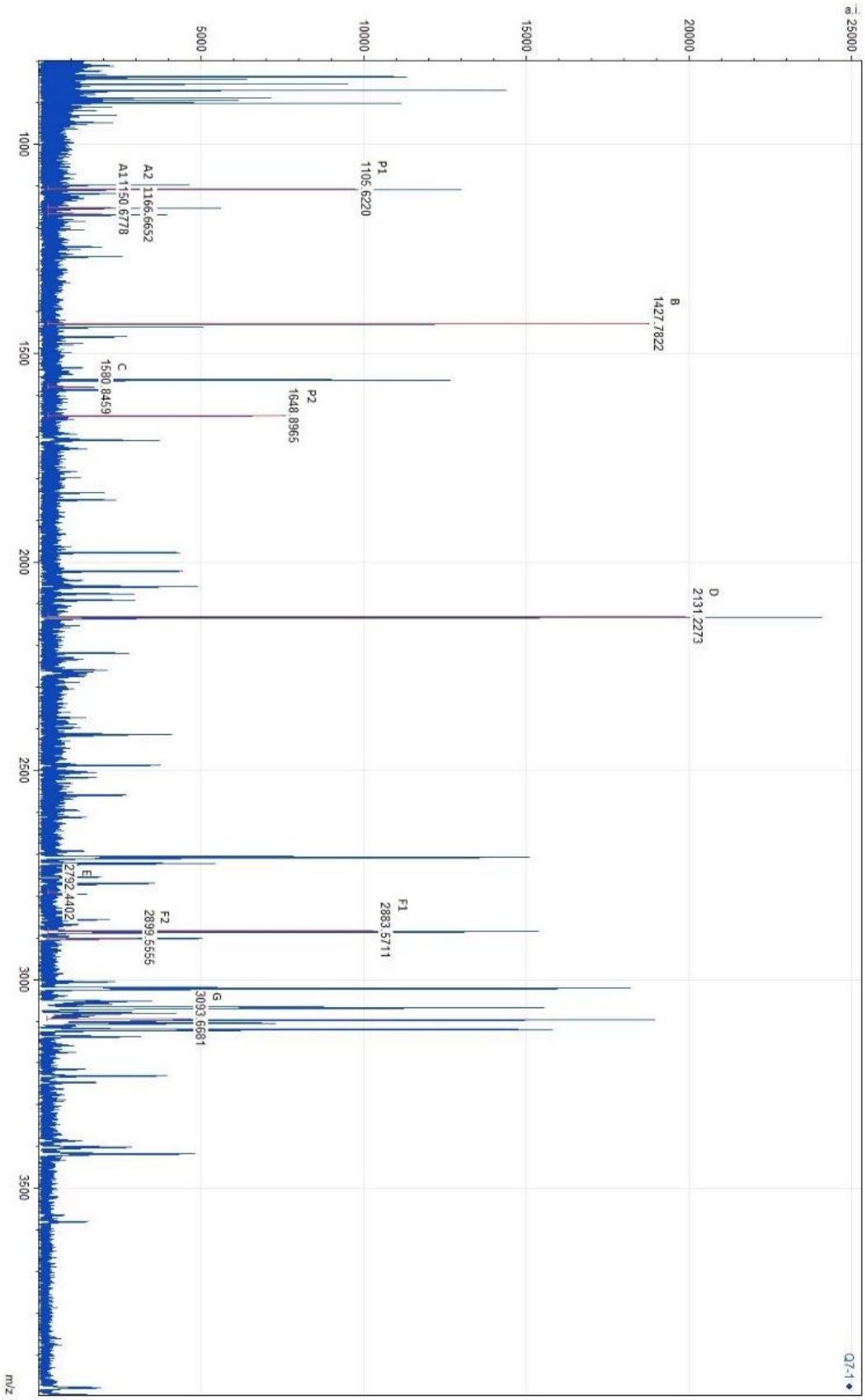
Q7-1
m/z
A1 1150.6778
A2 1166.6652
P1 1105.6220
B 1427.7822
C 1580.8459
P2 1648.8965
D 2131.2273
E 2792.4402
F2 2899.5555
F1 2883.5711
G 3093.6681

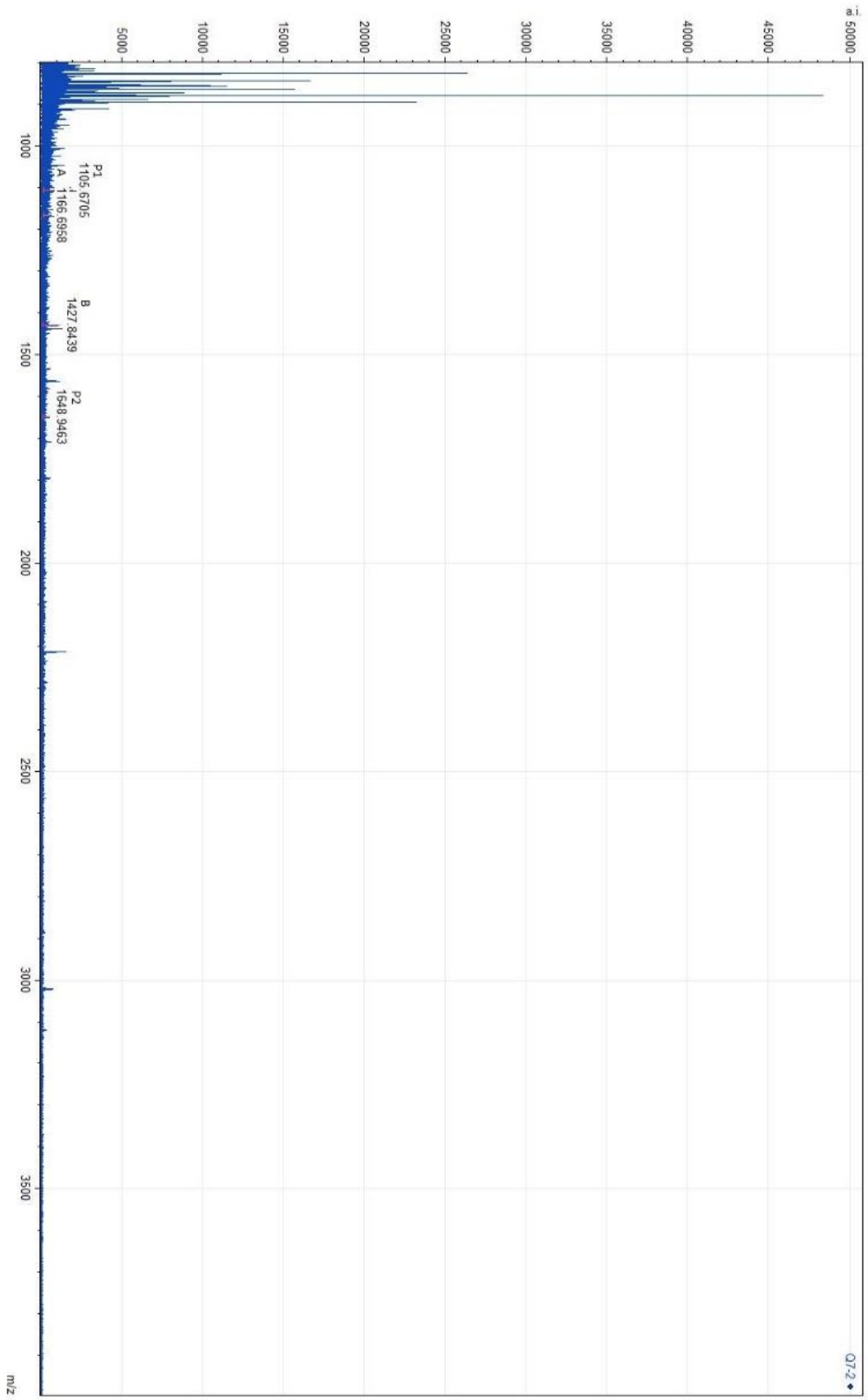
P1
1105.6705
A
1166.6958
B
1427.8439
P2
1648.9463
m/z
Q7-2

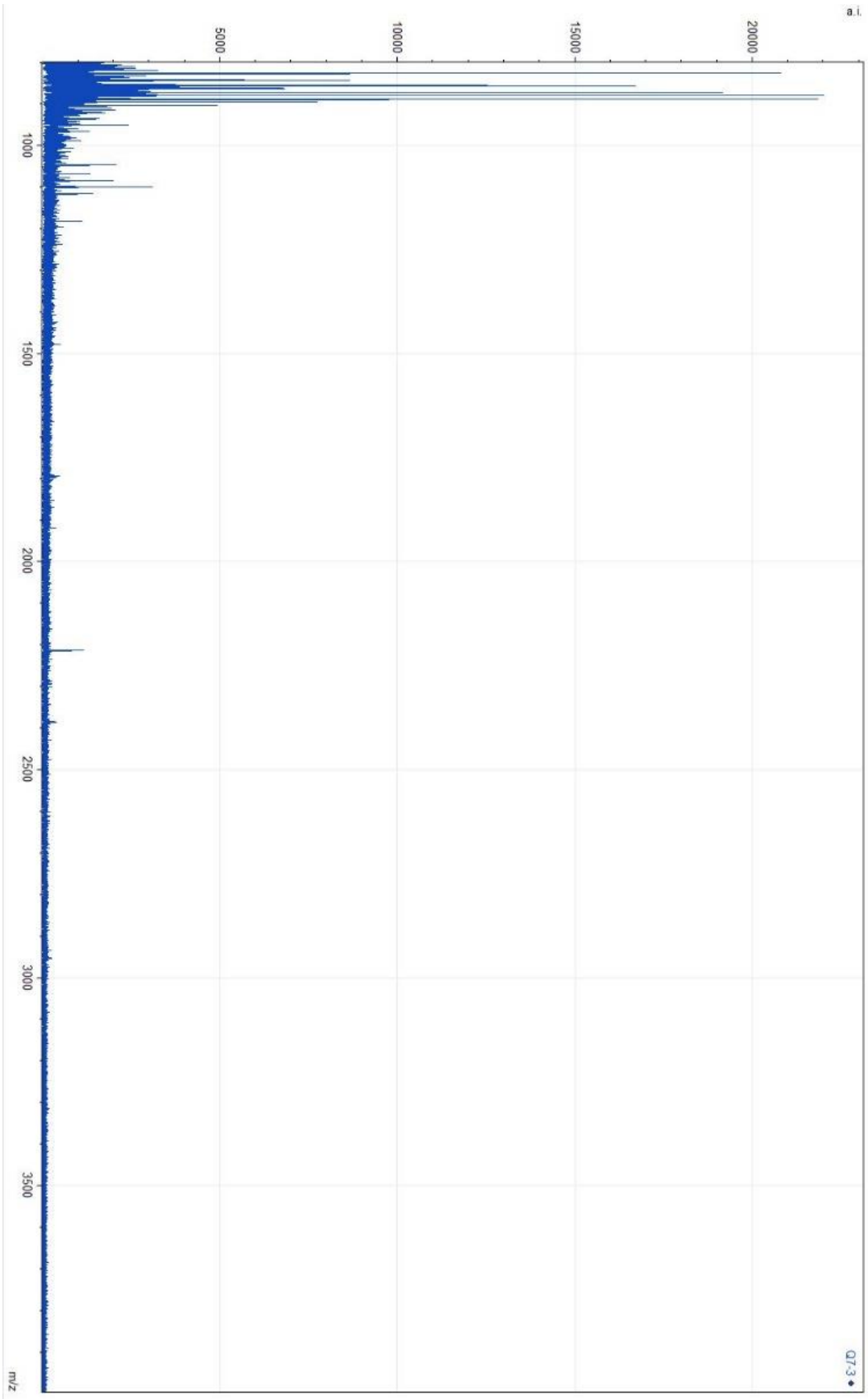
a.i.
5000
10000
15000
20000
1000
1500
2000
2500
3000
3500
m/z
Q1:3 ◆

D.2 Quinçay possible bone tools

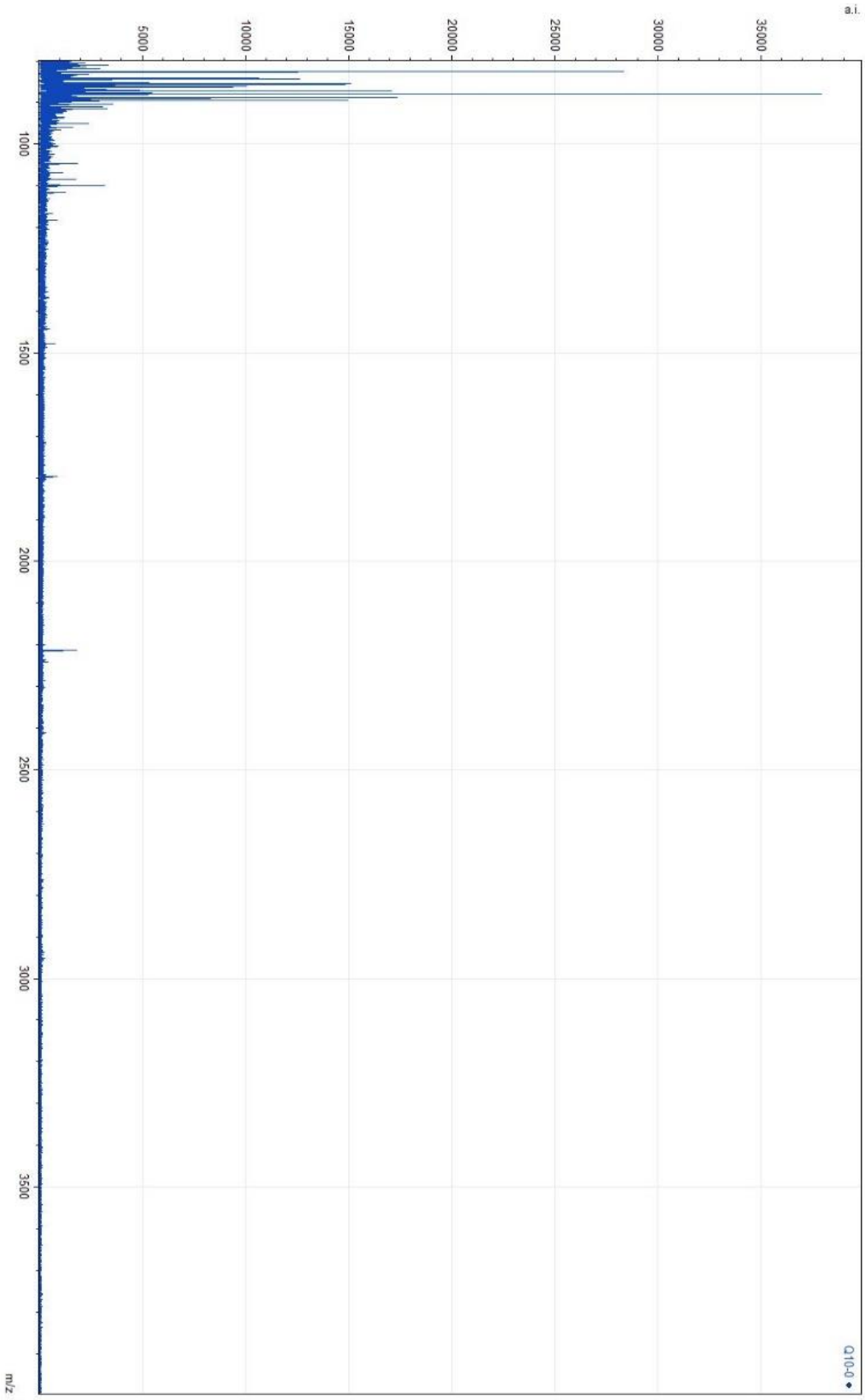

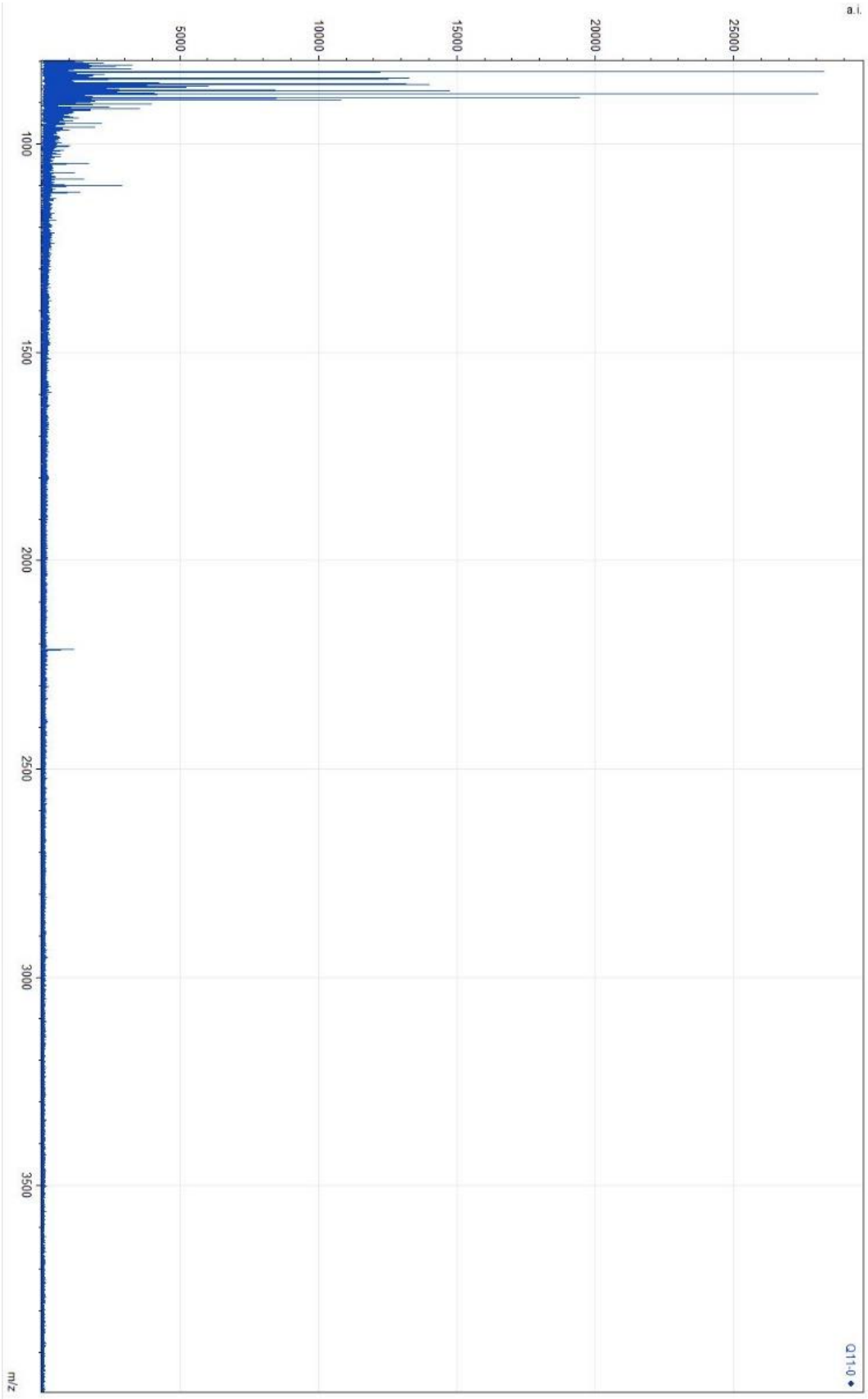
a.i.
5000
10000
15000
20000
25000
1000
1500
2000
2500
3000
3500
m/z
Q11-0

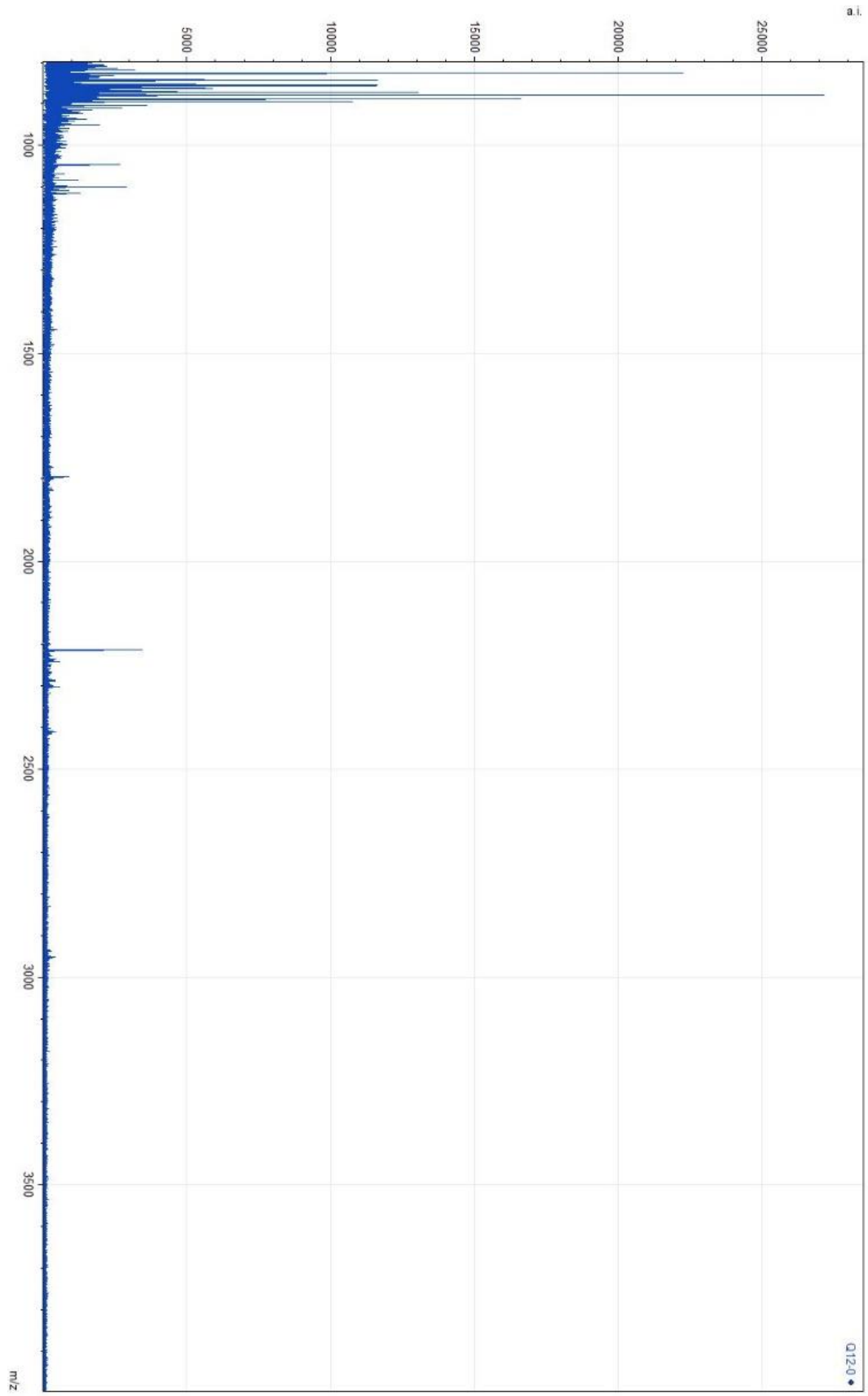
a.i.
5000
10000
15000
20000
25000
1000
1500
2000
2500
3000
3500
m/z
Q12-0

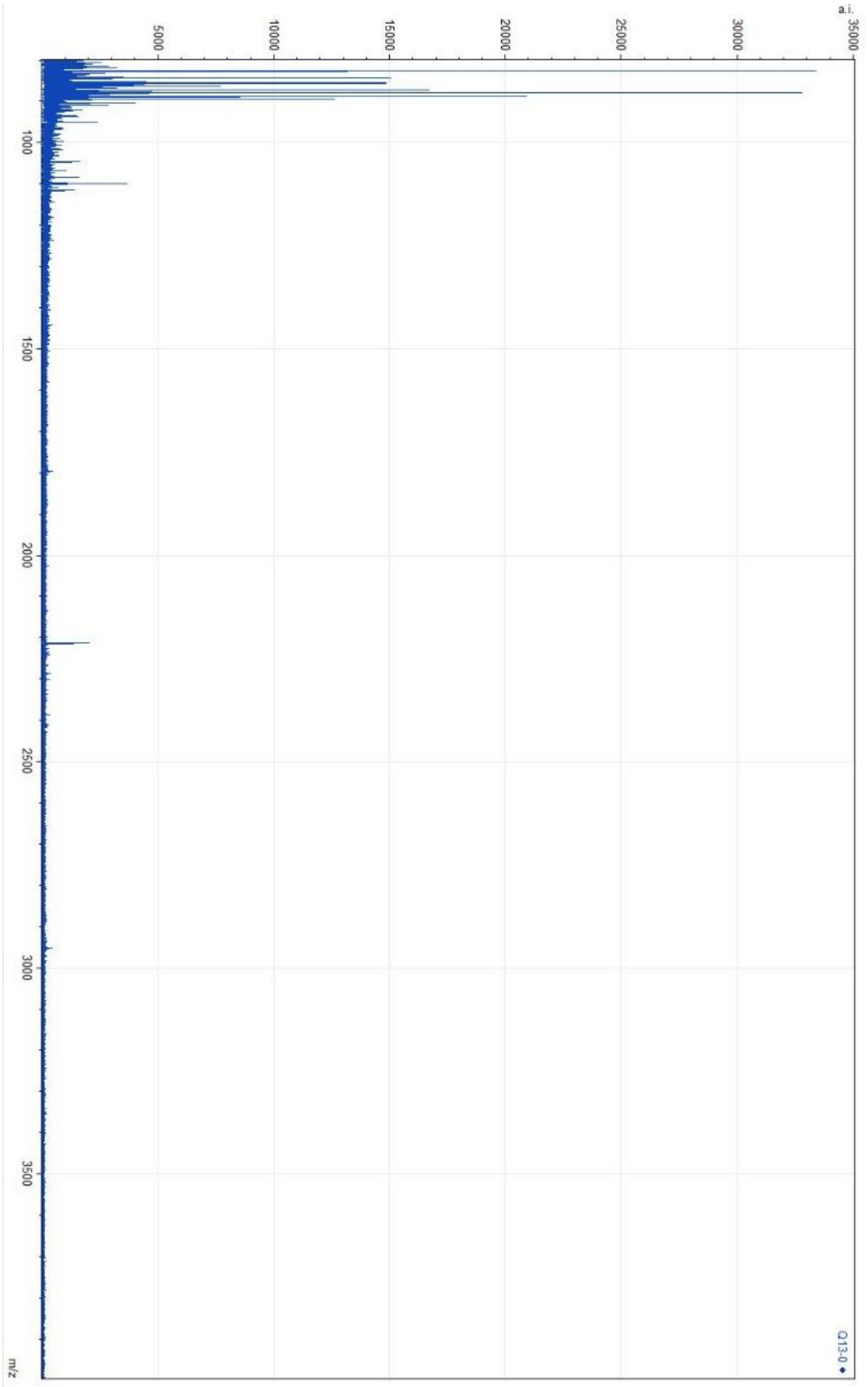
a.i.
5000
10000
15000
20000
25000
30000
35000
1000
1500
2000
2500
3000
3500
m/z
Q13-0

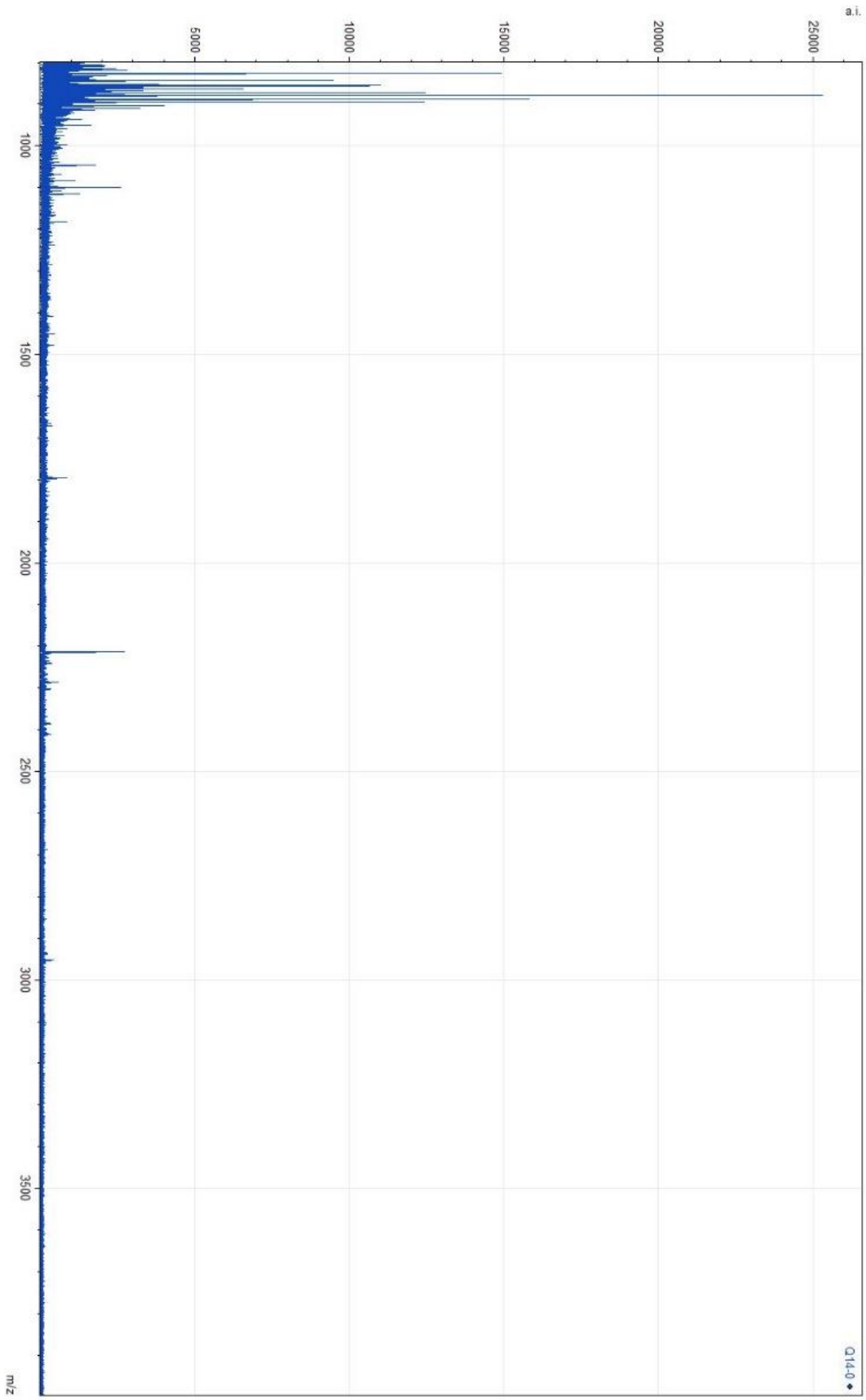
a.i.
5000
10000
15000
20000
25000
1000
1500
2000
2500
3000
3500
m/z
Q14-0

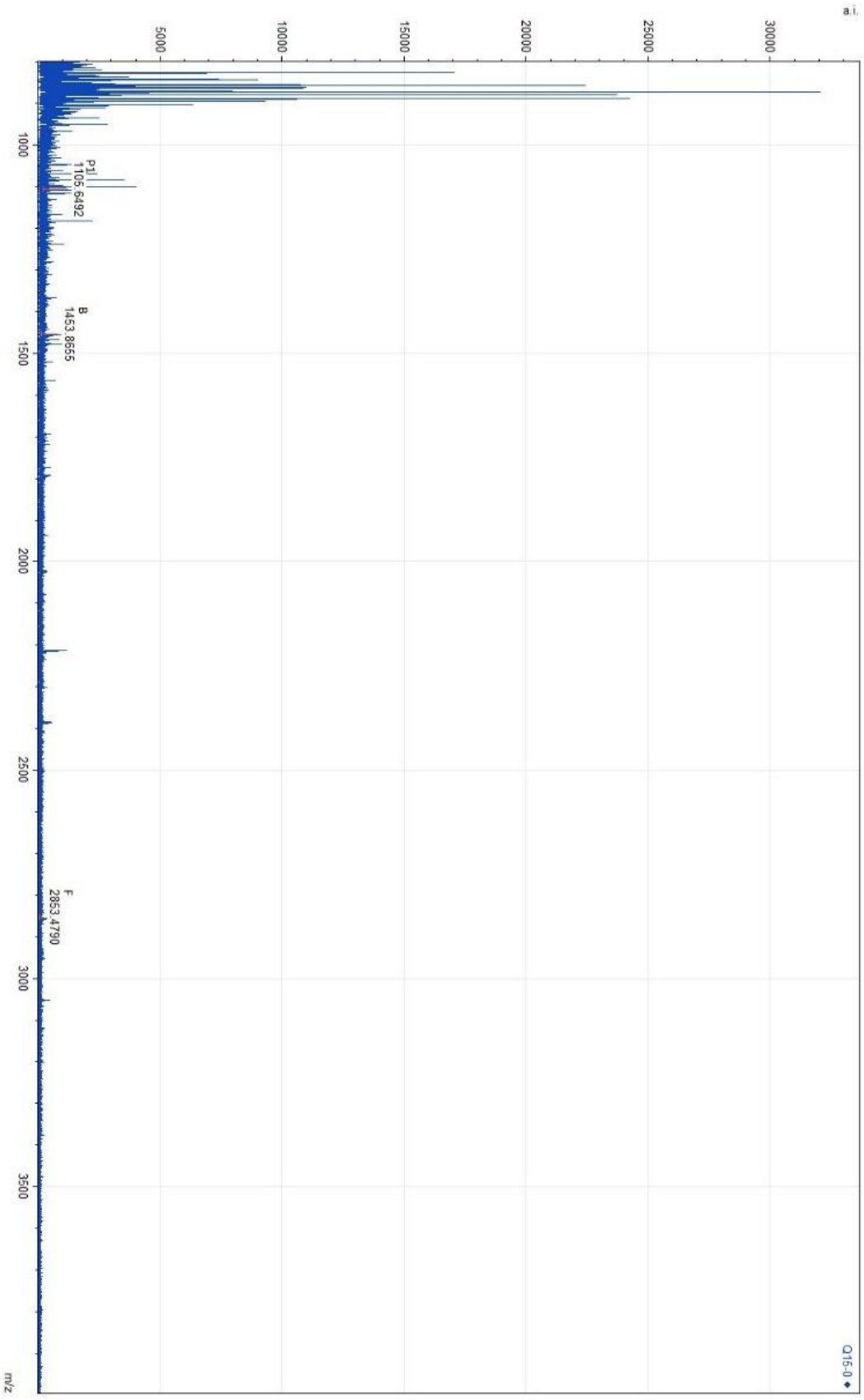
a.i.
5000
10000
15000
20000
25000
30000
1000
1500
2000
2500
3000
3500
m/z
P1
1105.6492
B
1453.8655
F
2853.4790
Q15-0

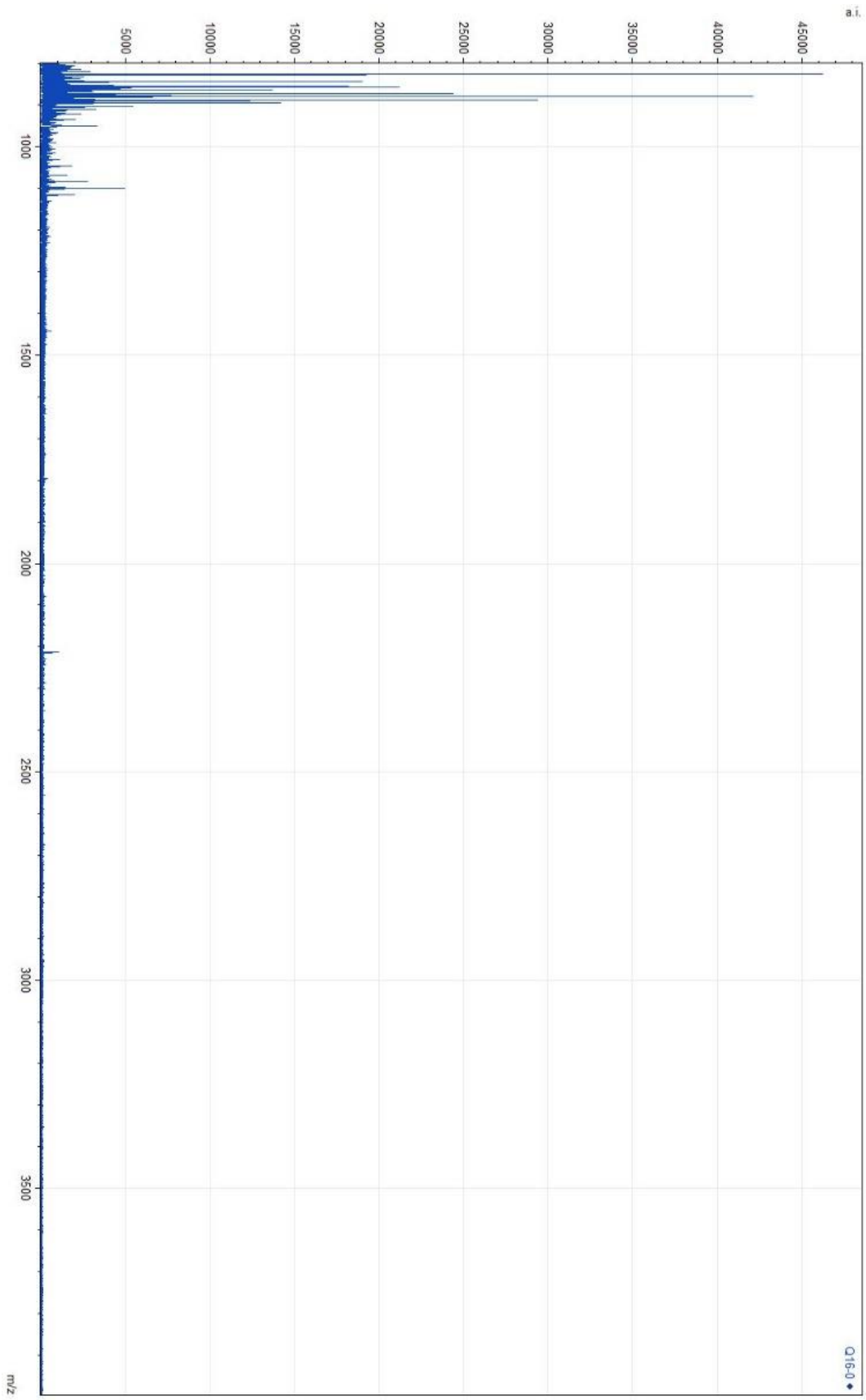
a.i.
5000
10000
15000
20000
25000
30000
35000
40000
45000
1000
1500
2000
2500
3000
3500
m/z
Q16-0

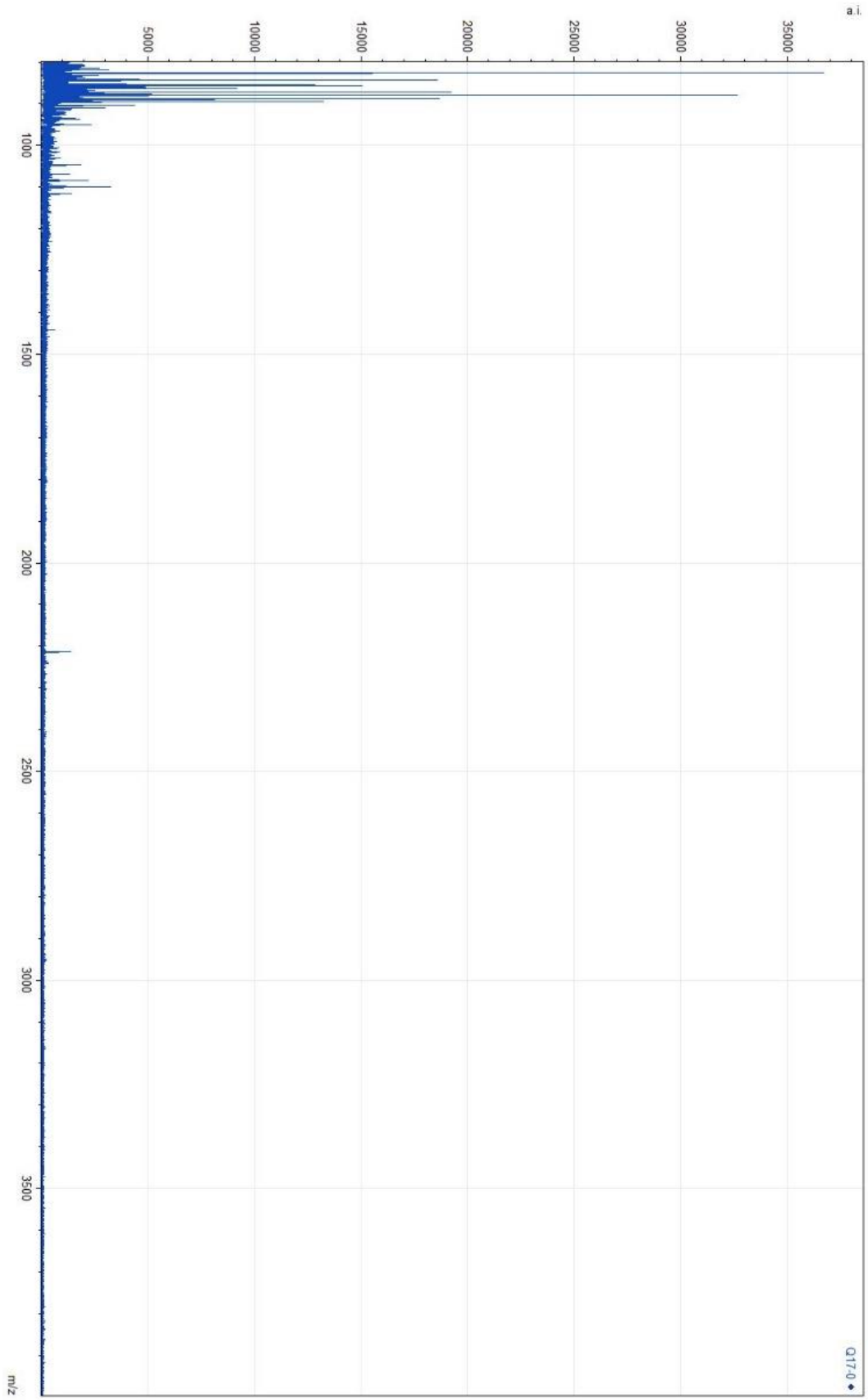
a.i.
5000
10000
15000
20000
25000
30000
35000
1000
1500
2000
2500
3000
3500
m/z
Q17-0

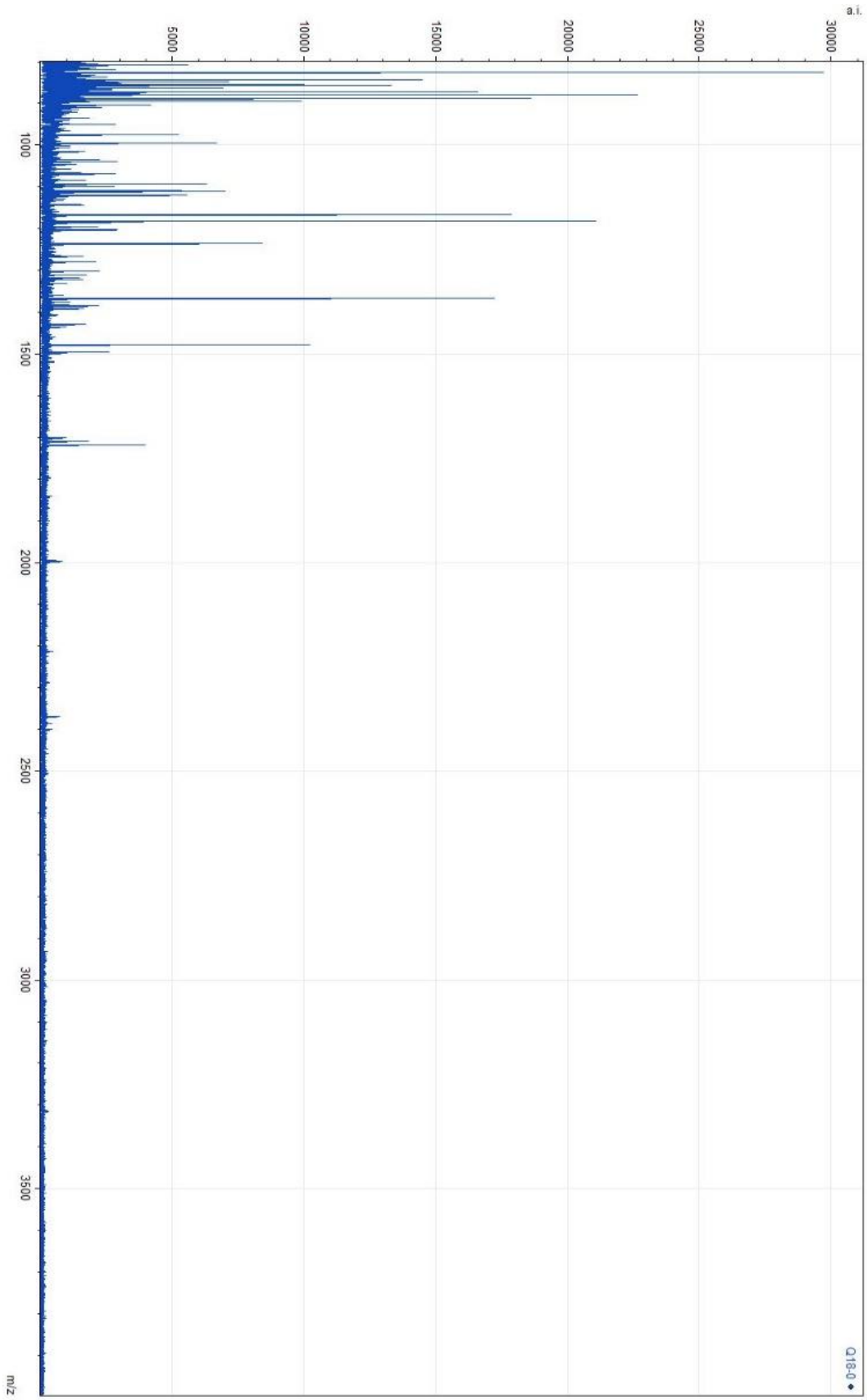
a.i.
5000
10000
15000
20000
25000
30000
1000
1500
2000
2500
3000
3500
m/z
Q18-0

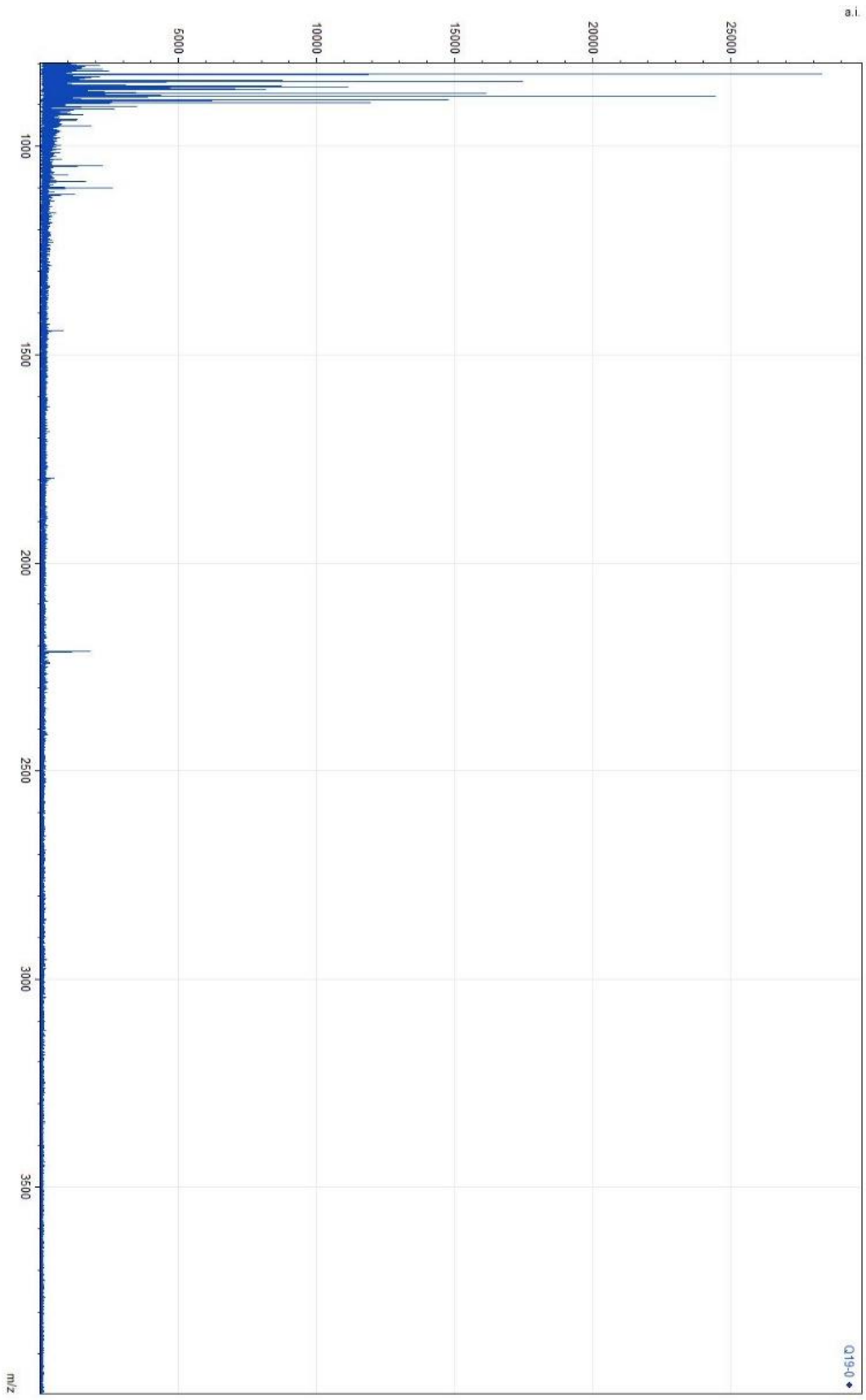
a.i.
5000
10000
15000
20000
25000
1000
1500
2000
2500
3000
3500
m/z
Q19-0

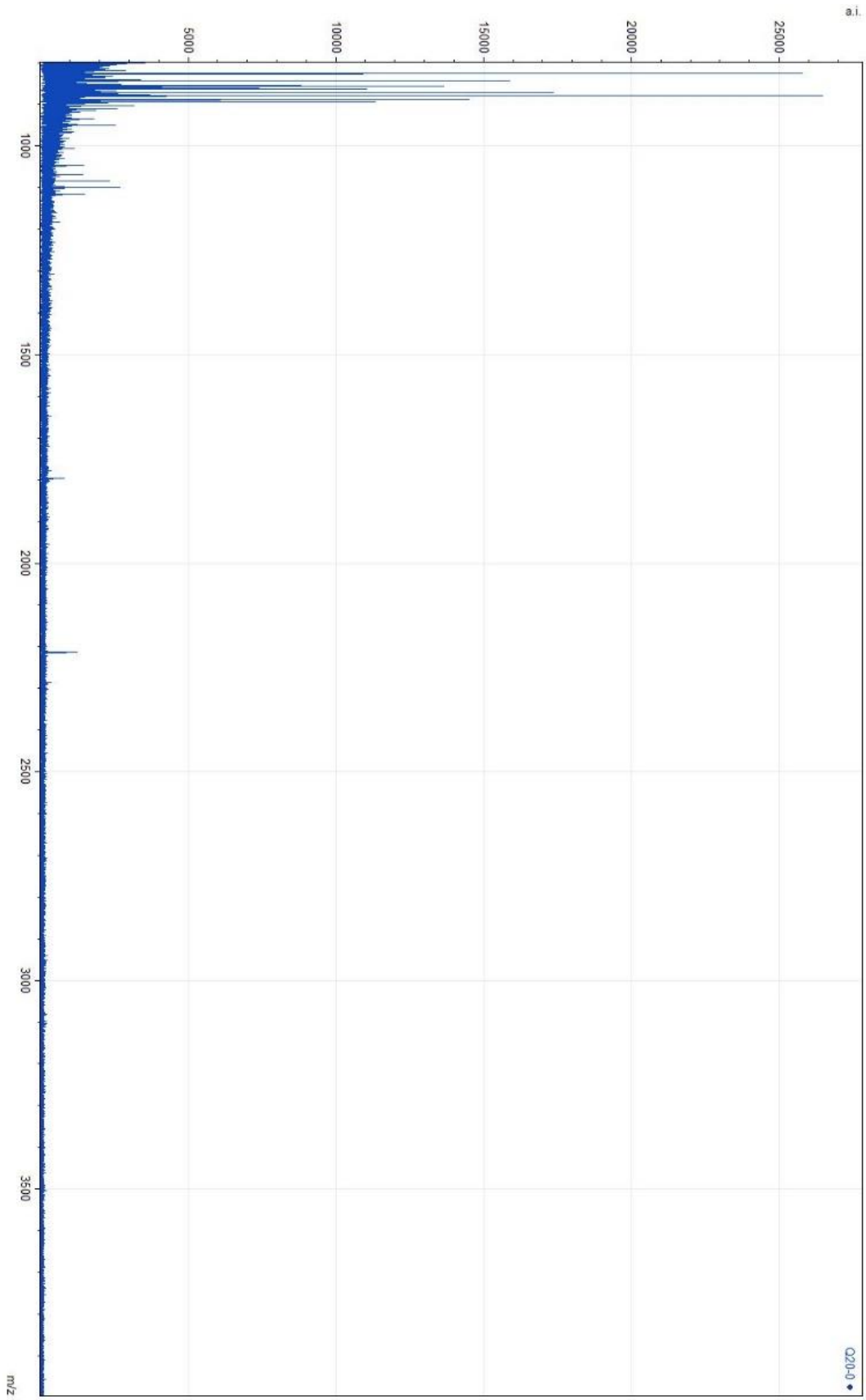
a.i.
5000
10000
15000
20000
25000
1000
1500
2000
2500
3000
3500
m/z
Q20-0

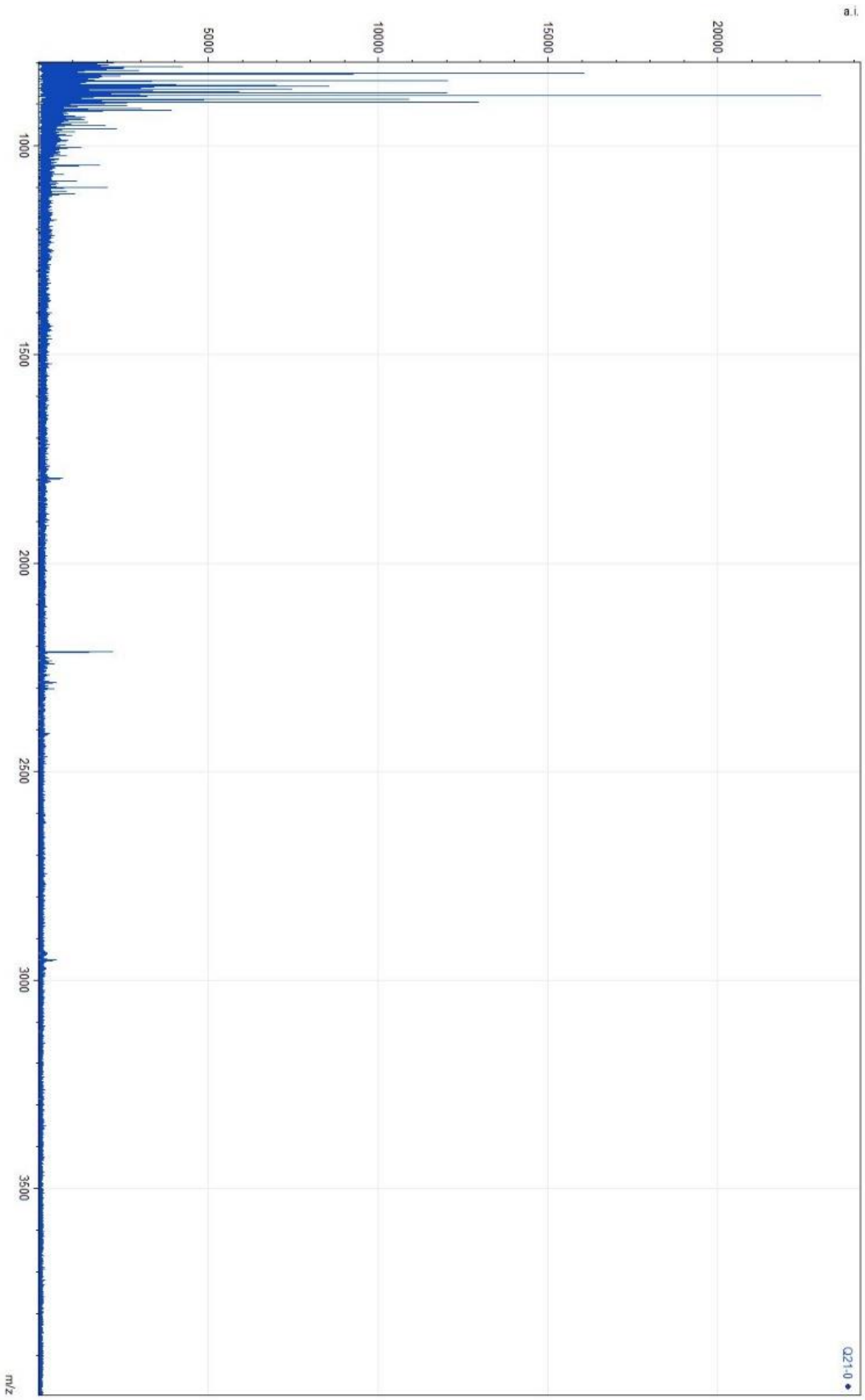
a.i.
5000
10000
15000
20000
1000
1500
2000
2500
3000
3500
m/z
Q21-0

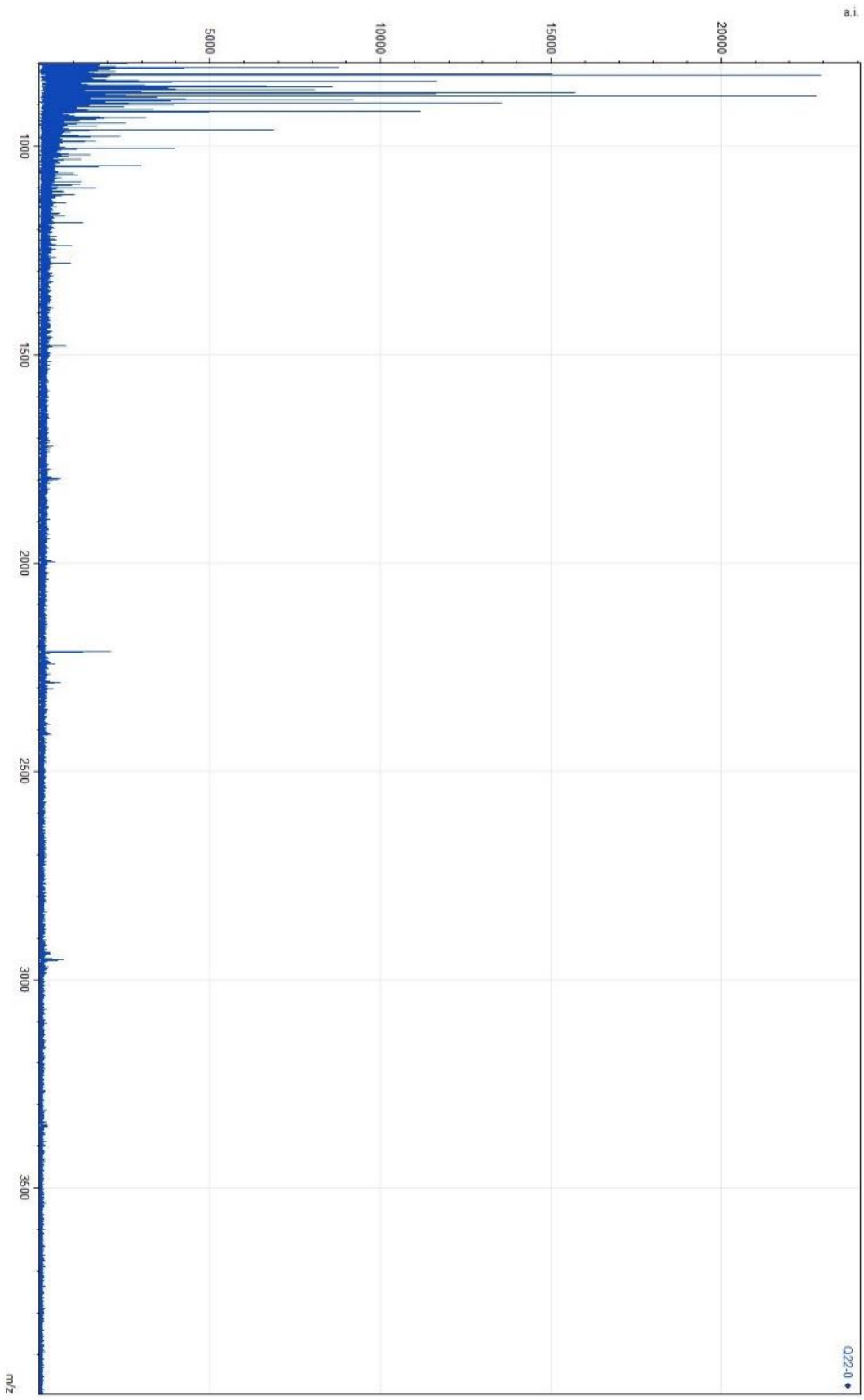
a.i.
5000
10000
15000
20000
1000
1500
2000
2500
3000
3500
m/z
Q22-0

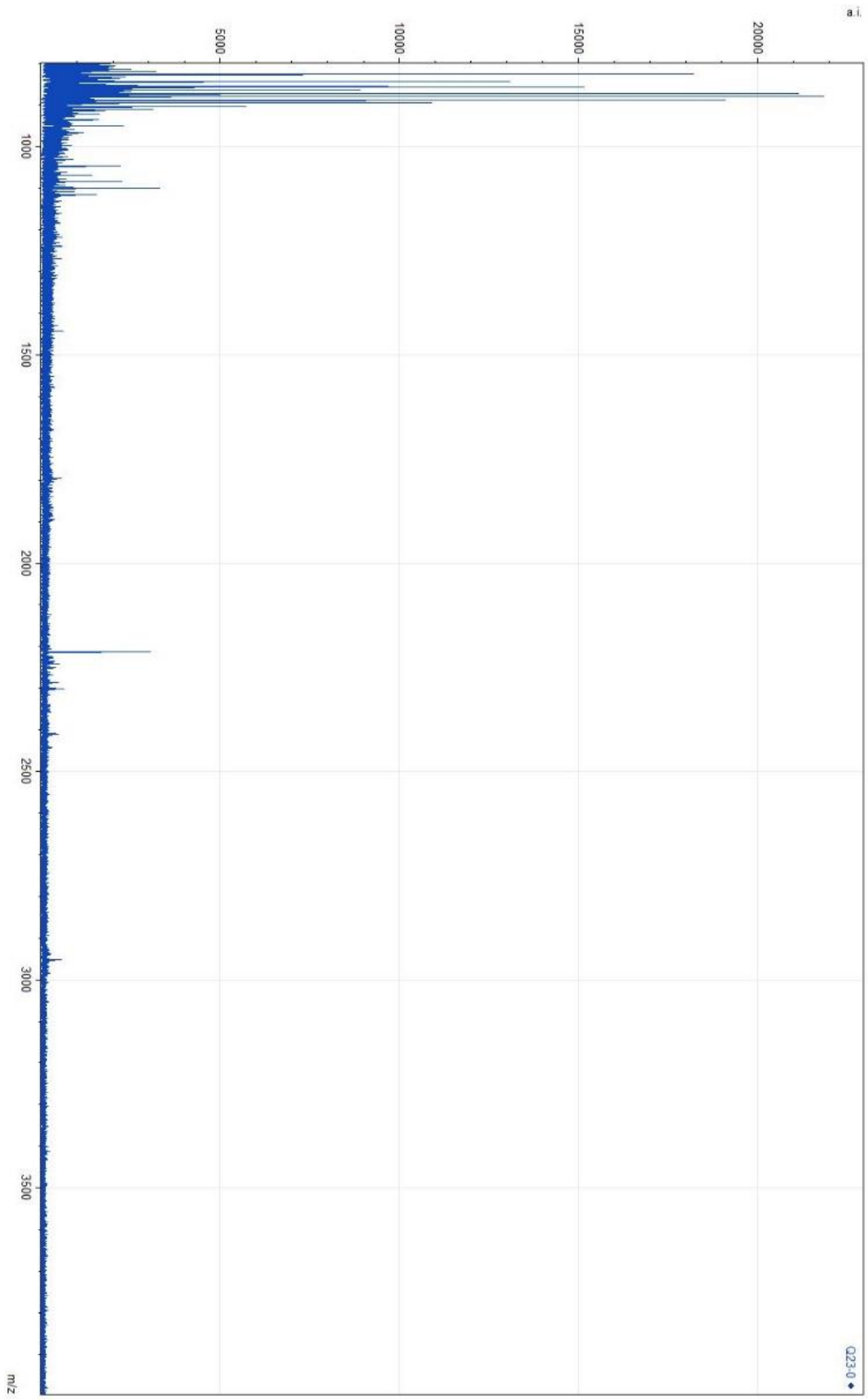
a.i.
5000
10000
15000
20000
1000
1500
2000
2500
3000
3500
m/z
Q23-0

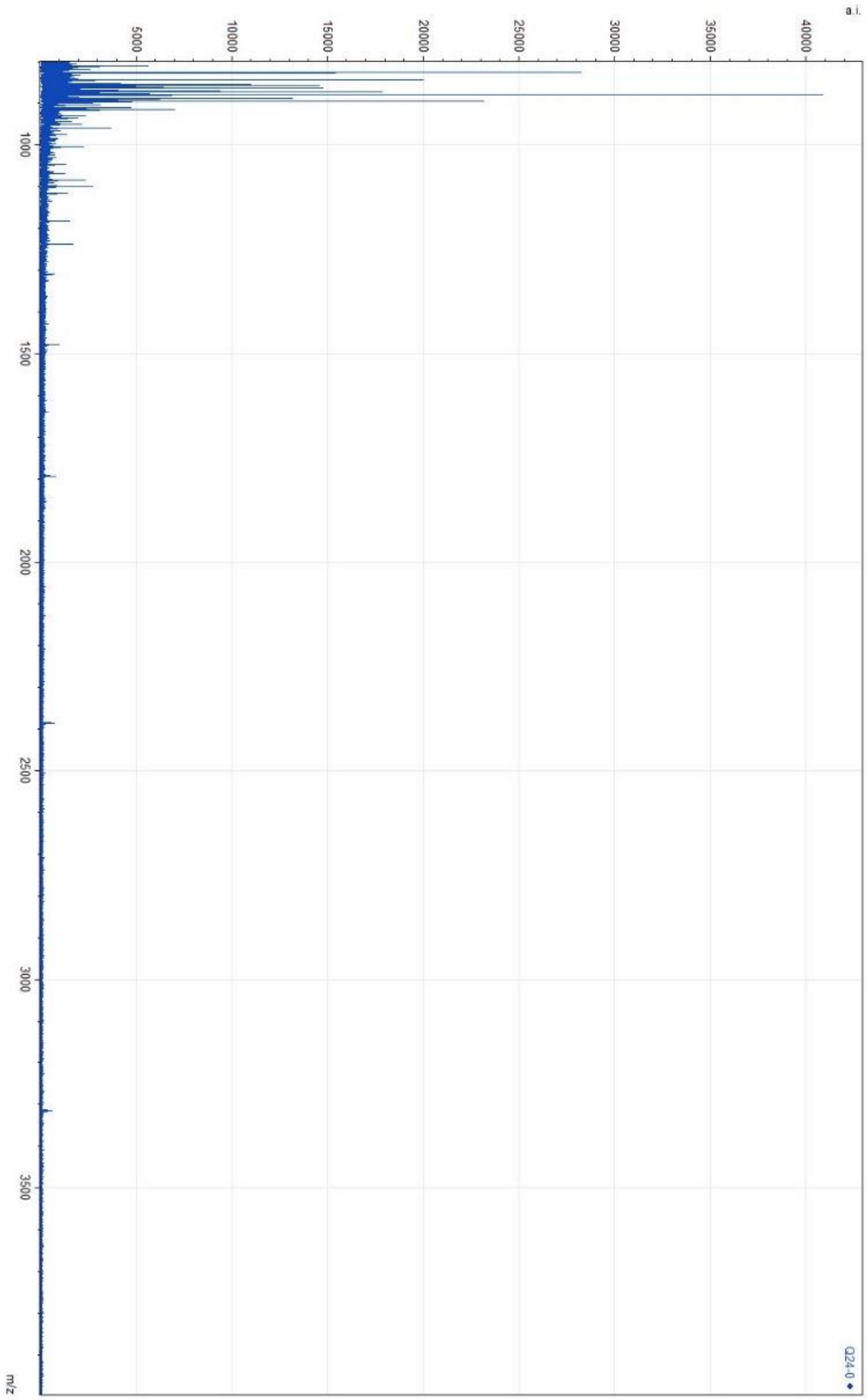
a.i.
5000
10000
15000
20000
25000
30000
35000
40000
1000
1500
2000
2500
3000
3500
m/z
Q24-0

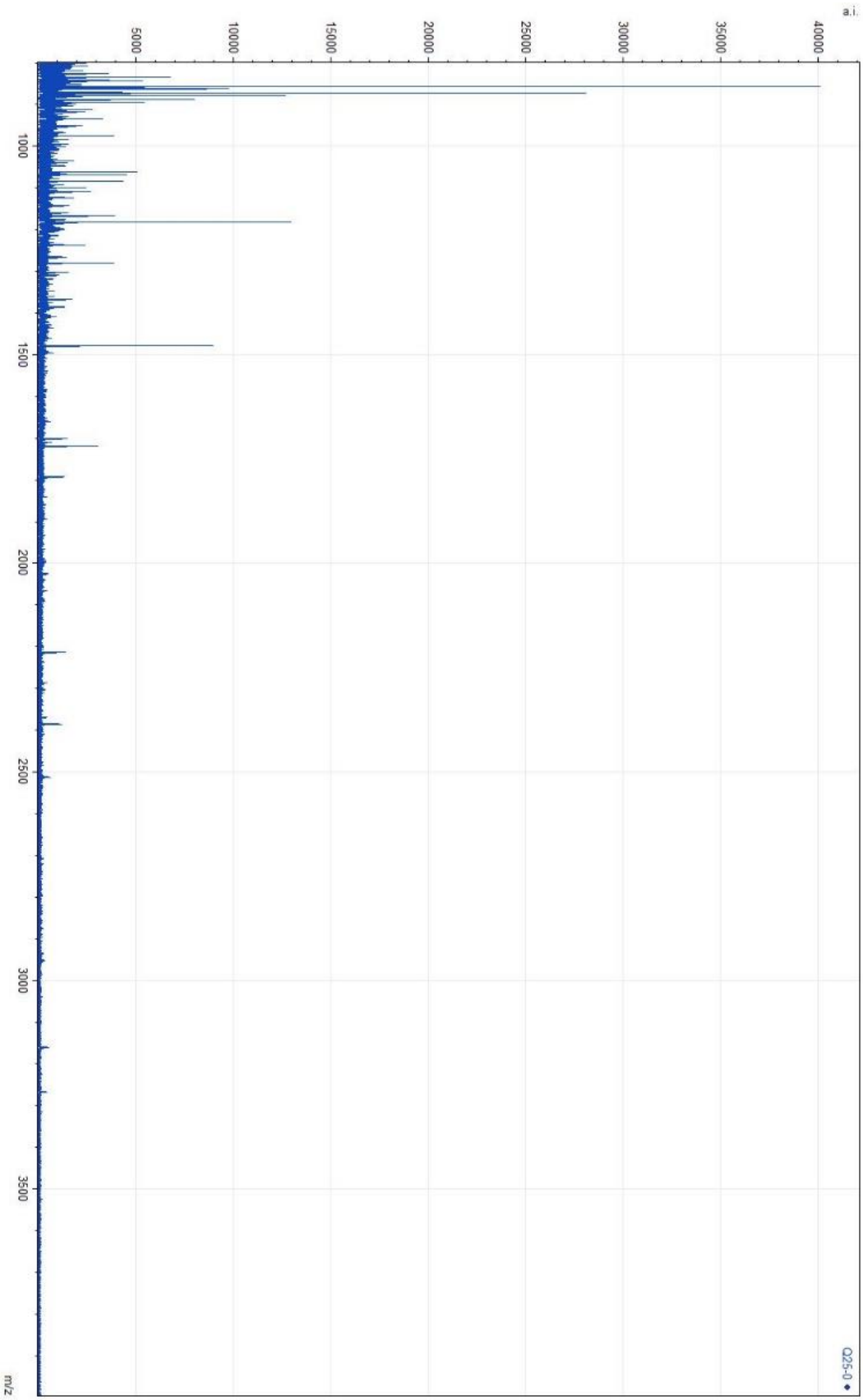
a.i.
5000
10000
15000
20000
25000
30000
35000
40000
1000
1500
2000
2500
3000
3500
m/z
Q25-0

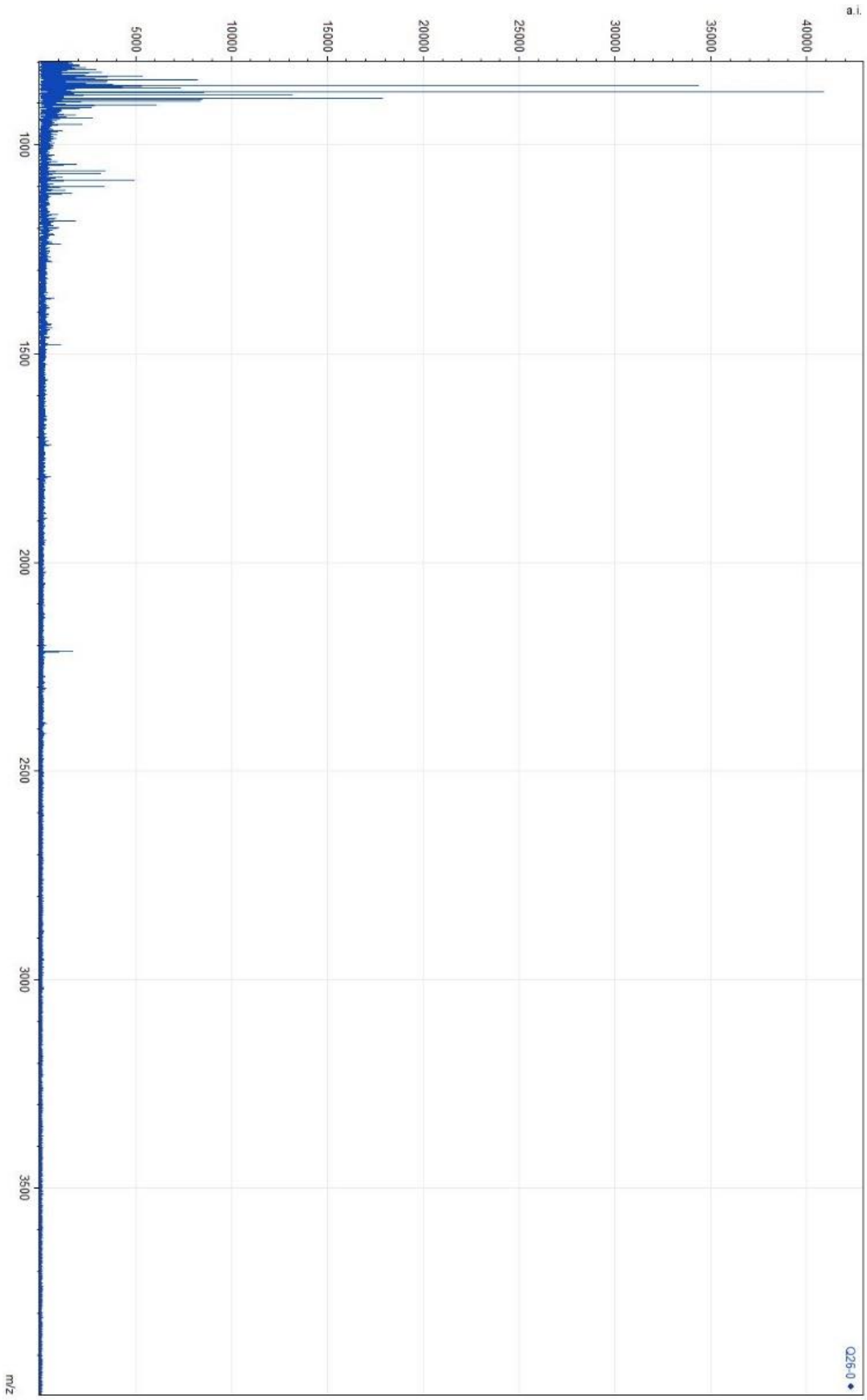
a.i.
5000
10000
15000
20000
25000
30000
35000
40000
1000
1500
2000
2500
3000
3500
m/z
Q26.0

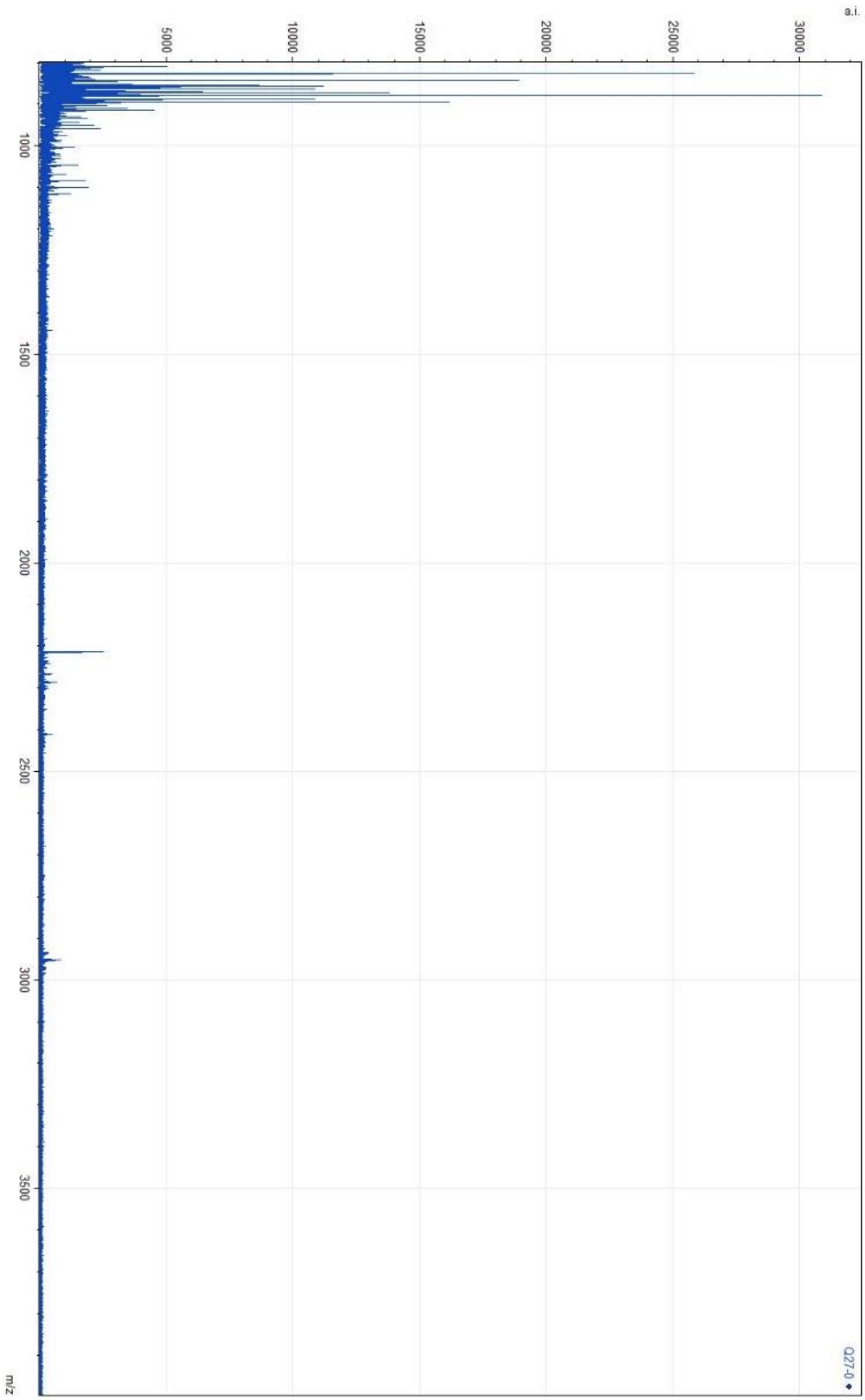
a.i.
5000
10000
15000
20000
25000
30000
1000
1500
2000
2500
3000
3500
m/z
Q27-0

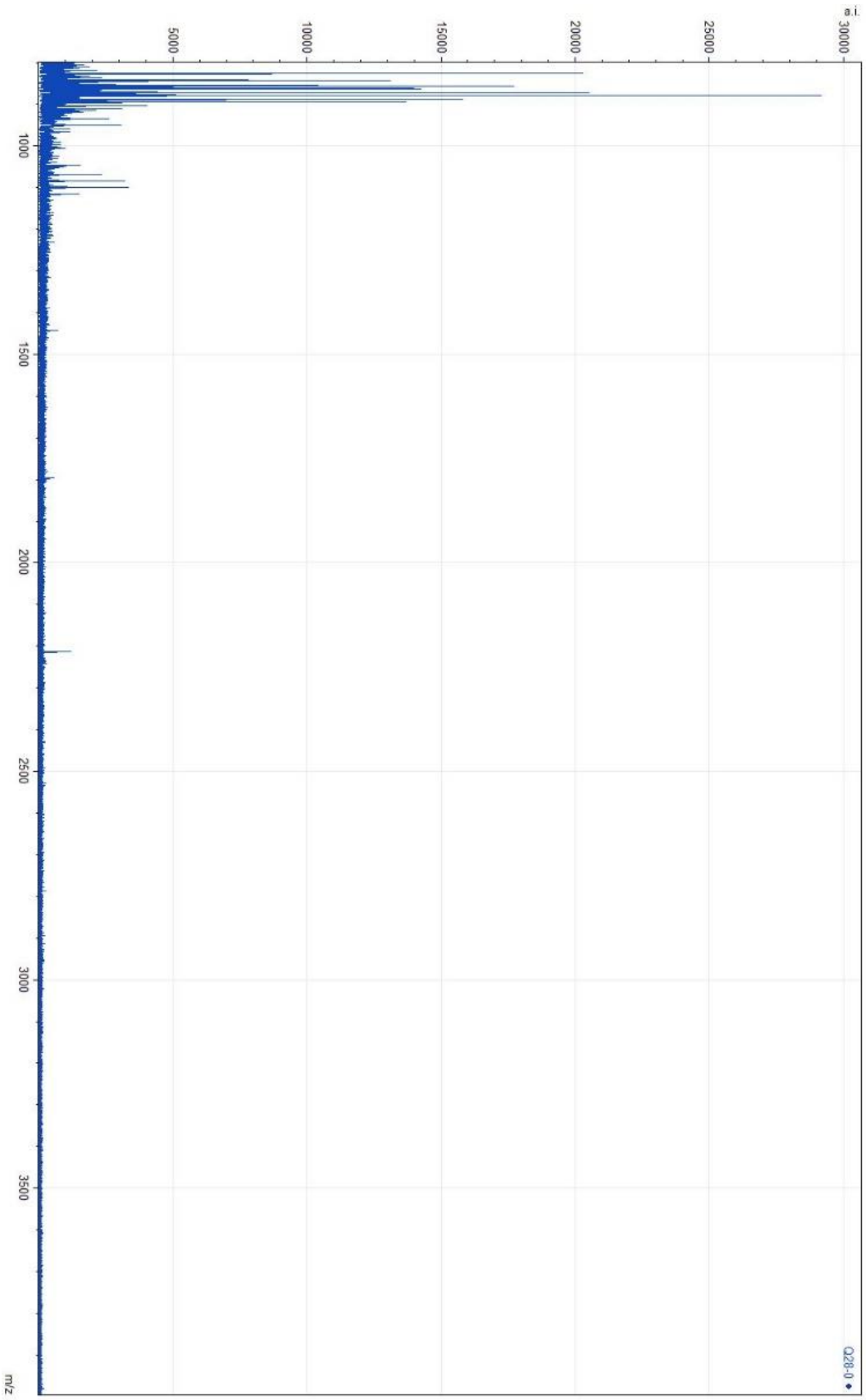
a.i.
5000
10000
15000
20000
25000
30000
1000
1500
2000
2500
3000
3500
m/z
Q28-0

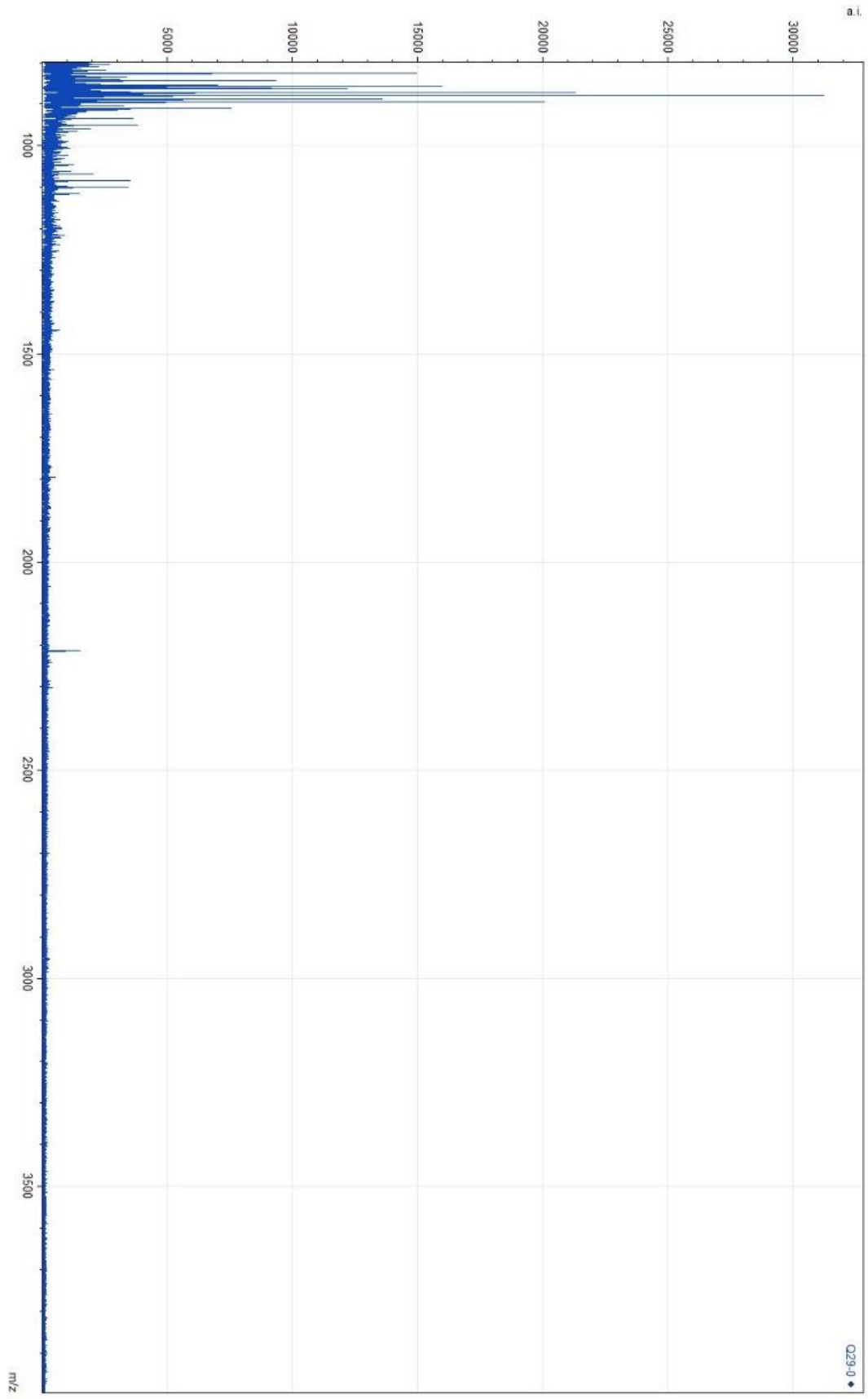
a.i.
5000
10000
15000
20000
25000
30000
1000
1500
2000
2500
3000
3500
m/z
Q29-0

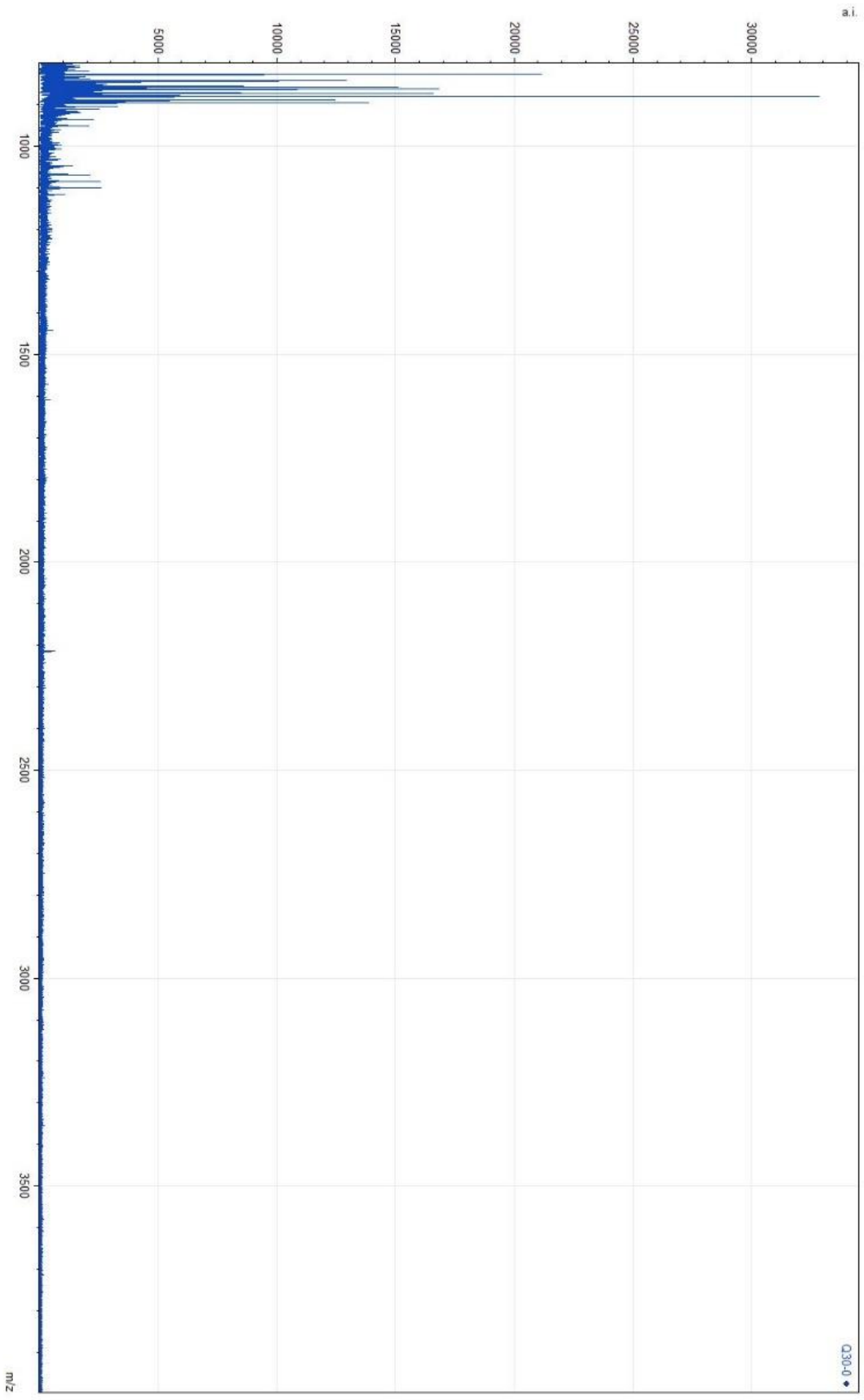
a.i.
5000
10000
15000
20000
25000
30000
1000
1500
2000
2500
3000
3500
m/z
Q30-0

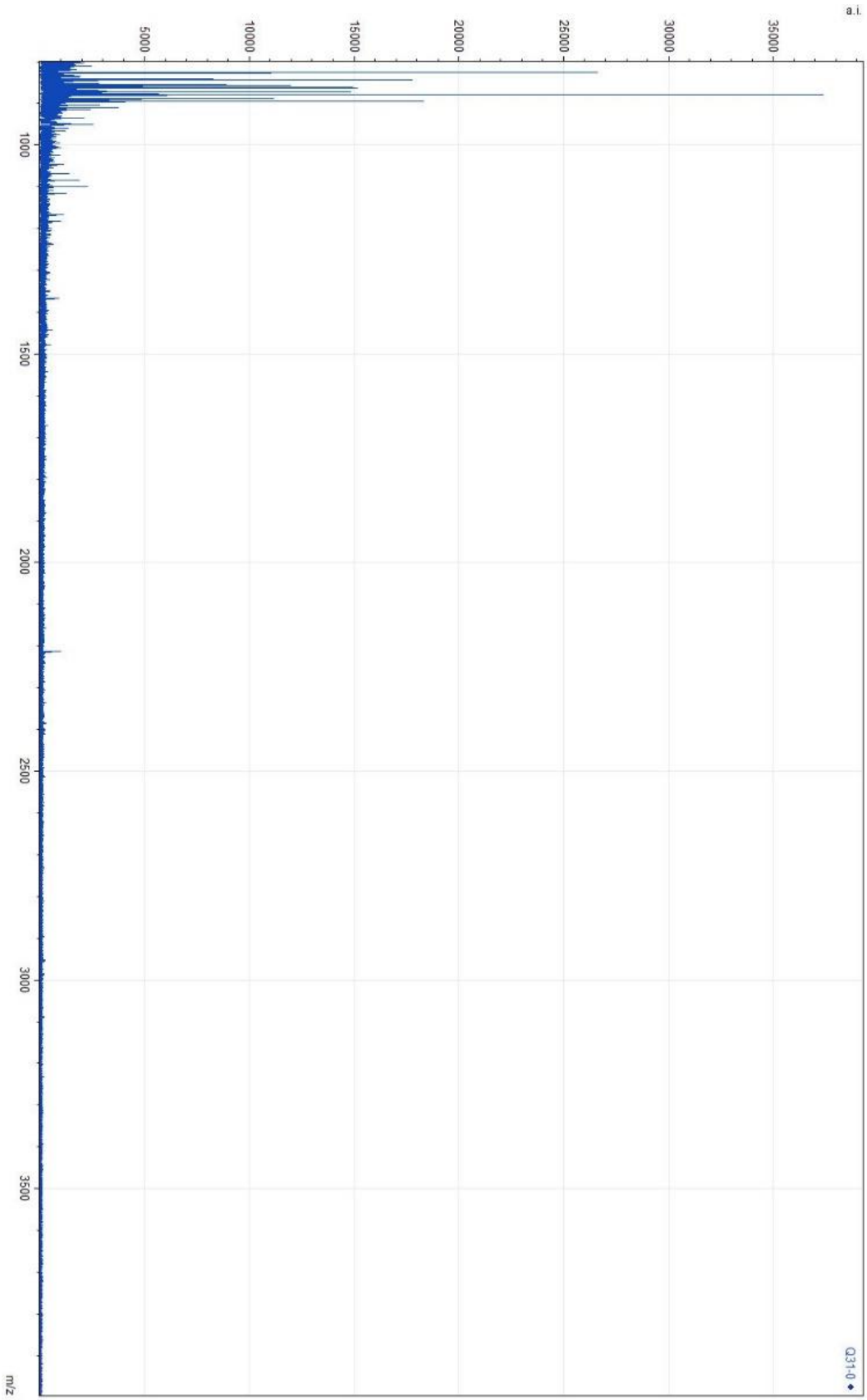
a.i.
5000
10000
15000
20000
25000
30000
35000
1000
1500
2000
2500
3000
3500
m/z
Q3 1-0 ◆

D.3 Mesolithic North Sea bone points

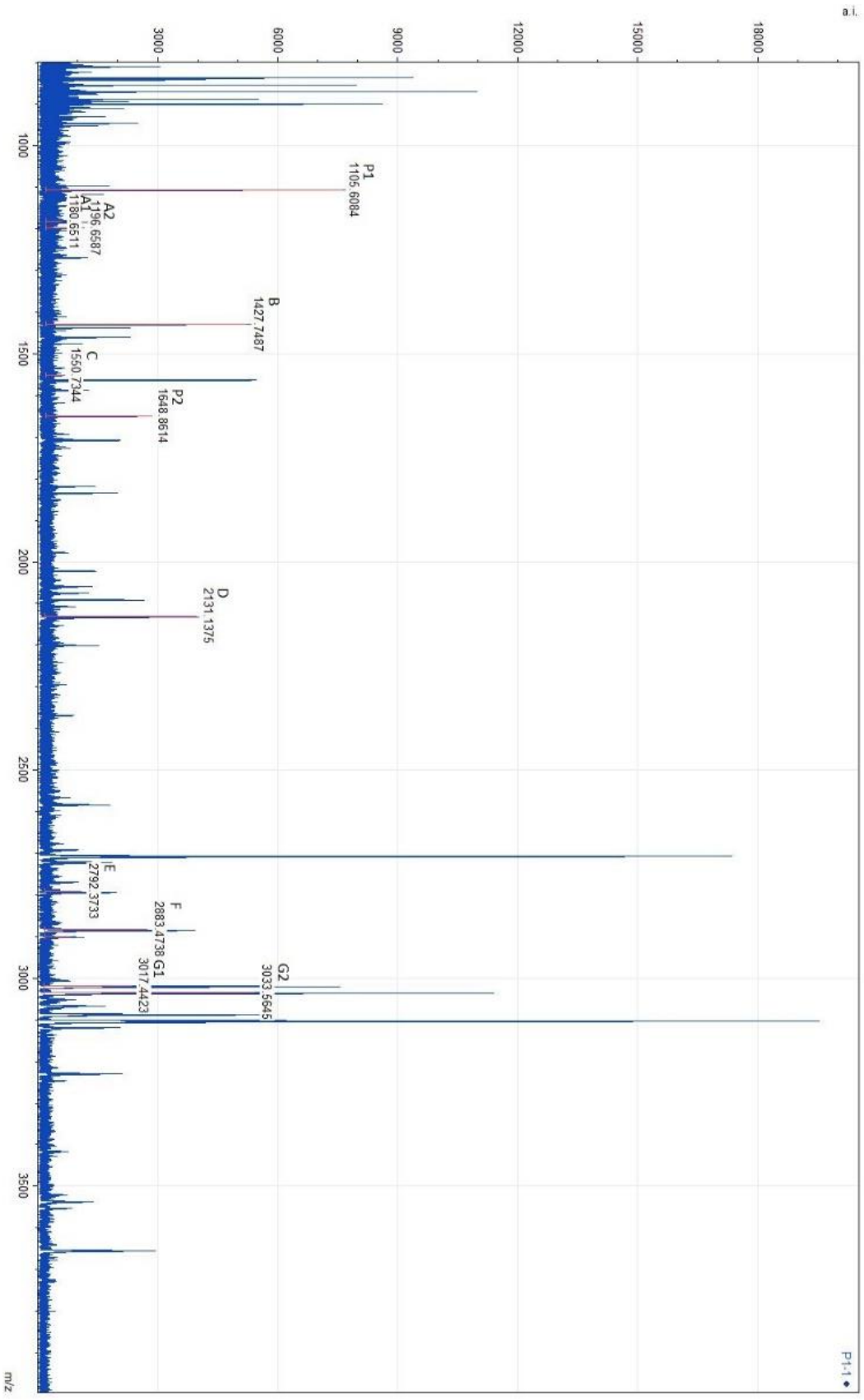

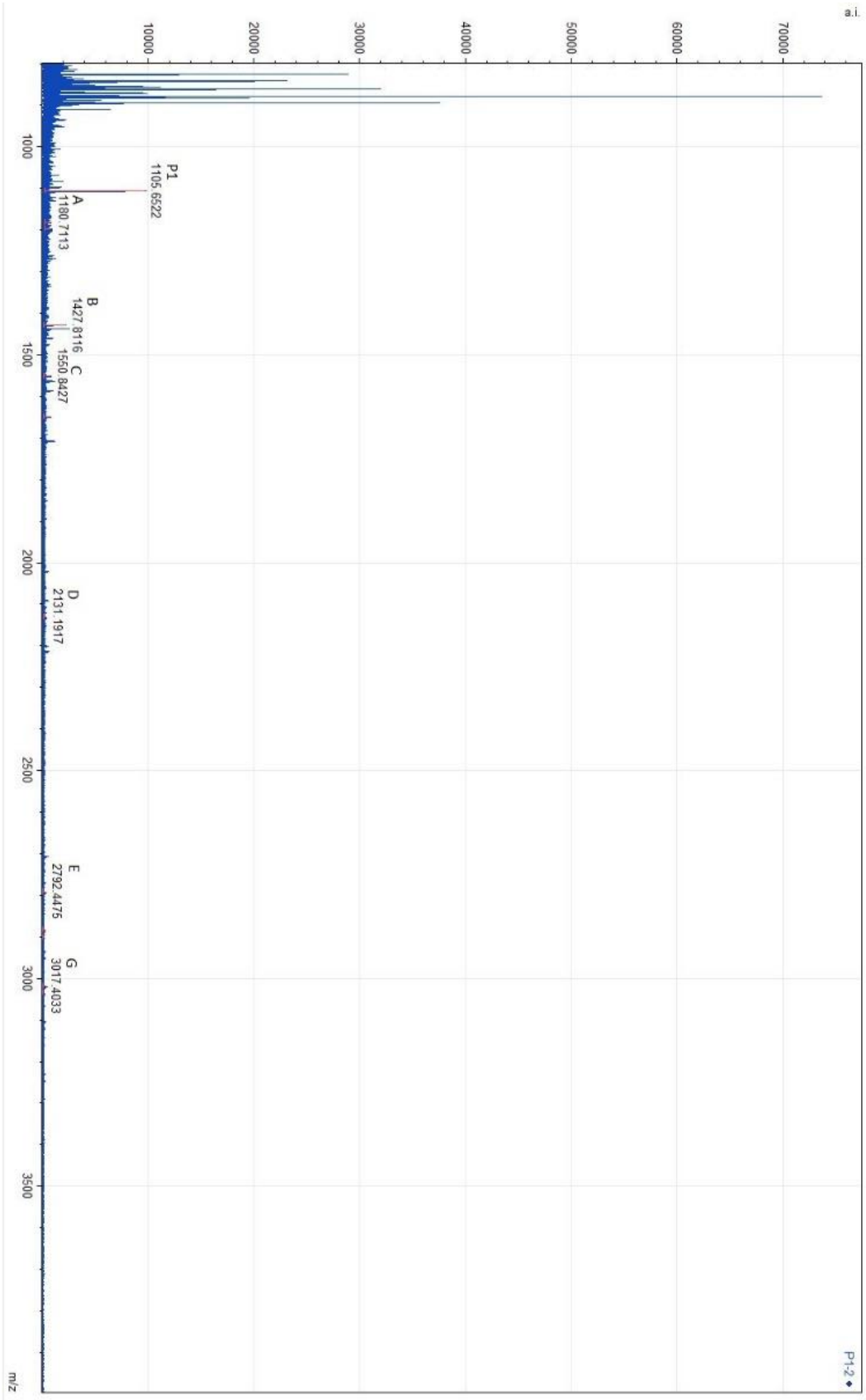
a.i.
70000
60000
50000
40000
30000
20000
10000
P1
1105.6522
A
1180.7113
B
1427.8116
C
1550.8427
D
2131.1917
E
2792.4475
G
3017.4033
1000
1500
2000
2500
3000
3500
m/z
P1-2

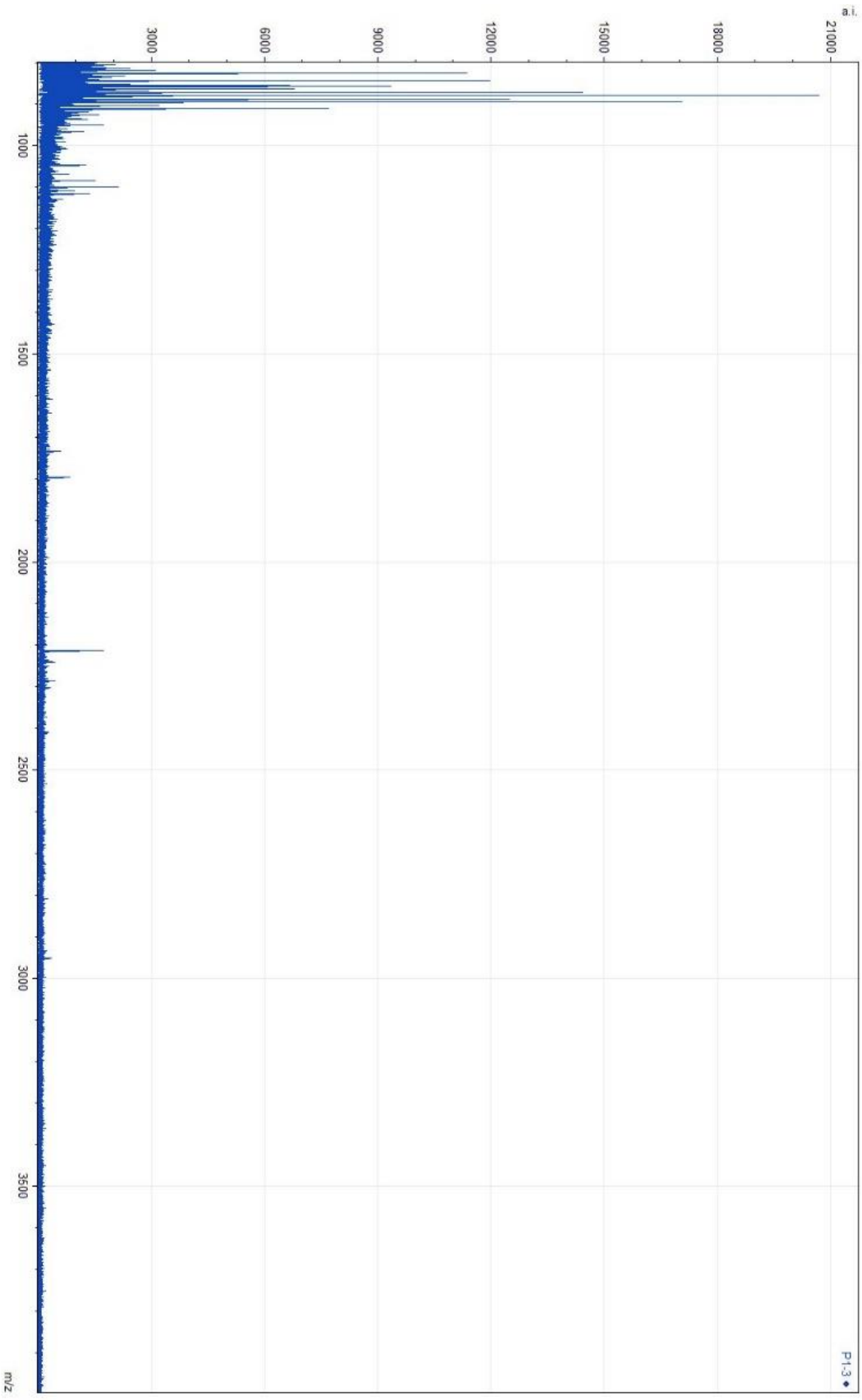
a.i.
3000
6000
9000
12000
15000
18000
21000
1000
1500
2000
2500
3000
3500
m/z
P1:3

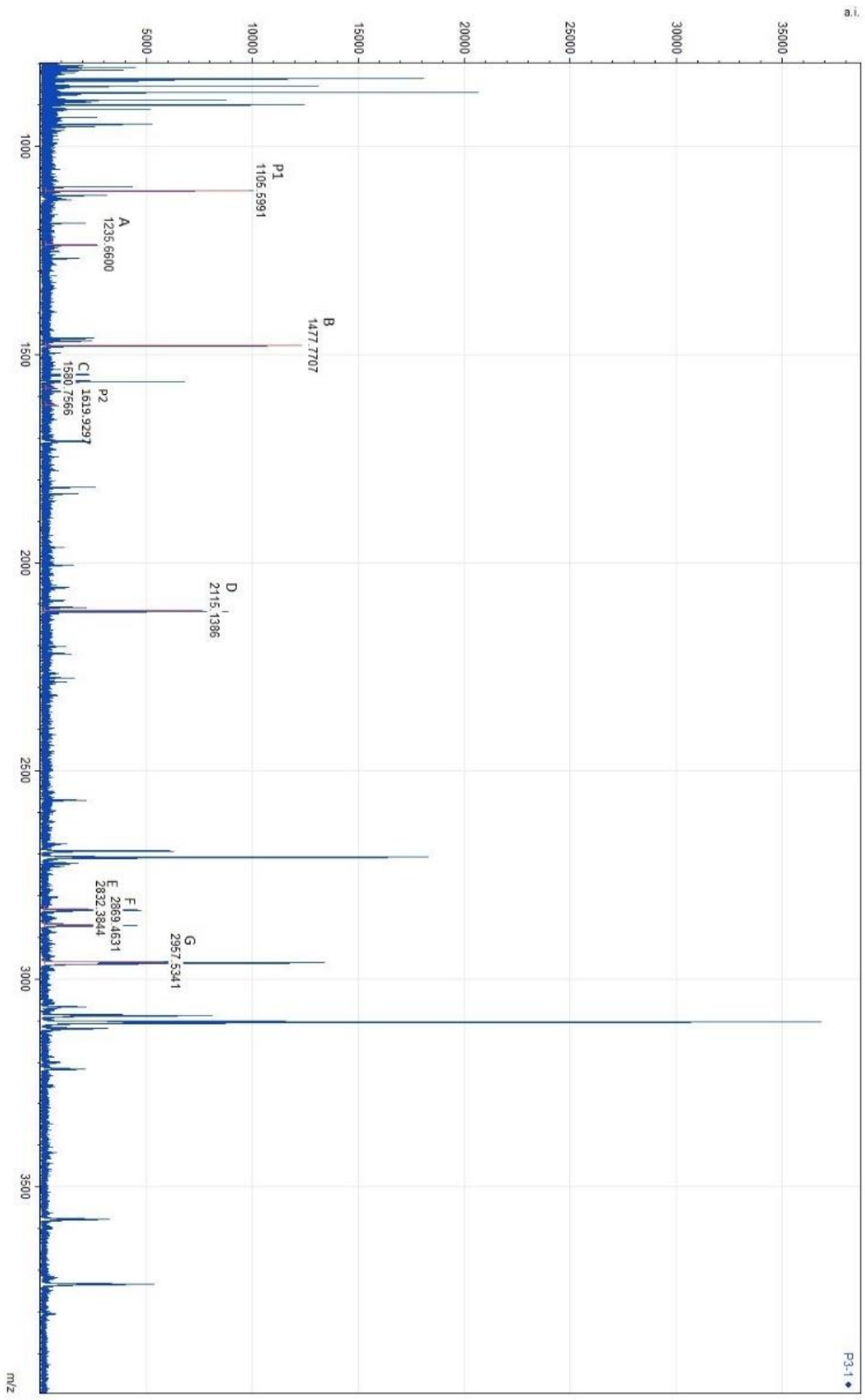
a.i.
5000
10000
15000
20000
25000
30000
35000
1000
1500
2000
2500
3000
3500
m/z
P1
1105.5991
A
1235.6600
B
1477.7707
C
1580.7566
P2
1619.9297
D
2115.1386
E
2832.3844
F
2869.4631
G
2957.5341
P3-1

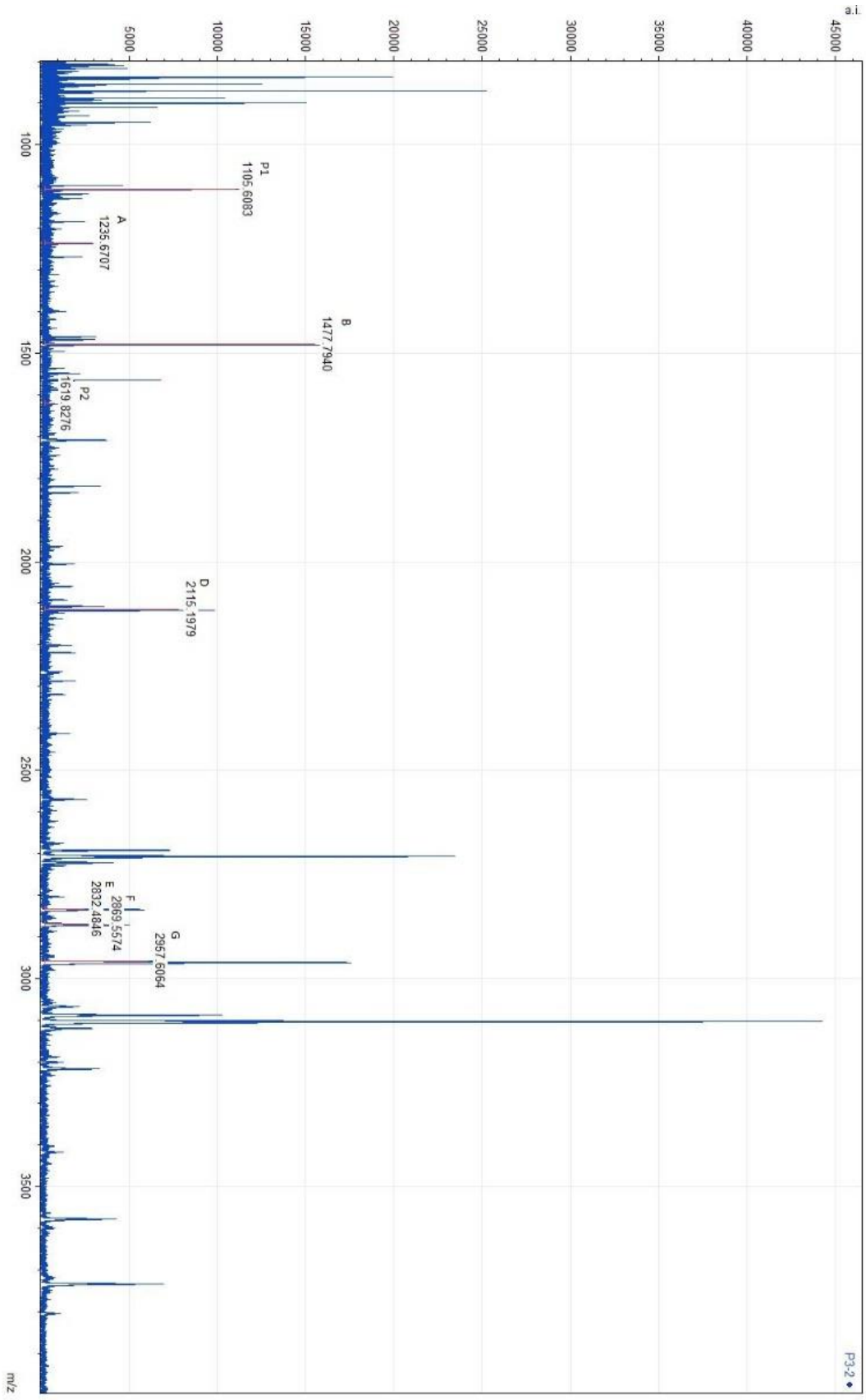
a.i.
5000
10000
15000
20000
25000
30000
35000
40000
45000
1000
1500
2000
2500
3000
3500
m/z
P1
1105.6083
A
1235.6707
B
1477.7940
P2
1619.8276
D
2115.1979
F
2869.5574
E
2832.4846
G
2967.6064
P3-2

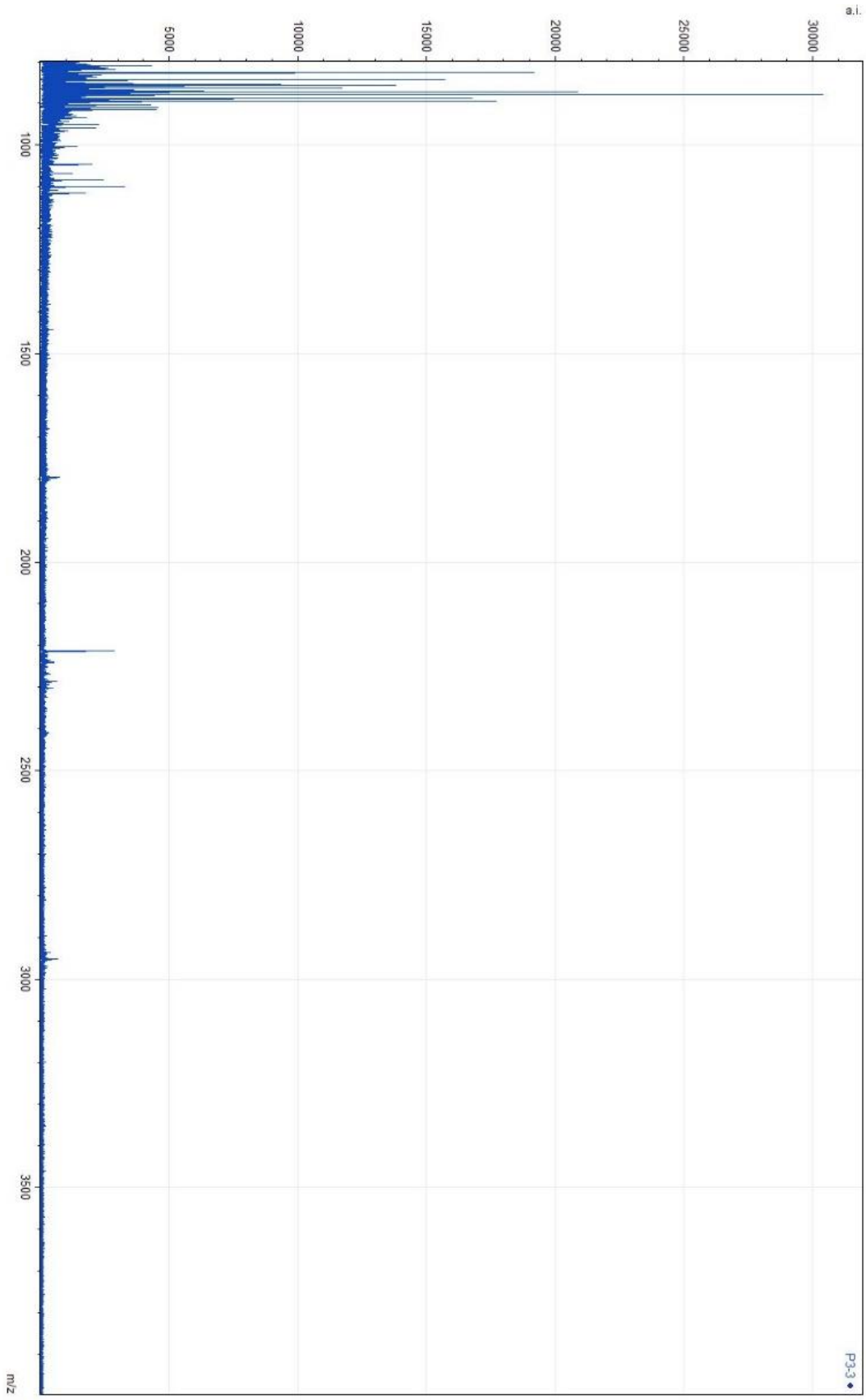
a.i.
5000
10000
15000
20000
25000
30000
1000
1500
2000
2500
3000
3500
m/z
P3-3

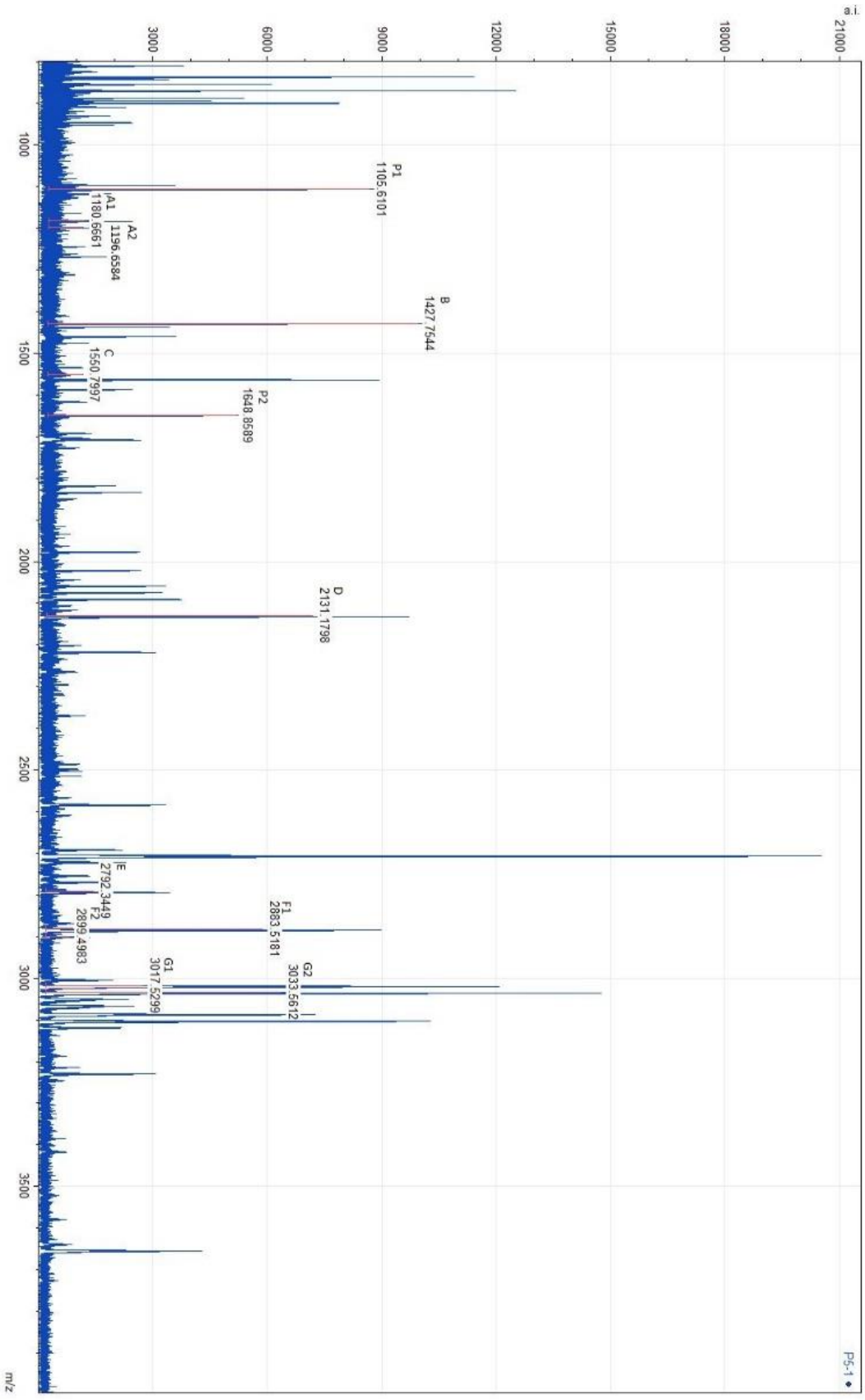
a.i.
21000
18000
15000
12000
9000
6000
3000
1000
1500
2000
2500
3000
3500
m/z
P1
1105.6101
A1
1180.6661
A2
1196.6584
B
1427.7544
C
1550.7997
P2
1648.8589
D
2131.1798
E
2792.3449
F2
2899.4983
F1
2883.5181
G1
3017.5299
G2
3033.5612
P5-1

a.i.
5000
10000
15000
20000
25000
30000
1000
1500
2000
2500
3000
3500
m/z
P1
1105.6367
A1
1180.7033
A2
1196.6845
B
1427.7928
C
1550.8285
P2
1648.8946
D
2131.2009
E
2792.3893
F
2883.5375
G1
3017.4795
G2
3033.5885
P5-2

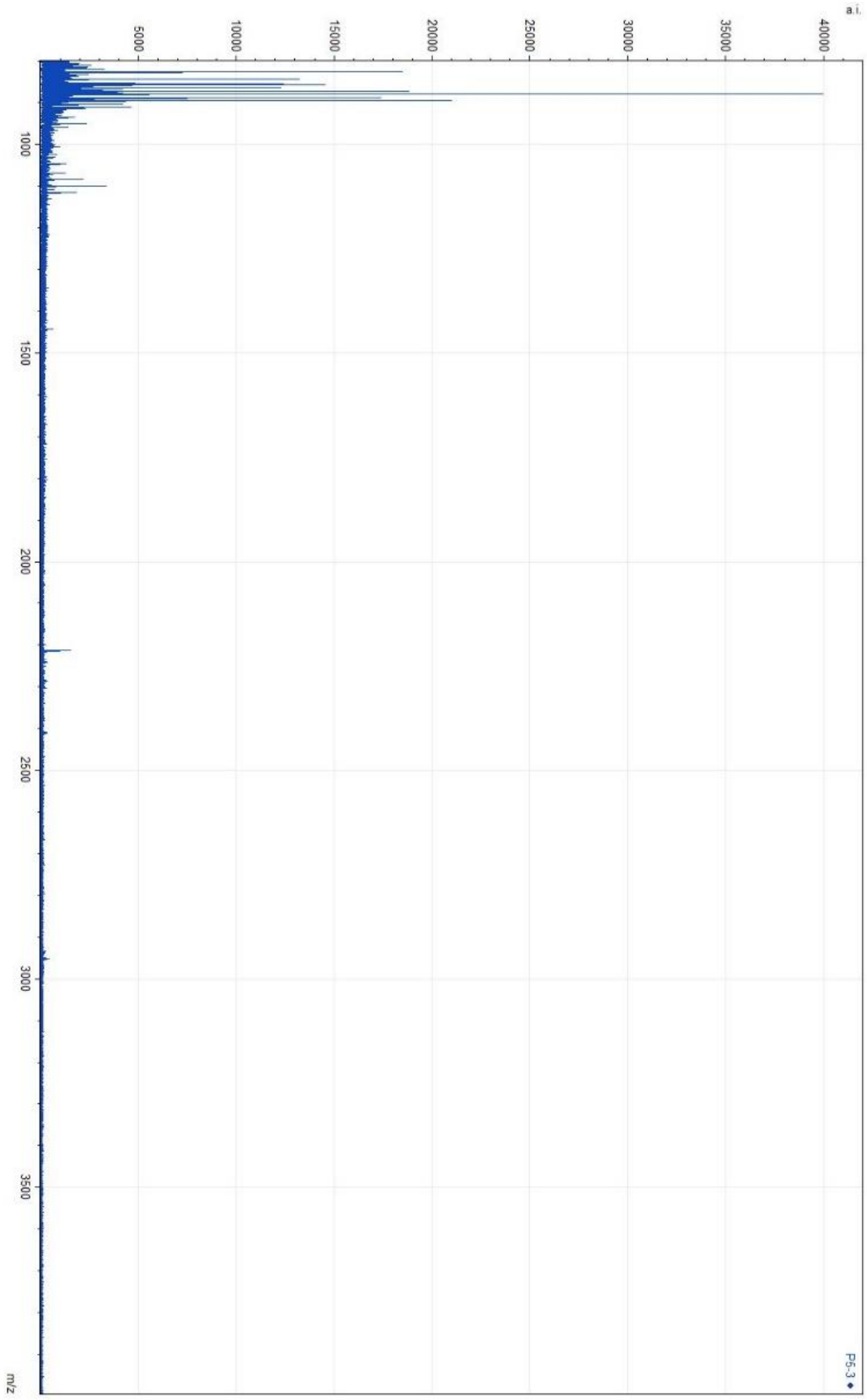
a.i.
5000
10000
15000
20000
25000
30000
35000
40000
1000
1500
2000
2500
3000
3500
m/z
P5-3

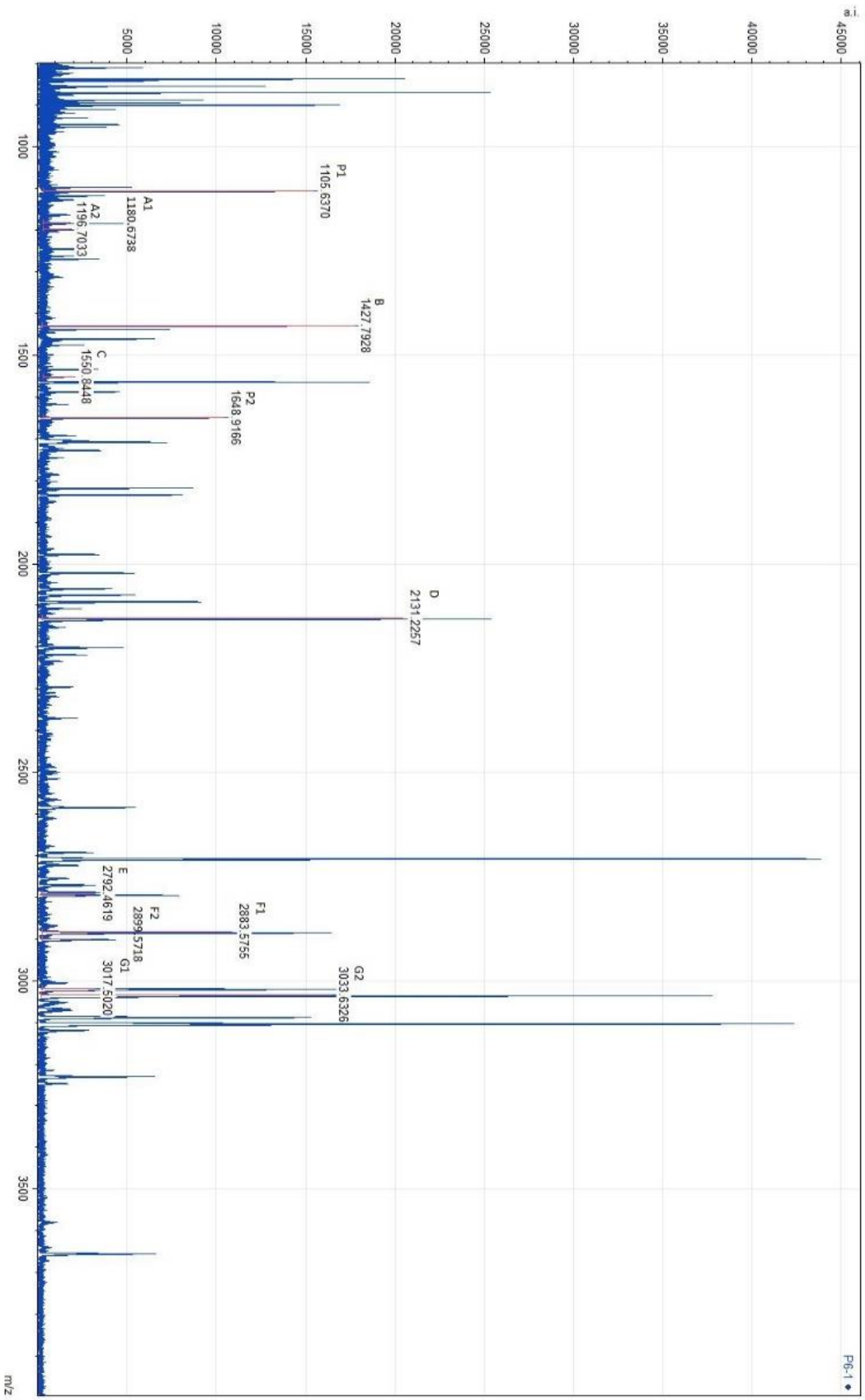
a.i.
45000
40000
35000
30000
25000
20000
15000
10000
5000
1000
1500
2000
2500
3000
3500
m/z
P1
1105.6370
A1
1180.6738
A2
1196.7033
B
1427.7928
C
1550.8448
P2
1648.9166
D
2131.2257
E
2792.4619
F2
2899.5718
F1
2883.5755
G1
3017.5020
G2
3033.6326
P6-1

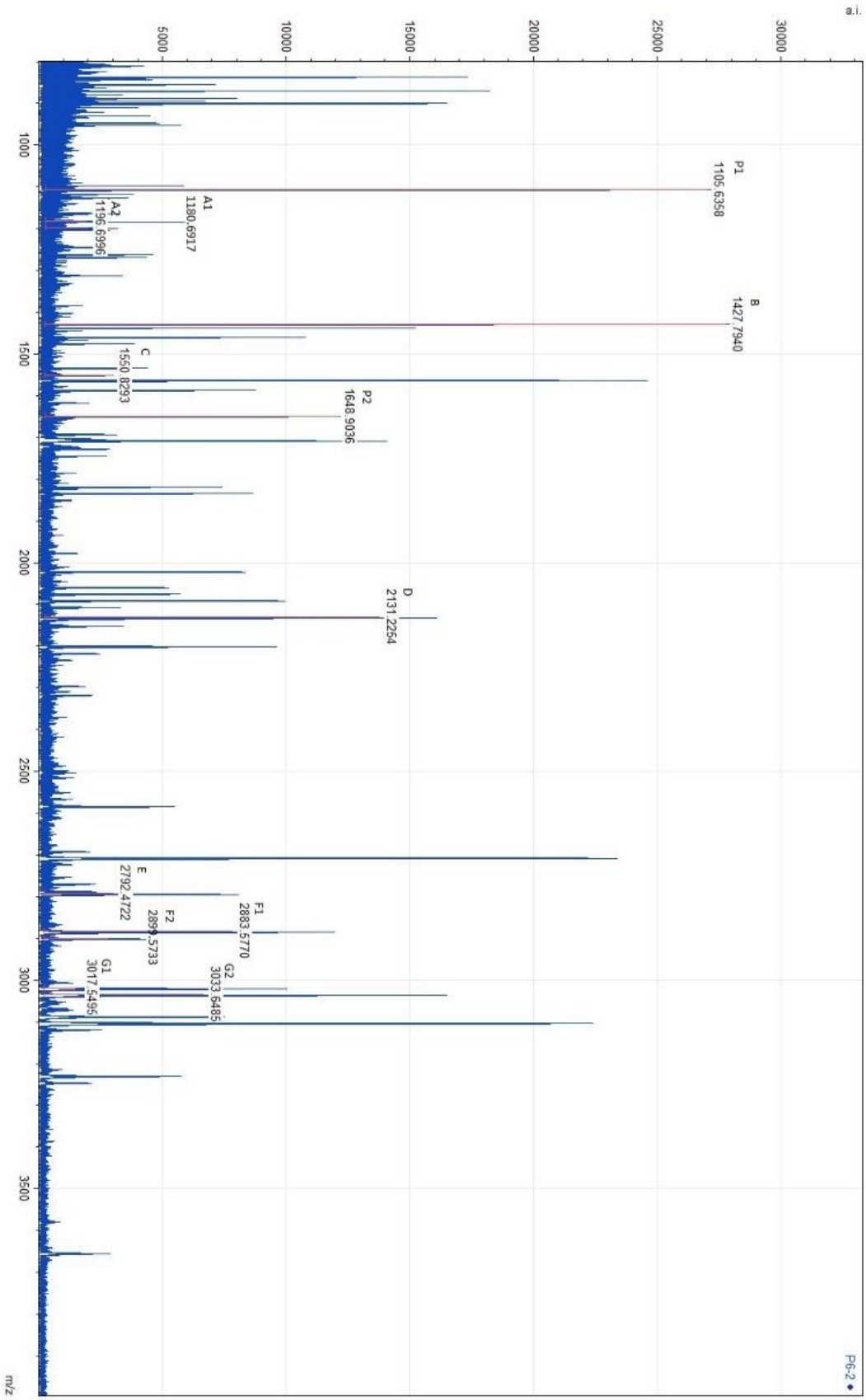
a.i.
5000
10000
15000
20000
25000
30000
1000
1500
2000
2500
3000
3500
m/z
P1
1105.6358
A1
1180.6917
A2
1196.6996
B
1427.7940
C
1550.8293
P2
1648.9036
D
2131.2254
E
2792.4722
F2
2894.5733
F1
2883.5770
G1
3017.6496
G2
3033.6485
P6-2

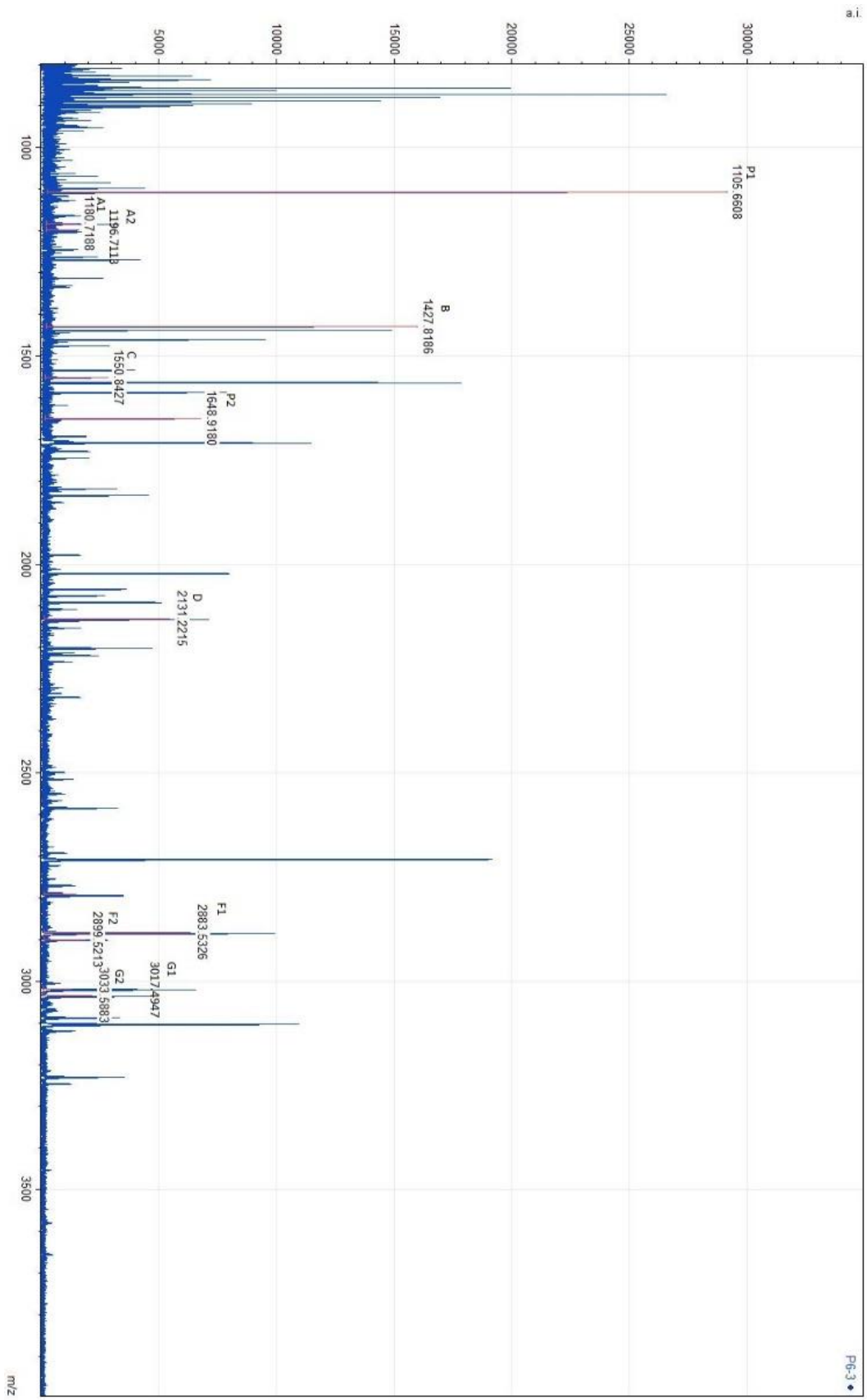
a.i.
5000
10000
15000
20000
25000
30000
1000
1500
2000
2500
3000
3500
m/z
P1
1105.6608
A1
1180.7188
A2
1196.7118
B
1427.8186
C
1550.8427
P2
1648.9180
D
2131.2215
F1
2883.5326
F2
2899.5213
G1
3017.4947
G2
3033.5883
P6-3

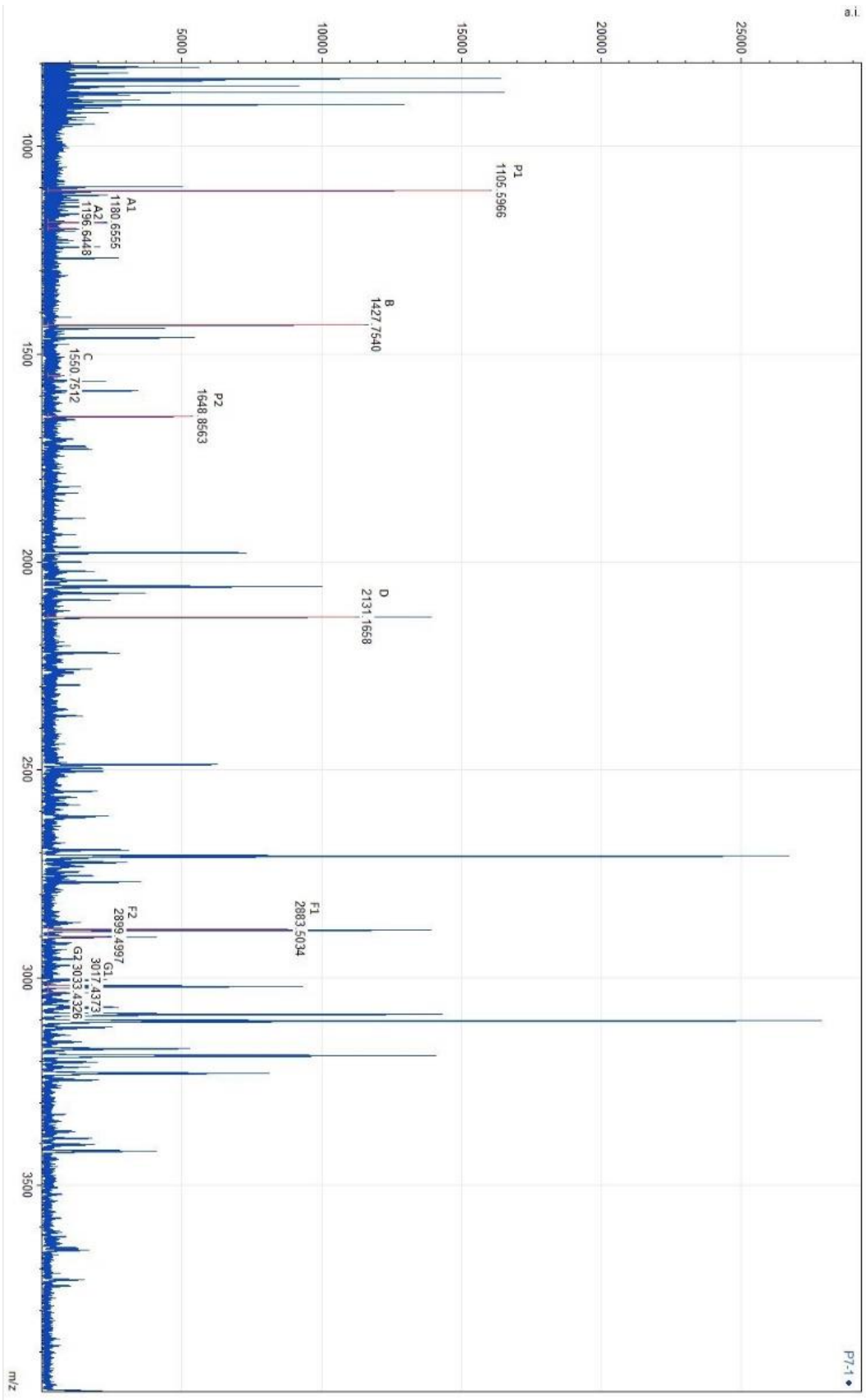
a.i.
5000
10000
15000
20000
25000
1000
1500
2000
2500
3000
3500
m/z
P1
1105.5966
A1
1180.6555
A2
1196.6448
B
1427.7540
C
1550.7512
P2
1648.8563
D
2131.1658
F1
2883.5034
F2
2899.4997
G1
3017.4373
G2
3033.4326
P7-1

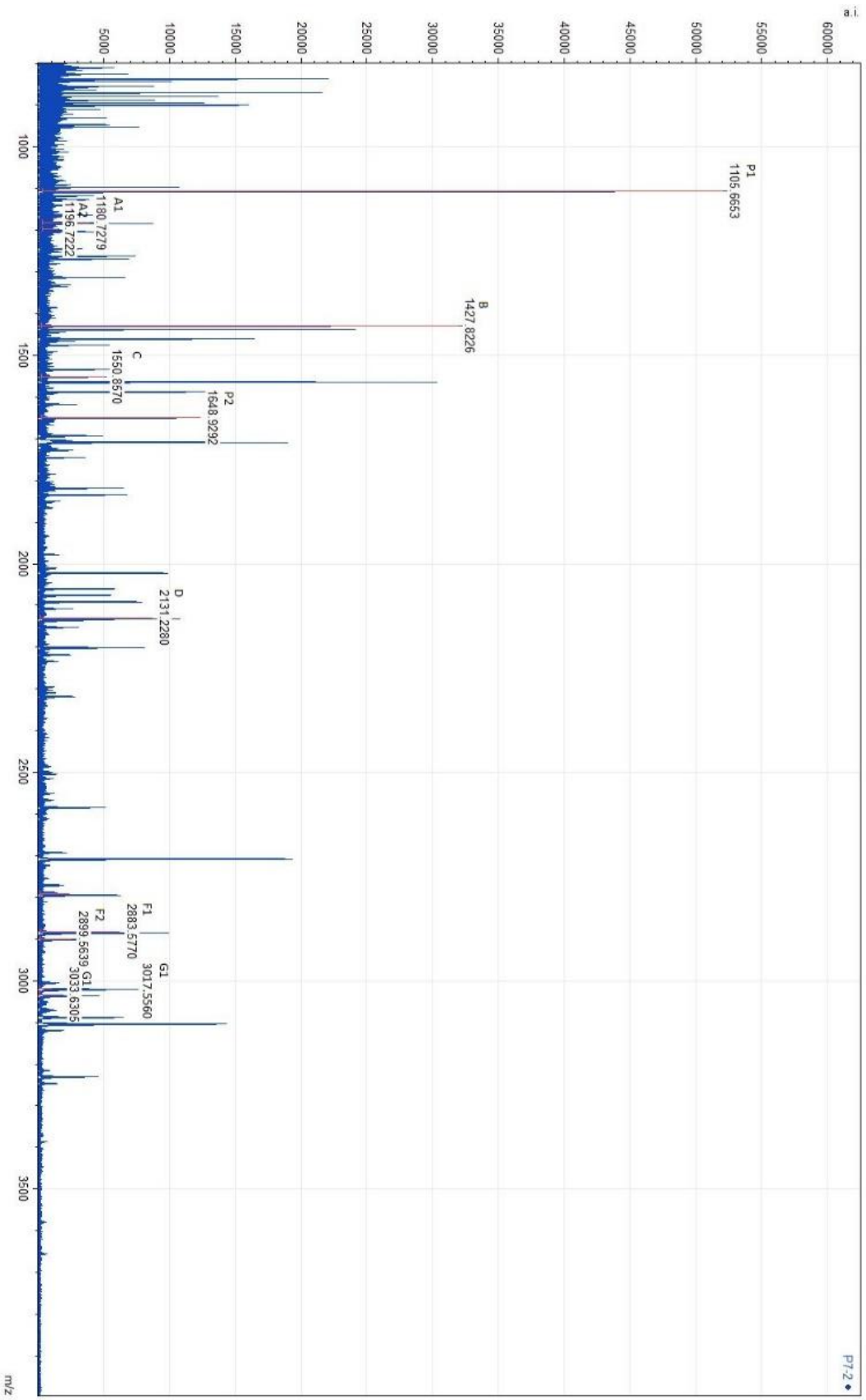
a.i.
P1
1105.6653
A1
1180.7279
A2
1196.7722
B
1427.8226
C
1550.8570
P2
1648.9292
D
2131.2280
F1
2883.5770
F2
2899.5639
G1
3017.5560
G1
3033.6305
m/z
P7-2

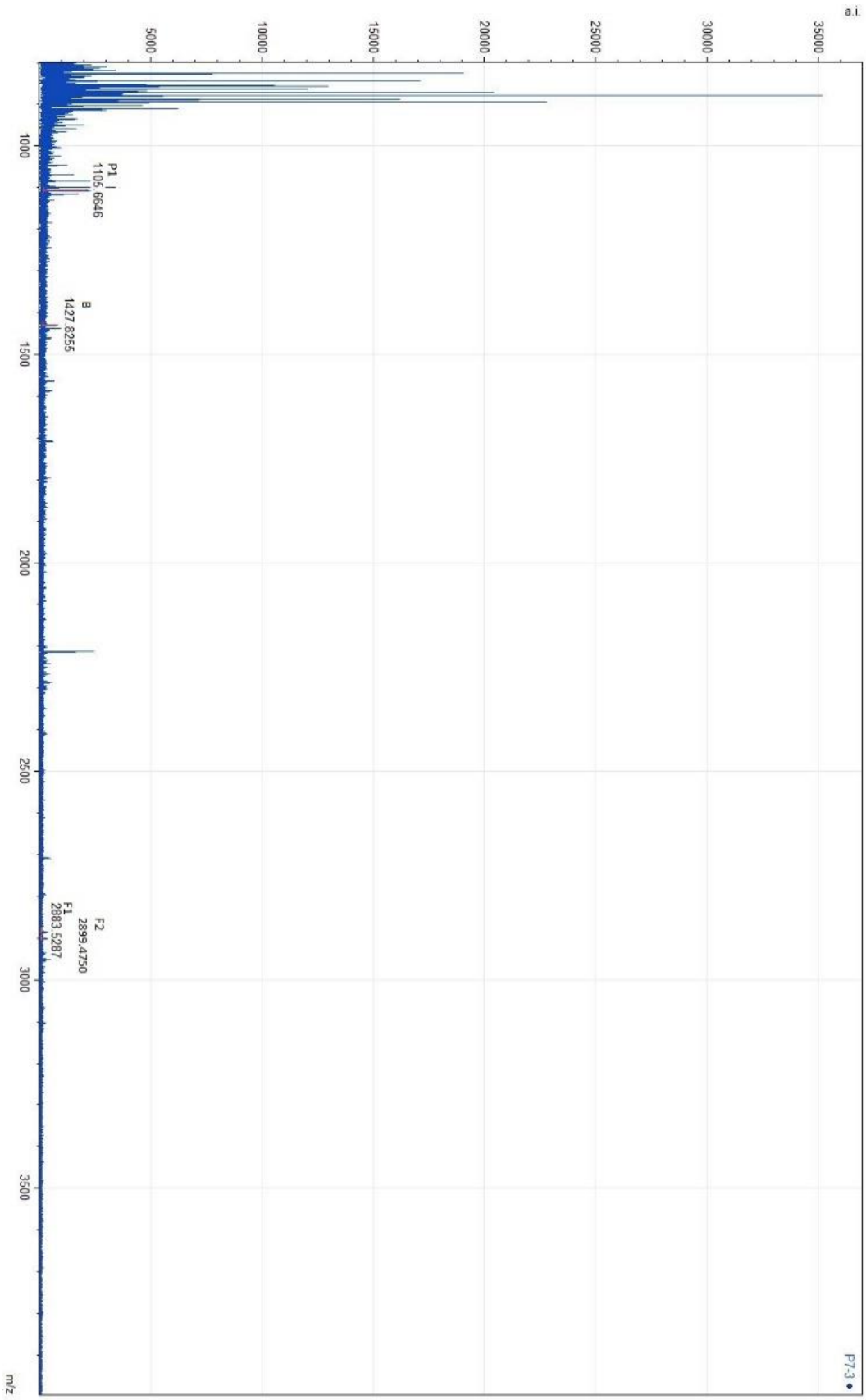
a.i.
5000
10000
15000
20000
25000
30000
35000
1000
1500
2000
2500
3000
3500
m/z
P1
1105.6646
B
1427.8255
F1
2883.5287
F2
2899.4750
P7-3

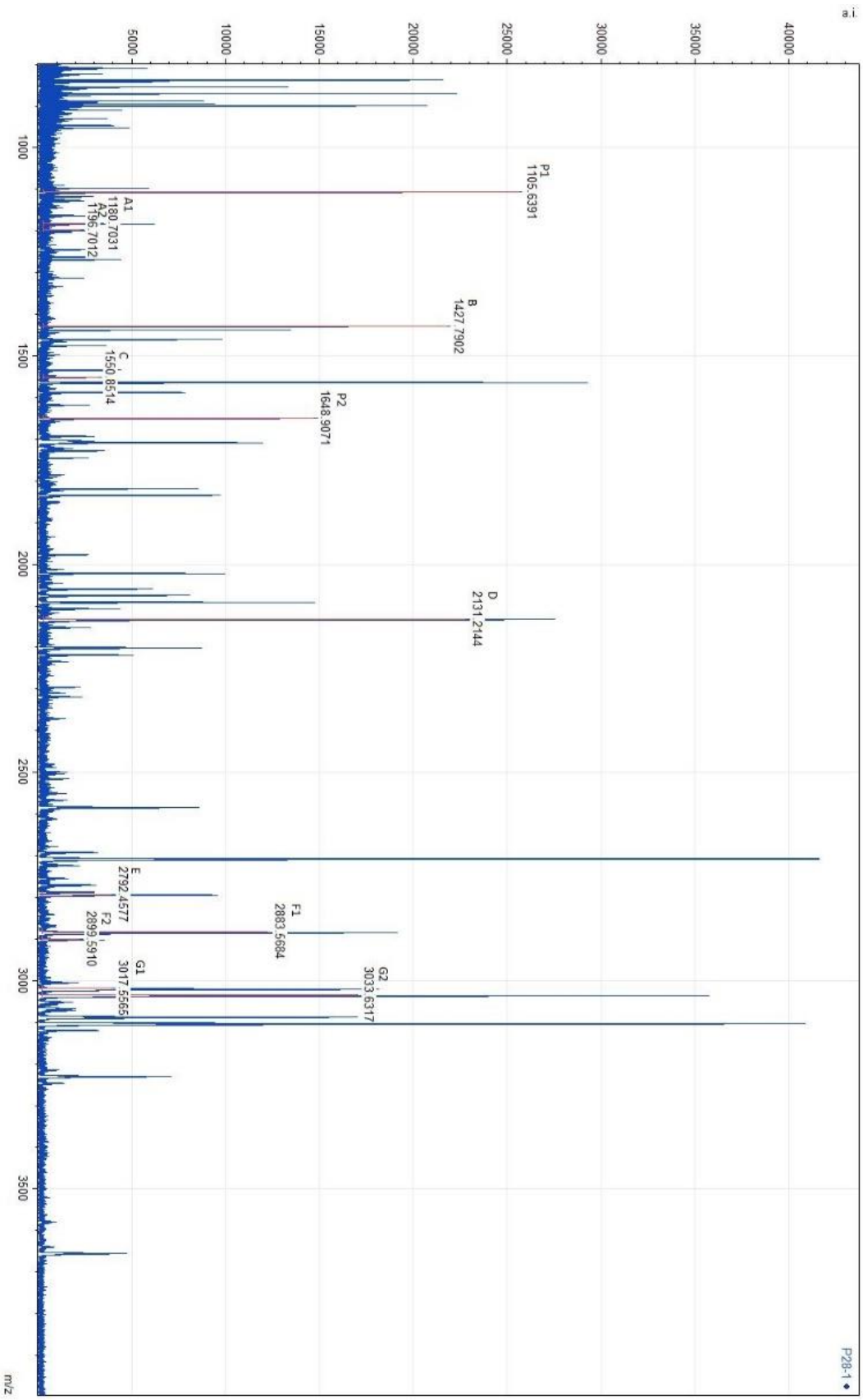
a.i.
5000
10000
15000
20000
25000
30000
35000
40000
1000
1500
2000
2500
3000
3500
m/z
P1
1105.6391
A1
1180.7031
1196.7012
B
1427.7902
C
1550.8514
P2
1648.9071
D
2131.2144
E
2792.4577
F2
2899.5910
F1
2883.5684
G1
3017.5565
G2
3033.6317
P28-1

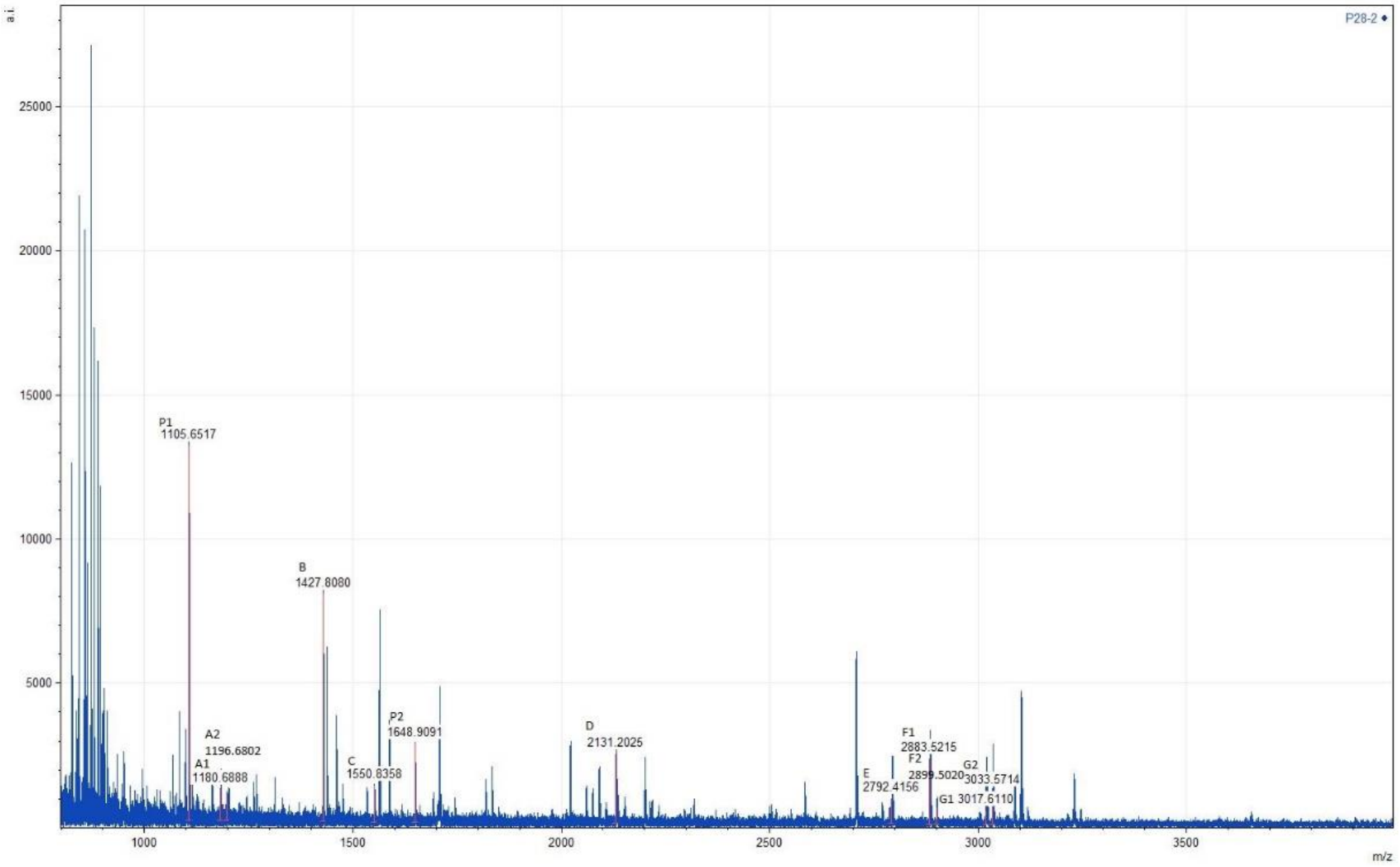
P28-2
a.i.
25000
20000
15000
10000
5000
P1
1105.6517
A2
1196.6802
A1
1180.6888
B
1427.8080
C
1550.8358
P2
1648.9091
D
2131.2025
E
2792.4156
F1
2883.5215
F2
2899.5020
G2
3033.5714
G1 3017.6110
1000
1500
2000
2500
3000
3500
m/z

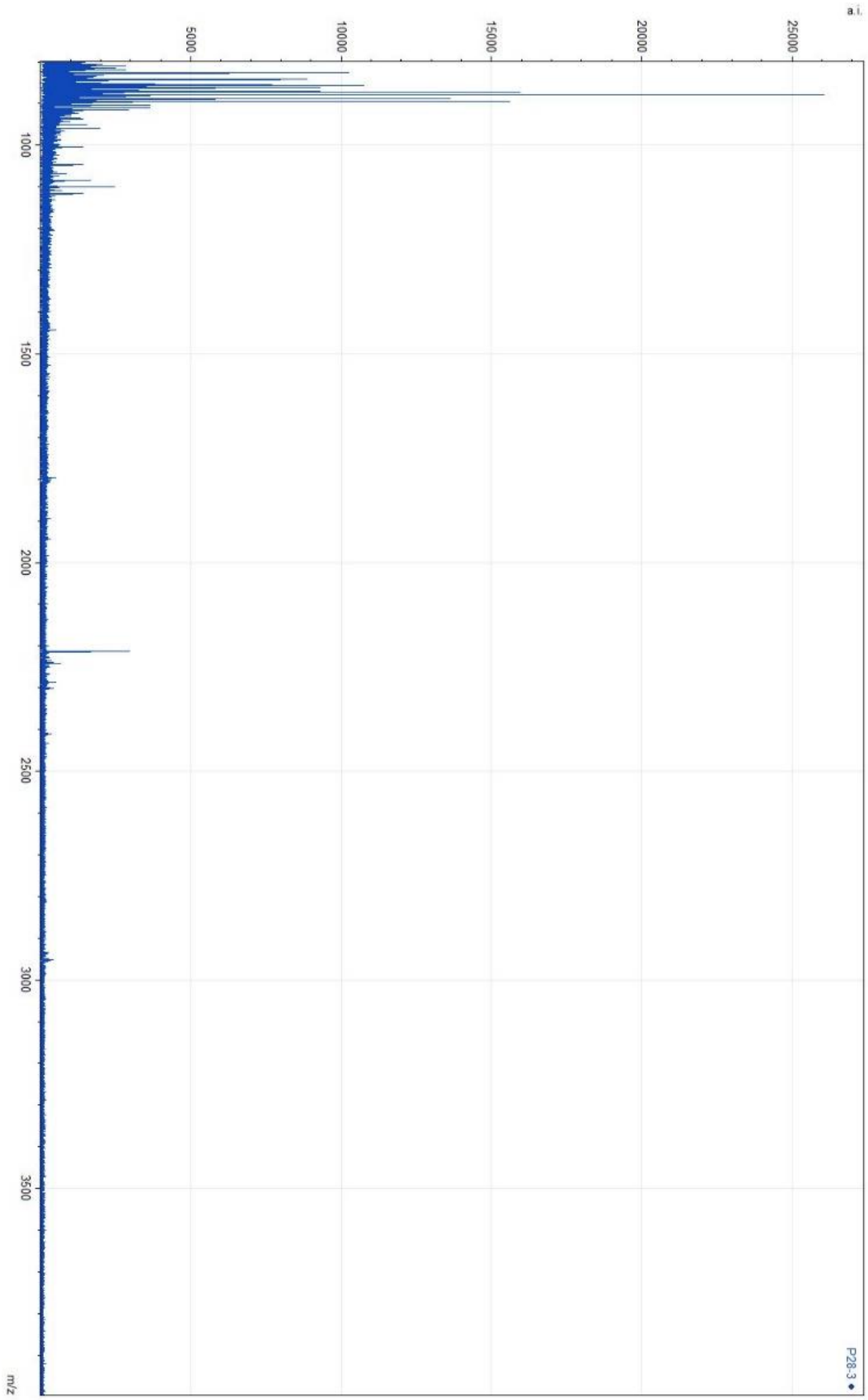
a.i.
5000
10000
15000
20000
25000
1000
1500
2000
2500
3000
3500
m/z
P28-3

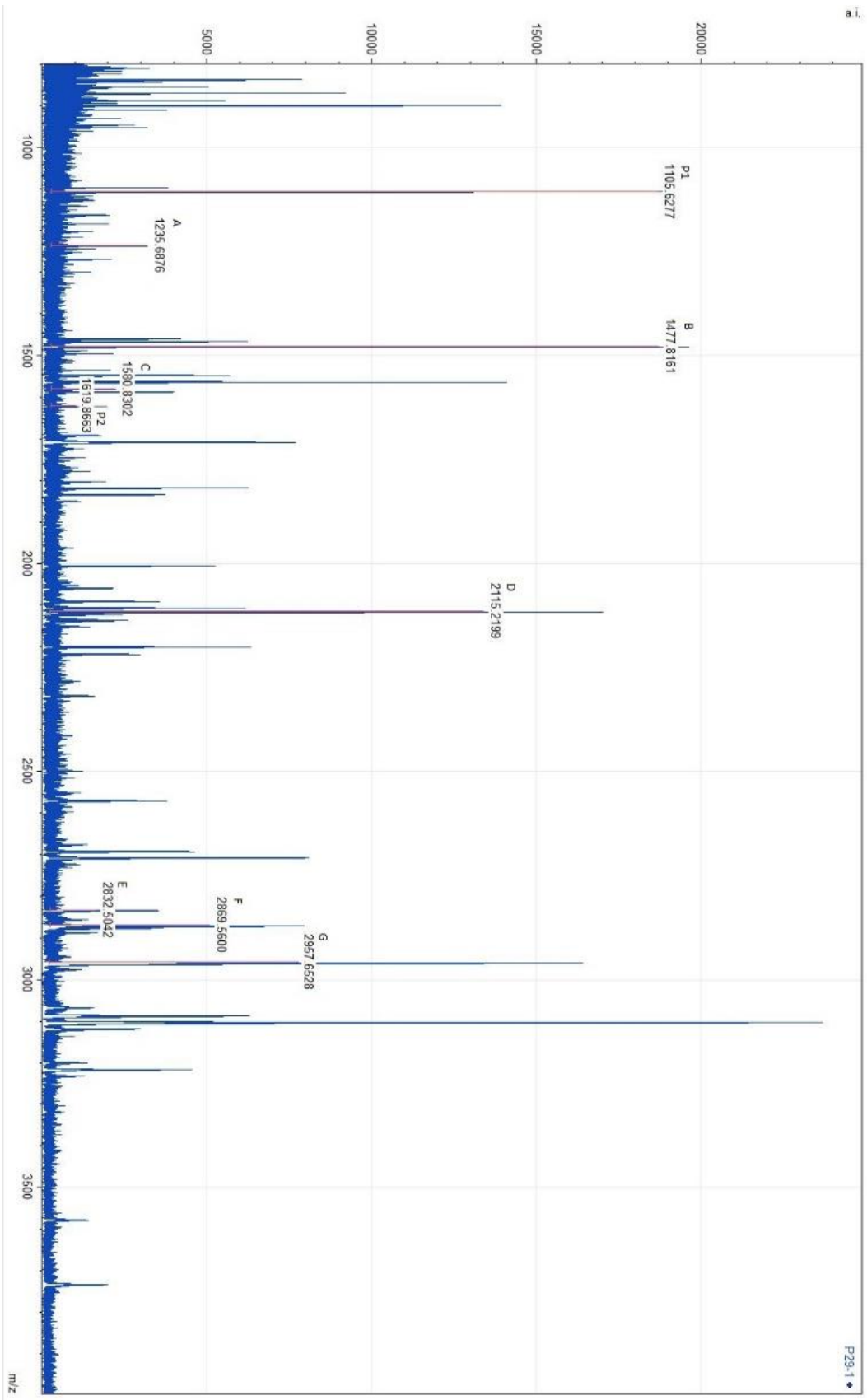
a.i.
P1
1105.6277
A
1235.6876
B
1477.8161
C
1580.8302
P2
1619.8663
D
2115.2199
E
2832.5042
F
2869.5600
G
2957.6528
P29-1
m/z

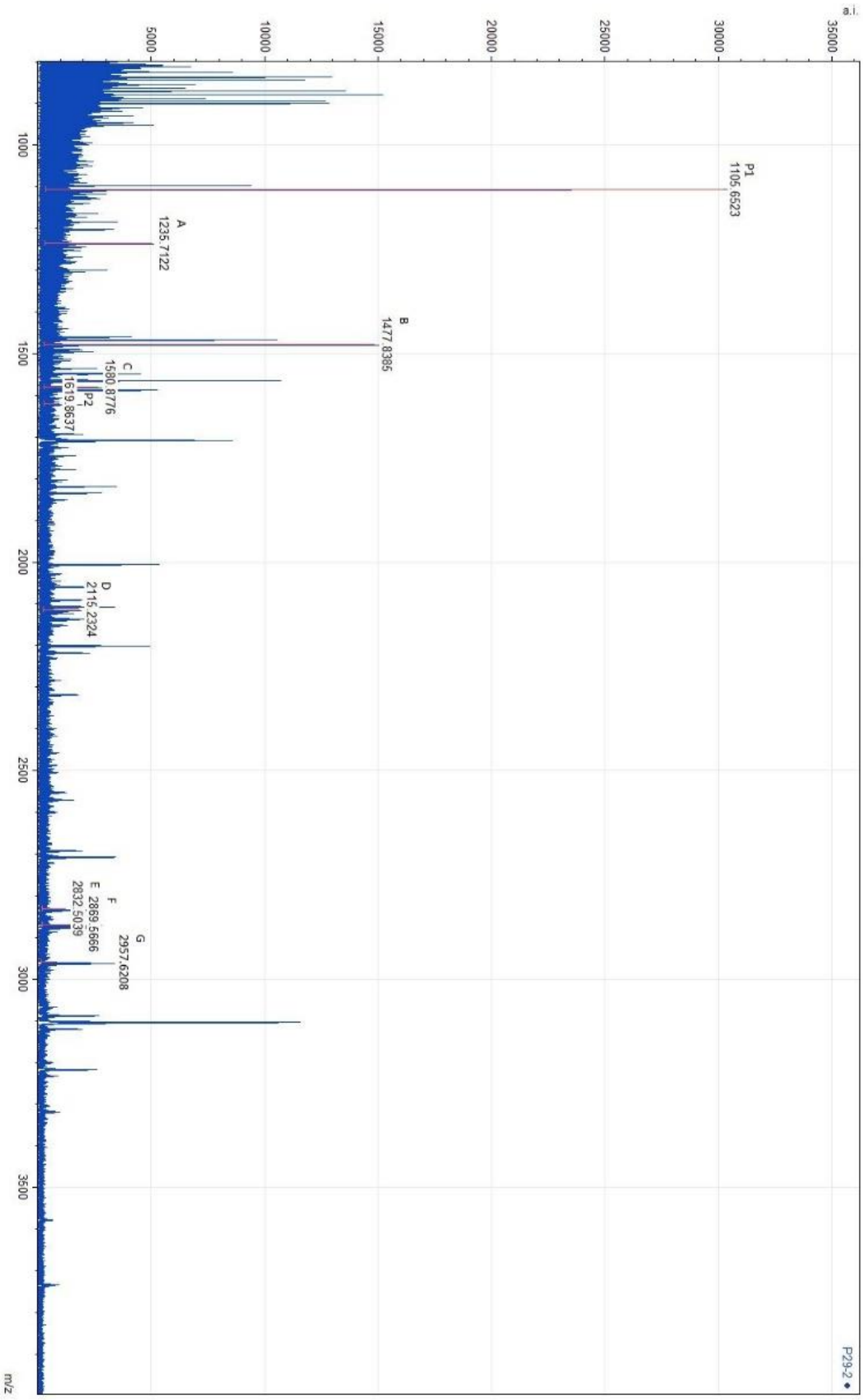
a.i.
35000
30000
25000
20000
15000
10000
5000
P1
1105.6523
A
1235.7122
B
1477.8385
C
1580.8776
P2
1619.8637
D
2115.2324
E
2832.5039
F
2869.5666
G
2957.6208
1000
1500
2000
2500
3000
3500
m/z
P29-2

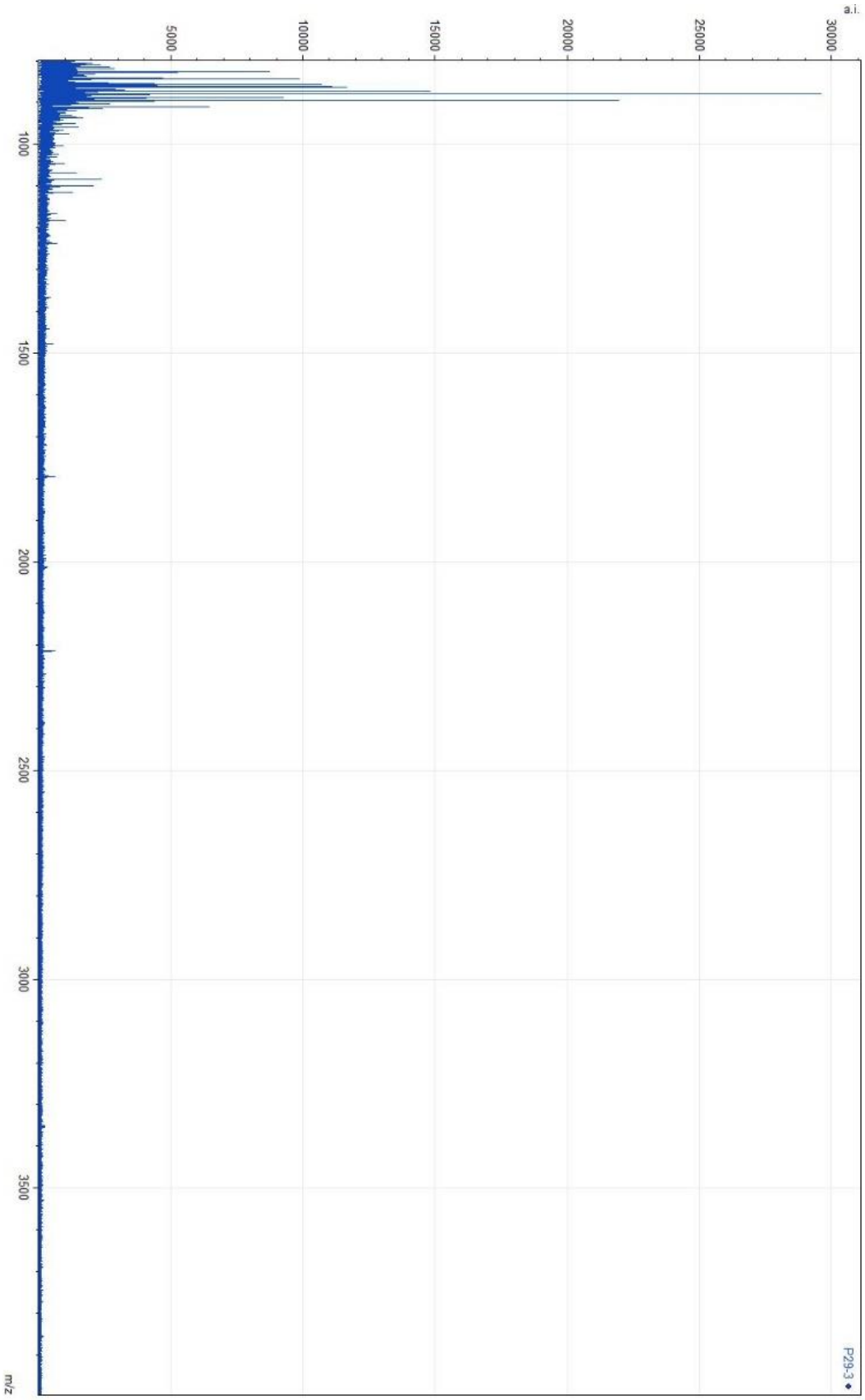
a.i.
5000
10000
15000
20000
25000
30000
1000
1500
2000
2500
3000
3500
m/z
P29-3

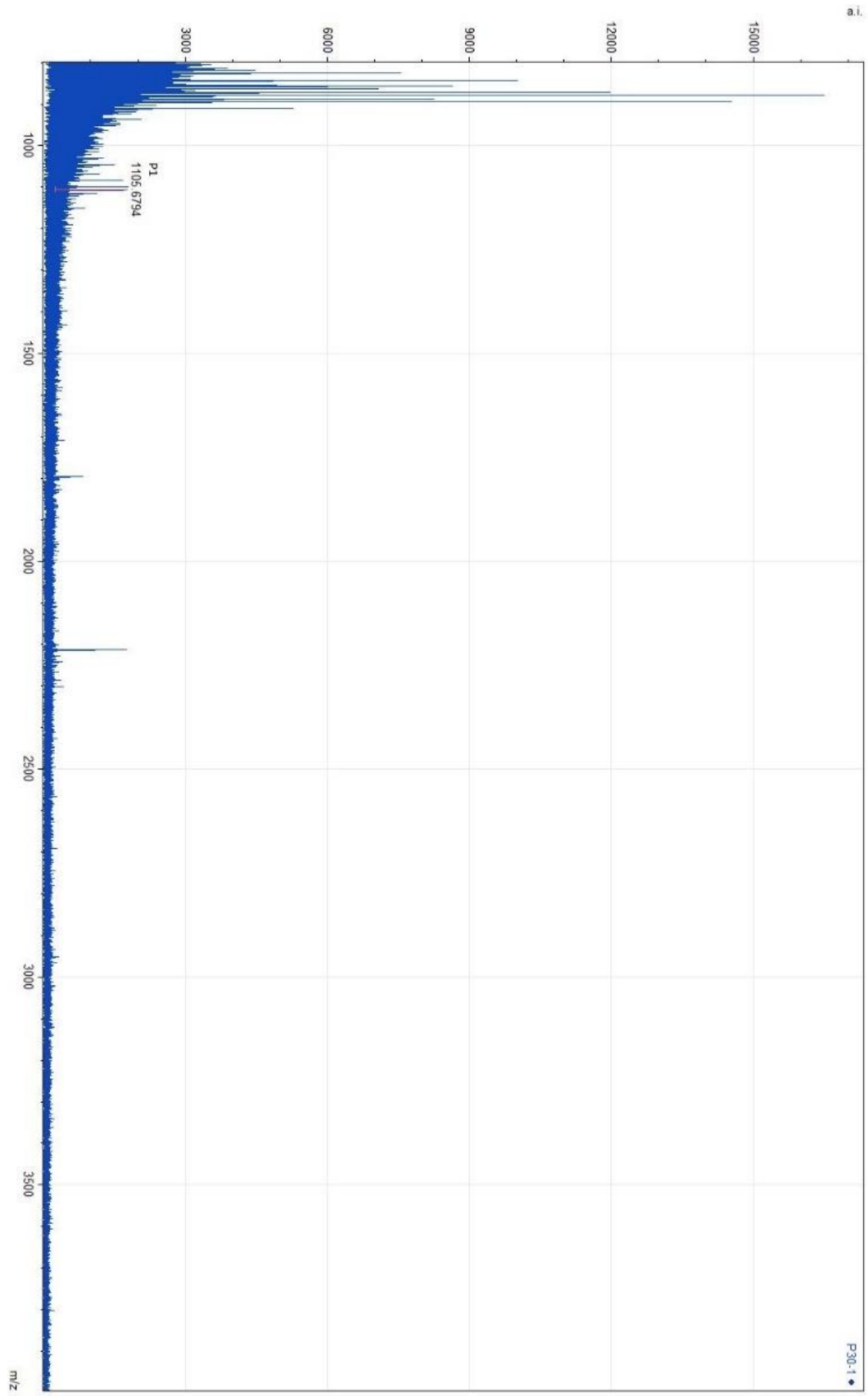
a.i.
3000
6000
9000
12000
15000
1000
1500
2000
2500
3000
3500
m/z
P1
1105.6794
P30-1

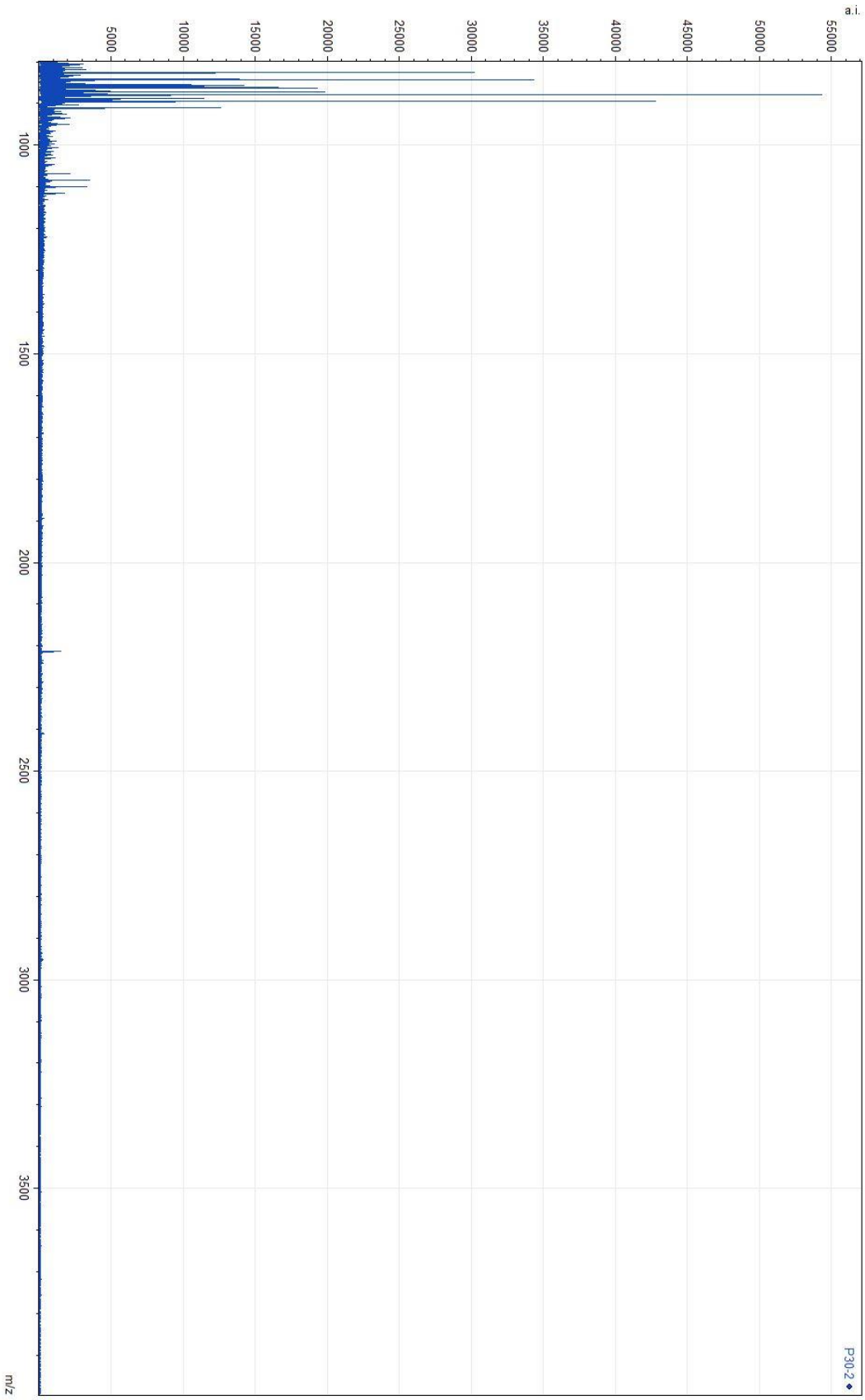
a.i.
5000
10000
15000
20000
25000
30000
35000
40000
45000
50000
55000
1000
1500
2000
2500
3000
3500
m/z
P30-2

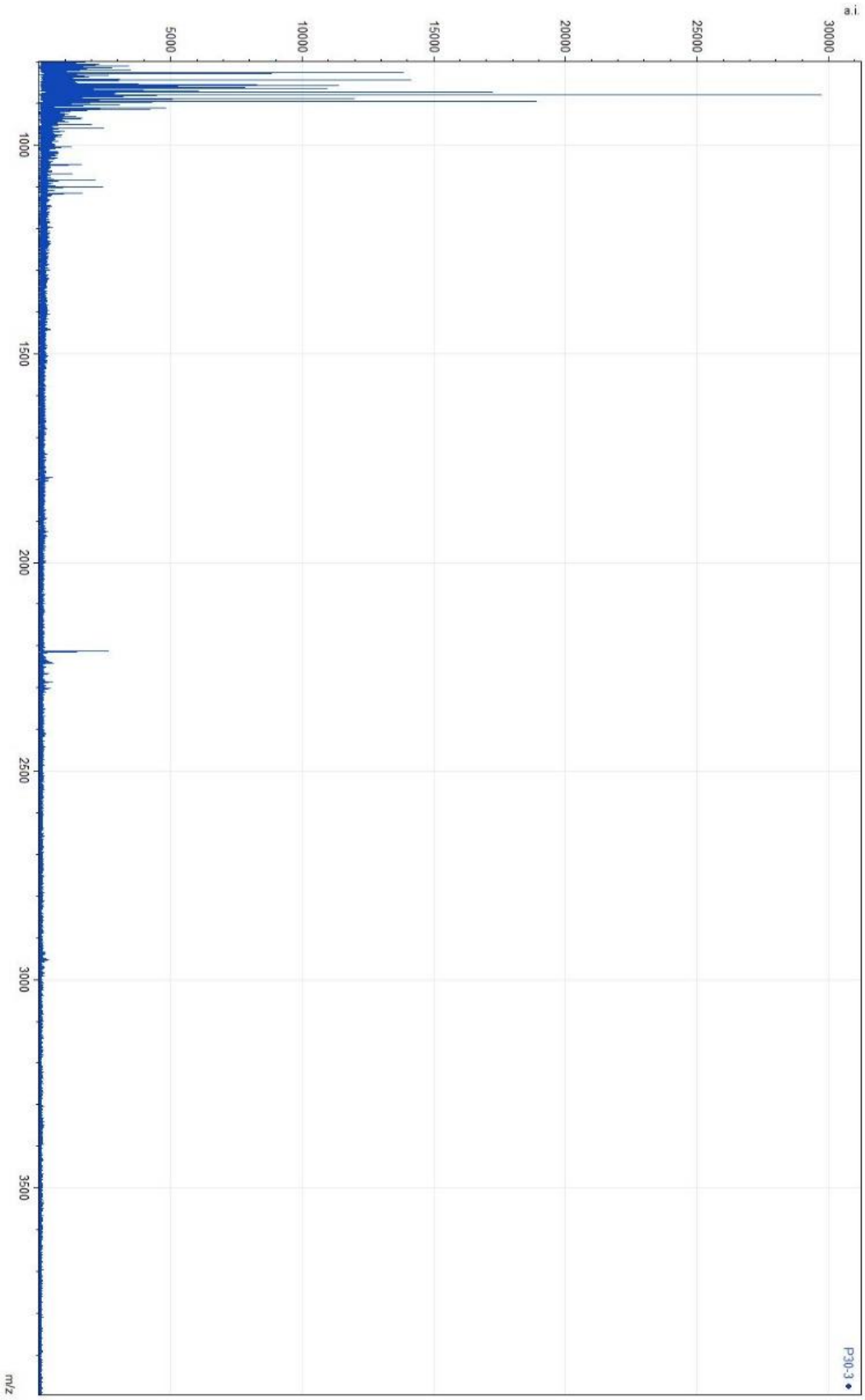
a.i.
5000
10000
15000
20000
25000
30000
1000
1500
2000
2500
3000
3500
m/z
P30-3

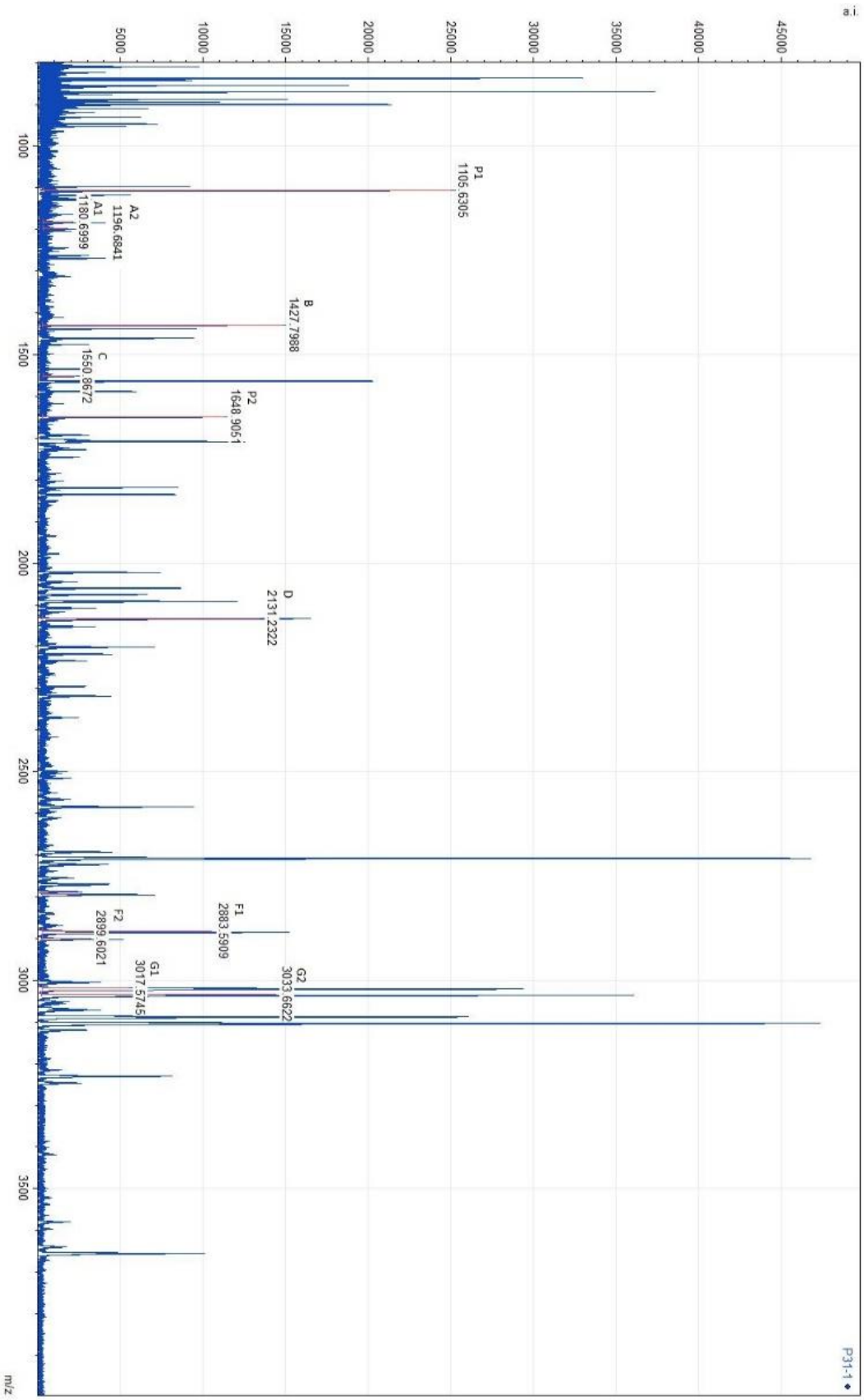
a.i
P1
1105.6305
A2
1196.6841
A1
1180.6999
B
1427.7988
C
1550.8672
P2
1648.9051
D
2131.2322
F1
2883.5909
F2
2899.6021
G1
3017.5745
G2
3033.6622
m/z
P31-1

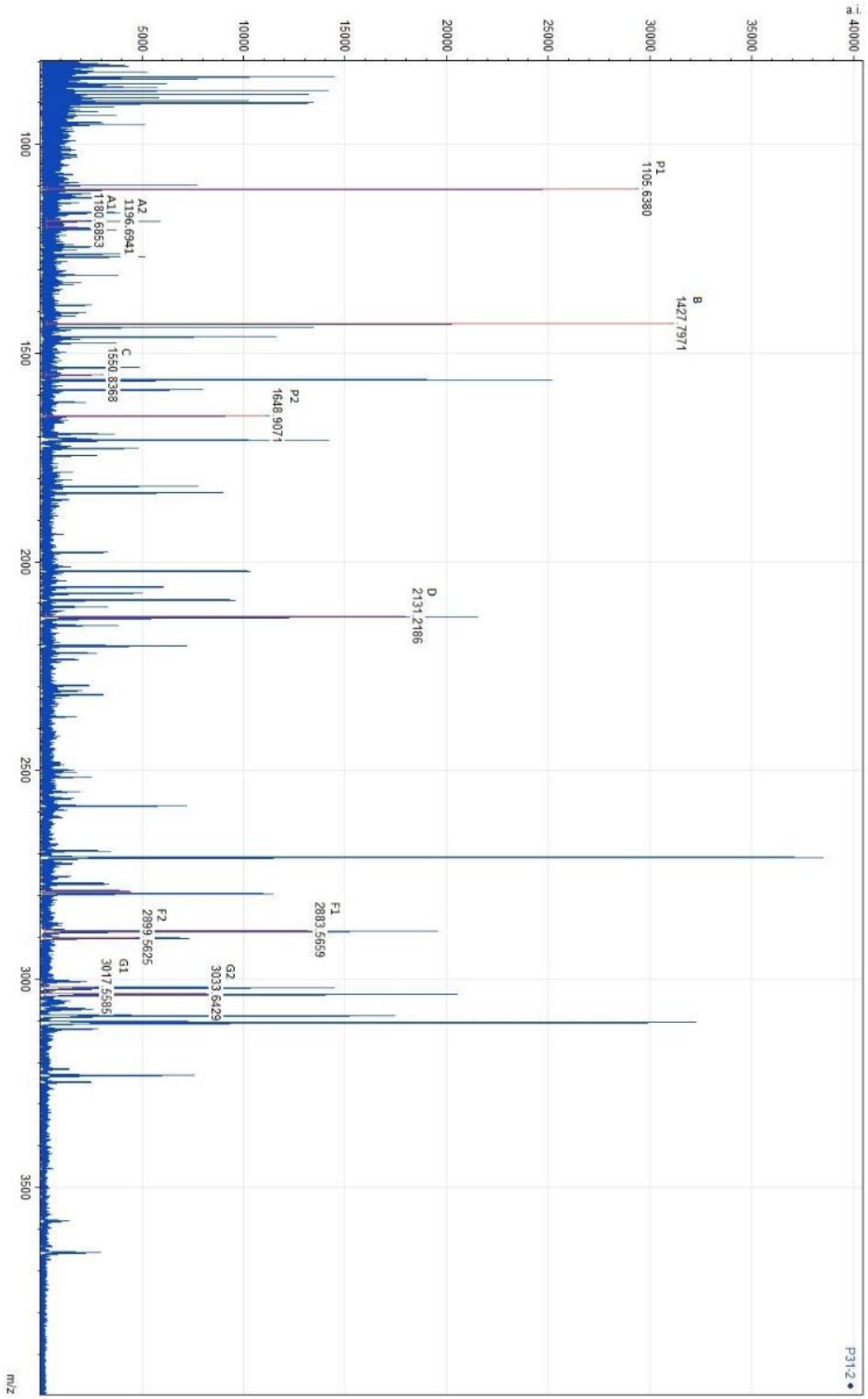
a.i.
40000
35000
30000
25000
20000
15000
10000
5000
1000
1500
2000
2500
3000
3500
m/z
P1
1105.6380
A2
1196.6941
A1
1180.6853
B
1427.7971
C
1550.8368
P2
1648.9071
D
2131.2186
F1
2883.5659
F2
2899.5625
G1
3017.5585
G2
3033.6429
P31-2

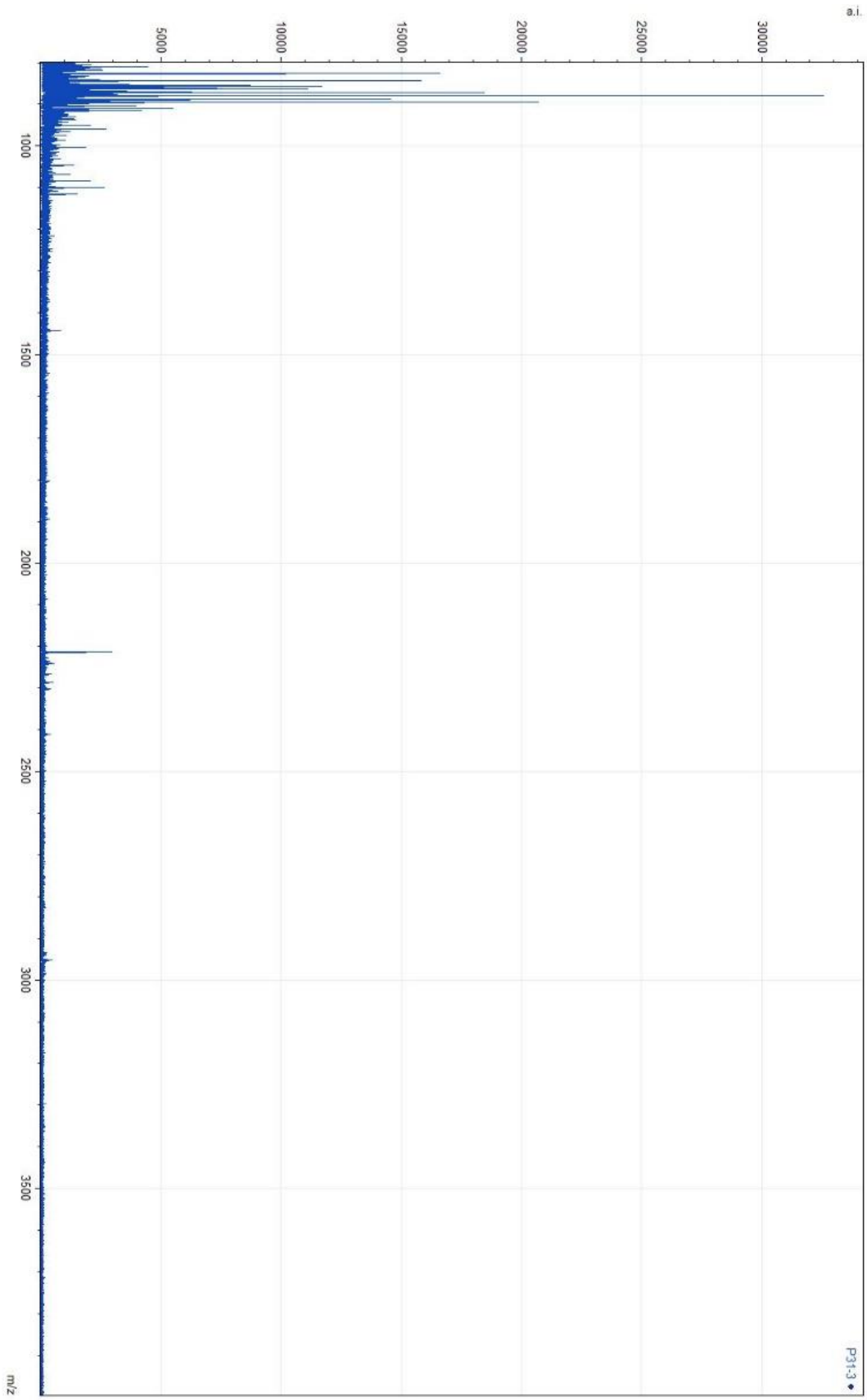
a.i.
5000
10000
15000
20000
25000
30000
1000
1500
2000
2500
3000
3500
m/z
P31-3

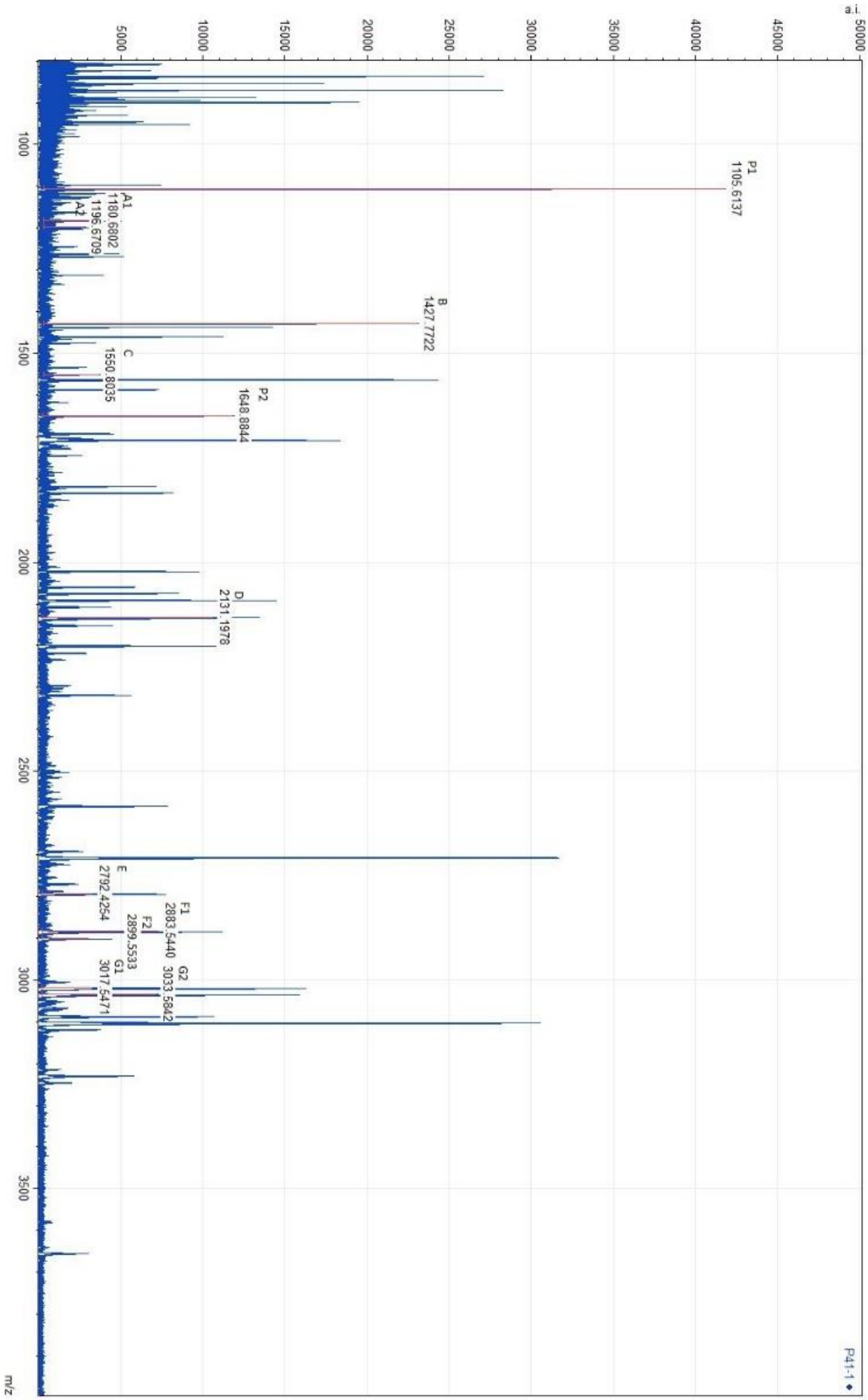
P1
1105.6137
A1
1180.6802
1196.6709
A2
B
1427.7722
C
1550.8035
P2
1648.8844
D
2131.1978
E
2792.4254
F1
2883.5440
F2
2899.5533
G1
3017.5471
G2
3033.5842
m/z
P41-1

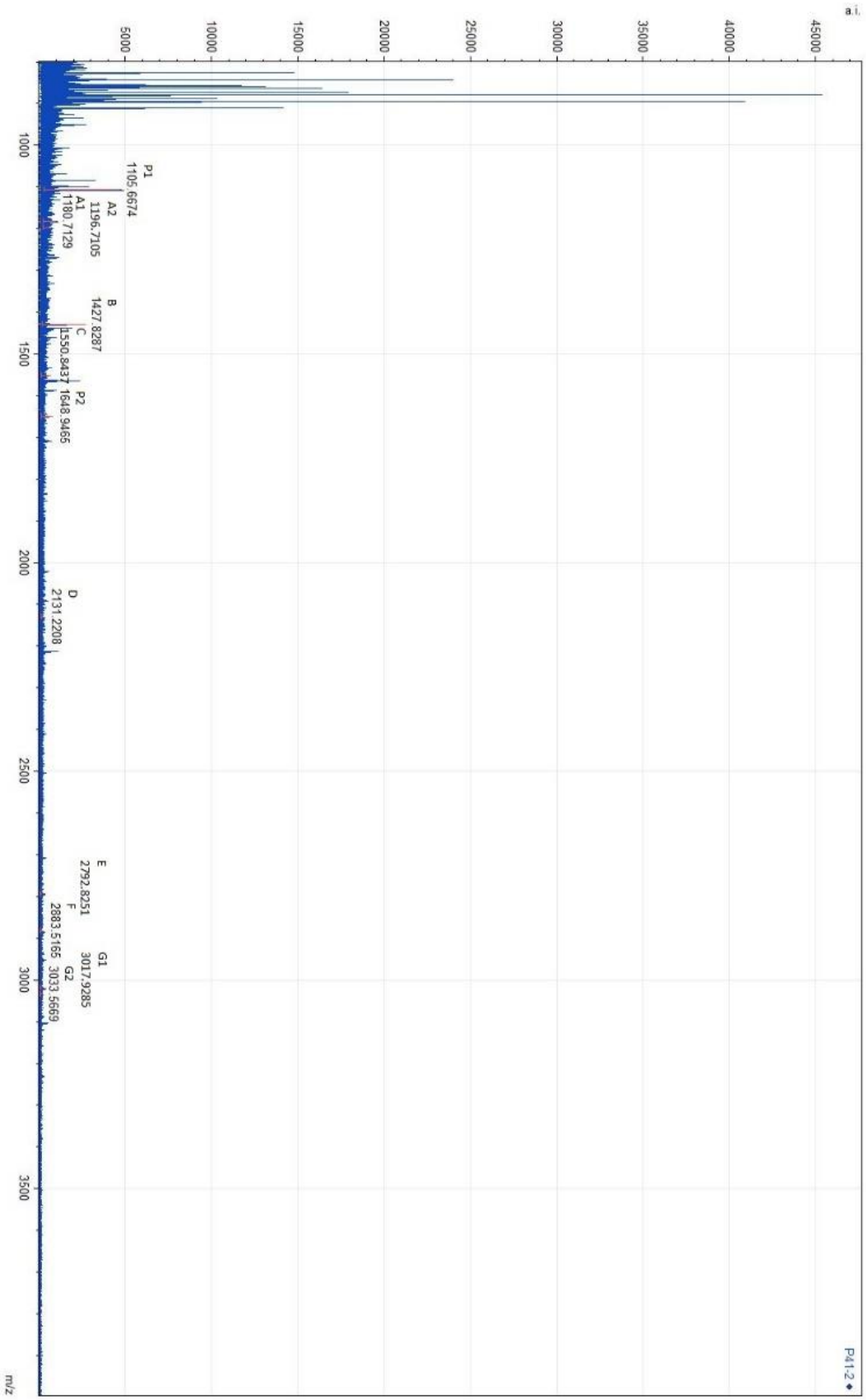
a.i.
P1
1105.6674
A2
1196.7105
A1
1180.7129
B
1427.8287
C
1550.8437
P2
1648.9466
D
2131.2208
E
2792.8251
F
2883.5165
G1
3017.9285
G2
3033.5669
P41-2
m/z

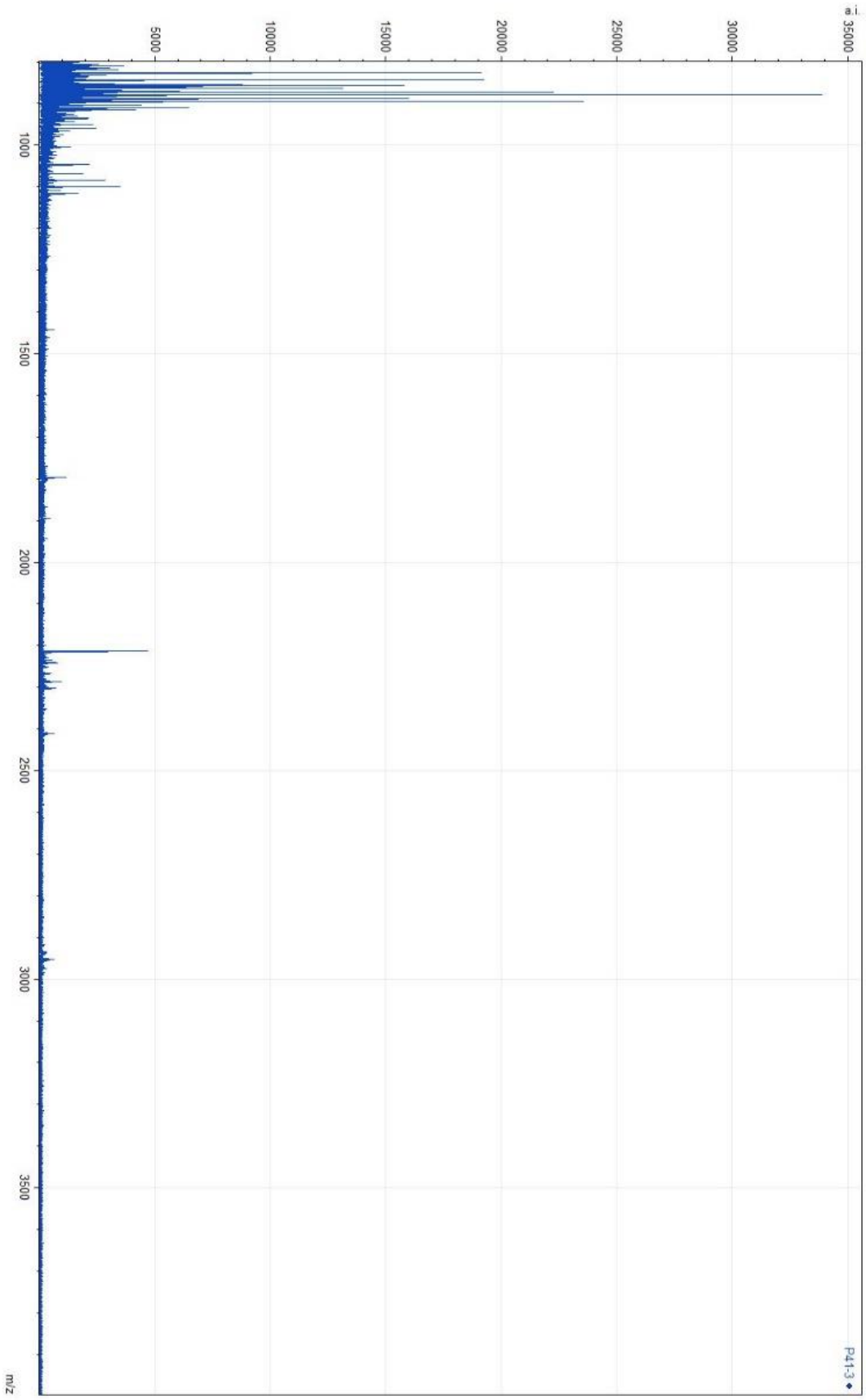
5000
10000
15000
20000
25000
30000
35000
1000
1500
2000
2500
3000
3500
m/z
P41-3